



Optimising laminated high-mass timber components assembled from a fibre-grown resource for building applications

by

Mohammad Derikvand

Master of Science in Natural Resources Engineering—Wood Science and Technology,
University of Tehran, 2012

Bachelor of Science in Natural Resources Engineering—Wood Science and Technology,
University of Mazandaran, 2008

Submitted in fulfilment of the requirements for the degree of

Doctor of Philosophy

College of Sciences and Engineering, University of Tasmania, Australia

April 2019

Statements

Declaration of originality

This thesis contains no material which has been accepted for a degree or diploma by the University or any other institution, except by way of background information and duly acknowledged in the thesis, and to the best of my knowledge and belief no material previously published or written by another person except where due acknowledgement is made in the text of the thesis, nor does the thesis contain any material that infringes copyright.

Authority of Access

This thesis may be made available for loan and limited copying and communication in accordance with the *Copyright Act 1968*.

Statement of Ethical Conduct

Not applicable.

Statement regarding published work contained in thesis

The statement of co-authorship for the research papers in this thesis is given in Chapter 4. The publishers of Paper II, Paper III, Paper V, Paper VI, and Paper VII will hold the copyright for that content and access to the material should be sought from the respective journals. The remaining published (i.e., Paper I and Paper IV) and non published content of the thesis may be made available for loan and limited copying and communication in accordance with the Copyright Act 1968.

Signed: 29/04/2019

Mohammad Derikvand

Acknowledgments

First and foremost, I would like to thank my primary supervisor Professor Gregory Nolan for giving me the opportunity to come to Australia and undertake my PhD under his supervision. Your support and encouragements always motivated me and made me believe in what I was doing within this PhD research. I would also like to thank my co-supervisor Dr. Nathan Kotlarewski, Dr. Hui Jiao, and Professor Andrew Chan for providing me with valuable feedback on my PhD research and reviewing my papers. My special thanks to both Dr. Nathan Kotlarewski from Australian Research Council Centre for Forest Value (ARC CFV) and Michael Lee from Centre for Sustainable Architecture with Wood (CSAW) for their advices on the methodology of this PhD research and assisting me in performing the relevant experimental investigations.

While doing my PhD, I was invited by Dr. Hui Jiao and Professor Andrew Chan to teach Timber Structures at the University of Tasmania's School of Engineering. Thank you, Hui and Andrew, for giving me this opportunity. I have developed a set of skills within this teaching opportunity and have achieved a lot of experience that will be extremely valuable in my future academic career.

This PhD research was undertaken under the Australian Research Council (ARC), Centre for Forest Value (CFV), University of Tasmania, TAS, Australia (Grant Reference: IC150100004). In the past three years, I had the opportunity to work closely with people from the ARC CFV and their industry partners. Without your support and encouragements, it would have been hard to conduct this PhD research as smoothly and cleanly as it eventually turned out to be. My special thanks to the ARC CFV director Professor Mark Hunt and the Centre's manager Dr. Mark Neyland who have always been supportive of my research.

As I was based at the University of Tasmania's discipline of Architecture and Design (A&D), I received enormous amount of technical advices and supports from the discipline's staff members while performing the experimental investigations of my project. My special thanks to the A&D workshop manager Robin Green for his help and advice during my PhD study. I would also like to thank Luke Dineen and Duncan Maxwell who assisted me in preparing the test specimens required for undertaking the experimental investigations of my PhD research.

I would like to extend my special thanks to my good colleagues and friends Maya Pangh, Kent Davis, Michelle Balasso, Dr. Mohammad Sadegh Taskhiri, and Janice Bowman for their support and help.

Last, but certainly not least, a special thanks to my parents and siblings. I started this journey with your unconditional support and encouragement in my quest for new challenges. I would like to dedicate this thesis to you as a small thank you for everything you have done for me. I will forever be grateful and indebted to you.

Preface

This is a thesis by publication, comprised of seven papers, that presents a PhD research aimed to develop and optimise high-value structural nail-laminated timber floor panels from fibre-managed eucalypt plantations.

The University of Tasmania’s *Guidelines for Incorporating Publications into a Thesis* suggests that “*As a general guideline, when the majority of a thesis is to be comprised of published papers, anywhere between three to eight papers (depending on the discipline) bracketed between a substantive general introduction chapter (that lays a coherent foundation for the research) and a general discussion and conclusion(s) chapter (that draws the findings together and provides a clear statement concerning the findings) would be considered acceptable, although this will ultimately be determined by the discipline*” (48TGuidelines for Incorporating Publications into a Thesis, 2018).

In this thesis by publication, a separate *State of the art* chapter (including a review of literature) and a separate *Methodology* chapter have also been included after the *Thesis Introduction* chapter to let the readers better understand the concept of this thesis and ways in which the experimental works within this PhD research have been performed. In addition, instead of presenting each paper as a separate chapter, the titles, publication status, and main goals of the seven papers in this thesis and ways in which they have been linked together are highlighted in a chapter named *Research Contributions*—with the full text of the papers being included in the Appendices. This is followed by a *Discussion and Conclusions* chapter that draws the findings together and provides clear statements concerning the findings as per the above University of Tasmania’s policy statement.

As each research paper must stand alone, there is some repetition in the methodologies and literature reviews presented in the seven papers outlined in this thesis.

I was awarded a PhD scholarship from the Australian Research Council Centre for Forest Value (ARC CFV). It must therefore be noted that the research presented in this thesis is mostly explored from an Australian perspective while still addressing a research problem with global importance.

Table of contents

Statements	i
Acknowledgments.....	ii
Preface	iv
Table of contents.....	v
List of tables.....	vii
List of figures.....	viii
Abstract.....	ix
Chapter 1: Thesis introduction.....	1
1.1. Introduction.....	1
1.2. Aim and scope of the thesis	1
1.3. Thesis rationale	2
1.4. Research gaps.....	2
1.5. Research questions.....	3
1.6. Thesis assumptions	4
1.7. Limitations	4
1.8. Layout of thesis.....	5
1.9. Summary	6
Chapter 2: State of the art	7
2.1. Introduction.....	7
2.2. Plantation hardwood resources and their uses in Australia.....	7
2.3. Plantation timber estate in Tasmania	8
2.4. The use of plantation eucalypt timber in structural products; opportunities and challenges	9
2.5. Potential mass laminated timber products from eucalypt plantations.....	12
2.6. Manufacturing process of mass laminated timber products.....	15
2.6.1. Harvesting and sawing of logs	15
2.6.2. Drying of timber boards.....	16
2.6.3. Structural grading of boards.....	18
2.6.4. End-to-end and side-to-side jointing of boards.....	18
2.7. Key studies on mass laminated timber from fibre-managed eucalypt plantations.....	19
2.8. Summary	21
Chapter 3: Methodology	23
3.1. Introduction.....	23
3.2. Harvesting and processing the required plantation eucalypt logs	23
3.3. Mapping the research problem.....	24
3.4. Development of research plan and experimental investigations.....	24
3.5. Summary.....	26

Chapter 4: Research contributions	27
4.1. Introduction.....	27
4.2. How the research questions were addressed	27
4.3. Statement of co-authorship	31
4.4. Summary	35
Chapter 5: Discussion and conclusions.....	36
5.1. Introduction.....	36
5.2. Producing sawn timber from plantation <i>E. nitens</i> pulplog and related challenges	36
5.3. Physical and mechanical properties of plantation <i>E. nitens</i> sawn timber	38
5.4. Structural performance of plantation <i>E. nitens</i> NLT panels	38
5.5. Methods for optimising plantation <i>E. nitens</i> NLT panels	39
5.6. Recommendations for future research	41
5.7. Epilogue	42
References.....	43
Appendices.....	51
Appendix A: Paper I	52
Appendix B: Paper II	56
Appendix C: Paper III.....	83
Appendix D: Paper IV	107
Appendix E: Paper V	121
Appendix F: Paper VI.....	146
Appendix G: Paper VII	164

List of tables

Tables are included in the relevant papers in the Appendices. No tables are included in the five chapters of this thesis.

List of figures

Figure 2. 1. Proportion of Australia’s hardwood plantations managed for sawlog and pulplog (ABARES, 2018).....	8
Figure 2. 2. Total plantation areas in Tasmania (ABARES 2018).....	8
Figure 2. 3. Plantation hardwood estate in Tasmania (ABARES, 2018).....	9
Figure 2. 4. Orientation of boards in vertical GLT (a) and CLT (b) panels.....	13
Figure 2. 5. Examples of different NLT and SLT panels (perspective view of the cross sections).....	14
Figure 2. 6. An idealised drawing of some common timber sawing patterns.	16
Figure 2. 7. Unrecoverable drying defects in 16-year-old unthinned and unpruned <i>E. nitens</i> . (a) and (b) show unrecoverable collapse, (c) shows end splitting, and (d) shows surface checking.	17

Abstract

In recent years, there has been a growing interest by the timber industry in Australia and worldwide in developing higher-value structural mass laminated timber products from fast-growing, fibre-managed plantation eucalypt resources (i.e., pulpwood eucalypt). The plantation eucalypt resources in Australia are predominantly managed to produce woodchips, which is considered as a low-value product. The timber from such plantation resources is of low-structural grade and contains a substantial number of strength-reducing features such as knots that can complicate its wider applications for structural purposes as individual boards.

This doctoral thesis aimed to develop and optimise higher-value structural nail-laminated timber (NLT) floor panels from fibre-managed plantation eucalypt timber. The target specie was *Eucalyptus nitens* (*E. nitens*), which is the main plantation hardwood specie in Tasmania. In parts of the experimental investigations of this thesis, however, tests have been done on plantation *Eucalyptus globulus* (*E. globulus*) as well to create a basis for comparison with *E. nitens*—*E. globulus* is the main plantation hardwood specie in Australia.

The experiments in this thesis were performed within three phases. The general aims and main findings of each phase are described as follow:

- In the first phase, the effectiveness of conventional timber processing regimes (i.e., harvesting, sawing, drying, and visual stress-grading) on fibre-managed plantation eucalypt and the physical and mechanical characteristics of the recovered sawn boards from this resource were determined. The aim of this phase was to investigate if the plantation eucalypt can be properly harvested, sawn, dried, and graded to produce sawn boards suitable for NLT production. Another aim of this phase was to create a profile of material characteristics for the plantation eucalypt sawn timber that can assist the development of NLT floor panels by better understanding the resource. Based on the results obtained in this phase, the conventional timber processing regimes used resulted in nominal sawn timber recovery rates of 25.8% for *E. nitens* and 31.8% for *E. globulus*. Considerable amounts of mechanical damages from debarker and sawing machines were detected in the recovered timber boards. Unrecoverable collapse, distortions, and surface checking were the main drying defects in the recovered boards. The visual stress-grading method showed no reliable accuracy in structural grading of plantation *E. nitens* timber. Alternative grading systems need to be developed for the structural use of this resource. A profile of visual, physical, and mechanical properties was created for the plantation eucalypt resources in this phase.
- In the second phase, NLT floor panels, with and without concrete topping, were constructed using different cross-sectional configurations and span lengths. Conventional methods were used in manufacturing these panels. The panels were subjected to both vibration and short-term four-point bending tests. The aim of this phase was to determine the short-term structural capacity of the NLT and NLT-concrete

floor panels made of randomly selected boards and to identify the best configuration for NLT production from the plantation eucalypt resources. The second aim of this phase was to identify any issues associated with the development of such products that can be addressed in the third phase of this doctoral research. Based on the results, all the test panels successfully passed the serviceability limit state (deflection and vibration) and strength limit state (bending moment capacity) requirements for structural floors in residential and office buildings. The best configuration of the panels was identified. A relatively high variation was observed in the bending characteristics of the panels. The conventional screw-type shear connectors used in producing the NLT-concrete panels resulted in a low composite action.

- In the third phase, based on the results obtained from the previous phases, innovative approaches were developed for the effective use of sawn fibre-managed plantation *E. nitens* in NLT and NLT-concrete production. The configuration and assembly methods of the NLT and NLT-concrete elements were optimised by developing appropriate timber-concrete connections and a new lamination system. The NLT panels (without concrete topping) produced using the new lamination system were subjected to short-term four-point bending test and long-term serviceability bending loads for 90 days to determine the bending creep deflection of the panels. The proposed lamination system reduced the variation in the MOE of the NLT panels. The results suggest that this lamination system can both customise the MOE of the panels and effectively maximise the use of lower-grade boards in NLT production.

Overall, the fibre-managed plantation *E. nitens* timber demonstrated appropriate short-term and long-term structural performances to be used in the construction of NLT floor panels for both residential and office buildings. Producing structural products from fibre-managed plantation eucalypt can create new markets for this resource and ensure a reliable supply of timber for the building construction sector in Australia. The use of such plantation resources will also be associated with some difficulties. These difficulties were discovered and are discussed in this thesis and relevant suggestions to address these difficulties are made through an agenda for future research.

Chapter 1: Thesis introduction

1.1. Introduction

In this chapter, the aim and context of this thesis are outlined. The thesis rationale, research gaps, research questions, assumptions surrounding the questions and limitations related to them are then described. Finally, the contents of each chapter of the thesis are highlighted.

1.2. Aim and scope of the thesis

According to the Australian Bureau of Agricultural and Resource Economics and Sciences (ABARES, 2018), Australia has a hardwood plantation estate of approximately 908,500 hectares. This plantation estate is predominantly comprised of *Eucalyptus nitens* (*E. nitens*) and *Eucalyptus globulus* (*E. globulus*). Both species are primarily managed for pulplog production. As Australia's hardwood timber sector still relies on native forests and imported wood products, there is a drive by the timber industry in developing higher-value structural products from the fibre-managed plantation eucalypt resources.

Finding a practical way to use fibre-managed plantation eucalypt in the Australian construction industry is challenging. Sawn timber from this resource has a low structural grade as it contains substantial strength-reducing features (SRFs) such as knots and surface checking. This could limit its use as individual boards in most structural applications. The effectiveness of using boards recovered from Australian fibre-managed plantation eucalypt resource for structural building applications in the form of mass laminated timber components—as opposed to individual boards—is still unknown and worthy of investigation. Sawn boards from this resource may have the potential to be used in producing innovative mass laminated timber products for building applications.

The main goal of this PhD research was to first characterise the physical and mechanical properties of timber recovered from fibre-managed eucalypt plantations and then investigate and optimise ways in which sawn boards from such planation resources can be used both effectively and efficiently in manufacturing higher-value nail-laminated timber (NLT) panels for structural flooring systems in both residential and office buildings. The target timber specie

in this research was *E. nitens*—this is the main hardwood plantation specie in Tasmania. In several parts of this research, however, tests have been done on fibre-managed plantation *E. globulus* timber as well to create a basis for comparison with *E. nitens*. *E. globulus* is the main hardwood plantation specie in Australia.

1.3. Thesis rationale

Given the significance and complexity of the issue as well as the lack of scientific information in this area, this PhD research investigates and addresses crucial parameters likely to influence the use of sawn fibre-managed plantation *E. nitens* in producing NLT for structural floor applications. The experimental and numerical investigations conducted in this PhD research lead to a robust understanding of the material properties of this timber resource and the way it can be used in producing NLT floors both effectively and efficiently. The outcomes of this PhD research may contribute to creating new markets for Australia's plantation hardwood industry as well by introducing reliable assembly techniques and procedures for producing NLT from the plantation eucalypt resources.

1.4. Research gaps

The possibility of using Australian fibre-managed plantation eucalypt in structural applications, as sawn boards and veneer-based products, has been studied in a few research projects in the past decade. Some of these studies are highlighted in Chapter 2. Despite these studies, there is still no information available on the performance of this plantation resource in NLT production. In addition, conventional methods of timber processing (i.e., harvesting, sawing, drying, and visual stress-grading) might be inadequate for fibre-managed plantation eucalypt timber, especially visual stress-grading method whose regulations and rules are designed based on the properties of mature native forest timber. This deficiency in the standard methods is an important obstacle against using this resource for mass laminated timber production. There is also a lack of information on the physical properties and short-term and long-term mechanical characteristics of fibre-managed plantation eucalypt timber that needs to be addressed before such a resource can be recommended for structural applications.

1.5. Research questions

The research in this thesis sought to address three general research questions as follow:

- Research question 1:

Are conventional timber processing regimes (harvesting, sawing, drying, and visual stress-grading) appropriate to produce sawn boards, suitable for NLT production, from fibre-managed eucalypt plantations?

To develop a practical method for producing NLT from fibre-managed plantation eucalypt resource, information is required on whether logs from this resource can be processed (i.e., harvested, sawn, dried, and graded) to produce sawn timber boards suitable for NLT production. Information is also required on the recovery rate of sawn boards, useable for NLT production, from such plantation resources. This research question aimed to fill the gap in knowledge in these areas through experimental investigations.

- Research question 2:

*Do timber sawn from fibre-managed plantation *E. nitens* and NLT floor panels assembled from this resource have satisfactory short-term structural properties especially when compared to the performance of other species?*

This research question aimed to create a profile of physical and mechanical properties of fibre-managed plantation *E. nitens* sawn timber and NLT panels. An important objective of this research question was to determine the differences between the physical and mechanical properties of sawn timber and NLT from this resource with those of sawn timber and mass laminated timber products from other species. Such information can help to understand the weaknesses and strengths of sawn timber and NLT from such a plantation resource, which can further be used to optimise the properties of the final product.

- Research question 3:

*How can the configuration of NLT floor panels assembled from sawn fibre-managed plantation *E. nitens* be optimised to improve their short-term and long-term structural performances?*

Considering the results obtained through answering the first and the second research questions, investigation of the third research question aimed to develop ways in which the configuration and assembly of the NLT panels in the previous phases of this thesis can be optimised to improve their structural performance. This research question also aimed to study the long-term structural performance of the NLT panels under sustained loads to fill the gap in knowledge in this area.

Through answering the above research questions, new knowledge and innovative manufacturing approaches were created which can provide guidance for the plantation forest and timber industry towards developing higher-value sawn timber and NLT floor products from the fibre-managed eucalypt plantations.

1.6. Thesis assumptions

The following general assumptions were considered within the research presented in this thesis:

- The Australian timber industry can use fibre-managed plantation *E. nitens* to develop effective solutions for new engineering and design applications. This topic is of growing interest as native hardwood species—used for their strength and visual properties—become protected because of government legislation and environmental preservation.
- Study on the physical properties and short-term and long-term mechanical characteristics of fibre-managed plantation *E. nitens* timber as well as establishing new target-based grading systems for using this resource in structural applications will shape the main body of the development of a possible NLT product from such a resource. This will result in a knowledge-based construction approach with a global value that could be used as an exemplar research project and applied in other countries that are facing the same problem in their timber construction sectors.

1.7. Limitations

The most important limitation in this PhD research related to the constrained amount of sawn fibre-managed plantation eucalypt available for performing the required experimental investigations. This plantation resource is generally managed to produce pulplog and is currently not available in the market as sawn timber. To perform the experimental investigations of this research, fibre-managed plantation eucalypt logs were harvested and

processed to produce sawn timber boards. However, the amount of recovered boards for this research was limited. Therefore, the number of specimens tested in some phases of this thesis, especially for NLT testing, had to be limited so that all the required experiments can be performed in a reasonable manner.

1.8. Layout of thesis

- Chapter 1: Introduction

This chapter introduces the general context and describes the research rationale, research questions, assumptions, limitations, and layout of this thesis.

- Chapter 2: State of the art

In this chapter, the general scope and topics concerning this thesis are highlighted. The status of plantation resources and their uses in Australia and Tasmania are discussed. The opportunities, drivers, and challenges related to the development of structural mass laminated timber from fibre-managed eucalypt plantations and potential mass laminated timber products and their configurations are highlighted and reviewed. The required manufacturing processes of mass laminated timber in general are also reviewed. Finally, a selection of key previous studies on developing mass laminated timber and other structural products from plantation eucalypt timber are summarised and discussed.

- Chapter 3: Methodology

This chapter outlines the methodology used in this PhD research including harvesting, sawing, drying, and finishing of the boards and the steps undertaken for producing and testing of NLT floor panels.

- Chapter 4: Research contributions

This chapter introduces the seven papers included in the thesis and provides details of co-authorship. The aims of each paper are given and information is provided on how the research questions were answered through these papers.

- Chapter 5: Discussion and conclusions

Considering the results reported in the seven outlined papers, the general findings as well as new knowledge and approaches created in this thesis are summarised in this chapter. Several recommendations and opportunities for future research are also included and discussed.

- Appendices:

The full text of the seven papers in this thesis are included in the Appendices section.

1.9. Summary

In this chapter, the general aims, context, and importance of this thesis by publication were introduced. A set of research questions and assumptions were developed to address specific gaps in knowledge related to the development of structural NLT floor panels from fibre-managed plantation eucalypt. A guide to this thesis was then created which highlighted the contents of the different chapters of this thesis.

Chapter 2: State of the art

2.1. Introduction

This chapter introduces the scope and relevant topics concerning this thesis. The statistics related to hardwood plantations and their uses in Australia and Tasmania are discussed. The statistics reported in this chapter are related to the year 2016-2017 based on the latest report by the Australian Bureau of Agricultural and Resource Economics and Sciences (ABARES, 2018). Opportunities and potential challenges associated with the development of any mass laminated timber component from fibre-managed plantation eucalypt are highlighted and discussed. Different types of mass laminated timber products and their configurations are reviewed. The manufacturing processes required to produce mass laminated timber in general are also highlighted. Finally, the key findings of previous studies on producing mass laminated timber from fibre-managed plantation eucalypt timber are discussed. Parts of the text of this chapter have been published in Paper I located in Appendix A.

2.2. Plantation hardwood resources and their uses in Australia

The hardwood plantation estate in Australia is predominantly comprised of *E. globulus* (or Southern blue gum) and *E. nitens* (or Shining gum). *E. globulus* makes up 51.7 per cent of the current estate while 25.7 per cent is *E. nitens* (ABARES, 2018). This hardwood plantation estate provides a resource of raw materials for fibre industries. The genetics of the current plantation hardwood estate have been selected for their fast growth to compliment short rotation cycles in unthinned and unpruned stands. While this plantation hardwood resource exists, Australia's hardwood timber sector still relies on milling logs from native forests and imported wood products (McGavin et al., 2015). Although native hardwood species are well regarded for their strength and visual properties, supply has decreased steadily from the 1970s (Nolan et al., 2005). Given this decline, there is a drive to develop higher-value solid wood products and corresponding applications in building construction for some part of the plantation hardwood resource in order to fill growing market gaps.

Such a large volume of plantation hardwood trees has the potential to provide a significant

portion of the timber resource required to service Australia's timber construction sector. However, most plantation hardwoods in Australia, mainly eucalypt species, are primarily managed for pulplog production. According to ABARES (2018), nearly 82 per cent of logs currently harvested from hardwood plantations are being used to produce pulplogs (Figure 2. 1). However, during the year 2016-17, a total of 17.9 per cent of logs from the hardwood plantations were harvested and used for sawlog production. This indicates an increase of 2.3 per cent compared to the year 2015-16.

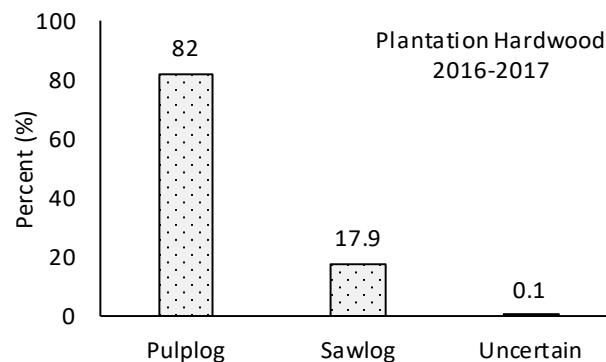


Figure 2. 1. Proportion of Australia's hardwood plantations managed for sawlog and pulplog (ABARES, 2018).

2.3. Plantation timber estate in Tasmania

Tasmania has approximately 309,900 ha of plantation trees (ABARES, 2018). In total, 75.5 per cent of the plantation estate in Tasmania is hardwood (Figure 2. 2). Softwood species also make up 24.5 per cent of the estate.

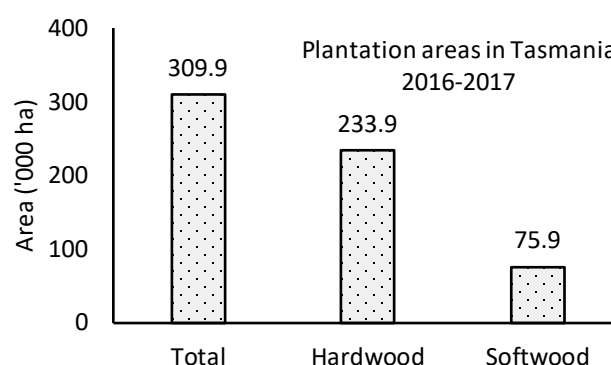


Figure 2. 2. Total plantation areas in Tasmania (ABARES 2018).

While the main plantation softwood species in Tasmania is Radiata pine (*Pinus radiata*), the plantation hardwood estate is predominately *E. nitens*—with a total area of 208,200 ha (Figure 2. 3). This counts for more than 89.1 per cent of the total area planted by *E. nitens* in Australia.

E. globulus makes up less than nine per cent of the plantation hardwood estate in Tasmania, whereas 2.82 per cent of the estate is planted with other hardwood species. In total, during the year 2016-17, around 85 per cent of the plantation hardwood estate in Tasmania was managed with short harvesting rotations for pulplog production.

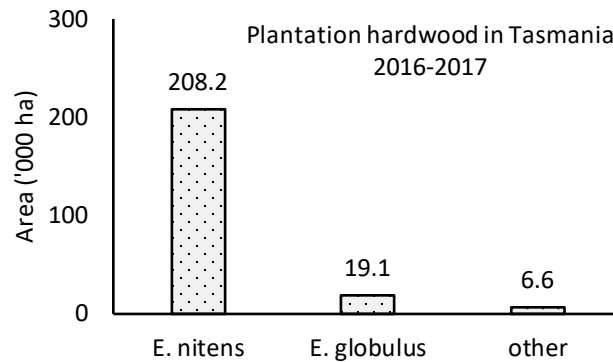


Figure 2. 3. Plantation hardwood estate in Tasmania (ABARES, 2018).

2.4. The use of plantation eucalypt timber in structural products; opportunities and challenges

Developing and producing engineered mass laminated timber components from structurally low-grade plantation eucalypt boards could generate a value-added product suite for a new plantation hardwood processing sector. It could support the markets expected to form as Australia's building professionals increasingly adopt timber-rich construction options for multi-residential and commercial buildings. Developing engineered products for building applications from structurally low-grade plantation eucalypt timber is a straightforward goal. However, commercial innovation and experimental works are also needed to find a practical process for using this material in a product that economically and structurally satisfies the requirements established in the Australian construction industry.

Due to the current economics of growing wood in Australia, fibre production drives management practices and most hardwood plantations are harvested between 15 to 20 years old. As a result, the diameter of logs potentially suitable for solid wood production is low. In addition, the stems are unthinned and unpruned. The lack of thinning produces tall but thin stems, while the lack of pruning results in regular branch stubs and other SRFs in the wood. Relatively unimportant for fibre production, both factors complicate recovery of solid wood products. This largely precludes its acceptance in appearance applications, but it may be suitable for a new generation of structural engineered products.

Sawing the logs and drying the boards from this resource presents challenges (Blackburn et al., 2010). Recovery from the small logs could be low without purpose-designed equipment, especially for *E. nitens* (Hamilton, 2007). The radial and tangential shrinkage rates for both *E. nitens* and *E. globulus* are high, and their sapwood is lyctus susceptible (Washusen, 2000; Washusen & Ilic, 2001). In conventional milling for appearance products, such species would be quarter sawn to reduce drying degrade and the sapwood removed. However, quarter sawing and sapwood exclusion reduce volume recovery from young logs with relatively wide sapwood bands. To increase recovery for mass laminated timber components, logs need to be sawn for volume and sapwood may need to be retained. Drying degradation in boards and lyctus susceptibility then need to be accommodated in later production stages.

The important initial stage in producing any mass laminated timber components from such resources is to establish a robust understanding of the resource's physical, mechanical, acoustical, and fire-resistant properties. While significant research into the properties of Australia's plantation species has occurred, much of this has focused on the properties of boards milled from logs from thinned and pruned stands grown in longer rotations (e.g., Washusen et al., 2009). Inadequate work has occurred on boards sawn for volume from logs recovered from unthinned and unpruned stands.

The multiplicity of knots, drying degradation features such as checks and unrecovered collapse, growth stress, the effects of tension wood, and non-uniform fibre orientation along the longitudinal axis can complicate the workability and performance of boards and groups of boards assembled into engineered timber components (Nolan et al., 2005; Hamilton, 2007). These complications need to be defined and understood. Factors that can influence the development of suitable, economic products from this resource include accelerated drying, drying degrade, board grading approaches, and methods of material assembly.

Logs cut for volume will produce a range of backsawn, quarter sawn, and transitional boards. If this resource is to be processed economically, accelerated drying is likely to be necessary, and the additional drying degradation generated in this variety of boards needs to be managed. However, the impact of the different types of drying degradation on board and panel workability and performance for each species and their increase with accelerated drying is not well understood. Additional checking is unlikely to be critical, but increased board deformation may create problems. These impacts need to be confirmed if a useful balance between drying speed and acceptable board degrade is to be identified.

Alternative grading rules are needed to accommodate plantation resources that will be used in mass engineered timber components. Existing visual stress-grading rules are rigorous and designed to ensure that the performance of an individual board for an unknown future application meets building standards. For individual boards with regular SRFs such as knots, the grading rules are constrictive and neglect to consider that multiple low-grade boards will be used in combination in a purpose-designed engineered component. While the individual boards may not be suitable to use as a single building element, such as a beam or post, they may contribute to the performance of a multi-member assembly such as Glue-Laminated Timber (GLT), NLT, and Stress-Laminated Timber (SLT) panels. Alternative grading rules can therefore potentially accommodate the patterns of features likely in each piece and their performance relative to board orientation in the finished panel.

In a high-mass laminated timber component, boards need to be joined along their length and side-to-side. An efficient end-to-end joining system is therefore vital to overcome length limitation and ensure efficient board utility. Finger jointing is the common end-to-end joining technique, but there is a lack of information on the effectiveness of finger joints in plantation eucalypt cut for volume and dried quickly. Simply docking out SRFs and re-joining clear sections will be labour-intensive and may make any final panel uneconomical in Australia. In addition to the SRFs in the wood, drying degradation may have a major influence on finger joint performance. Boards also need to be effectively joined side-to-side to make a panel: either glued, nail-laminated, or stress-laminated. Each approach will result in different structural performance in a panel (which needs to be defined) and in different opportunities in fabricating the panels economically.

Glue laminating panels requires skill in machining, adhesive management, and product assembly but can provide a reliable product from a varied resource (Uzel et al., 2018). Nail lamination is a more diverse process for regional producers to adopt but may only be viable if board deformation is constrained before assembly. Stress laminating may also be possible given the extensive range of large screws now available on the market (Crocetti et al., 2016).

Given the unique nature of the resource and the problem, a practical approach needs to be established where sawn boards are milled and joined into large elements by offering commercial solutions to assembling timber engineered component from plantation eucalypt into panels effectively.

Overall, drivers exist to develop higher-value structural products and corresponding applications in construction for some portion of Australia's extensive plantation hardwood resource. Repurposing the fibre-grown resource into purpose-designed timber engineered components suitable for building applications in Australia, such as structural flooring systems, to meet potential market gaps may be a solution. However, the form of the resources and their management complicates its use. Research is needed that seeks to understand and balance the technical, performance, and production issues along the supply chain: from the resource and the feedstock that may be recovered from it; through the production process in fabrication facilities of differing scale and skill level; to the products that have to provide satisfactory performance in a range of building applications.

2.5. Potential mass laminated timber products from eucalypt plantations

The use of mass laminated timber products in the construction of residential and office buildings has increased in popularity in recent years (Mohamed & Abdullah, 2014; Fink et al., 2015; Hayashi & Miyatake, 2015; Kandler et al., 2015; Ussher et al., 2017; Lu et al., 2018). Mass laminated timber products enable wide spans and can be designed and produced in a variety of sizes to suit different structural applications (Frühwald, 2001; Puettmann & Wilson, 2007; Khorasani, 2012). One of the biggest advantages of mass laminated timber products is that they enable the possibility of using structurally low-grade boards in combination with higher-grade ones. This allows for custom structural requirements in building components (Puettmann & Wilson, 2007) and could maximise the use of timber boards from lower grade levels in structural applications (Castro & Paganini, 2003). Therefore, mass laminated timber products have revolutionised the way timber could be used in building construction (Dietsch & Tannert, 2015; Scalet, 2015). Some of the most important mass laminated products currently used in building construction are outlined in the following.

GLT, also known as glulam, is one of the most popular structural timber products in building construction (Gasparri et al., 2015; Liao et al., 2017). There are varieties of timber products available in the market, however, Cross-laminated timber (CLT) and GLT are predominantly used. CLT is a mass timber product that is constructed of several layers of boards that are oriented at right angles to one another and glued together in panel form. CLT is regarded as a modern, engineered building product that has a high strength-to-weight ratio with exceptional dimensional stability and inherent fire performance (Mallo et al., 2014; Buck et al., 2016). CLT components can be prefabricated precisely and economically before installation, which results

in significant construction time saving (Gasparri et al., 2015). While CLT was developed in the early 1990s, its good seismic behavior has received particular attention during the last few years, resulting in an increase in popularity over other building materials (Pei et al., 2012; Shrestha et al., 2014; Latour & Rizzano, 2017).

Vertical GLT is also another type of glulam that is typically used as a beam or structural floor panel in buildings. The main difference between CLT and vertical GLT is the orientation of the boards in their construction. Unlike CLT, the laminations in vertical GLT is perpendicular to the short dimension of the panel's cross-section. In addition, in vertical GLT each layer (board) is oriented and glued parallel to the adjacent layer on the widest face of the boards (Figure 2. 4).

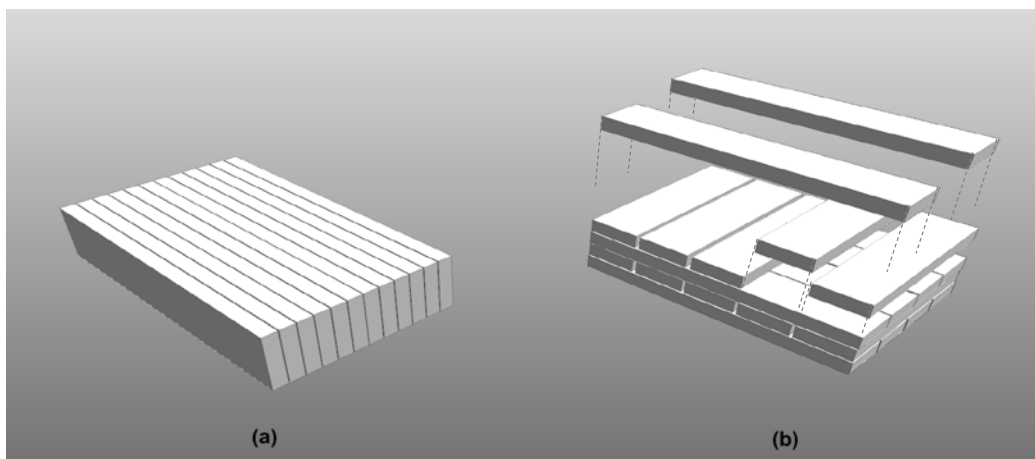


Figure 2. 4. Orientation of boards in vertical GLT (a) and CLT (b) panels.

Vertical GLT panels can also be constructed without glue by means of mechanical fasteners such as nails or screws. Although similar in shape, such a panel is no longer called GLT. If nails are used instead of glue in the construction of a vertically laminated timber panel, then the term ‘Nail-Laminated Timber’ (NLT) is used (Hong, 2017; Smith et al., 2017). Although not frequently used in practice, NLT panels can also be produced using short screws. NLT panels can be effectively adapted to use in structural flooring systems (Hong, 2017; Robertson et al., 2018).

Depending on the application, long screws or all-thread rods can be used in the construction of vertically laminated timber panels as well. Such a panel is referred to as ‘Stress-Laminated Timber’ (SLT). SLT panels are similar to NLT panels. However, instead of nailing, all the laminations are clamped and stressed together on their widest faces by means of steel stressing (all-thread) rods. One of the most important advantages of SLT panels is that they can provide

increased load transfer (Grant, 2010). This characteristic makes SLT an appropriate product for constructing timber bridge structures. The load transfer between the laminations is developed by means of friction, which is a function of the pressure that the stressing rods produce between the laminates along the length of the panel (Grant, 2010). Another important advantage of SLT is that it can also be constructed with lower-quality timber than is needed in the construction of other laminated timber products (Ritter et al., 1991).

Mass laminated timber panels can be produced with different geometries and sizes in the cross-section as well. They can be a pure timber panel, or a timber composite panel cast with concrete (Weckendorf et al., 2016; Hong, 2017). When used in structural floor systems, casting concrete on top of a mass laminated timber panel results in higher bending strength and stiffness, improved vibration behavior and acoustic separation as well as increased thermal mass and fire resistance (Yeoh et al., 2010, 2011). Such floor systems are referred to as timber-concrete composite (TCC) floors. TCC floors are normally fabricated by connecting a solid concrete slab to a timber component through shear connectors. In TCC floors, the concrete slab is designed to predominantly resist compression, whereas the timber component is designed to resist tension and bending. In such a composite system, the TCC connectors transfer shear loads between the two components. The TCC connection system must be stiff and strong enough to provide an effective composite action. When designed properly, TCC floors can benefit from the high compressive strength of concrete and the high tensile strength of timber.

Some examples of NLT and SLT panels, with and without concrete topping, are depicted in Figure 2. 5.

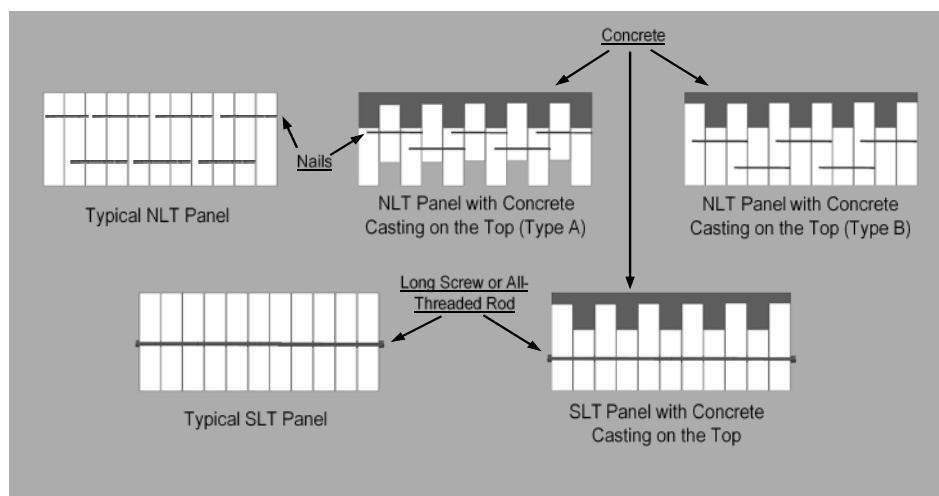


Figure 2. 5. Examples of different NLT and SLT panels (perspective view of the cross sections).

2.6. Manufacturing process of mass laminated timber products

In the following sections, all the required manufacturing steps of mass laminated timber products in general, from harvesting to the final prefabrication step, are described. Some of these steps were used in processing fibre-managed plantation eucalypt timber in this PhD research—which are described in more details in Chapter 3.

2.6.1. Harvesting and sawing of logs

While many issues are associated with the harvesting process that can affect the quality of the final product, tree selection is an important step. Unlike for pulplog production, where the logs volume could be the main consideration, tree selection for sawlog production is dependent on a range of different parameters. Among the most important parameters in tree selection for sawlog, regardless of species, are modulus of elasticity (MOE) and small end diameter of the tree (Madhoushi & Daneshvar, 2016). Non-destructive techniques can be used for measuring MOE of standing trees before harvesting using acoustic wave velocity (Farrell et al., 2012; Madhoushi & Daneshvar, 2016).

After tree selection and harvesting, due to the difference between the moisture content (MC) of the logs and the relative humidity (RH) of the environment, the logs start to lose their MC quickly. This causes end-grain checks and cracks in the cross-section of the logs. To prevent checking at the cross-section, the logs could be end-greased in the forest before transporting to the sawmill.

At modern sawmills, the logs first pass through an automated scanner to identify the best sawing pattern based on the shape and diameter of the logs. In traditional sawmills, however, this process is done by a human operator. The most common sawing patterns at sawmills are plain sawing, quarter sawing, and rift sawing (Figure 2. 6). Each sawing pattern can result in different types of boards. Timber boards can be typically classified by the grain direction at their cross sections, which is also a function of the sawing pattern.

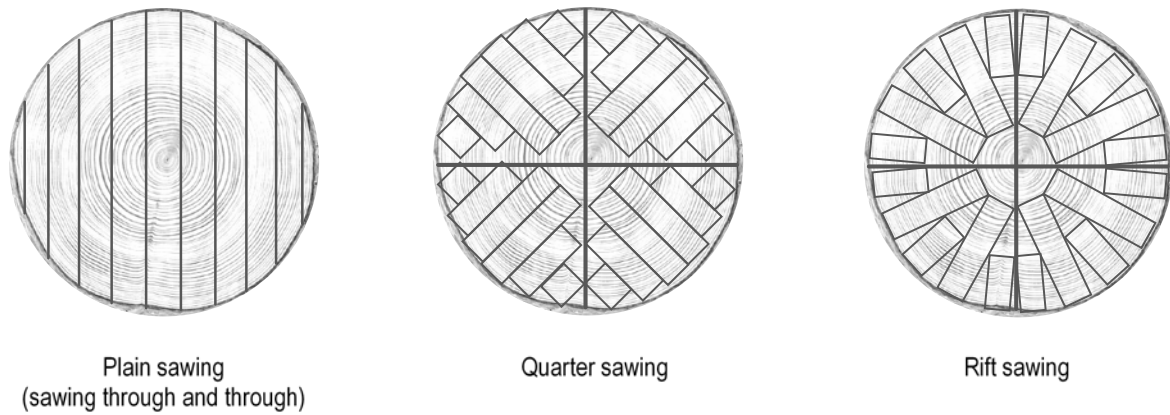


Figure 2. 6. An idealised drawing of some common timber sawing patterns.

After identifying the best sawing pattern, the logs are cut into boards by means of appropriate sawing methods. The logs can be sawn by a series of parallel saw cuts (sawing through and through) or by turning of the logs as sawing proceeds (sawing around). In the next step, another saw cuts the boards into structural sizes and the boards are then ready for the drying stage.

2.6.2. Drying of timber boards

Drying sawn boards is an important step during the manufacturing process of mass laminated timber products. Water is stored in wood in two forms: free water and cell water (or bound water). Free water is stored in the vessels (cells cavities), while bound water is stored as an integral part in the cell walls.

The mechanism of losing MC (water) in timber has two main phases (Gezici-Koç et al., 2017). In the first phase, the wood starts to lose free water as soon as the logs are cut. This phase is done slowly by air drying and is a function of RH and temperature of the environment (Gezici-Koç et al., 2017). The sawn boards need to be kept in the drying yard for several months (usually between four to 12 months for hardwoods) until the boards reach an MC value at which all the free water is removed from the vessels and released to the atmosphere. The wood at this point, which is called ‘Fibre-Saturation Point’ (FSP), normally has an MC between 25 to 30 per cent—depending on the species, the FSP range can be different.

In the second phase, the wood loses its bound water. Once the FSP is reached, the bound water is released from the wood cells. However, this phase is critical and requires a controlled environment with a higher temperature and a lower RH than the first phase. Any rapid decrease in MC below the FSP can cause adverse shrinkage in the boards, which may result in a variety

of drying defects such as end checking and surface checking. Hence, each specie should be dried using their specific drying schedule (Pleschberger al., 2013). This is usually achieved by industrial kilns where the boards can be stacked and dried effectively. Kiln drying is a conventional method for drying timber to any desired MC under the FSP. Depending on the drying schedule and the intended service conditions, the boards are usually dried in the kiln to approximately 12 ± 4 per cent.

During the kiln drying process, the boards may produce some recoverable and/or unrecoverable drying defects. Recoverable drying defects usually include deformations at the cross-section along the length of the boards, such as twist, cup, and bow. Unrecoverable drying defects include checking, end splitting, and unrecoverable collapse (Wentzel-Vietheer et al., 2013) (Figure 2. 7).



Figure 2. 7. Unrecoverable drying defects in 16-year-old unthinned and unpruned E. nitens. (a) and (b) show unrecoverable collapse, (c) shows end splitting, and (d) shows surface checking.

For collapse prone species, most companies use a re-conditioning process to recover the deformations in the boards using a high-temperature steam chamber. The deformations are usually recovered to a reasonable degree. After re-conditioning, a finishing process is followed to cut the boards to a final structural size.

2.6.3. Structural grading of boards

Visual stress-grading and machine stress-grading are the most common methods for structural grading of timber (Brunetti et al., 2016).

Visual stress-grading of timber is based on assessing the board's surfaces and detecting the SRFs such as knots, checks, end splits, slope of grain, shake, decay, and limb trace (Stapel & van de Kuilen, 2014). The boards with major SRFs normally receive a lower grade than ones with smaller or less SRFs. In this method, the SRFs can be detected by either a human operator (seen and judged by eye) or an automated SRFs scanner.

The use of machine stress-grading method is also quite widespread. Machine stress-grading is a non-destructive method of measuring the stiffness (MOE) of timber. During the stress grading process, the boards are passed through a testing machine that measures the MOE by applying a controllable amount of load along the longitudinal axis of the boards (Stapel & van de Kuilen, 2014). The load is usually applied on the face of the boards (minor axis). In some companies, a visual stress-grading process is also followed after the machine stress-grading to detect any SRF that may have negative impacts on the edgewise stiffness of the boards. The boards are then sorted based on the grade level that they receive during the grading processes.

2.6.4. End-to-end and side-to-side jointing of boards

One of the advantages of mass laminated timber products is that they could be produced in any required span lengths. To enable this, an appropriate end-to-end jointing method needs to be used to overcome any length limitation in the boards. The most commonly used technique for this purpose is finger jointing (Lara-Bocanegra et al., 2017). In this method, finger profiles (either vertical or horizontal profiles) are cut into the cross-section of the boards and then the two mating parts (board pieces) are glued and jointed together using a structural adhesive. Finger jointing is known as the most effective end jointing technique for producing mass laminated timber (Lara-Bocanegra et al., 2017). Butt joints can also be used effectively for the manufacture of NLT panels (Robertson et al., 2018).

Depending on the product type, various side-to-side jointing techniques are available to use in the production of mass laminated timber. For CLT and GLT panels, the laminations are simply jointed together by means of gluing and then pressing. For NLT and SLT type panels, the laminations are fitted and jointed together by means of mechanical fasteners such as all-thread

rods, nails, and screws. Side-to-side jointing of boards is the final step of producing mass laminated timber.

The produced mass laminated timber usually needs to go through a prefabrication process before they can be used in building construction. Prefabrication of mass laminated timber components is an offsite process that helps to eliminate high-risk site activities and reduce building construction time (Ahvenainen & Sousa, 2016). With the benefit of a panelised building construction system, the high level of prefabrication of mass laminated timber components leads to efficient, precise, and fast manufacturing and erection processes. A typical prefabrication process of mass laminated timber building elements includes an offsite digital design and then pre-cut to manufacture the timber elements. After pre-cutting, the prefabricated mass laminated timber components are ready to be transported and installed on site effectively (Ramage et al., 2017).

2.7. Key studies on mass laminated timber from fibre-managed eucalypt plantations

Several previous studies were aimed at developing sawn timber and structural/non-structural elements from plantation eucalypt resources (e.g., Reid & Washusen, 2001; Piter et al., 2007; Washusen et al., 2009; Carrasco et al., 2013; Franke & Marto, 2014; Zitto et al., 2014; Christoforo et al., 2015; Satchell, 2015; Petruski et al., 2016; Underhill, 2016; Dugmore, 2018; Majano-Majano et al., 2019). In most of these studies, however, either the target resources were sawlog plantations or the source of the timber has not been indicated (sawlog plantation vs pulplog plantation). Available information on the performance of fibre-managed plantation eucalypt species (i.e., pulpwood eucalypt) in the construction of mass laminated timber is limited to only a few previous studies that are discussed and highlighted in the following.

The feasibility of producing CLT from fast-grown small-diameter eucalypt (*Eucalyptus urophylla* × *Eucalyptus grandis*) was evaluated by Liao et al. (2017). These researchers investigated the impacts of various parameters, including adhesive spread rate, pressing pressure, and pressing time duration, on the shear strength, percentage of wood failure, and delamination rate of CLT. It was found that the mechanical characteristics of eucalypt CLT were comparable to those of commercially available CLT from softwood. It was also concluded that CLT from fast-grown small-diameter eucalypt (*Eucalyptus urophylla* × *Eucalyptus grandis*) is promising for structural purposes.

Although producing CLT from plantation eucalypt was reported to be feasible by Liao et al. (2017), Lu et al. (2018) indicated that “*eucalyptus bonded with commercial one-component polyurethane adhesive usually provides poor resistance to delamination and shear force*”. These researchers studied the impacts of adhesive type and priming surface of eucalypt CLT layers on shear strength, percentage of wood failure, and delamination rate of CLT made of small-diameter eucalypt at both dry and wet states. The results of this study indicated that the properties of eucalypt CLT were comparable to those of commercial softwood CLT. It was found that priming treatment using hydroxymethylated resorcinol was effective to improve the bond performance and mechanical characteristics of CLT made of small-diameter eucalypt.

Dugmore et al., (2019) studied the bonding quality of CLT made of fibre-managed *Eucalyptus grandis* (*E. grandis*) timber. These researchers concluded that *E. grandis* CLT made with one-component polyurethane adhesive can obtain a good bonding quality with the right processing variables (i.e., clamping pressure and stress relief grooves). They also demonstrated that the bonding quality of *E. grandis* CLT is affected significantly by wood density.

Lara-Bocanegra et al. (2017) indicated that “*Eucalyptus globulus is one of the hardwood species growing in Europe with the best mechanical properties and great natural durability*”. These researchers aimed to develop high performance *E. globulus* finger-joints using one-component polyurethane adhesive for the construction of engineered laminated hardwood products. The effects of failure modes, MOE and density of wood, geometric parameters, and assembly pressure on the finger-joint bending strength were evaluated. These researchers demonstrated that high performance finger-joints can be obtained from *E. globulus* to produce engineered laminated products using one-component polyurethane adhesive.

Pröller et al. (2018) reported that green edge-gluing of plantation *Eucalyptus grandis* timber could be an appropriate solution to overcome drying distortions in the use of sawn boards from such a resource, making it a more appropriate resource for mass laminated timber production.

In a recent research project at the University of Tasmania, Pangh et al. (2019) evaluated the bending performance of three-ply CLT panels made of fibre-managed plantation *E. nitens* and *E. globulus*. These researchers indicated that “*Due to the high volume of available plantation eucalyptus resources, there is an opportunity to test the properties of these plantation species to identify the potential for streamlining some of the resource into value added structural applications for the Australian construction and building industry*”. They demonstrated that *E.*

globulus CLT has a higher bending capacity than *E. nitens* CLT. These researchers also demonstrated that the bending capacity of the CLT panels were meaningfully affected by the stress-grade of the boards used. Based on the failure modes observed, they indicated that the adhesion properties of the two plantation timber species are determining factor in the overall bending capacity of the CLT panels.

Given the results of the above studies, gluing of the boards recovered from fibre-managed eucalypt plantations is associated with important challenges. This is predominantly due to the multiplicity of SRFs and drying defects such as unrecoverable collapse in the timber that can influence its bond quality. In addition, the poor adhesive penetration, high internal stress, and high proportion of juvenile wood contributes to the poor bond quality of the timber recovered from such plantation resources (Lu et al., 2018). The challenges associated with gluing of the boards from fibre-managed plantation eucalypt resources may suggest that producing mass laminated timber using mechanical fasteners, such as NLT, might be a better solution. NLT is a mechanically laminated product and its structural performance is independent of the adhesion properties of the timber species used.

Despite the above studies, there is no information available on the performance of Australian fibre-managed plantation eucalypt in mass laminated timber production. The available information to date is related to producing sawn timber (Washusen et al., 2000, 2004; Hamilton, 2007; Blackburn et al., 2010, 2011, 2014; Farrell et al., 2012) and veneer-based products (McGavin et al., 2015; Blackburn et al., 2018) from these plantation resources. More details related to the previous studies on the topic are given in relevant papers in the Appendices.

2.8. Summary

Overall, opportunities exist in developing higher-value structural mass laminated timber products from fibre-managed eucalypt plantations that can add value to and create new markets for these plantation resources. Such a product development, however, is associated with important challenges that need to be investigated and properly addressed. The potential challenges include the recovery rate of useable boards, issues related to timber processing (especially grading), natural and drying defects, low adhesion performance, and the lack of knowledge on short-term and long-term mechanical performance of timber from these plantation resources. Most of these challenges have been discussed and addressed in the

experimental investigations in this thesis.

Chapter 3: Methodology

3.1. Introduction

In this chapter, the methodology used in the thesis is described in three sections. The procedures used for harvesting and processing of the required plantation *E. nitens* and *E. globulus* logs are described. Information related to the mapping of the research problem are presented. The experimental investigations in the thesis are then described in three phases. More details related to the methods used in each experimental phase are included in their relevant papers in Appendices.

3.2. Harvesting and processing the required plantation eucalypt logs

The *E. nitens* and *E. globulus* logs in this PhD research were harvested from two fibre-managed plantation sites in the north of Tasmania. Both resources were unthinned and unpruned. The plantation *E. nitens* resource was 16 years old and the plantation *E. globulus* resource was 26 years old. The plantation sites were managed by Forico Pty Limited, which is the largest private forestry management company in Tasmania. The harvesting operation was performed in 2016. Approximately 29 m³ butt logs with an average length of 5500 mm were obtained for each species. The logs were processed using conventional timber processing facilities that are used for processing logs from native forests. The logs were sawn using the plain sawing method described in section 2.6.1. After sawing of the logs, the recovered boards were stored in a local mill yard for two months and then dried in an industrial kiln. The boards were then passed through a finishing step and shipped to the laboratory for testing processes. The finished boards had a nominal thickness of 35 mm. The nominal widths of the boards were 70 mm, 90 mm, 120 mm, and 140 mm. The lengths of the boards used for each experimental step of this thesis are described in the relevant paper.

E. nitens and *E. globulus* are respectively the most widely planted hardwood species in Tasmania and Australia—which is why they were selected for this research. The difference in the age of the two resources (i.e., 16 years old versus 26 years old) could create some insight into whether a longer rotation harvest cycle can improve the wood quality of the fibre-managed

plantation eucalypt resources.

3.3. Mapping the research problem

To properly establish a research strategy, a list of key research and previous studies relevant to the topic of this thesis was created—the most important ones are presented in Chapter 2 and the rest are given in relevant papers in the Appendices. The findings of the previous studies on the use of structurally low-grade timber of fibre-managed plantation *E. nitens* in engineered wood products were analysed. With a focus on fibre-managed plantation eucalypt resources, the investigations into issues associated with the use of fast-growing wood species in producing mass laminated timber building components were reviewed. Current claims and standards for the performance of mass laminated timber floor systems were analysed. Finally, based on the reviewed literature and the results of previous studies, different options for developing and evaluating mass laminated timber from plantation *E. nitens* were identified. NLT was selected as the target product to be investigated in this thesis. NLT is a mechanically laminated product and, unlike CLT and GLT, its strength and stiffness are independent of the adhesion properties of the timber used. This could enable the use of highly featured (low-grade) timber without any pre-thicknessing processes—which are usually required for producing CLT and GLT from hardwood (Lu et al., 2018). NLT production requires no high-tech equipment or necessarily unique manufacturing facilities and can be even produced locally in a variety of sizes to suit different structural applications.

3.4. Development of research plan and experimental investigations

The experimental investigations were conducted in three phases. Each phase had several experimental programs that are described in the following.

The first phase was generally aimed to study the effectiveness of conventional timber processing regimes, including harvesting, sawing, drying and visual stress-grading, on fibre-managed plantation *E. nitens* timber. It aimed to determine if the fibre-managed plantation *E. nitens* can be properly processed to produce sawn boards useable for NLT production. This phase was started by identifying and characterising major SRFs and processing defects of plantation *E. nitens* boards through inspection and measurement processes. After identifying the major SRFs, the impacts of these features on the bending strength and stiffness of the boards were evaluated by means of four-point bending test. Considering the results obtained, a series of target-based rules were introduced to improve the performance of visual stress-grading of

plantation *E. nitens* boards. The above-mentioned experiments, except visual stress-grading, were also applied on the fibre-managed plantation *E. globulus* boards to create a basis for comparison with the plantation *E. nitens*. The performance of different non-destructive techniques, including Artificial Neural Network modelling and acoustic wave velocity measurement, in predicting the bending strength and stiffness of the plantation *E. globulus* timber was also investigated. Another aim of this phase was to create a profile of material characteristics for the plantation *E. nitens* timber. The static bending properties, compressive, tensile, and shear strengths, cleavage, impact bending, and hardness of the plantation *E. nitens* timber were studied using small clear wood samples. The profile of material characteristics of the plantation *E. nitens* timber was established based on the test results. The results obtained from the first phase are given in Paper II, Paper III, and Paper IV.

The second phase of the experiments was aimed to find the best panel configurations for producing NLT from the plantation *E. nitens* timber. Different panel construction methods including timber-only and timber-concrete floors were investigated. The best panel configurations were identified through testing short-term bending moment capacity and vibration of the panels based on the relevant standard requirements. The same testing program was also applied on the plantation *E. globulus* timber to create a basis for comparison with the plantation *E. nitens*. The results obtained from the second phase are given in Paper V.

The third phase of the experiments was aimed to optimise the properties of NLT panels based on the relevant issues discovered in the second phase. The selected panel configuration was optimised through developing appropriate timber-concrete connections and a lamination system that can customise the bending properties and maximise the use of lower-grade boards in NLT production. This phase also aimed to investigate the long-term bending creep behavior of the NLT panels under uniformly distributed loads based on Australian Standard. The impacts of structural grade of timber and environmental conditions (temperature and RH) on the bending creep deflection of the NLT panels made of plantation *E. nitens* were studied. The results obtained from the third phase are given in Paper VI and Paper VII.

Finally, as provided in Chapter 5, a set of conclusions were developed based on the results obtained in the three phases. Potential solutions to the problems that arose during harvesting, sawing, drying, and grading processes of fibre-managed plantation eucalypt timber were proposed. Considering both effectiveness and efficiency factors, a series of recommendations were provided for developing NLT floor products from fibre-managed eucalypt plantations.

3.5. Summary

This chapter described the methodology employed towards answering the thesis's questions. The information related to the harvesting and processing of the timber species used was provided and the experimental investigations performed in this thesis were described in three phases. More details related to these experiments as well as the results obtained and their analyses are provided in seven papers that are introduced in Chapter 4.

Chapter 4: Research contributions

4.1. Introduction

This chapter introduces the seven papers included in this thesis and provides information on how the thesis's questions were addressed through the presentation of these papers. Papers I, II, III, IV, V, and VII have been published. Paper VI is under review for publication by an international journal. The statement of co-authorship, title, publication status, and descriptions of the aims of each paper are provided. The papers in their entirety are located in Appendices. The full text of these papers is replicated in the same submission format required by the relevant journal—with minor changes in their text font consistent with the font used in the text of this thesis.

4.2. How the research questions were addressed

Paper I is an editorial piece that discussed drivers, opportunities, and challenges associated with developing mass laminated timber products from fibre-managed plantation eucalypt timber. It described the plantation eucalypt estate and their uses in Australia and possible challenges associated with processing (i.e., sawing, drying, and grading) of the timber recovered from such plantation resources. It then described different product options from fibre-managed plantation eucalypt timber and established the main foundation for this PhD research. The research plans in this thesis were developed based on the initial discussions presented in this paper. Parts of the text of this paper were included in Chapter 2.

Papers II, III, and IV are original research articles, which reported the visual, physical, and mechanical characteristics of fibre-managed plantation eucalypt timber and ways in which these characteristics are affected by different parameters. These papers addressed the first research question of this thesis on “*Are conventional timber processing regimes (harvesting, sawing, drying, and visual stress-grading) appropriate to produce sawn boards, suitable for NLT production, from fibre-managed eucalypt plantations?*” and parts of the second research question (related to sawn timber) on “*Do timber sawn from fibre-managed plantation *E. nitens* and NLT floor panels assembled from this resource have satisfactory short-term structural*

properties especially when compared to the performance of other species?”.

When a plantation resource that is managed to produce pulplog is going to be considered as a sustainable raw material for mass laminated timber production, there is a need to make sure that the logs harvested from such a resource can be properly processed to produce useable sawn timber boards. This plays a major role in determining the efficiency and potential profitability of using such a resource. Prior to this PhD research there was a gap in the knowledge in this area that needed to be appropriately explored before any effective structural product can be developed from such a plantation resource.

The investigations reported in Paper II were aimed to evaluate the effectiveness of visual stress-grading and conventional harvesting, sawing, and drying procedures on fibre-managed *E. nitens* plantation. The most common natural and processing SRFs and defects of the boards were identified and their influence on the flexural properties of the boards were examined. The results of this experimental work on the characteristics of the timber influenced the development of an appropriate NLT floor system in the next stages of this PhD research.

Paper III described the recovery rate, flexural properties, and visual characteristics of sawn fibre-managed plantation *E. globulus* to create a basis for comparison with *E. nitens*—which was an objective of the second research question of this thesis. This paper also reported on the effectiveness of conventional timber processing regimes and ways in which different parameters may influence the flexural properties of sawn fibre-managed plantation *E. globulus*. The effectiveness of different non-destructive methods for predicting the bending properties of plantation *E. globulus* boards were also reported. The experiments reported in this paper used the same testing methods developed in Paper II to evaluate the visual characteristics, natural and processing defects, basic density, and bending properties of the boards. The aim was to investigate how the measured characteristics differ between *E. globulus* and *E. nitens* timber reported in Paper II.

The investigations reported in Paper IV were performed to characterise the physical and mechanical properties of small clear wood samples from fibre-managed plantation *E. nitens* timber. The aim was to create a profile of physical and mechanical properties of plantation *E. nitens* timber and investigate ways in which various parameters influence these properties. This has been done by testing small clear wood samples obtained from six different *E. nitens* logs. The studied mechanical properties included static MOE and modulus of rupture (MOR), shear,

compressive, and tensile strengths, impact bending, cleavage, and hardness. This experimental work was performed to identify the strengths and weaknesses of the plantation *E. nitens* timber and to see how the properties of the timber compare to other species.

Paper V is an original research article that addressed the remaining parts of the second research question (related to NLT panels) on “*Do timber sawn from fibre-managed plantation E. nitens and NLT floor panels assembled from this resource have satisfactory short-term structural properties especially when compared to the performance of other species?*” and the third research question on “*How can the configuration of NLT floor panels assembled from sawn fibre-managed plantation E. nitens be optimised to improve their short-term and long-term structural performances?*”.

After discovering the challenges in processing, grading, and characterisation of the plantation *E. nitens* timber in Papers II to IV, the investigations reported in Paper V were aimed to produce and determine the short-term bending capacities of NLT and NLT-concrete floor panels from such plantation resources. The panels were made using conventional construction systems with randomly selected timber boards from both plantation *E. nitens* and *E. globulus*. The conventional screw-type shear connectors were used to produce the NLT-concrete panels. All the NLT and NLT-concrete panels were subjected to both vibration and four-point bending tests. The properties of the panels were verified against the limit state design requirements for serviceability and bending strength of structural floor systems in both residential self-contained dwelling and office buildings. These properties were compared to those of commercially available mass laminated timber products reported in the literature.

Papers VI and VII are original research articles aimed to optimise the construction of the NLT and NLT-concrete panels to improve their structural performances based on the results obtained in the experimental investigations reported in Paper V. Papers VI and VII addressed the third research question of this thesis on “*How can the configuration of NLT floor panels assembled from sawn fibre-managed plantation E. nitens be optimised to improve their short-term and long-term structural performances?*”.

One of the most important issues discovered and discussed in Paper V was the low structural efficiency of the conventional screw-type shear connectors used in the construction of the NLT-concrete floor panels. The use of a shear connector with a higher structural efficiency will result in floor panels with higher strength/stiffness and better vibration behavior. This enables the

possibility of using such a product in long span floor systems. Therefore, the investigations reported in Paper VI were aimed to optimise the structural capacity of the NLT-concrete elements made of plantation *E. nitens* timber by developing and utilising more appropriate shear connection systems. Several types of different timber-concrete connection systems were examined to find the best solution to use in NLT-concrete floor panels made of plantation *E. nitens* timber. In the development of such connections, specific criteria were considered with respect to structural performance and the cost and ease of manufacture.

As reported in Paper V, when timber boards are randomly nail-laminated together, the resulting NLT panels will have a relatively high variability in their structural performances. Furthermore, even though the test panels showed an appropriate structural capacity under short-term loading conditions, their performance under sustained loads remained unknown. Therefore, the aim of Paper VII was to optimise the NLT panels made of plantation *E. nitens* timber by developing a lamination system that can reduce the variabilities in the bending performance of NLT panels and maximise the use of low-grade boards in the construction of such products. The bending performance of *E. nitens* NLT panels were examined under both short-term and long-term loads. The effectiveness of visual stress-grading method in the development of the NLT panels and the influence of environmental conditions on the long-term bending creep deflection of the panels were also evaluated and discussed.

4.3. Statement of co-authorship

The following people and institutions contributed to the publication of work undertaken as part of this thesis:

Candidate	Mohammad Derikvand, Australian Research Council, Centre for Forest Value, University of Tasmania, Australia
Author 1	Gregory Nolan Centre for Sustainable Architecture with Wood (CSAW), University of Tasmania, Australia, Primary supervisor
Author 2	Nathan Kotlarewski, Australian Research Council, Centre for Forest Value, University of Tasmania, Australia, Co-supervisor
Author 3	Hui Jiao School of Engineering, AMC, University of Tasmania, Australia, Co- supervisor
Author 4	Andrew Chan School of Engineering, AMC, University of Tasmania, Australia, Co- supervisor
Author 5	Michael Lee Centre for Sustainable Architecture with Wood (CSAW), University of Tasmania, Australia

Author details and their roles:

Paper I, Derikvand, M., Nolan, G., Jiao, H., & Kotlarewski, N. (2016). What to do with structurally low-grade wood from Australia's plantation eucalyptus; building application?. *BioResources*, 12(1), 4-7.

Authors and their roles: The candidate was the primary author of this paper with 80% contribution. Author 1, Author 2, and Author 3 contributed respectively 10%, 5%, and 5% to the text of this paper.

Paper II, Derikvand, M., Kotlarewski, N., Lee, M., Jiao, H., Chan, A., & Nolan, G. (2018). Visual stress grading of fibre-managed plantation Eucalypt timber for structural building applications. *Construction and Building Materials*, 167, 688-699.

Authors and their roles: The candidate was the primary author of this paper with 80% contribution who conceptualised the research presented in the paper, performed the literature review, developed the methodology, conducted the experimental investigations and the data analysis, and prepared the original draft paper. Author 1, Author 2, Author 3, Author 4, and Author 5 (4% contribution each) provided supervision, technical expertise, and collaborated with the candidate in optimising the concept and methodology of the work and editing the draft paper.

Paper III, Derikvand, M., Kotlarewski, N., Lee, M., Jiao, H., & Nolan, G. (2018). Flexural and visual characteristics of fibre-managed plantation Eucalyptus globulus timber. *Wood Material Science & Engineering*, 1-10.

Authors and their roles: The candidate was the primary author of this paper with 80% contribution who conceptualised the research presented in the paper, performed the literature review, developed the methodology, conducted the experimental investigations and the data analysis, and prepared the original draft paper. Author 1, Author 2, Author 3, and Author 5 (5% contribution each) provided supervision, technical expertise, and collaborated with the candidate in optimising the concept and methodology of the work and editing the draft paper.

Paper IV, Derikvand, M., Kotlarewski, N., Lee, M., Jiao, H., & Nolan, G. (2019). Characterisation of Physical and Mechanical Properties of Unthinned and Unpruned Plantation-Grown Eucalyptus nitens H. Deane & Maiden Lumber. *Forests*, 10(2), 194.

Authors and their roles: The candidate was the primary author of this paper with 80% contribution who conceptualised the research presented in the paper, performed the literature review, developed the methodology, conducted the experimental investigations and the data analysis, and prepared the original draft paper. Author 1, Author 2, Author 3, and Author 5 (5% contribution each) provided supervision, technical expertise, and collaborated with the candidate in optimising the concept and methodology of the work and editing the draft paper.

Paper V, Derikvand, M., Jiao, H., Kotlarewski, N., Lee, M., Chan, A., & Nolan, G. (2019). Bending performance of nail-laminated timber constructed of fast-grown plantation eucalypt.

European Journal of Wood and Wood Products, 1-17.

Authors and their roles: The candidate was the primary author of this paper with 75% contribution who conceptualised the research presented in the paper, performed the literature review, developed the methodology, conducted the experimental investigations and the data analysis, and prepared the original draft paper. Author 1, Author 2, Author 3, Author 4, and Author 5 with 5% contribution each provided supervision, technical expertise, and collaborated with the candidate in optimising the concept and methodology of the work, conducting the experimental investigations, and editing the draft paper.

Paper VI, Derikvand, M., Kotlarewski, N., Lee, M., Jiao, H., Chan, A., & Nolan, G. Timber-concrete composite connections for hybrid nail-laminated timber floor systems. Under review.

Authors and their roles: The candidate was the primary author of this paper with 80% contribution who conceptualised the research presented in the paper, performed the literature review, developed the methodology, conducted the experimental investigations and the data analysis, and prepared the original draft paper. Author 1, Author 2, Author 3, Author 4, and Author 5 with 4% contribution each provided supervision, technical expertise, and collaborated with the candidate in optimising the concept and methodology of the work, conducting the experimental investigations, and editing the draft paper.

Paper VII, Derikvand, M., Kotlarewski, N., Lee, M., Jiao, H., Chan, A., & Nolan, G. (2019). Short-term and long-term bending properties of nail-laminated timber constructed of fast-grown plantation eucalypt. *Construction and Building Materials*, 211, 952-964.

Authors and their roles: The candidate was the primary author of this paper with 80% contribution who conceptualised the research presented in the paper, performed the literature review, developed the methodology, conducted the experimental investigations and the data analysis, and prepared the original draft paper. Author 1, Author 2, Author 3, Author 4, and Author 5 with 4% contribution each provided supervision, technical expertise, and collaborated with the candidate in optimising the concept and methodology of the work, conducting the experimental investigations, and editing the draft paper.

We the undersigned agree with the above stated “proportion of work undertaken” for each of the above published (or submitted) peer-reviewed manuscripts contributing to this thesis:

Signed

Candidate: 29/04/2019

Author 1: 10/04/2019

Author 2: 10/04/2019

Author 3: 11/04/2019

Author 4: 10/04/2019

Author 5: 10/04/2019

Primary supervisor and head of school declaration

Professor Gregory Nolan

Primary supervisor

Centre for Sustainable Architecture with Wood

University of Tasmania

Date: 10/04/2019

Professor Mark Hunt

Head of School

School of Science and Technology

University of Tasmania

Date:

4.4. Summary

In this chapter, the relations between the thesis's questions described in Chapter 1 and the research papers included in this thesis were described. A clear statement of co-authorship and details related to the title, aim, and publication status of the papers were then provided. The PhD candidate was the primary author and writer in these papers with the highest contribution. While each of these papers include their own discussion and conclusion sections, all the findings are drawn together with clear statements concerning the findings in the next chapter as per the University of Tasmania's *Guidelines for Incorporating Publications into a Thesis*.

Chapter 5: Discussion and conclusions

5.1. Introduction

This chapter discusses and concludes the main findings of the research papers included in this thesis and ways in which they have answered the thesis's questions. Recommendations for future research are also provided in a separate section to further extend the knowledge around fibre-managed eucalypt plantations and potential structural product development from such resources.

5.2. Producing sawn timber from plantation *E. nitens* pulplog and related challenges

Within the objectives of Paper II and Paper III, the visual characteristics and recovery rate of sawn boards as well as the effectiveness of conventional timber processing regimes (i.e., harvesting, sawing, drying, and grading) on plantation *E. nitens* and *E. globulus* were determined. These findings provided answers to the first and parts of the second research questions of this thesis (related to sawn timber) outlined in Chapter 1.

Based on the results obtained, it could be concluded that the recovery rate of sawn boards with high structural grade from these plantation resources is relatively low, especially for *E. nitens* that was 10 years younger than the *E. globulus*. The use of such plantation resources in structural products, such as NLT panels, is therefore challenged with the low recovery rate of useable sawn boards. To make it an economically viable procedure, solutions are of interest to the timber industry that can maximise the use of lower-grade boards in the construction of such structural products.

The current visual stress-grading method described in AS 2082 (2007) was found to be unsuitable for structural grading of fibre-managed plantation *E. nitens* timber. This could be due to the high variation in the density (which is not visually measurable) and therefore the mechanical properties of the resource. In addition, the current visual stress-grading method does not directly consider localised variation in the grain orientation of the boards—although it was found to have a significant influence on the bending properties of the plantation *E. nitens*

timber. The grading rules in the future should consider localised variation in the grain orientation directly as a grade-determining parameter. Overall, the findings of this study indicated that alternative structural grading methods must be developed for this plantation resource before it can effectively be used in any structural products. Machine stress-grading could be a potential method for grading plantation *E. nitens* timber, which can provide more accurate estimate of the actual grade of the boards than visual stress-grading. Numerical models developed using Artificial Neural Networks could also be used to improve the accuracies of a potential grading method for such plantation resources. Artificial Neural Network models have shown a good performance in predicting the MOE and MOR of plantation *E. globulus* timber using visual characteristics (as presented in Paper III). The log dynamic MOE also showed moderate significant correlations with the MOE of the boards. The log dynamic MOE can be used as a tool to segregate and select plantation eucalypt logs appropriate for sawn board production.

The sawn timber boards recovered from the two plantation eucalypt resources had significant number of knots and knotholes—which could be considered as the main natural SRFs of the resources. The most frequent processing defects of plantation *E. nitens* and *E. globulus* were found to be mechanical damages from debarker and sawing processes. These damages appeared on a significant number of sawn boards during the manufacturing process. Some other important defects, which arose during the drying of the sawn boards, were unrecoverable collapse, end split, surface checking, and drying distortion. These characteristics of sawn boards from fibre-managed eucalypt plantations will influence the development of any structural products from these resources. Unrecoverable collapse and surface checking could present challenges in producing a product that requires a timber resource with good adhesion properties—as these defects may influence the bond quality in such products (Darmawan et al., 2015). Unrecoverable collapse did not appear to have any important influence in the production of NLT panels (manufactured and tested in Paper V)—which is a product that uses mechanical fasteners (nails) instead of glue.

In general, fibre-managed plantation *E. nitens* and *E. globulus* logs can be processed to produce sawn timber boards with a nominal recovery rate of 25.8% for *E. nitens* and 31.8% for *E. globulus*. It can be concluded, however, that the conventional timber processing regimes applied did result in some considerable processing defects in the recovered boards. This can suggest some new topics for future research aiming to optimise these processes for

manufacturing higher-quality sawn boards from fibre-managed plantation eucalypt resources.

5.3. Physical and mechanical properties of plantation *E. nitens* sawn timber

To address parts of the second research question of this thesis (related to sawn timber), a profile of material characteristics of sawn fibre-managed plantation *E. nitens* was created through experimental investigations.

In several parts of this thesis, in Paper II, Paper IV, Paper V, and Paper VI, the density of the sawn fibre-managed plantation *E. nitens* was determined. It could be concluded that there is a high variation in the density of the plantation *E. nitens* timber. As most mechanical properties were highly correlated to the density (see Paper IV), such a high variation in the density can influence the accuracy of any structural grading method that relies on density as a grade determining parameter—such as the visual stress-grading method tested in this PhD research. The density of plantation *E. globulus* timber boards was also determined in Paper III. The density of the plantation *E. globulus* timber (498.3 kg/m³ reported in Paper III) was only slightly higher than that of the plantation *E. nitens* timber (480.6 kg/m³ reported in Paper II).

The bending MOE and MOR of the plantation *E. nitens* and *E. globulus* sawn boards were determined in Paper II and Paper III, respectively. The plantation *E. globulus* timber had 4.6 % higher MOE and 6.1 % higher MOR than the plantation *E. nitens* timber. Such differences were only minor—even though the *E. globulus* resource was 10 years older than the *E. nitens* resource. It must be noted, however, that the timber boards tested in this thesis were a limited representation on a large resource and the results obtained only indicate what can be expected in the whole resource.

In Paper IV, the profile of physical and mechanical properties of the plantation *E. nitens* timber was created that can be used as a reference for performing numerical modelling on any potential structural products from this resource. This included bending MOE (10.38 GPa) and MOR (53 MPa), shear strength parallel (5.5 MPa) and perpendicular to the grain (8.5 MPa), compressive strength parallel (42.8 MPa) and perpendicular to the grain (4.1 MPa), tensile strength perpendicular to the grain (3.4 MPa), impact bending (23.6 J/cm²), cleavage (1.6 kN), and Janka hardness (23.2 MPa).

5.4. Structural performance of plantation *E. nitens* NLT panels

In this section, the results related to the structural performance of timber-only NLT panels from

plantation *E. nitens* timber are discussed. The short-term structural performance of plantation *E. nitens* NLT panels was determined and compared to that of plantation *E. globulus* NLT panels in Paper V. The long-term bending performance of plantation *E. nitens* NLT panels was also determined in Paper VII. The findings related to the short-term and long-term performances of plantation *E. nitens* NLT panels contributed to providing answers to the second and the third research questions of this thesis (related to NLT panels).

The results obtained suggest that, for span lengths up to 3600 mm, the short-term stiffness and strength of the plantation *E. nitens* NTL panels are well beyond the limit state design requirements for structural floor systems in both office and residential buildings. No important difference was found between the stiffness of the *E. nitens* NLT panels with that of the *E. globulus* ones. This result could be due to the fact that the boards used in the construction of these panels were randomly selected from ungraded boards. The MOR of the *E. globulus* NLT panels, however, was higher than that of the *E. nitens* panels. The MOE and MOR of the NLT panels constructed of the two plantation species were superior to those of some commercially important mass laminated timber products reported in the literature. The fundamental natural vibration frequency values of the NLT panels from both species with span length of 3300 mm were above the recommended minimum range of 8-10 Hz for residential and office floors. The two plantation timber species demonstrated appropriate short-term bending performances to be used in the construction of structural floor systems.

The long-term bending creep deflection of the *E. nitens* NLT panels (reported in Paper VII) was highly correlated to the daily variations in the RH of the environment and the structural grade of the boards used. The predicted bending creep deflection of the panels using a nonlinear regression model developed in Paper VII showed that the panels with span lengths up to 3600 mm are highly likely to still meet the serviceability requirements for deflection after 50 years at service.

5.5. Methods for optimising plantation *E. nitens* NLT panels

Methods for improving the structural capacity of plantation *E. nitens* NLT panels were examined in Paper V, Paper VI, and Paper VII. These included addition of a concrete slab to the NLT panels (Paper V), development of innovative timber-concrete connections (Paper VI), and utilisation of a lamination system that can customise the bending performance of the panels (Paper VII). The findings of these papers provided answers to the third research question of

this thesis on “*How can the configuration of NLT floor panels assembled from sawn fibre-managed plantation *E. nitens* be optimised to improve their short-term and long-term structural performances?*”.

The results reported in Paper V indicated that the addition of a concrete slab to the NLT panels improves their structural bending performance. Under the limit state design loads, all the NLT-concrete panels from both *E. nitens* and *E. globulus* were still in the linear-elastic range up to 4600 mm span length. The vibration behavior of the NLT panels also improved by adding the concrete slab. However, when the span length increased from 3300 mm to 4600, the fundamental natural vibration frequency of the NLT-concrete panels decreased significantly. The fundamental natural vibration frequency of the panels with 4600 mm span length was only marginally above the recommended range of 8-10 Hz. The structural efficiency of the conventional screw-type shear connectors used in the construction of the NLT-concrete panels was also relatively low. This problem was discussed further in Paper VI.

In Paper VI, six types of different timber-concrete connections were developed and tested for the NLT-concrete elements. An innovative connection system comprised of two steel plates welded together with a reinforcing bar showed 2.3 times more shear strength and 2.9 times more stiffness than the screw-type shear connectors used in the construction of NLT-concrete panels in Paper V. This connection system can be used in the construction of *E. nitens* NLT-concrete floor panels to improve their structural capacity and enable the possibility of span lengths longer than 4600 mm.

Apart from the connection type, another way to improve the structural performance of the NLT panels is to customise the construction of the NLT component itself to meet specific level of structural capacity. In Paper V, it was observed that manufacturing NLT panels using randomly selected boards will result in a relatively high variation in the properties of the panels. A new lamination system was therefore developed in Paper VII to overcome this problem. This lamination system uses lower-grade and higher-grade boards, with known MOE, in an alternate arrangement resulting in more consistent bending performances. Using this lamination system, specific stiffness levels can be targeted for NLT panels during the manufacturing process. Based on the results, the targeted stiffness values were more than 97% close to the actual stiffness of the NLT panels in the end.

It was demonstrated that the presented lamination system can maximise the use of lower-grade

boards in NLT production. The use of such a lamination system in producing NLT from fibre-managed *E. nitens* plantation can represent a solution to the low recovery rate of high-grade boards from this resource.

It was also demonstrated that the structural grade of the boards has a significant influence on the stiffness of the NLT panels. As reported in Paper VII, the current visual stress-grading method was incapable of accurately estimating the actual MOE of the *E. nitens* boards. The MOE of *E. nitens* NLT panels, therefore, cannot be properly estimated based on the visual stress-grading results. A highly accurate prediction of the MOE of *E. nitens* NLT panels manufactured using the presented lamination system can be made by linear regression models when the actual MOE of the boards is used as the regressor. This suggests that a grading system that can give a close estimate of the actual MOE of the boards would be preferable to use in the production of NTL panels with predictable structural capacity and less variable structural performance.

5.6. Recommendations for future research

Considering the results obtained in this PhD research, several subjects can be recommended for future research aimed at developing structural products from fibre-managed eucalypt plantations.

The use of timber in any structural application requires a good estimate of their structural capacity, which is achievable using an appropriate grading system. While the current Australian visual stress-grading method is shown to be unreliable on plantation *E. nitens* timber, machine stress-grading of this resource might represent some potential. This will require performing relevant trial on a considerably large sample size to provide a reliable reference that the timber industry can utilise for their product development.

For the development of any structural grading method, the allowable design stress values of the timber are mandatory. These values must be obtained by testing a large sample size of timber obtained from different sites and trees of different characteristics to take into account the possible variability in the properties between trees and plantation sites.

Another important area that requires further development is drying. There were several issues arising during the drying process of the plantation *E. nitens* timber, such as unrecoverable collapse, distortions, and checking. These issues could be addressed in future research aiming

at producing a more effective drying schedule for such plantation resources.

It could be also suggested to future research to study the structural capacity of NLT-concrete panels from the plantation *E. nitens* resources using longer span lengths—as it was observed that with increased span length the serviceability of the panels could be challenged. Such panels can be manufactured using the proposed timber-concrete connections in this thesis to study their composite efficiency as well.

5.7. Epilogue

Providing a general guidance for the timber industry, the findings of this PhD research have explored ways in which producing alternative structural NLT products can add value to plantation eucalypt resources in Australia that are currently being managed to produce woodchips—a low-value commodity export. The results obtained have contributed to creating new knowledge in the areas related to sawn timber production, structural grading, and production and optimisation of NLT from fibre-managed eucalypt plantations. Practical methods have been developed in this PhD research that can be used in NLT production from such plantation resources. The opportunities and potential challenges associated with such product development were investigated and discussed through experiments and answering the three research questions presented in Chapter 1.

Overall, the results obtained have demonstrated a good potential for using fibre-managed eucalypt plantations in NLT production. The most important challenges at this stage could be the relatively low recovery rate of useable boards, drying issues, and structural grading of the boards from such plantation resources—which opens up new topics and stimulates future innovative research in this area.

References

A

- Ahvenainen, J., & Sousa, H. S. (2016). Multistorey building made of CLT: How to design it right?. *Construir em madeira*, 95-118.
- AS 2082. (2007). Timber - Hardwood - Visually stress graded for structural purposes. Standards Australia, Australia.
- Australian Bureau of Agricultural and Resource Economics and Sciences (ABARES). (2016). Australian plantation statistics 2016, Australian Bureau of Agricultural and Resource Economics and Sciences, Canberra, August. CC BY 3.0. Available at: agriculture.gov.au/abares/publications
- Australian Bureau of Agricultural and Resource Economics and Sciences (ABARES). (2018). Australian plantation statistics 2018, Australian Bureau of Agricultural and Resource Economics and Sciences, Canberra, August. CC BY 3.0. Available at: <https://data.gov.au/data/dataset/f688dfa9-7af4-485b-8b04-4363616c8978>

B

- Blackburn, D. P., Hamilton, M. G., Harwood, C. E., Innes, T. C., Potts, B. M., & Williams, D. (2011). Genetic variation in traits affecting sawn timber recovery in plantation-grown *Eucalyptus nitens*. *Annals of Forest Science*, 68(7), 1187.
- Blackburn, D. P., Hamilton, M. G., Harwood, C. E., Innes, T. C., Potts, B. M., & Williams, D. (2010). Stiffness and checking of *Eucalyptus nitens* sawn boards: genetic variation and potential for genetic improvement. *Tree genetics & genomes*, 6(5), 757-765.
- Blackburn, D., Hamilton, M., Williams, D., Harwood, C., & Potts, B. (2014). Acoustic wave velocity as a selection trait in *Eucalyptus nitens*. *Forests*, 5(4), 744-762. <https://doi.org/10.3390/f5040744>
- Blackburn, D., Vega, M., Yong, R., Britton, D., & Nolan, G. (2018). Factors influencing the production of structural plywood in Tasmania, Australia from *Eucalyptus nitens* rotary peeled veneer. *Southern Forests: a Journal of Forest Science*, 1-10.
- Brunetti, M., Burato, P., Cremonini, C., Negro, F., Nocetti, M., & Zanuttini, R. (2016). Visual and machine grading of larch (*Larix decidua* Mill.) structural timber from the Italian Alps. *Materials and Structures*, 49(7), 2681-2688.
- Buck, D., Hagman, O., Wang, A., & Gustafsson, A. (2016). Further Development of Cross-Laminated Timber (CLT): Mechanical Tests on 45° Alternating Layers. In *World Conference on Timber Engineering (WCTE 2016)*, Vienna, August 22-25 2016. Vienna

University of Technology, Austria.

C

- Carrasco, E. V. M., Duarte, R. S., Alves, R. C., & Mantilla, J. N. R. (2013). Determination of *Eucalyptus grandis* boards properties through non-destructive testing. *International Journal of Applied Science and Engineering Research*, 2(5), 493-501.
- Castro, G., & Paganini, F. (2003). Mixed glued laminated timber of poplar and *Eucalyptus grandis* clones. *Holz als Roh-und Werkstoff*, 61(4), 291-298.
- Christoforo, A. L., Panzera, T. H., Brandão, L. C., de Araújo, V. A., Silva, D. A. L., & Lahr, F. A. R. (2015). Comparison among the Longitudinal Modulus of Elasticity in *Eucalyptus grandis* Timber Beams by Alternative Methodologies. *International Journal of Materials Engineering*, 5(4), 77-81.
- Crocetti, R., Ekholm, K., & Kliger, R. (2016). Stress-laminated-timber decks: state of the art and design based on Swedish practice. *European Journal of Wood and Wood Products*, 74(3), 453-461.

D

- Darmawan, W., Nandika, D., Massijaya, Y., Kabe, A., Rahayu, I., Denaud, L., & Ozarska, B. (2015). Lathe check characteristics of fast growing sengon veneers and their effect on LVL glue-bond and bending strength. *Journal of Materials Processing Technology*, 215, 181-188.
- Derikvand, M., Jiao, H., Kotlarewski, N., Lee, M., Chan, A., & Nolan, G. (2019a). Bending performance of nail-laminated timber constructed of fast-grown plantation eucalypt. *European Journal of Wood and Wood Products*, 77(3), 421-437.
- Derikvand, M., Kotlarewski, N., Lee, M., Jiao, H., & Nolan, G. (2018a). Flexural and visual characteristics of fibre-managed plantation *Eucalyptus globulus* timber. *Wood Material Science & Engineering*, 1-10.
- Derikvand, M., Kotlarewski, N., Lee, M., Jiao, H., & Nolan, G. (2019b). Characterisation of physical and mechanical properties of unthinned and unpruned plantation-grown *Eucalyptus nitens* H. Deane & Maiden lumber. *Forests*, 10(2), 194.
- Derikvand, M., Kotlarewski, N., Lee, M., Jiao, H., Chan, A., & Nolan, G. (2018b). Visual stress grading of fibre-managed plantation Eucalypt timber for structural building applications. *Construction and Building Materials*, 167, 688-699.
- Derikvand, M., Kotlarewski, N., Lee, M., Jiao, H., Chan, A., & Nolan, G. (2019c). Short-term and long-term bending properties of nail-laminated timber constructed of fast-grown plantation eucalypt. *Construction and Building Materials*, 211, 952-964.

Derikvand, M., Nolan, G., Jiao, H., & Kotlarewski, N. (2017). What to Do with Structurally Low-Grade Wood from Australia's Plantation Eucalyptus; Building Application?. *BioResources*, 12(1), 4-7.

Dietsch, P., & Tannert, T. (2015). Assessing the integrity of glued-laminated timber elements. *Construction and Building Materials*, 101, 1259-1270. <https://doi.org/10.1016/j.conbuildmat.2015.06.064>

Dugmore, M. K. (2018). Evaluation of the bonding quality of *E. grandis* cross-laminated timber made with a one-component polyurethane adhesive (Doctoral dissertation, Stellenbosch: Stellenbosch University).

Dugmore, M., Nocetti, M., Brunetti, M., Naghizadeh, Z., & Wessels, C. B. (2019). Bonding quality of cross-laminated timber: Evaluation of test methods on *Eucalyptus grandis* panels. *Construction and Building Materials*, 211, 217-227.

F

Farrell, R., Innes, T. C., & Harwood, C. E. (2012). Sorting *Eucalyptus nitens* plantation logs using acoustic wave velocity. *Australian forestry*, 75(1), 22-30. <https://doi.org/10.1080/00049158.2012.10676382>

Fink, G., Frangi, A., & Kohler, J. (2015). Probabilistic approach for modelling the load-bearing capacity of glued laminated timber. *Engineering Structures*, 100, 751-762. <https://doi.org/10.1016/j.engstruct.2015.06.015>

Franke, S., & Marto, J. (2014). Investigation of *Eucalyptus globulus* wood for the use as an engineered material. In *World Conference on Timber Engineering*, August 10-14, Quebec, Canada.

Frühwald, E. (2001). Investigation of stability of glulam roof trusses with large spans. Diploma Thesis, Lund Institute of Technology, Sweden.

G

Gasparri, E., Lucchini, A., Mantegazza, G., & Mazzucchelli, E. S. (2015). Construction management for tall CLT buildings: From partial to total prefabrication of façade elements. *Wood Material Science & Engineering*, 10(3), 256-275.

Gavran, M. (2015). Australian Plantation Statistics 2015 update, Australian Bureau of Agricultural and Resource Economics and Sciences, http://www.agriculture.gov.au/abares/publications/display?url=http://143.188.17.20/anrdl/DAFFService/display.php?fid=pb_aplnsd9abfs20150513_11a.xml, viewed 21 May 2015.

Gezici-Koç, Ö., Erich, S. J., Huinink, H. P., van der Ven, L. G., & Adan, O. C. (2017). Bound and free water distribution in wood during water uptake and drying as measured by 1D

magnetic resonance imaging. *Cellulose*, 24(2), 535-553.

Grant, G. (2010). Evaluation of timber floor systems for fire resistance and other performance requirements (Doctoral dissertation), University of Canterbury, New Zealand.

H

Hamilton, M. G. (2007). The genetic improvement of *Eucalyptus globulus* and *E. nitens* for solidwood production (Doctoral dissertation, University of Tasmania).

Hayashi, T., & Miyatake, A. (2015). Recent research and development on sugi (Japanese cedar) structural glued laminated timber. *Journal of Wood Science*, 61(4), 337-342. <https://doi.org/10.1007/s10086-015-1475-x>

Hong, K. E. M. (2017). Structural performance of nail-laminated timber-concrete composite floors (Doctoral dissertation, University of British Columbia).

K

Kandler, G., Füssl, J., Serrano, E., & Eberhardsteiner, J. (2015). Effective stiffness prediction of GLT beams based on stiffness distributions of individual lamellas. *Wood Science and Technology*, 49(6), 1101-1121. <https://doi.org/10.1007/s00226-015-0745-5>

Khorasani, S. R. (2012). Finite-element simulations of glulam beams with natural cracks (Master Thesis), Blekinge Institute of Technology, Sweden.

L

Lara-Bocanegra, A. J., Majano-Majano, A., Crespo, J., & Guaita, M. (2017). Finger-jointed *Eucalyptus globulus* with 1C-PUR adhesive for high performance engineered laminated products. *Construction and Building Materials*, 135, 529-537.

Latour, M., & Rizzano, G. (2017). Seismic behavior of cross-laminated timber panel buildings equipped with traditional and innovative connectors. *Archives of Civil and Mechanical Engineering*, 17(2), 382-399.

Liao, Y., Tu, D., Zhou, J., Zhou, H., Yun, H., Gu, J., & Hu, C. (2017). Feasibility of manufacturing cross-laminated timber using fast-grown small diameter eucalyptus lumbers. *Construction and Building Materials*, 132, 508-515.

Lu, Z., Zhou, H., Liao, Y., & Hu, C. (2018). Effects of surface treatment and adhesives on bond performance and mechanical properties of cross-laminated timber (CLT) made from small diameter *Eucalyptus* timber. *Construction and Building Materials*, 161, 9-15.

M

- Madhoushi, M., & Daneshvar, S. (2016). Predicting the static modulus of elasticity in eastern cottonwood (*Populus deltoides*) using stress wave non-destructive testing in standing trees. *European Journal of Wood and Wood Products*, 74(6), 885-892.
- Majano-Majano, A., Lara-Bocanegra, A., Xavier, J., & Morais, J. (2019). Measuring the Cohesive Law in Mode I Loading of *Eucalyptus globulus*. *Materials*, 12(1), 23. <https://doi.org/10.3390/ma12010023>
- Mallo, M. F. L., & Espinoza, O. A. (2014). Outlook for cross-laminated timber in the United States. *BioResources*, 9(4), 7427-7443.
- McGavin, R. L., Bailleres, H., Fehrmann, J., & Ozarska, B. (2015). Stiffness and density analysis of rotary veneer recovered from six species of Australian plantation hardwoods. *BioResources*, 10(4), 6395-6416. DOI: 10.15376/biores.10.4.6395-6416
- Mohamed, S., & Abdullah, R. (2014). Timber use practices in Malaysia's construction industry: single-family residential building sector. *Pertanika Journal of Tropical Agricultural Science*, 37(4), 475-482.

N

- Nolan, G. B., Greaves, B. L., Washusen, R., Parsons, M., & Jennings, S. (2005). Eucalypt Plantations for Solid Wood Products in Australia-A Review 'If you don't prune it, we can't use it'. Forest & Wood Products Australia Ltd., Project No.: PN04.3002.

P

- Pei, S., van de Lindt, J. W., & Popovski, M. (2012). Approximate R-factor for cross-laminated timber walls in multistory buildings. *Journal of Architectural Engineering*, 19(4), 245-255.
- Petrauski, S. M. F. C., Silva, J. D. C., Petrauski, A., & Lucia, R. M. D. (2016). Analysis of eucalyptus glued-laminated timber porticos structural performance. *Revista Árvore*, 40(5), 931-939.
- Piter, J. C., Cotrina, A. D., Zitto, M. S., Stefani, P. M., & Torrán, E. A. (2007). Determination of characteristic strength and stiffness values in glued laminated beams of Argentinean *Eucalyptus grandis* according to European standards. *Holz als Roh-und Werkstoff*, 65(4), 261-266.
- Pleschberger, H., Teischinger, A., Müller, U., & Hansmann, C. (2013). Mechanical characterization of lumber of small-diameter hardwood species after different drying schedules. *Drying Technology*, 31(9), 1056-1062.
- Pröller, M., Nocetti, M., Brunetti, M., Barbu, M. C., Blumentritt, M., & Wessels, C. B. (2018). Influence of processing parameters and wood properties on the edge gluing of green *Eucalyptus grandis* with a one-component PUR adhesive. *European Journal of Wood and*

Wood Products, 1-10.

Puettmann, M. E., & Wilson, J. B. (2007). Gate-to-gate life-cycle inventory of glued-laminated timbers production. *Wood and Fiber Science*, 37, 99-113.

R

Ramage, M. H., Burrige, H., Busse-Wicher, M., Fereday, G., Reynolds, T., Shah, D. U., ... & Allwood, J. (2017). The wood from the trees: The use of timber in construction. *Renewable and Sustainable Energy Reviews*, 68, 333-359.

Reid, R., & Washusen, R. (2001). Sawn timber from 10-year-old pruned *Eucalyptus nitens* (Deane & Maiden) grown in an agricultural riparian buffer. In *Third Australian Stream Management Conference proceedings: the value of healthy streams* (pp. 27-29).

Ritter, M. A., Geske, E. A., McCutcheon, W. J., Moody, R. C., Wacker, J. P., & Mason, L. E. (1991, September). Methods for assessing the field performance of stress-laminated timber bridges. In *Proceedings of the 1991 International Conference on Timber Engineering*. Londres, Inglaterra. pgs (pp. 3319-3326).

Robertson, M., Holloway, D., & Taoum, A. (2018). Vibration of suspended solid-timber slabs without intermediate support: assessment for human comfort. *Australian Journal of Structural Engineering*, 19(4), 266-278.

S

Satchell, S. D. (2015). Evaluating profitability of solid timber production from 15 year old pruned and thinned *Eucalyptus nitens* (Deane & Maiden) in Canterbury (Master's dissertation, University of Canterbury).

Scalet, T. (2015). *Cross Laminated Timber as Sustainable Construction Technology for the Future*. Helsinki Metropolia University of Applied Sciences, Finland.

Shrestha, R., Lewis, K., & Crews, K. I. (2014). Introduction to cross laminated timber and development of design procedures for Australia and New Zealand. In *Australasian Conference on the Mechanics of Structures and Materials*. Southern Cross University.

Smith, R. E., Griffin, G., Rice, T., & Hagehofer-Daniell, B. (2018). Mass timber: evaluating construction performance. *Architectural Engineering and Design Management*, 14(1-2), 127-138.

Stapel, P., & van de Kuilen, J. W. G. (2014). Efficiency of visual strength grading of timber with respect to origin, species, cross section, and grading rules: A critical evaluation of the common standards. *Holzforschung*, 68(2), 203-216.

U

- Underhill, I. (2016). The Development and Assessment of Engineered Wood Products Manufactured from Low Grade Eucalyptus Plantation Thinnings (Doctoral dissertation, Griffith University).
- Ussher, E., Arjomandi, K., Weckendorf, J., & Smith, I. (2017). Prediction of motion responses of cross-laminated-timber slabs. *Structures* 11, 49-61.
- Uzel, M., Togay, A., Anil, Ö., & Söğütü, C. (2018). Experimental investigation of flexural behavior of glulam beams reinforced with different bonding surface materials. *Construction and Building Materials*, 158, 149-163.

W

- Washusen, R. (2000). Shrinkage of solid wood during drying and its relationship to tree form in 11-year-old Eucalyptus globulus Labill. In *Proceedings of 26th Forest Products Research Conference: Research developments and industrial applications and Wood Waste Forum*, Clayton, Victoria, Australia, 19-21 June 2000 (pp. 47-48). CSIRO Forestry and Forest Products.
- Washusen, R., & Ilic, J. (2001). Relationship between transverse shrinkage and tension wood from three provenances of Eucalyptus globulus Labill. *Holz als Roh-und Werkstoff*, 59(1-2), 85-93.
- Washusen, R., Blakemore, P., Northway, R., Vinden, P., & Waugh, G. (2000). Recovery of dried appearance grade timber from Eucalyptus globulus Labill, grown in plantations in medium rainfall areas of the Southern Murray-Darling Basin. *Australian Forestry*, 63(4), 277-283.
- Washusen, R., Harwood, C., Morrow, A., Northway, R., Valencia, J. C., Volker, P., ... & Farrell, R. (2009). Pruned plantation-grown Eucalyptus nitens: Effect of thinning and conventional processing practices on sawn board quality and recovery. *New Zealand Journal of Forestry Science*, 39(1), 39-55.
- Washusen, R., Reeves, K., Hingston, R., Davis, S., Menz, D., & Morrow, A. (2004). Processing pruned and unpruned Eucalyptus globulus managed for sawlog production to produce high value products. Australian Government, Forest and Wood Products Research and Development Corporation PN03, 1315, Melbourne, Victoria.
- Weckendorf, J., Toratti, T., Smith, I., & Tannert, T. (2016). Vibration serviceability performance of timber floors. *European Journal of Wood and Wood Products*, 74(3), 353-367.
- Wentzel-Vietheer, M., Washusen, R., Downes, G. M., Harwood, C., Ebdon, N., Ozarska, B., & Baker, T. (2013). Prediction of non-recoverable collapse in Eucalyptus globulus from near infrared scanning of radial wood samples. *European Journal of Wood and Wood Products*, 71(6), 755-768.

Y

Yeoh, D., Fragiacomio, M., & Deam, B. (2011). Experimental behaviour of LVL–concrete composite floor beams at strength limit state. *Engineering Structures*, 33(9), 2697-2707.

Yeoh, D., Fragiacomio, M., De Franceschi, M., & Heng Boon, K. (2010). State of the art on timber-concrete composite structures: Literature review. *Journal of structural engineering*, 137(10), 1085-1095.

Z

Zitto, M. S., Köhler, J., & Piter, J. C. (2014). Load-carrying capacity of timber-to-timber joints of fast-growing Argentinean *Eucalyptus grandis* with nails of small diameter laterally loaded in double shear: analysis according to the criterion adopted by European standards. *European Journal of Wood and Wood Products*, 72(1), 21-31.

Appendices

Appendix A: Paper I

Publication reference: Derikvand, M., Nolan, G., Jiao, H., & Kotlarewski, N. (2016). What to do with structurally low-grade wood from Australia's plantation eucalyptus; building application?. *BioResources*, 12(1), 4-7.

What to Do with Structurally Low-Grade Wood from Australia's Plantation Eucalyptus; Building Application?

Mohammad Derikvand, Gregory Nolan, Hui Jiao, and Nathan Kotlarewski

About one million hectares of plantation hardwoods, mostly eucalyptus trees of different sub-species (*E. nitens* and *E. globulus*), are annually being managed in Australia, which provides a promising resource of raw materials for fibre industries. However, the timber boards required by the Australian hardwood sector are still being either imported from other countries or harvested from the native forests. There is a need to find a practical way to use the plantation eucalyptus in the Australian timber industry. However, the fibre-managed plantation eucalyptus produces structurally low-grade timber which could not be used as individual boards for structural applications—such as building construction. Unsuitable for appearance applications, the structurally low-grade boards may be suitable for producing innovative high-mass engineered timber products. This editorial will briefly discuss drivers, opportunities, and challenges associated with conducting such a research project.

Keywords: Plantation hardwood; Structurally low-grade wood; Timber building; Eucalyptus

The Australian Bureau of Agricultural and Resource Economics and Sciences (ABARES) estimates that more than two million hectares of plantation softwood and hardwood species exist in Australia—with a total area of 976,400 hectares for hardwood plantations (Gavran 2014). Such a large volume of plantation hardwood trees has the potential to provide a significant portion of the wood resource required to service Australia's timber construction sector. However, most plantation hardwoods in Australia are eucalyptus species, primarily managed for pulp log production. According to ABARES, nearly 84.4 per cent of logs currently harvested from hardwood plantations are being used in Australia's pulp and paper industries or exported as woodchips. Current plantation hardwood genetics have been selected for their fast growth to compliment short rotation cycles in largely unthinned and unpruned stands. Recovered plantation hardwood logs generally produce structurally low-grade timber when sawn, producing boards that contain strength-reducing characteristics. While this plantation hardwood resource exists, Australia's hardwood lumber sector still relies on milling logs from native forests and imported wood species (McGavin *et al.* 2015). Although native hardwood species are well regarded for their strength and visual properties, supply has decreased steadily from the 1970s (Nolan *et al.* 2005). Given this decline in supply and the lack of expansion in the plantation softwood estate, there is a drive to develop higher-value solid wood products and corresponding applications in building construction for some part of the plantation hardwood resource in order to fill growing market gaps. The aim of this editorial is to highlight and discuss the main issues likely to impact the development of any high-mass timber components manufactured from structurally low-grade boards recovered from Australia's plantation eucalypts.

Developing and producing engineered high-mass timber components—such as Glue Laminated Timber (GLT) and Nail Laminated Timber (NLT) panels—from structurally low-grade

plantation hardwood boards could be one option. Not competing with the current softwood processing sector, this approach could generate a value-added product suite for a new plantation hardwood processing sector. It could also support the markets expected to form as Australia's building professionals increasingly adopt timber-rich construction options for multi-residential and commercial buildings. Developing engineered products for building applications from structurally low-grade plantation eucalypt timber is a straightforward goal; however, commercial innovation and experimental works are also needed to find a practical process for using this material in a product that economically and structurally satisfies the requirements established in the Australian construction industry.

Eucalyptus globulus (known as Tasmanian or Southern blue gum) and *Eucalyptus nitens* (known as Shining gum) are the major plantation hardwood species grown in Australia. Southern blue gum makes up 54.6 per cent of the current estate while 24.2 per cent is Shining gum (Gavran 2014). The estate was mainly planted after 1995, and both species were selected for their high growth rate. The overwhelming majority of the estate was planted and is managed in unthinned and unpruned stands to economically maximise fibre production. The lack of thinning produces tall but thin stems, while the lack of pruning results in regular branch stubs in the wood—especially in Shining gum. While relatively unimportant for fibre production, both factors complicate recovery of solid wood products. Due to the current economics of growing wood in Australia, fibre production drives management practices and most hardwood plantations are harvested between 15 to 20 years old. As a result, the diameter of logs potentially suitable for solid wood production is low—averaging 345 mm at the small end diameter. Since the stems are unpruned, the wood includes regular knots and other natural features. This largely precludes its acceptance in appearance applications, but it may be suitable for a new generation of structural engineered products. Sawing the logs and drying the boards from this resource presents challenges. Recovery from the small logs is low without purpose-designed equipment, and both species are prone to cell collapse during drying—again, especially Shining gum. The radial and tangential shrinkage rates for both species are high, and their sapwood is lyctus susceptible. In conventional milling for appearance products, these species would be quarter sawn to reduce drying degrade and the sapwood removed. However, quarter sawing and sapwood exclusion reduce volume recovery from young logs with relatively wide sapwood bands. To increase recovery for high-mass timber components, logs need to be sawn for volume and sapwood may need to be retained. Drying degradation in boards and lyctus susceptibility then need to be accommodated in later production stages.

The important initial stage in producing any high-mass timber components from this material is to establish a robust understanding of the resource's physical, mechanical, acoustical, and fire-resistant properties. While significant research into the properties of Australia's plantation species has occurred, much of this has focused on the properties of boards milled from logs from thinned and pruned stands grown in longer rotations. Inadequate work has occurred on boards sawn for volume from logs recovered from unthinned and unpruned stands. The multiplicity of knots, drying degradation features such as checks and unrecovered collapse, growth stress, the effects of tension wood, and non-uniform fiber orientation along the longitudinal axis can complicate the workability and performance of boards and groups of boards assembled into engineered timber components. These complications need to be defined and understood. Factors that can influence the development of suitable, economic products from this resource include accelerated drying, drying degrade, board grading approaches and methods of material assembly.

Logs cut for volume will produce a range of backsawn, quarter sawn, and transitional boards. If this resource is to be processed economically, accelerated drying is likely to be necessary, and the additional drying degradation generated in this variety of boards needs to be managed. However, the impact of the different types of drying degradation on board and panel workability and performance for each species and their increase with accelerated drying is not well understood. Additional checking is unlikely to be critical, but increased board deformation may create problems. These impacts need to be

confirmed if a useful balance between drying speed and acceptable board degrade is to be identified. Alternative grading rules are also needed to accommodate plantation resources that will be used in high-mass engineered timber components. Existing structural grading rules are rigorous and designed to ensure that the performance of an individual board for an unknown future application meets building standards. For individual boards with regular strength reducing characteristics such as knots, the grading rules are constrictive and neglect to consider that multiple low-grade boards will to be used in combination in a purpose-designed engineered component. While the individual boards may not be suitable to use as a single building element, such as a beam or post, they may contribute to the performance of a multi-member assembly such as GLT and NLT panels. Alternative grading rules can therefore potentially accommodate the patterns of features likely in each piece and their performance relative to board orientation in the finished panel.

Simply docking out strength-reducing characteristics and rejoining ‘clear’ sections will be labour-intensive and make any final panel uneconomical. In a high-mass timber component, boards need to be joined along their length and side-to-side. An efficient end-to-end joining system is therefore vital to overcome length limitation and ensure efficient board utility. Finger jointing is the common end-to-end joining technique, but there is a lack of information on the effectiveness of finger joints in plantation eucalypt cut for volume and dried quickly. In addition to the features in the wood, drying degradation may have a major influence on finger joint performance. Boards also need to be effectively joined side-to-side to make a panel: either glued, nail-laminated, or stress laminated. Each approach will result in different structural performance in a panel (which needs to be defined) and in different opportunities in fabricating the panels economically. Glue laminating panels requires skill in machining, adhesive management, and product assembly but can provide a reliable product from a varied resource. Nail lamination is a more diverse process for regional producers to adopt, but may only be viable if board deformation is constrained before assembly. Stress laminating may now also be possible given the extensive range of large screws now available on the market. Given the unique nature of the resource and the problem, innovative approaches are needed. An approach where sawn boards are milled, joined, and green glued into large elements before seasoning, may not offer a commercial solution to assembling timber engineered component from Shining and Southern blue gum into panels, but the response of this material to green gluing may inform more efficient ways of assembling dry boards effectively.

This editorial indicates that drivers exist to develop higher-value solid wood products and corresponding applications in construction for some portion of Australia’s extensive plantation hardwood resource. Unsuitable for appearance applications, recovered boards may be suitable for novel and innovative high-mass engineered timber components. Repurposing the fibre-grown resource into purpose-designed timber engineered components suitable for building construction in Australia to meet potential market gaps may be a solution. However, the form of the resources and their management complicates its use. Research is needed that seeks to understand and balance the technical, performance, and production issues along the supply chain: from the resource and the feedstock that may be recovered from it; through the production process in fabrication facilities of differing scale and skill level; to the products that have to provide satisfactory performance in a range of building applications.

References Cited

- Gavran, M. (2014). “Australian Plantation Statistics 2014 Update,” Department of Agriculture, Fishier, and Forestry,
http://www.agriculture.gov.au/abares/publications/display?url=http://143.188.17.20/anrdl/DAFFService/display.php?fid=pb_aplnsd9abfs20140910_11a.xml)

- McGavin, R. L., Bailleres, H., Fehrmann, J., and Ozarska, B. (2015). "Stiffness and density analysis of rotary veneer recovered from six species of Australian plantation hardwoods," *BioResources* 10(4), 6395-6416. DOI: 10.15376/biores.10.4.6395-6416
- Nolan, G., Washusen, R., Jennings, S., Greaves, B. and Parsons, M. (2005). "Eucalypt plantations for solid wood products in Australia - A review," Forest & Wood Products Australia Ltd., Project No.: PN04.3002.

Appendix B: Paper II

Publication reference: Derikvand, M., Kotlarewski, N., Lee, M., Jiao, H., Chan, A., & Nolan, G. (2018). Visual stress grading of fibre-managed plantation Eucalypt timber for structural building applications. *Construction and Building Materials*, 167, 688-699.

Visual Stress Grading of Fibre-Managed Plantation Eucalypt Timber for Structural Building Applications

Mohammad Derikvand, Nathan Kotlarewski, Michael Lee, Hui Jiao, Andrew Chan, Gregory Nolan

Abstract

The aim of this study was to examine the impacts of visual characteristics, strength-reducing features (SRFs), and basic density on the mechanical properties of fibre-managed plantation Eucalypt timber to create effective structural grade groups. It is the intension that the results found in this study can lead to the development of a visual stress grading method for fibre-managed plantation timber in the future and influence the development of new applications for the resource in structural elements for the built environment. The plantation specie investigated in this study was *Eucalyptus Nitens*–390 sawn timber boards. The most important visual characteristics and SRFs likely to influence the mechanical properties of the boards were visually identified and measured before the boards were divided into designated groups for sampling. The impacts of the visual characteristics, SRFs, and basic density of the boards within each group on modulus of elasticity (MOE) and modulus of rupture (MOR) were determined using four-point bending test. The statistical analyses suggest three structural grade groups can categorise the resource. Strong correlations were found between MOE, MOR, and basic density with the visual characteristics and SRFs of the boards in the three grade groups.

Keywords: timber; *Eucalyptus nitens*; visual grading; basic density; bending strength; strength-reducing features.

1. Introduction

The reliability and design flexibility of timber-rich construction makes wood products an attractive option for designers and builders. It is widely recognised that timber is:

- Environmentally friendly because wood is biodegradable, recyclable, and renewable (De Araujo et al., 2016; Fidan et al., 2016).
- A sustainable building material that is widely available in nature as long as the harvested trees are replaced by new plantings (Ramage et al., 2017).
- Very low in production energy compared to other building materials such as concrete, steel, and aluminum (Santi et al., 2016).
- Structurally effective due to its high strength-to-weight capacity ratio (Chuquitaype & Elghazouli, 2016; Ramage et al., 2017).
- An effective, natural insulator because of its porous structure (Li et al., 2016).
- Light and easy to work with (Yasar et al., 2017).
- Naturally beautiful with a featured pattern that adds character and warmth.

With the increased effectiveness and sophistication of high-mass laminated timber products, demand for timber solutions in different structural applications has rapidly increased in recent decades — especially in building construction (Yasar et al., 2017). However, timber's availability for construction is also an important issue. Using fast growing plantation species like Eucalypts on short rotation harvest cycles could be a viable and necessary contemporary solution to this issue. Eucalypts are the main plantation hardwood species in the world and most are planted and managed for fibre production. While efficient for fibre production, the forestry practices used in a fibre-focused management regime generally produces small logs of low-grade wood. It is challenging to find a practical way to use fibre-managed Eucalypt in the timber and construction industry as the sawn timber and veneer recovered from this resource is young, highly variable, and has substantial strength-reducing features (SRFs) such as knots and drying defects (Nolan et al., 2005; Blackburn et al., 2010, 2011). These can limit its use in structural applications (Derikvand et al., 2017).

The Australian National Construction Code (NCC) regulates all structural applications in buildings and consequently establishes the minimum 'fit-for-purpose' requirements for structural timber. To satisfy the NCC's requirements, structural timber elements have to comply with either the requirement of the relevant structural grading standards or have independent engineering certification of their structural performance. For hardwood, the relevant structural grading standard is Australian Standard (AS) 2082 (Timber - Hardwood - Visually stress graded for structural purposes, Standards Australia 2007). Grading under AS 2082 (Standards Australia 2007) is based on the visual examination of the SRFs and other attributes of each board and allocation to it of a structural grade. Combining this structural grade with the species' typical mechanical properties assigns a stress grade to the board. In practice, this method assumes a direct correlation between the assessed visual SRFs of the board and its structural properties and is based on correlations established on testing relationships between the visual characteristics and mechanical properties of mature wood from native forests. By contrast, fibre-managed Eucalypt plantations are quickly grown and often harvested at 15 to 20 years old. They yield

logs and recovered timber that contain a high percentage of SRFs and juvenile wood. As a result, they are likely to have physical and mechanical properties that are completely different in value and in the relationship between SRFs and structural capacity from those of mature native forest wood of the same species. Given this, the methods for visual stress grading of hardwood in the current standard may not be relevant to such a resource. In this process, the origin of boards (plantation or native forests) and the specific requirements in the target application for the boards need to be taken into account. Boards may be graded and sold as individual commodity items for use in an unknown application in buildings or graded and incorporated into a purpose design component. Parts of these issues have already been addressed in previous studies (Kline et al., 2000; Piter et al., 2004; Lycken et al., 2006; Adell Almazán et al., 2008; Roblot et al., 2008; Krzosek 2011; Muñoz et al., 2011; Stapel and van de Kuilen 2014; Feio and Machado 2015; Viguier et al., 2015; Nicoletta et al., 2017). However, the relevance of visual stress grading of timber to fibre-managed plantation species is still unknown.

The goal of this study was to investigate the effects of visual characteristics and SRFs on the mechanical properties of timber boards recovered from fibre-managed plantation *Eucalyptus nitens* (*E. nitens*) and create effective structural grade groups that can be used to inform the development of a practical visual grading method for the resource. *E. nitens* was selected in this study as it is one of the most widely planted fast-growing eucalypt species in Australia. Due to its abundance, there is interest in developing new applications for the resource especially in the built environment. Specific objectives of the study:

- Investigated the nominal recovery rate and dressed-board recovery of fibre-managed plantation *E. nitens*—sawn, dried, and dressed using standard commercial procedures.
- Created a profile of material characteristics of fibre-managed plantation *E. nitens* by assessing the visual characteristics, SRFs, basic density, and moisture content (MC) of recovered boards.
- Categorised the boards into different groups based on their wood quality, SRFs, and other visual characteristics.
- Determined the modulus of elasticity (MOE) and modulus of rupture (MOR) of the boards from different quality groups to evaluate the correlations between the visual characteristics, SRFs, and basic density with the mechanical properties of the boards under uniaxial bending loads.
- Developed regression models to predict MOE and MOR values using the visual characteristics, SRFs, and basic density of the boards.
- Developed effective structural grade groups for the boards based on the results obtained.

2. Materials and Methods

2.1. Harvesting, Sawing, and Drying Processes

For this study, 29.30 m³ of *E. nitens* logs were harvested from a 16 years old fibre-managed plantation on the north of Tasmania, Australia. The average small-end diameter of the logs was 345 mm. After

harvested, the logs were sawn and the boards dried using standard commercial procedures. This ensured that the results would align to any future production system that used the same equipment suite and processes. Logs were sawn into boards of four nominal widths: 75 mm, 100 mm, 125 mm, and 150 mm, and a nominal 38 mm thickness. To maximise volume recovery rate, logs were plain sawn and the sapwood was retained. The lengths of the recovered boards varied. The average lengths by width were 4551 mm, 4391 mm, 4551 mm, and 4582 mm respectively. The boards were dried in pre-dryers for nine weeks under rack weights and then air-dried in the mill yard for three weeks. After reconditioning, they were dried in conventional kilns to a nominal MC of 12%. The rack weights were kept on the boards during the entire drying processes to decrease possible distortions in the boards due to rapid drying. The dry boards were finally square dressed to widths of 70 mm, 90 mm, 120 mm, and 140 mm, and a thickness of 35 mm.

2.2. Assessment of Visual Characteristics

In total, 390 boards with the four different widths were studied for a broad range of various visual characteristics and SRFs.

2.2.1. Knots and Knotholes

Knots are one of the features that can significantly affect the mechanical properties of timber and wood products (Kretschmann and Hernandez 2006; Muñoz et al., 2011; Koman et al., 2013) and the dimensions of knots in the piece are one of the key factors in the current visual stress grading standards. In this study, face knots (both loose and tight knots) with a diameter larger than 1/4 of the width of the boards were considered major knots. This boundary diameter for major knots was chosen as timber boards that have face knots with diameters equal to or smaller than 1/4 of the width of the boards can still be graded as either Structural Grade No. 1 (the best grade) or Structural Grade No. 2 in AS 2082 (Standards Australia 2007). The frequency and type of major knots were assessed in each board.

The existence of knotholes on the boards was also assessed. This criterion was mainly an indicator of the presence or absence of knotholes not their quantity or dimensions.

2.2.2. Surface checks

Surface checks with individual lengths exceeding 1/4 of the length of the boards and or surface checks with a width larger than 3 mm were examined and reported. Boards that have surface checks with a length and or a width equal to or smaller than the aforementioned values can still be graded as Structural Grade No. 1 according to AS 2082 (Standards Australia 2007)—hence, they were not considered as major surface checks in this study.

2.2.3. End splits

The length and width of end splits were measured on each board and the percentage of boards with major end splits was reported. Major end splits in this study are those that had a length larger than or equal to the width of the boards.

2.2.4. Wane

Wane is the under-bark surface of a log that appears on the edge of a sawn timber board. The amount of wane on each board was assessed and the percentage of boards with significant amount of wane was reported. Wane larger than 1/10 of the cross-sectional area, wane on the face of the boards exceeding 1/2 of the board's width, and wane on the edge of the boards exceeding 1/3 of the board's thickness were considered as significant—according to the criteria described for Structural Grade No .1 in AS 2082 (Standard Australia 2007).

2.2.5. Insect trace and fungal decay

Most standards include insect trace and fungal decay as important visual stress grading parameters for timber. Loss in the mechanical properties due to fungal decay may be severe, especially by the time that decay becomes visually apparent (Bower et al., 2003). The boards in this study were carefully inspected to detect any possible insect trace and decay.

2.2.6. Drying distortions

Distortion frequently occurs because of differential shrinkage along and across the timber during the drying process. The types of drying distortions that occur include bow, crook (spring), twist, diamonding, and cupping. Bow, crook, and twist appear along the length of the boards while diamonding and cupping can be detected across the face of the boards. In this study, bow, crook, and twist were measured for each board and the percentage of boards with impermissible bow, crook, and twist under AS 2082 (Standards Australia 2007) is reported. The boards used in this study were square-dressed, which is a conventional processing step at the mill level. This removes or significantly reduces diamonding and cupping distortions. Hence, the amount of diamonding and cupping distortions of the test boards was insignificant and therefore disregarded in this study.

2.2.7. Slope of grain

Bower et al. (2003) describes slope of grain as “the length through which a deviation in the grain occurs”. Slope of grain is one of the most important factors that affects the stiffness and strength properties of timber. A board's mechanical properties can significantly decrease with an increase in the slope of grain in it (Baño et al., 2011; Viguier et al., 2015). Slope of grain can vary from one part of the board to another, especially in long and high-feature boards. In this study, the maximum slope of grain

along the longitudinal axis was detected and measured for each board according to AS 1080.2 (Standards Australia 2006). Grain deviation around knots as well as localised variations in the slope of grain were disregarded—in accordance with AS 1080.2 (Standards Australia 2006).

2.2.8. Mechanical damages and unrecoverable collapse

Mechanical damage on boards usually occurs due to debarking and or sawing deviation. Unrecoverable collapse appears during the drying process. The loss of cross section area of the boards due to mechanical damages and unrecoverable collapse may influence the mechanical properties. The percentage of boards with mechanical damages and unrecoverable collapse as well as the loss of volume of the boards due to these parameters were assessed in this study.

2.2.9. Percentage of clear wood

The percentage of clear wood is an important factor that influences the mechanical properties of timber products, even though this factor is not directly considered in the current visual stress grading standards. Clear wood in this study refers to parts of each board, with at least 500 mm continuous length, that can meet the grade requirements for structural grade ‘one’ boards under AS 2082 (Standards Australia 2006). This allows no face knots larger than 1/7 of the width and or no edge knot larger than 1/7 of the thickness of the board. In addition, surface checking longer than 1/4 of the length of the boards is not allowed. Therefore, the diameter of knots and knotholes as well as the length of surface checks on the boards were considered for calculating the percentage of clear wood. Furthermore, areas of the boards that represented any insect trace, fungal decay, wane, mechanical damages, unrecoverable collapse, and end splits were excluded from the measurement of clear wood.

2.3. Segregation of the Boards

After identifying the most important visual characteristics and SRFs of the resource, the boards were divided into five quality groups based on their visual characteristics. Group one had the least extent of apparent SRFs and group five had the most extent of apparent SRFs. The segregation was based on the percentage of clear wood in each board, the number of continuous clear wood pieces, the type of knots on the edge and face of the boards, and surface checks as shown in Table 1.

Parameters such as mechanical damages, unrecoverable collapse, knothole, wane, number of knots, insect trace, fungal decay, and end split were taken into account by the measurement of the percentage of clear wood in each board and had an indirect effect on the segregation of the boards.

Table 1. Criteria used for the segregation of the boards.

Criteria	Group one	Group two	Group three	Group four	Group five
Percentage of clear wood	≥ 80% in total and in not more than three continuous clear pieces or ≥ 60% in only one continuous clear piece.	≥ 60% to < 80% in total or ≥ 40% to < 60% in only one continuous clear piece.	≥ 40% to < 60% in total or ≥ 35% to < 40% in only one continuous clear piece.	≥ 20% to < 40% in total.	≥ 0% to < 20% in total.
Type of knots on the edge and face of the board	Round and oval knots	Any	Any	Any	Any
Surface checking	Not allowed	Allowed	Allowed	Allowed	Allowed
Insect trace/fungal decay	Not allowed	Not allowed	Not allowed	Not allowed	Not allowed

2.4. Physical and Mechanical Tests

2.4.1. Static Four-point Bending test

The relationship between the visual characteristics and the actual mechanical properties of the boards was tested in four-point edgewise bending in accordance with the test procedure described in AS 4063.1 (Standards Australia 2010). Three boards were selected from each of the five quality groups for each board width using a simple random sampling (SRS) method. With this method, each board in each group had an equal probability of selection. One test sample, with a length equal to 20 times the width of the board, was cut from each selected boards and subjected to a static four-point bending test. Careful attention was taken during the sampling process to avoid selecting more than one board from the same log for each treatment. The experimental design of the four-point bending test is shown in Table 2.

Table 2. Experimental design of the static four-point bending test.

Species	Width (mm)	Group one ^a	Group two	Group three	Group four	Group five	Total No. of Samples
<i>E. nitens</i>	70	3	3	3	3	3	15
	90	2	3	3	3	3	14
	120	1	3	3	3	3	13
	140	1	3	3	3	3	13
Total No. of Samples							55

^a: Less than three boards could meet the requirements of group one in boards with 90 mm, 120 mm, and 140 mm widths. Hence, no average value is reported for the mechanical properties of these treatments. The results obtained from these treatments however were included in the statistical analysis described in section 0 (where all the results were analysed as one dataset).

In total, 55 samples with a good range of different visual characteristics and SRFs were tested. MOE and MOR values were calculated for the test samples using Equation 1 and Equation 2 (AS 4063.1, Standards Australia 2010).

Equation 1,

$$MOE = \frac{23l^3}{108bd^3 \left(\frac{\varphi_2 - \varphi_1}{F_2 - F_1} \right)}$$

Equation 2,

$$MOR = \frac{3F_{max} a}{bd^2}$$

where, b and d are the thickness and the width of boards (mm); l is the span length (mm); F_2 and F_1 are respectively 40% and 10% of the maximum load (F_{max}) at failure point (N); φ_2 and φ_1 are maximum displacement (mm) at F_2 and F_1 loads, respectively.

The failure mode and the total number and type of knots in the test samples and the loading zone particularly were counted with each test (see Figure 1). It was assumed that, due to stress concentration factor, total number of knots in the loading zone can potentially have a high impact on the bending properties of the boards. Hence, in addition to the various SRFs and visual characteristics, the concentration of knots in this zone and their possible impacts on MOE and MOR values were considered.

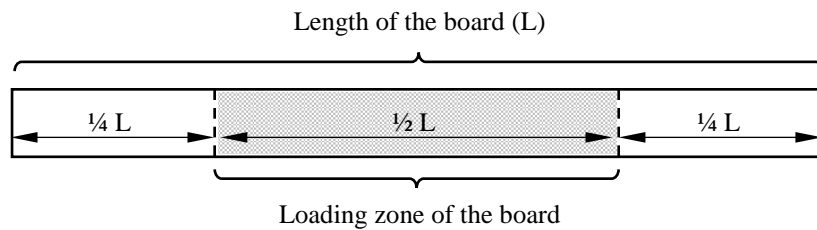


Figure 1. Loading zone in a test board.

2.4.2. Basic Density and MC

Three samples were recovered from separate areas of each tested board to determine its basic density and MC. These samples were free from defects and had a nominal cross-sectional area of $35 \times 35 \text{ mm}^2$. In total, 165 samples were collected and assessed. The basic density was calculated using Equation 3.

$$\rho = \frac{m_1}{V} \times \frac{100}{(100 + w)}$$

where, ρ is the basic density (kg/m^3); m_t is the mass of the sample at the time of testing (kg); V is the volume of the samples before oven-drying (m^3); w is the MC of the sample at the time of testing.

The MC was calculated using Equation 4.

Equation 4,

$$w = \frac{m_1 - m_0}{m_0} \times 100$$

where, m_0 is the oven-dry mass of the sample (kg).

2.5. Data Evaluation

IBM SPSS Statistics software (version 23) was used for this study's statistical analysis. Normality of the data obtained was determined using Kolmogorov-Smirnov test. Parametric statistical analyses were performed to test for statistical significance using one-way analysis of variance (ANOVA) test. The Duncan's test was conducted to analyse the differences between the independent groups when the ANOVA showed any significant impact for the test variables. The correlations between the studied variables were analysed using linear regression analysis and the Pearson correlation coefficient.

3. Results and Discussions

3.1. Recovery Rates of the Resource

When considering a timber resource for sawlog production, the recovery rate of the useable boards from the logs plays an important role in determining the efficiency and potential profitability of using such a resource. The higher the recovery rate of the useable boards, the higher the economic value of the resource. The nominal recovery rate and the dressed-board recovery rate of the *E. nitens* resource in this study were 25.8% and 22.32%, respectively. The nominal recovery rate was calculated based on the volume of the dried boards before the final planning stage divided by the volume of the harvested logs. The dressed-board recovery rate was calculated in the same way but based on the volume of all the boards that could successfully pass the final planning process at the thickness of 35 mm, regardless of their lengths.

3.2. Visual Characteristics and SRFs

The profile of common visual characteristics and SRFs in the *E. nitens* boards, obtained from 390 samples, are given in Table 3. The average volume of clear wood in the resource was 26.3%. The average individual lengths of clear wood pieces were 1252 mm, 952 mm, 946 mm, and 805 mm in board widths of 70 mm, 90 mm, 120 mm, and 140 mm respectively. The individual length of clear wood pieces in the boards varied from a minimum of 500 mm to a maximum of about 5000 mm (Figure 2).

More than 60% of the continuous clear wood pieces in the resource had a length between 500 mm to 1000 mm. Lengths of clear wood smaller than 500 mm were not measured.

Table 3. Visual characteristics and major SRFs of the fibre-managed *E. nitens* boards.

Measured items	Width of boards			
	70 mm	90 mm	120 mm	140 mm
Average length of boards (mm)	4551	4391	4551	4582
Clear wood (%)	60.8	24.7	22.1	13.6
Average length of continuous clear wood pieces (mm)	1252	952	946	805
Boards with end split (%)	48.6	58.8	67.7	73.8
Boards with knothole (%)	60.6	89.7	77.4	77.9
Boards with major knots (%)	95.4	98.9	100	100
Boards with mechanical damage/unrecoverable collapses (%)	45.9	51.5	54.8	64.8
Boards with significant bow (%)	11	0	0	4.1
Boards with significant crook (%)	14.7	0	0	8.2
Boards with significant twist (%)	0	0	0	0
Boards with significant surface checks (%)	18.4	47.4	64.5	63.9
Boards with wane (%)	21.1	13.4	4.8	12.3
Boards with fungal decay and/or insect trace (%)	0	0	0	0
Loss of volume due to mechanical damages/unrecoverable collapses (%)	8	10.7	9.6	15.7
Multiplicity of knots	5.4	6.8	6.8	9.1
Predominant slope of grain	1:15 \geq	1:15 \geq	1:10 to 1:15	1:15 \geq



Figure 2. Distribution of the length of continuous clear wood pieces in the boards.

Knots were the most frequent SRF in the resource, followed respectively by knothole, end splits, mechanical damage/unrecoverable collapse, surface checks, wane, and distortion along the length of the boards (i.e., bow and crook). The resource was free from fungal decay and insects attack. Knots and

knothole are common in the unpruned fibre managed *E. nitens* resource. While revised silvicultural techniques can reduce knot frequency, these have to be applied early in the tree's growth (Nolan et al., 2005). Consequently, knots and knothole will continue to be common SRF of timber recovered from unpruned stands currently in the ground. Another solution to knot frequency is finger jointing as major knots and knotholes can be docked out and remaining sections joined to make more structural reliable pieces. Though finger jointing is effective, this method may not be an efficient solution for this resource as the volume of clear wood was low at only 26.3 % of the recovered boards and 5.9% of the harvested logs.

The other important visual characteristic in the resource was mechanical damage that was also associated with unrecoverable collapse. These are problems arising from processing of the boards during harvesting, sawing, and drying steps. Mechanical damage was mainly from debarkers and sawing machines, while unrecoverable collapse appeared during the drying process. A significant loss in the volume of clear wood was noted in the resource due to mechanical damages and unrecoverable collapse. The loss of volume of clear wood ranged from 8% in the 70 mm boards to 15.7% in the 140 mm boards (Table 3). These negative characteristics could be reduced by utilising methods that are more appropriate for sawn timber production during harvesting, sawing, and drying processes. Inadequate sawing accuracy could intensify the development of unrecoverable collapse. The final planning process may remove unrecoverable collapse from the boards' surfaces if accurate sawing strategies are utilised (Washusen et al., 2009).

Surface checks, end splits, and distortion in the boards were substantial. These also appeared during the drying process, which suggests that the drying process for the resource needs to be reviewed and effectively modified. The amount of surface checks can significantly decrease if the logs are sawn using a quarter sawing pattern (Washusen et al., 2009). However, quarter sawing of the logs also decreases the total recovery rate of the boards (Washusen et al., 2004; 2007; 2009). The resource was free from twist distortion and the highest bow and crook rates appeared in the 70 mm boards. The 90 mm and 120 mm boards were also free from any significant distortions.

The resource proved to have a good range of slope of grain. The majority of the resource had a slope of grain of 1:15 or better. Less than 2% of the boards had the highest slope of grain of > 1:6 (Figure 3).

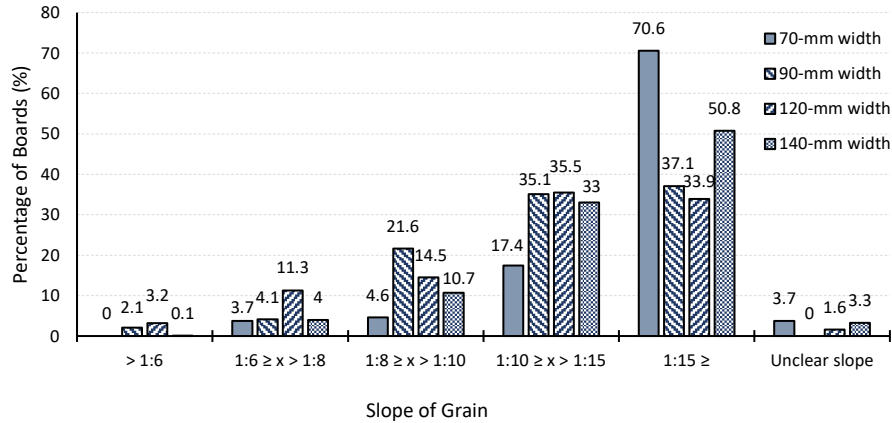


Figure 3. Variation of slope of grain in the boards.

3.3. Physical and Mechanical Properties

3.3.1. MOE, MOR, Basic Density, and MC

The overall average MOE and MOR values of the boards are given in Table 4. The average MC of the boards was $11.10 \pm 0.89\%$. The average basic density of the resource was $480.58 \pm 49.46 \text{ kg/m}^3$. The basic density of the fibre-managed *E. nitens* in this study was comparable to that of a plantation *E. nitens* resource studied by Blackburn et al. (2012).

In total, 27.27% of the boards tested in this study showed an MOE value between 12.0 GPa to 15.9 GPa, 41.83% of the boards had MOE values between 10.0 GPa to 11.9 GPa, and 25.45% of the boards showed MOE values between 8.0 GPa to 9.9 GPa. Only 5.45% of the boards exhibited an MOE less than 8.0 GPa. The mean MOE and MOR values of the 16-year-old unthinned and unpruned *E. nitens* were lower than that of 22-year-old thinned and pruned plantation *E. nitens* reported by Washusen et al. (2009) (Table 4). The samples tested by these researchers were obtained from the pruned parts of the logs, which is mainly consist of clear wood. However, the samples tested in the present study contained several SRFs and were not obtained from clear wood. This could be one of the reasons for the differences between the MOE and MOR values of the two resources. The other reasons could be the differences between the ages of the two resource, the sawing patterns, and the applied forestry regimes.

Table 4. Recovery rate, MOE, and MOR values of the fibre-managed *E. nitens* in this study against those of thinned and pruned plantation *E. nitens* reported by Washusen et al. (2009).

Species	Age	Thinned	Pruned	Sawing strategy	Nominal recovery rate (%)	MOE (GPa)	MOR (MPa)
Fibre-managed <i>E. nitens</i> ^a	16	No	No	Plain sawing	25.80	10.80 ± 1.88	43.55 ± 14.37
Plantation <i>E. nitens</i> ^b	22	6 years	6 years	Backsawn	29.8 ^c to 31.2 ^d	12.0 ^e to 13.2 ^f	99.0 ^g to 108.1 ^h

a: *E. nitens* tested in this study.

b: *E. nitens* tested by Washusen et al. (2009).

c, e, and g: these values are obtained from butt logs.

d, f, and h: these values are obtained from upper logs.

3.3.2. Modes of Failure

Predominant failure modes in the samples tested under bending loads were grain tension failure (40% of the samples) (Figure 4a), face and edge knot failures (45.45% of the samples) (Figure 4b), compression failure (9.1% of the samples) (Figure 4c), and catastrophic failure (5.45% of the samples) (Figure 4d). Most edge knot failures, observed in almost 12% of the samples, occurred in quartersawn boards.

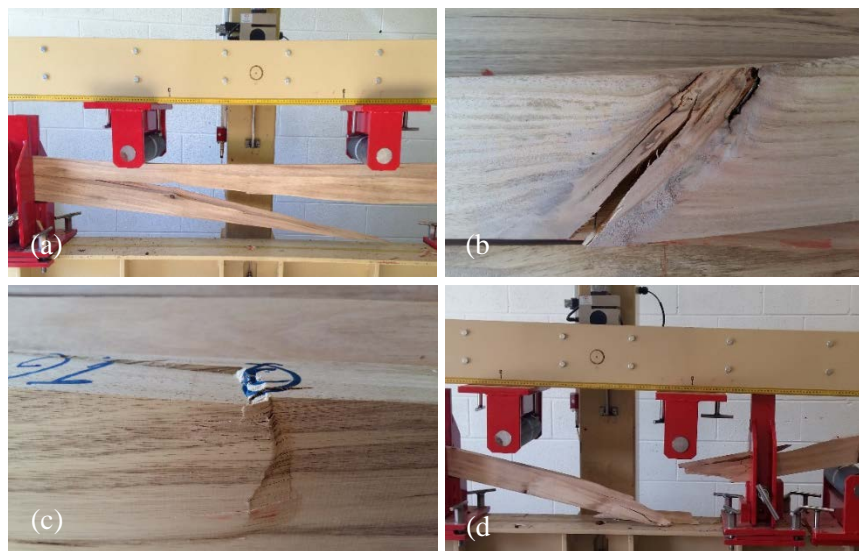


Figure 4. Failure modes of the boards under four-point bending load.

Different types of the above-mentioned failure modes were observed during the testing process. Compression failure occurred in boards that had the highest MOE and MOR values, whereas knot failure resulted in boards with the lowest MOE and MOR values. The average MOE and MOR values

in the boards with compression failure mode was 13.06 GPa and 56.52 MPa respectively. In the boards with knot failure mode the average MOE and MOR values were respectively 9.98 GPa and 38.18 MPa.

3.3.3. Impacts of Visual Characteristics, SRFs, and basic density on MOE and MOR

In the following sections, the boards tested under bending are referred to as the tested boards and the boards from which the tested boards were extracted are referred to as the source boards. The impacts of visual characteristics and SRFs of the source boards and the tested boards on MOE and MOR values are given in Table 5. For the statistical analysis, the results of the mechanical testing of the tested boards were listed against the data obtained from the assessment of visual characteristics of the tested boards and their respective source boards to determine statistical significance—as one dataset regardless of the treatments shown in Table 2.

Table 5. The ANOVA results for the impacts of visual characteristics, SRFs, and basic density on MOE and MOR values.

Independent variables	MOE	MOR
Slope of grain	***	***
Ring angle	**	NS
Ring angle \times Slope of grain	***	**
Width of boards	NS	NS
Percentage of clear wood in the source boards	NS	NS
Percentage of clear wood in the tested boards	***	***
Total number of knots in the source boards	NS	NS
Total number of knots in the tested boards	NS	*
Number of knots in the loading zone of the tested boards	**	**
Type of knots in the tested boards	**	**
Basic density	***	NS

NS = not significant; * = significant at $P < 0.05$; ** = significant at $P < 0.01$; *** = highly significant at $P < 0.001$.

The impact of slope of grain on the mechanical properties of the tested boards was highly significant ($p < 0.001$). The average MOE decreased by 32.02% with the increase in the slope of grain from $1:15 \geq$ to $1:6 \geq X > 1:8$ (Table 6). The same increase in the slope of grain caused 53% reduction in the average MOR in the tested boards. Even though the samples tested in this study were not obtained from clear wood, the strength reduction impact of slope of grain was close to that suggested by Bower et al. (2003)—which was reported to be 60% for wood in general.

Table 6. The average MOE and MOR values of the boards as a function of slope of grain.

Variable	Slope of grain	N	Mean (GPa)	Duncan's groups	COV (%)	Min. (GPa)	Max. (GPa)
MOE	1:15 \geq	22	11.82	A	12.18	10.05	15.94
	1:10 \geq X > 1:15	15	10.91	AB	10.54	9.64	12.87
	1:8 \geq X > 1:10	12	10.19	B	21.2	7.8	15.05
	1:6 \geq X > 1:8	6	8.03	C	10.83	6.62	8.82
Variable	Slope of grain	N	Mean (MPa)	Duncan's groups	COV (%)	Min. (MPa)	Max. (MPa)
MOR	1:15 \geq	22	51.36	A	24.07	12.7	74.3
	1:10 \geq X > 1:15	15	45.19	AB	23.86	23.2	60
	1:8 \geq X > 1:10	12	36.95	B	35.94	13.6	58.4
	1:6 \geq X > 1:8	6	24.02	C	24.65	15.1	30.8

N = Number of replicates; COV = Coefficient of variance.

The MOE values were significantly affected by annual ring angle ($p < 0.01$) (Table 5). The highest MOE values were obtained when the angle between the loading direction and annual rings axis was $0^\circ \pm 15^\circ$ (i.e., backsawn boards). The lowest MOE was obtained when the loading direction was perpendicular to the annual rings ($90^\circ \pm 15^\circ$ or quartersawn boards). The average MOE fell somewhere between that of backsawn boards and quartersawn boards when the angle between the loading direction and annual rings was $45^\circ \pm 15^\circ$ (i.e., transitional-sawn boards). There was no significant difference between the MOE values of transitional-sawn and quartersawn boards (Table 7).

Table 7. The average MOE and MOR values of the boards as a function of annual ring angle.

Variable	Annual Ring Angle	N	Mean (GPa)	Duncan's groups	COV (%)	Min. (GPa)	Max. (GPa)
MOE	$0^\circ \pm 15^\circ$	22	11.9	A	14.29	8.81	15.94
	$45^\circ \pm 15^\circ$	14	10.24	B	12.3	6.62	12.03
	$90^\circ \pm 15^\circ$	19	9.94	B	19.01	7.35	15.05
Variable	Annual Ring Angle	N	Mean (MPa)	Duncan's groups	COV (%)	Min. (MPa)	Max. (MPa)
MOR	$0^\circ \pm 15^\circ$	22	47.6	A	24.6	20.8	74.3
	$45^\circ \pm 15^\circ$	14	42.93	A	33.19	12.7	63.3
	$90^\circ \pm 15^\circ$	19	39.34	A	42.04	13.6	65.5

The impact of annual ring angle on MOR values was non-significant ($p > 0.05$). Four of the quartersawn boards tested in this study had a high slope of grain of $1:6 \geq X > 1:8$ —that was the worst slope of grain in the tested boards. The average MOE and MOR values in these four boards were as low as 8.19 GPa and 23.12 MPa, respectively. By contrast, only one of the backsawn boards and one of the transitional-sawn boards had the same slope of grain of $1:6 \geq X > 1:8$. Hence, the slope of grain in the four boards intensified the overall impact of annual ring angle on the mechanical properties of the tested boards. The ANOVA results also support this argument as the interaction effect of slope of grain and annual

ring angle on the MOE and MOR values was highly significant ($p < 0.001$ for MOE and $p < 0.01$ for MOR) (Table 5). This could be one of the reasons for such a difference in the mechanical properties of quartersawn boards versus backsawn and transitional-sawn boards. There was no statistically significant difference ($p > 0.05$) between the mechanical properties of boards from the four different widths (Table 5).

The statistical analysis revealed that the percentage of clear wood in the source boards had no significant impact on the mechanical properties of the tested boards ($p > 0.05$), whereas the mechanical properties was highly affected by the percentage of clear wood in the tested boards ($p < 0.001$ for both MOE and MOR) as presented in Table 5. This suggests that the visual characteristics of long boards could not necessarily be representative of the mechanical properties when the boards are cut to a subsequent length. However, with the current visual stress-grading procedures, timber boards are only graded based on their original length at the mill. Based on the results obtained in this part of the study, a two-step visual stress grading process may be more reliable—the first step at the mill and the second step when the boards are cut to the final dimensions. The highest MOE and MOR values were obtained with the tested boards that had a total percentage of clear wood of ≥ 80 (Table 8). The average MOE and MOR values decreased by, respectively, 21.85% and 36.76% with the decrease in the percentage of clear wood from ≥ 80 to < 40 .

Table 8. The average MOE and MOR values of the boards as a function of the percentage of clear wood in the tested boards.

Variable	Clear wood (%)	N	Mean (GPa)	Duncan's groups	COV (%)	Min. (GPa)	Max. (GPa)
MOE	≥ 80	29	11.76	A	11.9	9.75	15.94
	$70 \leq X < 80$	9	10.38	AB	22.25	7.35	15.05
	$40 \leq X < 70$	11	9.5	B	16.84	6.62	12.57
	< 40	6	9.19	B	10.34	8.27	10.72
Variable	Clear wood (%)	N	Mean (MPa)	Duncan's groups	COV (%)	Min. (MPa)	Max. (MPa)
MOR	≥ 80	29	51.03	A	20.03	31.1	74.3
	$70 \leq X < 80$	9	38.68	B	44.52	12.7	57.3
	$40 \leq X < 70$	11	33.98	B	36.32	15.1	56.7
	< 40	6	32.27	B	37.09	13.6	45.4

Total number of knots in the source boards had no important impact on the MOR values ($p > 0.05$). However, the impact of total number of knots in the tested boards on the MOR values was significant at 95% level of confidence (Table 5). The average MOR decreased significantly as the total number of knots in the tested boards increased. The total number of knots in either the source boards or the tested boards did not significantly affect the MOE values ($p > 0.05$).

Both MOE and MOR values were meaningfully affected by the number of knots in the loading zone of the tested boards ($p < 0.01$) as presented in Table 5. With an increase in the number of knots in the

loading zone of the tested boards from zero to four, the average MOE decreased by 23.40% (Table 9). The same increase in the number of knots in the loading zone of the tested boards reduced the average MOR values substantially by 40.72%.

Table 9. The average MOE and MOR values of the boards as a function of number of knots in the loading zone of the tested boards.

Variable	No. Knots in the loading zone	N	Mean (GPa)	Duncan's groups	COV (%)	Min. (GPa)	Max. (GPa)
MOE	0 (No knots)	13	12.22	A	14.4	9.75	15.94
	1	18	10.98	AB	9.93	8.81	12.89
	2	8	10.72	AB	14.27	8.29	12.57
	3	9	9.59	B	28.68	6.62	15.05
	4	7	9.36	B	5.66	8.32	10.01
Variable	No. Knots in the loading zone	N	Mean (MPa)	Duncan's groups	COV (%)	Min. (MPa)	Max. (MPa)
MOR	0 (No knots)	13	57.07	A	16.47	33.8	74.3
	1	18	42.53	B	27.65	12.7	56.3
	2	8	38.43	B	42.62	15.1	63.3
	3	9	38.19	B	40.74	13.6	57.3
	4	7	33.83	B	24.06	22.5	42.1

The type of knots in the tested boards significantly affected both MOE and MOR values ($p < 0.01$). Spike knots reduced the average MOE values by 24.47%—the average MOE was 12.64 GPa in boards with no knots. The MOE reduction impact of round knots, however, was 14.52%. Spike knots also decreased the MOR values by 41.14%—the average MOR was 60.93 MPa in boards with no knots. The MOR values decreased by 29.96% in boards with round knots.

The average MOE values of the boards were significantly affected by basic density ($p < 0.001$), whereas the effect of basic density on the average MOR values was insignificant ($p > 0.05$).

A linear regression analysis was performed to see if the MOE and MOR values of the tested boards could be predicted. The results indicated that the MOE of the tested boards might not reliably be predicted by their individual basic density—the determination coefficient was as low as $R^2=0.355$. The average difference between the predicted values of MOE using density and the empirical data was 11.43% (Figure 5). The results also indicated that the MOR values of the tested boards could not be predicted by their individual basic density—the average difference was 36.43% with $R^2= 0.076$ (Figure 6). Likewise, the MOR values could not be predicted reliably by MOE—the average difference was 24.97%, although the determination coefficient improved to $R^2= 0.511$. The determination coefficient for predicting the MOR values based on both MOE and basic density was $R^2= 0.546$. This result

indicated that the MOR values for the 16-year-old *E. nitens* might not be satisfactorily predicted by MOE and or basic density themselves. This finding is in good agreement with those reported in the previous studies on other wood species from both native and pruned plantation forests (Johansson et al., 1992; Larsson et al., 1998; Steiger and Arnold 2009; Washusen et al., 2009; Ranta-Maunus et al., 2011; Olsson et al., 2012; Lukacevic et al., 2015).

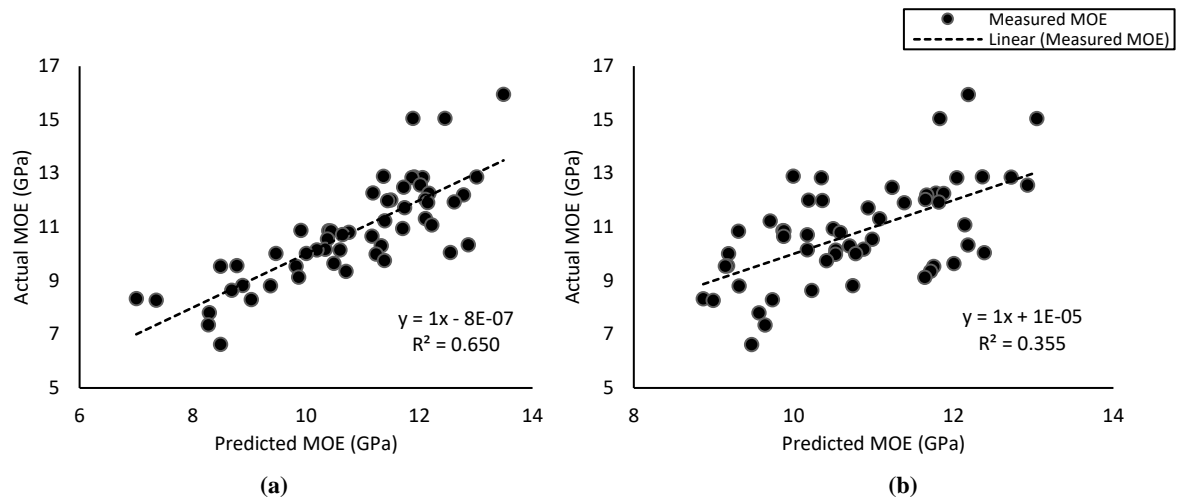


Figure 5. Correlation between actual MOE and predicted MOE values using Equation 5 (a) and basic density (b).

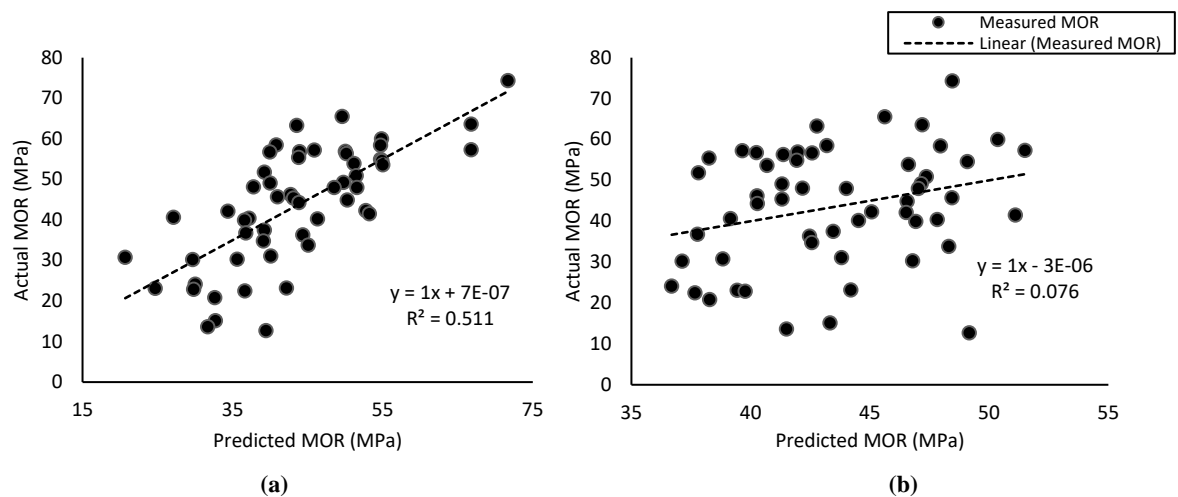


Figure 6. Correlation between actual MOR and predicted MOR values using MOE (a) and basic density (b).

The determination coefficient for the prediction of MOE considerably improved up to $R^2 = 0.650$ when the other indicating parameters including slope of grain, annual ring angle, percentage of clear wood, number of knots in the loading zone, and type of knots in the tested boards were included in the analysis.

With Equation 5, the average difference between the predicted MOE values and the empirical data reduced to 7.74% ($R^2 = 0.650$).

Equation 5,

$$MOE_{(GPa)} = (D \times a1) + (R \times a2) + (S \times a3) + (C \times a4) + (N \times a5) + (T \times a6) + a7$$

where, D is the basic density of the plantation *E. nitens* timber within the range of $480.58 \pm 49.46 \text{ kg/m}^3$. R is annual ring angle: 1 for annual ring angle $0^\circ \pm 15^\circ$; 2 for annual ring angle $45^\circ \pm 15^\circ$; 3 for annual ring angle $90^\circ \pm 15^\circ$. S is slope of grain: 1 for slope of grain $1:15 \geq$; 2 for slope of grain $1:10 \geq X > 1:15$; 3 for slope of grain $1:8 \geq X > 1:10$; 4 for $1:6 \geq X > 1:8$. C is clear wood: 1 for clear wood $< 40\%$; 2 for clear wood $40\% \leq X < 70\%$; 3 for clear wood $70\% \leq X < 80\%$; 4 for clear wood $\geq 80\%$. N is number of knots in the loading zone. T is type of knots: 0 for boards with no knots; 1 for boards with round/oval knots; 2 for boards with spike knots. $a1$ to $a7$ are regression coefficients as follow: $a1 = 0.016$; $a2 = -0.395$; $a3 = -0.490$; $a4 = 0.060$; $a5 = -0.266$; $a6 = -0.354$; $a7 = 5.720$.

Equation 5 is valid for *E. nitens* timber. When the same procedure was followed for the MOR values of the test boards, with all the indicating parameters plus MOE included, the predicted results for a few samples could not satisfactorily be fitted to the empirical data, resulting in a high average difference of 22.55%, even though the determination coefficient improved considerably to $R^2 = 0.617$. In these samples, sudden failures occurred before they can reach their maximum load-carrying capacities. The possible reason for such a phenomenon could be found in the failure modes of these samples. The samples failed due to the existence of knots on the tension zone of the board (Figure 7a and Figure 7b), localised variation in the slope of grain in the tension zone (Figure 7c), and brittle failure around knots in the loading zone of the board (Figure 7d). This result suggests that the location of knots across the width of the board as well as localised variation in the slope of grain could be important in determining the maximum load-carrying capacity and MOR values of the boards. These two criteria are disregarded in most current standard methods such as AS 2082 (Standards Australia 2007). This observation is also in agreement with the findings of Lukacevic et al. (2015). These researchers indicated that the position of knots along the length and also across the width of the boards is so important that it can be used as a non-destructive indicating parameter to estimate the strength properties of the boards.

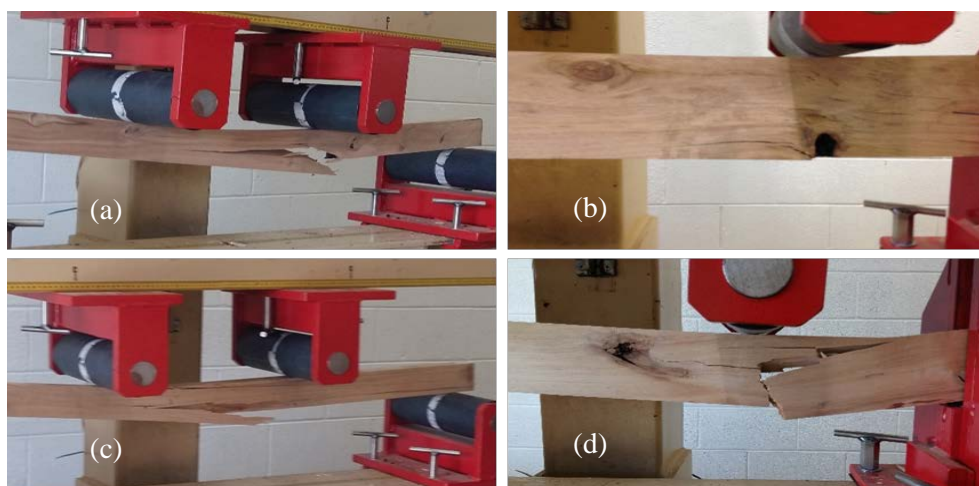


Figure 7. Sudden failure in a few samples tested under four-point bending load.

3.3.4. Development of grade classes

The average MOE and MOR values for the five wood quality groups are depicted in Figure 8. No significant correlation was found between the mechanical properties and basic density of the tested boards against the wood quality groups that were established based on the visual characteristics, SRFs, and percentage of clear wood in the source boards (Table 10).

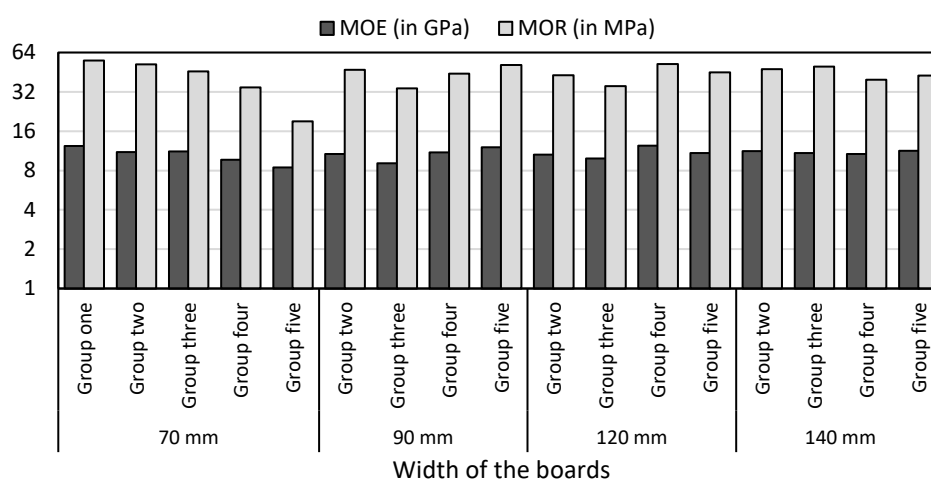


Figure 8. Average MOE and MOR values of boards in each wood quality group.

Table 10. The correlation between the wood quality groups and MOE, MOR, and basic density of the tested boards.

Indicating parameters	Wood quality Groups		
	Pearson Correlation	Sig. (2-tailed)	N

MOE	0.106	0.442	55
MOR	0.069	0.615	55
Basic density	0.095	0.491	55 ^a

^a: Three samples were tested for each board (i.e., $3 \times 55 = 165$ samples in total)

This result indicates that the visual characteristics of the source boards could not necessarily be representative of the mechanical properties and basic density of the tested boards. Hence, a successful grading system needs to be established based on the final dimensions of the boards, which is determined according to their target applications—this is not currently considered in the grading procedures of hardwoods at the mill level.

An attempt was made to create effective structural grade groups that can ensure reasonable correlations between the visual characteristics and SRFs with the mechanical properties and basic density of the boards. The tested boards were re-arranged in different groups, but this time based on their mechanical properties, instead of their visual characteristics (repeating the process in the reverse order). The visual characteristics of the tested boards in each strength/stiffness class were analysed and the most frequent combinations of the visual characteristics and SRFs in each group were identified. The statistical analyses were then re-performed to determine the importance of correlations between the visual characteristics and SRFs with the mechanical properties of the tested boards in the new grade groups. The best correlations between the mechanical properties and the visual characteristics and SRFs were found when the tested boards were divided into the following three grade groups:

- Grade group A: MOE between 12 GPa to 15.9 GPa and corresponding MOR values.
- Grade group B: MOE between 10 GPa to 11.9 GPa and corresponding MOR values.
- Grade group C: MOE less than 10 GPa and corresponding MOR values.

The correlations between the suggested grade groups and MOE, MOR, basic density, and visual characteristics and SRFs (except type of knots) of the tested boards were highly significant at 99% level of confidence (Table 11). The density varied significantly between the three grade groups ($p < 0.001$) (Table 12). The average basic density decreased by 13.15% from grade group A to grade group C.

Table 11. The correlation between the three grade groups and MOE, MOR, basic density, and visual characteristics of the tested boards.

Indicating parameters	Grade group		
	Pearson Correlation	Sig. (2-tailed)	N
MOE	-0.877**	0	55
MOR	-0.646**	0	55
Ring angle	0.474**	0	55
Slope of grain	0.580**	0	55
Ring angle \times Slope of grain	0.524**	0	55
Percentage of clear wood	-0.561**	0	55

Total number of knots	0.345**	0.01	55
Number of knots in the loading zone	0.529**	0	55
Type of knots	0.225	0.099	55
Basic density	-0.528**	0	55

** = Correlation is significant at the 0.01 level (2-tailed).

Table 12. The average basic density values in the three grade groups.

Grade level	N	Basic density (kg/m ³)	SD	Duncan's group
Grade A	15	521.27	41.68	A
Grade B	23	474.66	39.03	B
Grade C	17	452.70	47.03	B

Analysing the data obtained suggested that most of the tested boards in the three MOE classes had the combinations of visual characteristics and SRFs shown in Table 13.

Table 13. Predominant combinations of visual characteristics and SRFs in the three grade groups.

Grade Level	Ring angle	Slope of grain	Clear wood	Total No. of Knots	No. of Knots in the loading zone	Probability *
Grade A	0°	1:10 ≥	≥ 80	≤ 2	≤ 1	75.00% in group A 16.67% in group B 8.33% in group C
Grade B	45° and 90°	1:10 ≥	≥ 70	≤ 3	≤ 2	81.25% in group B 12.50% in group A 6.25% in group C
Grade C	45° and 90°	1:10 <	Any	≥ 1	≥ 1	100% in group C

*: This shows the possible grade level that a board may receive if they can meet the combination of features in the respective group.

While this was not an objective of this paper, if the criteria given in Table 13 is going to be used for grading of fibre-grown *E. nitens*, the probability of existence of over-graded boards in grade group A might be 25%. Using the criteria identified for grade group B, 12.50% of the boards might be downgraded and 6.25% of the boards might be over-graded. None of the boards might be over-graded with the criteria identified for grade group C. A bigger sample size in future research may improve the accuracy of such a method. It must be noted that there could be levels of uncertainty and inconsistency associated both with this method and with visual grading of timber in the first place—as suggested in previous studies as well (Kline et al., 2000; Roblot et al., 2008). As an instance, the results in the present study showed that the strength/stiffness of the boards are higher when the slope of grain is 1:10 or lower. However, some of the boards that were categorised in the grade group C, which was the worst grade group, had a slope of grain equal to 1:10 or even better. Another example is the annual ring angle. Based

on the results, the strength/stiffness of the boards is the highest when the annual ring angle is $0^\circ \pm 15^\circ$ (backsawn boards). However, the stiffness in some of the boards with the annual ring angle of $0^\circ \pm 15^\circ$ was as low as 8.5 GPa (which includes in grade group C). The same issues are associated with the current standard methods on visual grading of timber. Laboratory testing on visually graded boards in previous studies revealed that a small percentage of the boards exhibited a strength class below their respective grade level, while a high percentage of the boards were meaningfully stronger than their suggested grade level in the relevant standard (Kretschmann and Hernandez 2006). While this gives a reasonable safety factor from an engineering point of view, there is a good chance that using the current visual stress grading methods significant amounts of quality boards are downgraded. On the other hand, over-graded boards, even a small percentage, can be dangerous as they might be used under load levels that they are unable to carry. Therefore, the effectiveness of the current standard methods for visual stress grading of timber needs to be addressed considering these issues in the future studies.

4. Conclusions

The following conclusions were drawn from the results obtained in the present study and the statistical analyses:

- The recovery rate of boards from the 16-year-old fibre-managed plantation *E. nitens* in this study was lower than that of a 22-year-old thinned and pruned plantation *E. nitens* reported in the literature.
- Knots and knotholes were the most important SRFs of the boards recovered from fibre-managed plantation *E. nitens*.
- Substantial mechanical damages, unrecoverable collapse, surface checks, end splits, and drying distortions were associated with the boards recovered from the resource. This may suggest that current harvesting, sawing, and drying regimes are unsuitable for this process.
- The visual characteristics and quality of long boards could not necessarily be representative of the mechanical properties when the boards are cut to a subsequent length. Hence, a two-step visual stress grading process may be more reliable—the first step at the mill and the second step when the boards are cut to the final dimensions required in their target applications.
- MOE and MOR of the fibre-managed *E. nitens* boards were significantly affected by annual ring angle, slope of grain, number of knots in the loading zone, and type of knots. The MOE of the boards was significantly affected by basic density. The impact of total number of knots on MOR values as well as the interaction impact of annual ring angle and slope of grain on both MOE and MOR values were also statistically significant.
- MOR values could not be predicted satisfactorily by either basic density or MOE of the boards. MOE values might be predicted using a multiple linear regression equation that was developed

in this study based on the correlations between the visual characteristics and SRFs with mechanical properties of the boards. It might be possible to develop the same procedure for other species based on relevant laboratory testing in future studies.

- Three structural grade groups with their respective criteria were proposed for fibre-managed plantation *E. nitens* boards in this study. Strong correlations were found between the three grade groups and the visual characteristics, SRFs, basic density, and mechanical properties of the boards.

Acknowledgment

This study was carried out under the Australian Research Council, Centre for Forest Value, University of Tasmania, TAS, Australia (Grant Reference: IC150100004). The financial support from Forest and Wood Products Australia Limited (FWPA), Melbourne, VIC, Australia is acknowledged (Grant Number: PNB387-1516). The authors are grateful for the support from Forico Pty Ltd. in providing the logs and Britton Brothers Pty Ltd. for the milling of the logs and seasoning of the boards.

References

- [1] Almazán, F. A., Prieto, E. H., Martitegui, F. A., & Richter, C. (2008). Comparison of the Spanish visual strength grading standard for structural sawn timber (UNE 56544) with the German one (DIN 4074) for Scots pine (*Pinus sylvestris* L.) from Germany. *Holz als Roh-und Werkstoff*, 66(4), 253-258. <https://doi.org/10.1007/s00107-008-0241-9>.
- [2] AS 2082 (2007). Timber - Hardwood - Visually stress graded for structural purposes. Standards Australia, Australia.
- [3] AS 4063.1 (2010). Characterisation of structural timber, Part 1: Test Methods. Standards Australia, Australia.
- [4] AS 1080.2 (2006). Timber - Methods of test - Slope of grain. Standards Australia, Australia.
- [5] Baño, V., Arriaga, F., Soilán, A., & Guaita, M. (2011). Prediction of bending load capacity of timber beams using a finite element method simulation of knots and grain deviation. *Biosystems Engineering*, 109(4), 241-249. <https://doi.org/10.1016/j.biosystemseng.2011.05.008>
- [6] Blackburn, D. P., Hamilton, M. G., Harwood, C. E., Innes, T. C., Potts, B. M., & Williams, D. (2011). Genetic variation in traits affecting sawn timber recovery in plantation-grown *Eucalyptus nitens*. *Annals of Forest Science*, 68(7), 1187. <https://doi.org/10.1007/s13595-011-0130-y>
- [7] Blackburn, D., Farrell, R., Hamilton, M., Volker, P., Harwood, C., Williams, D., & Potts, B. (2012). Genetic improvement for pulpwood and peeled veneer in *Eucalyptus nitens*. *Canadian Journal of Forest Research*, 42(9), 1724-1732. <https://doi.org/10.1139/x2012-105>
- [8] Blackburn, D., Hamilton, M., Harwood, C., Innes, T., Potts, B., & Williams, D. (2010). Stiffness and checking of *Eucalyptus nitens* sawn boards: genetic variation and potential for genetic improvement. *Tree Genetics & Genomes*, 6(5), 757-765. <https://doi.org/10.1007/s11295-010-0289-7>

- [9] Bower, J. L., Shmulsky, R., & Haygreen, J. G. (2003). *Forest products and wood science-an introduction*. Iowa State Press, Ames, IA.
- [10] Chuquitaype, C. M., & Elghazouli, A. Y. (2016). Chapter 8 Design of Timber Structures. In *Seismic Design of Buildings to Eurocode 8* (pp. 213-234). Crc Press.
- [11] De Araujo, V. A., Cortez-Barbosa, J., Gava, M., Garcia, J. N., de Souza, A. J. D., Savi, A. F., ... & Lahr, F. A. R. (2016). Classification of wooden housing building systems. *BioResources*, 11(3), 7889-7901. <https://doi.org/10.15376/biores.11.3.DeAraujo>
- [12] Derikvand, M., Nolan, G., Jiao, H., & Kotlarewski, N. (2017). What to do with structurally low-grade wood from Australia's plantation eucalyptus; building application?. *BioResources*, 12(1), 4-7. <https://doi.org/10.15376/biores.12.1.4-7>
- [13] Feio, A., & Machado, J. S. (2015). In-situ assessment of timber structural members: Combining information from visual strength grading and NDT/SDT methods—A review. *Construction and Building Materials*, 101, 1157-1165. <https://doi.org/10.1016/j.conbuildmat.2015.05.123>
- [14] Fidan, M. S., Yaşar, Ş. Ş., Yaşar, M., Atar, M., & Alkan, E. (2016). Effect of seasonal changes on the combustion characteristics of impregnated cedar (*Cedrus libani* A. Rich.) wood. *Construction and Building Materials*, 106, 711-720. <https://doi.org/10.1016/j.conbuildmat.2015.12.133>
- [15] Johansson CJ, Brundin J, Gruber R (1992) Stress grading of swedish and german timber—a comparison of machine stress grading and three visual grading systems. Tech. Rep. 23, Swedish National Testing and Research Institute.
- [16] Kline, D. E., Surak, C., & Araman, P. A. (2000). A lumber grading system for the future: an update evaluation. In *Proceedings, 28th Annual Hardwood Symposium*. 123-129.
- [17] Koman, S., Feher, S., Abraham, J., & Taschner, R. (2013). Effect of knots on the bending strength and the modulus of elasticity of wood. *Wood Research*, 58(4), 617-626.
- [18] Kretschmann, D. E., & Hernandez, R. (2006). Grading timber and glued structural members. In *Primary Wood Processing* (pp. 339-390). Springer Netherlands.
- [19] Krzosek, S. (2011). Timber strength grading of *Pinus sylvestris* L. using a visual method according to Polish Standard PN-82/D-94021 and German Standard DIN 4074. *Wood Research*, 56(3), 435-440.
- [20] Larsson, D., Ohlsson, S., Perstorper, M., & Brundin, J. (1998). Mechanical properties of sawn timber from Norway spruce. *European Journal of Wood and Wood Products*, 56(5), 331-338. <https://doi.org/10.1007/s001070050329>
- [21] Li, T., Zhu, M., Yang, Z., Song, J., Dai, J., Yao, Y., ... & Hu, L. (2016). Wood composite as an energy efficient building material: guided sunlight transmittance and effective thermal insulation. *Advanced Energy Materials*, 6(22). <https://doi.org/10.1002/aenm.201601122>.
- [22] Lukacevic, M., Füssl, J., & Eberhardsteiner, J. (2015). Discussion of common and new indicating properties for the strength grading of wooden boards. *Wood Science and Technology*, 49(3), 551-576. <https://doi.org/10.1007/s00226-015-0712-1>
- [23] Lycken, A. (2006). Comparison between automatic and manual quality grading of sawn softwood. *Forest Products Journal*, 56(4), 13-18.

- [24] Muñoz, G. R., Gete, A. R., & Saavedra, F. P. (2011). Implications in the design of a method for visual grading and mechanical testing of hardwood structural timber for designation within the European strength classes. *Forest Systems*, 20(2), 235-244. <https://doi.org/10.5424/fs/2011202-9771>
- [25] Nicoletta, T., Valdés, M., De Nicolo, B., & Fragiaco, M. (2017). Grading of low-quality wood for use in structural elements. In *Wood in Civil Engineering*. InTech. <https://doi.org/10.5772/67129>.
- [26] Nolan, G. B., Greaves, B. L., Washusen, R., Parsons, M., & Jennings, S. (2005). Eucalypt Plantations for Solid Wood Products in Australia-A Review 'If you don't prune it, we can't use it'. Forest & Wood Products Research & Development Corporation, Vic. Australia.
- [27] Olsson, A., Oscarsson, J., Johansson, M., & Källsner, B. (2012). Prediction of timber bending strength on basis of bending stiffness and material homogeneity assessed from dynamic excitation. *Wood Science and Technology*, 46(4), 667-683. <https://doi.org/10.1007/s00226-011-0427-x>
- [28] Piter, J. C., Zerbino, R. L., & Blaß, H. J. (2004). Visual strength grading of Argentinean *Eucalyptus grandis*. *Holz als Roh-und Werkstoff*, 62(1), 1-8. <https://doi.org/10.1007/s00107-003-0433-2>
- [29] Ramage, M. H., Burrige, H., Busse-Wicher, M., Fereday, G., Reynolds, T., Shah, D. U., ... & Allwood, J. (2017). The wood from the trees: The use of timber in construction. *Renewable and Sustainable Energy Reviews*, 68, 333-359. <https://doi.org/10.1016/j.rser.2016.09.107>
- [30] Ranta-Maunus, A., Denzler, J. K., & Stapel, P. (2011). Strength of European timber. Part 2. Properties of spruce and pine tested in Gradewood project. VTT Technical Research Centre of Finland, Espoo, Finland.
- [31] Roblot, G., Coudegnat, D., Bleron, L., & Collet, R. (2008). Evaluation of the visual stress-grading standard on French Spruce (*Picea excelsa*) and Douglas fir (*Pseudotsuga menziesii*) sawn timber. *Annals of Forest Science*, 65(8), pp 812. <https://doi.org/10.1051/forest:2008071>
- [32] Santi, S., Pierobon, F., Corradini, G., Cavalli, R., & Zanetti, M. (2016). Massive wood material for sustainable building design: the Massiv-Holz-Mauer wall system. *Journal of Wood Science*, 62(5), 416-428. <https://doi.org/10.1007/s10086-016-1570-7>
- [33] Stapel, P., & van de Kuilen, J. W. G. (2014). Efficiency of visual strength grading of timber with respect to origin, species, cross section, and grading rules: A critical evaluation of the common standards. *Holzforschung*, 68(2), 203-216. <https://doi.org/10.1515/hf-2013-0042>
- [34] Steiger, R., & Arnold, M. (2009). Strength grading of Norway spruce structural timber: revisiting property relationships used in EN 338 classification system. *Wood Science and Technology*, 43(3-4), 259-278. <https://doi.org/10.1007/s00226-008-0221-6>
- [35] Viguier, J., Jehl, A., Collet, R., Bleron, L., & Meriaudeau, F. (2015). Improving strength grading of timber by grain angle measurement and mechanical modeling. *Wood Material Science & Engineering*, 10(1), 145-156. <https://doi.org/10.1080/17480272.2014.951071>
- [36] Washusen, R., Harwood, C., Morrow, A., Northway, R., Valencia, J. C., Volker, P., ... & Farrell, R. (2009). Pruned plantation-grown *Eucalyptus nitens*: Effect of thinning and conventional processing practices on sawn board quality and recovery. *New Zealand Journal of Forestry Science*, 39(1), 39-55.
- [37] Washusen, R., Harwood, C., Morrow, A., Valencia, J.C., Volker, P., Wood, M., Innes, T., Ngo Dung, Northway, R. and Bojadzic, M. (2007) Goulds Country *Eucalyptus nitens* Thinning Trial: Solid Wood Quality and Processing Performance Using Conventional Processing Strategies. Technical Report 168. CRC for Forestry.

- [38] Washusen, R., Reeves, K., Hingston, R., Davis, S., Menz, D., & Morrow, A. (2004). Processing pruned and un-pruned blue gum (*Eucalyptus globulus*) to produce high value products. Forest and Wood Products Research and Development Corporation Report PN03, 1315, 25-27, Melbourne, Australia.
- [39] Yasar, Ş. Ş., Fidan, M. S., Yaşar, M., Atar, M., & Alkan, E. (2017). Combustion properties of impregnated spruce (*Picea orientalis* L.) wood. *Construction and Building Materials*, 143, 574-579. <https://doi.org/10.1016/j.conbuildmat.2017.03.141>

Appendix C: Paper III

Publication reference: Derikvand, M., Kotlarewski, N., Lee, M., Jiao, H., & Nolan, G. (2018). Flexural and visual characteristics of fibre-managed plantation *Eucalyptus globulus* timber. Wood Material Science & Engineering, 1-10.

Flexural and visual characteristics of fibre-managed plantation *Eucalyptus globulus* timber

Mohammad Derikvand, Nathan Kotlarewski, Michael Lee, Hui Jiao, and Gregory Nolan

Abstract: The main goal of this study was to investigate the visual characteristics, recovery rate, and flexural properties of sawn boards from a fibre-managed plantation *Eucalyptus globulus* resource as a potential raw material for structural building applications. The impacts of the visual characteristics, strength-reducing features, and variation in basic density and moisture content on the bending modulus of elasticity (MOE) and modulus of rupture (MOR) of the boards were investigated. The reliabilities of different non-destructive methods in predicting MOE and MOR of the boards were evaluated, including log acoustic wave velocity measurement and numerical modellings. The MOE and MOR of the boards were significantly affected by the slope of grain, percentage of clear wood, and total number of knots in the loading zone of the boards. The normal variation in basic density significantly influenced the MOE of the boards while its effect on the MOR was insignificant. The numerical models developed using the artificial neural network (ANN) showed better accuracies in predicting the MOE and MOR of the boards than traditional multi-regression modelling and log acoustic wave velocity measurement. The ANN models developed in this study showed more than 78.5% and 79.9% success in predicting the adjusted MOE and MOR of the boards, respectively.

Keywords: plantation Eucalypt; timber processing; bending test; acoustic wave velocity; artificial neural network; non-destructive testing.

Introduction

The plantation hardwood estate in Australia is mainly *Eucalyptus globulus* (*E. globulus*) (Gavran 2015). The majority of this estate exists in unthinned and unpruned stands that are

managed in short rotation cycles and exported as wood chips (Gavran 2015). Plantation stands that are unthinned and unpruned produce thin stems with substantial strength-reducing features (SRFs) such as knots. Both factors affect the recovery rate of useable sawn board from this resource. Australia's hardwood timber sector predominantly relies on mill logs from native forests and imported wood products however, there is an interest in the timber industry to establish practical ways to use fibre-grown plantation eucalypt in Australia's solid wood products industry (Derikvand et al. 2017, 2018).

Most *E. globulus* plantations are harvested at an early age between 15 to 20 years old (Gavran 2015). As a result, log diameter is small compared to logs from mature, native forests. The timber boards recovered from these plantation logs contain a considerable amount of SRFs when sawn. This complicates the performance and workability of individual boards (Nolan *et al.* 2005, Derikvand *et al.* 2017) and limits the potential of using this resource in structural building applications. The effectiveness of processing procedures (i.e., harvesting, sawing, and drying) can also influence both the quality of the boards and the efficiency of using this resource for sawn timber production (Connell 2003, Derikvand *et al.* 2018).

In order to utilise the resource effectively in structural applications and to establish the relevant allowable stress values, it is important to understand the resource's physical and mechanical characteristics. The need for an effective structural grading system for timber boards recovered from fibre-managed estate is therefore warranted. For hardwood, the relevant grading standards (such as AS 2082, Standards Australia 2007) are generally based on segregating the boards into different structural grades using their visual characteristics and SRFs as indicating parameters—which is known as visual stress grading. The grading methods described in such standards are based on the correlations between the visual characteristics and SRFs with the mechanical properties of the boards. In order to inform the development of a relevant visual stress grading method for fibre-managed *E. globulus* resource, it is vital to

understand the correlations between the visual characteristics and SRFs with the mechanical properties (strength and stiffness) of the resource.

Previous studies have demonstrated that some of the mechanical properties of timber, such as its flexural properties, might be predicted using relevant non-destructive techniques (NDTs) as well—which can further be used to improve the accuracy of structural grading of timber (Jones and Emms 2010, Wang *et al.* 2013, Denzler *et al.* 2015). Estimating the modulus of elasticity (MOE) of logs and determining its correlation with the static MOE of the recovered boards is one of the most widely used NDTs for predicting the MOE of timber in previous studies (Farrell *et al.* 2012, Merlo *et al.* 2014, Urhan *et al.* 2014). This method requires log's acoustic wave velocity (AWV) and green density to calculate the log MOE.

The AWV measurement technique, both log AWV and standing tree AWV, had shown acceptable performances as a predictor of stiffness of sawn boards in previous studies (Edlund *et al.* 2006, Mackenzie *et al.* 2009, Jones and Emms 2010, Blackburn *et al.* 2014, Merlo *et al.* 2014, Urhan *et al.* 2014, Denzler *et al.* 2015). Farrell *et al.* (2012) demonstrated that the static MOE of plantation *Eucalyptus nitens* (*E. nitens*) timber can be predicted using log MOE (calculated by log AWV and green density) and regression models with more than 54% accuracy. This accuracy could vary between species and within species at different sites (Legg and Bradley 2016). Wang *et al.* (2013) demonstrated that a regression model with log AWV as the regressor has a moderate accuracy of 40% in predicting the static MOE of Douglas-fir (*Pseudotsuga menziesii*) timber. These researchers indicated that log AWV combined with other criteria including log diameter or log vertical position in tree could be a better predictor of the boards' static MOE and visual grading yield than log AWV alone.

Numerical models can also be used to estimate the flexural stiffness and strength of timber. Artificial Neural Network (ANN) is among the most effective modelling techniques for predicting different physical and mechanical properties of timber and timber products, as

reported in previous studies (Mansfield *et al.* 2007, Esteban *et al.* 2009, Fernández *et al.* 2012, Tiryaki and Aydın 2014, Bardak *et al.* 2016, García-Iruela *et al.* 2016, Fu *et al.* 2017). ANN modelling consists of a complex system of information processing which is made up of a number of highly interconnected processing elements called artificial neurons (Grazide *et al.* 2015). An ANN model is generally constructed of three layers: input layer which can contain several input factors, hidden layer, and output layer containing one or multiple target outputs as shown in Figure 1.

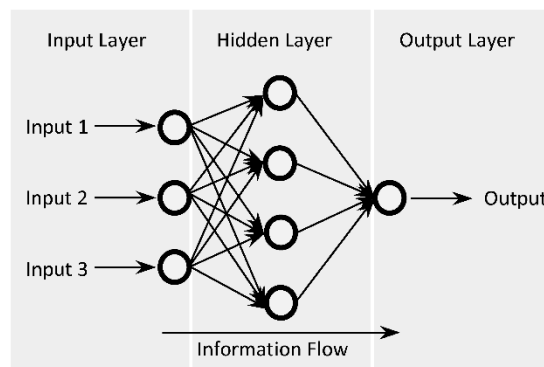


Figure 1. Structure of an ANN model with three input factors, one hidden layer with four neurons, and one target output.

An ANN model estimates the designated outputs based on the statistical information related to the correlation between the characteristics introduced in input layer and the target output(s) in output layer. The statistical information can be obtained by relevant experimental studies. The ANN modelling technique has shown acceptable capabilities for the prediction of flexural properties of timber in previous studies. Esteban *et al.* (2016) developed an ANN model using several input factors, including boards' density, width and thickness, moisture content (MC), ultrasonic wave propagation velocity, and visual grading, that could predict the static MOE of *Abies pinsapo* Boiss. timber with 75% accuracy. García-Iruela *et al.* (2016) compared the accuracies of ANN modelling and traditional multi-linear regression (MLR) modelling in predicting the static MOE of radiata pine (*Pinus radiata* D. Don.) timber. These

researchers demonstrated that ANN modelling using ultrasonic technique has a higher MOE prediction accuracy than traditional MLR modelling when the two methods use the same input factors. Despite these studies, only one reference could be found in the literature with respect to the effectiveness of ANN modelling in predicting the modulus of rupture (MOR) of timber in bending. Mansfield *et al.* (2007) reported that an ANN model with different input factors, including density, MC, microfibril angle, can predict the MOR of western hemlock (*Tsuga heterophylla* Raf.) with a moderate accuracy ranged from 43.8% to 56.1%.

The present study aimed to investigate the visual and flexural properties of fibre-managed plantation *E. globulus* timber sawn into boards as a potential raw material for structural building applications.

The study's specific objectives were to: a) Evaluate the recovery rate and the effectiveness of the conventional timber processing regimes for producing sawn boards from fibre-managed *E. globulus* plantation, b) Identify the most frequent and important visual characteristics and SRFs of the sawn boards from the resource, c) Determine any correlations between the MOE and MOR of the boards with the visual characteristics, SRFs, and variation in basic density and MC of the boards, d) Compare the effectiveness of using log AWV, traditional MLR modelling, and ANN modelling methods in predicting MOE and MOR of the boards.

Materials and Methods

Plantation site and harvesting

A 26-year-old fibre-managed plantation *E. globulus* resource on the north of Tasmania (Australia) was selected as the study site. In total, 29.08 m³ logs were harvested for this study. The volume of each log was calculated by measuring the length, small-end diameter, and large-end diameter of the log and then applying the relevant mathematical computations. The debarking process took place in the forest utilising conventional harvester/debarker machines

that are normally used for pulplog production. The average small-end diameter of the logs was 403 mm.

Sawing, drying, and planning regimes

Using a plain sawing pattern, the logs were sawn to four nominal widths: 75 mm, 100 mm, 125 mm, and 150 mm. The sapwood was retained. The sawing pattern generated quartersawn (annual ring angle = $90^{\circ} \pm 15^{\circ}$), backsawn (annual ring angle = $0^{\circ} \pm 15^{\circ}$), and transitional boards (annual ring angle = $45^{\circ} \pm 15^{\circ}$). The recovered boards were pre-dried for a nine-week period under rack weights and then air-dried for three weeks. The boards were then reconditioned and dried in conventional kiln equipment to a target MC of 12%. The rack weights were kept on the boards during the drying process to decrease distortions. After the drying stage, the boards were planed/dressed to final dimensions at the thickness of 35 mm. The final widths of the boards were 70 mm, 90 mm, 120 mm, and 140 mm. The average length of the finished boards was 4848.5 mm and a total of 444 boards were recovered from the resource.

Laboratory testing

Assessment of the recovery rate, visual characteristics, SRFs, and processing defects of the boards

The nominal recovery rate of the boards was calculated for the resource using Equation 1.

$$NR = \frac{V_0}{V_L} \quad (1)$$

where, NR is the nominal recovery rate of the boards (%); V_0 is the volume of the boards before the final planning stage calculated by measuring the cross-sectional area and length of the boards (m^3); V_L is the volume of the harvested logs (m^3).

The recovered boards (444 boards) were visually assessed and the information regarding their visual characteristics, SRFs, percentage of clear wood (PCW), and any processing defects or damages were recorded for each board. The criteria used for these assessments are summarised in Table 1 (Derikvand et al. 2018).

Table 1. Criteria used for visual assessment of the boards.

Measured items	Criteria used for the measurement
PCW (%)	Total length of clear wood pieces in the resource with individual lengths equal to or larger than 500 mm divided by total length of all the boards.
Average length of clear wood pieces (mm)	Total length of clear wood pieces with individual lengths equal to or larger than 500 mm divided by total number of clear wood pieces in the resource
End split (%)	Number of boards with end split equal to or larger than the width of the boards divided by total number of boards (TNB)
Knothole (%)	Number of boards with at least one knothole divided by TNB
Major knots (%)	Number of boards with at least one knot with a diameter equal to or larger than 1/4 of the width of the board divided by TNB
Significant bow (%)	Number of boards with impermissible bow (according to AS 2082) divided by TNB
Significant crook (%)	Number of boards with impermissible crook (according to AS 2082) divided by TNB
Significant twist (%)	Number of boards with impermissible twist (according to AS 2082) divided by TNB
Significant surface checks (%)	Number of boards with surface checks with individual length exceeding 1/4 of the length of the boards divided by TNB
Wane (%)	Number of boards with wane exceeding 1/10 of the cross-sectional area or 1/2 of the width of the boards divided by TNB
Fungal decay and/or insect trace (%)	Number of boards with fungal decay and/or insect trace divided by TNB
Multiplicity of knots	Total number of major knots in the resource divided by TNB
Predominant slope of grain	One of the following groups, measured according to AS1080.2: Slope of grain = > 1:6 Slope of grain = 1:6 \geq X > 1:8 Slope of grain = 1:8 \geq X > 1:10 Slope of grain = 1:10 \geq X > 1:15 Slope of grain = 1:15 >
Damages from debarker	Number of boards with any debarker damage larger than 100 mm in length divided by TNB
Damages from sawing process	Number of boards with any sawing damage larger than 100 mm in length divided by TNB
Unrecoverable collapse	Number of boards with unrecoverable collapse from drying step larger than 100 mm in length divided by TNB

Evaluation of the static MOE and MOR of the boards

The boards were divided into five groups based on their SRFs and PCW. Group one had the highest PCW ($\geq 80\%$) and the least apparent SRFs, whereas group five had the lowest PCW ($\geq 0\%$ to $< 20\%$) and the most apparent SRFs (Derikvand et al. 2018). Continuous clear wood pieces with a length shorter than 500 mm, mechanical damages, unrecoverable collapse, major face and edge knots, knotholes, fungal decay, insect trace, wane, and end split were excluded from the measurement of the PCW in each board. Three samples were then randomly selected from each of the five groups from each board widths (i.e., 70 mm, 90 mm, 120 mm, and 140

mm) for the static bending test. The three replicates in each treatment were selected from three different logs. In total, 60 boards were selected and cut to a final length equal to 20 times the width of the boards in accordance with AS 4063.1 (Standards Australia 2010) for the static four-point bending test.

The boards were tested edgewise and loading continued until failure. The maximum applied load, deflection, and failure mode were recorded for each boards. The MOE and MOR values of the boards were calculated in accordance with the procedure described in AS 4063.1 (Standards Australia 2010).

Basic density and MC measurement

Three samples were cut from each board tested under bending for the measurement of basic density and actual MC at the time of bending test. The samples were taken from different areas along the length of the boards and were free from defects. The nominal cross section area of the samples was $35 \times 35 \text{ mm}^2$. The total number of samples tested for basic density and MC was 180 samples. Equation 2 was used to calculate the basic density.

$$\rho_b = \frac{m_0}{V} \times \frac{100}{(100+w)} \quad (2)$$

where, ρ_b is the basic density (kg/m^3); m_0 is the oven-dry mass of the sample (kg); V is the volume of the samples before oven-drying (m^3); w is the MC of the sample at the time of testing.

The MC of the tested boards was calculated based on the oven-dry mass of the samples.

Statistical analysis

Statistical analysis of the empirical data in this study was performed using IBM SPSS Statistics software (version 23). The MOE and MOR values were adjusted based on the actual MC of each board in accordance with AS 2878 (Standards Australia 2000). The average adjusted

MOE, MOR, basic density, and MC were then calculated for each test treatment. The results were then re-grouped as one dataset and the impacts of the test variables on the MOE and MOR of the boards were studied using analysis of variance (ANOVA) test. For the ANOVA in the study, the visual characteristics and SRFs were used as fixed factors and the basic density and MC were used as covariates.

Prediction of the adjusted MOE and MOR of the boards

Log AWV measurement

In order to create a basis for comparison with the other prediction models developed in this study, the AWV of logs was measured and used to calculate the log MOE and the results were then used to predict the adjusted MOE and MOR of the boards by means of linear regression analysis. Six logs were randomly selected for this purpose. The AWV measurement was conducted on each log using the Director HM200TM. From each of the six logs, one disc was cut and used for measuring the log's green density (i.e., the disc weight divided by the disc volume). The log MOE was then calculated using the following equation (Farrell *et al.* 2012):

$$\text{Log MOE} = \rho_g \times \text{AWV}^2 \quad (3)$$

where, ρ_g is the log's green density (kg/m^3).

The log MOE values were compared with those obtained from static bending test of the boards recovered from each log.

ANN modelling

In this study, two separate ANN models were designed for the prediction of adjusted MOE and MOR of the boards. A feedforward multilayer perceptron network was used in the modelling. Both models were made of two hidden layers. The first hidden layer and the second hidden layer had 15 and four neurons, respectively. The back-propagation algorithm was used for training the ANN models. The activation (transfer) function used was Hyperbolic Tangent (Equation 4).

$$f(x) = \frac{2}{1+e^{(-2x)}} - 1 \quad (4)$$

where, $f(x)$ and x are the output and the input values of the neuron, respectively.

The transfer function used produces outputs in the interval -1 to 1. Hence, the data set should be normalised accordingly to improve the generalisation ability of the network (Esteban *et al.* 2009). Equation 5 was used to normalise the data set for the ANN modelling in this study (Esteban *et al.* 2009, Fernández *et al.* 2012).

$$X_2 = \frac{X_1 - X_{min}}{X_{max} - X_{min}} \quad (5)$$

where, X_2 is the normalised data, X_1 is the original data, and X_{max} and X_{min} are the maximum and minimum values in the original data set before the normalisation.

It was assumed that any visual characteristics and SRFs that have significant influences on the bending properties of the timber can increase the accuracy of the ANN models when used as input factors. Accordingly, annual ring angle, slope of grain, PCW, and another factor named SGAR (slope of grain \times annual ring angle) were selected and used as input factors in these models based on the statistical analysis results. The SGAR factor created in this study represents the interaction impact of slope of grain and annual ring angle on the mechanical properties of the boards, which can improve the prediction ability of the ANN models. The basic density and MC of the boards were used as input covariates. The structure of the ANN model was the same for the prediction of both adjusted MOE and MOR of the boards. However, the adjusted MOE values of the boards were also included in the model as an input covariate for the prediction of the adjusted MOR values. The models were trained using the data obtained from half of the tested samples and then validated using the data obtained from the rest of the samples—i.e., 30 samples for each step. The overall determination coefficients (R^2) was used to investigate the performance of the proposed models.

MLR modelling

For the MLR modelling in this study the input variables were the same as in the ANN modelling for the prediction of both adjusted MOE and MOR. In addition, simple linear regression models were also developed utilising only a single variable as the input (i.e., basic density variable to predict the MOE of the boards and basic density and MOE variables to predict MOR of the boards separately). The R^2 values were used to investigate the accuracy of the models.

Results and Discussions

The recovery rates, visual characteristics, SRFs, and processing defects of the boards

The nominal recovery rate of the resource was 31.8%. Around 42.7% of the dressed boards were clear wood pieces with at least 500 mm individual lengths—this is equal to 11.6% of the harvested logs. The PCW, SRFs, and visual characteristics of the boards are shown in Table 2—obtained from 444 boards.

Table 2. Characteristics of the fibre-managed *E. globulus* boards (from 444 boards).

Measured items	Width of boards			
	70 mm	90 mm	120 mm	140 mm
Average length of boards (mm)	4345	4756	5087	5206
PCW (%)	52	51.8	47.1	29.6
Average length of clear wood pieces (mm)	1151	1109	1049	987
End split (%)	30.4	37.1	35.5	56.3
Knothole (%)	60	77.4	90.3	87.5
Major knots (%)	93.9	98.4	98.9	98.2
Significant bow (%)	3.5	0	0	1.8
Significant crook (%)	0.8	0	0	0.9
Significant twist (%)	0	0	0	0
Significant surface checks (%)	11.3	25	26.9	39.3
Wane (%)	17.4	18.5	6.5	6.2
Fungal decay and/or insect trace (%)	0.9	4.8	1.1	4.4
Multiplicity of knots	5.3	5.4	6.1	6.9
Predominant slope of grain	1:15 \geq	1:15 \geq	1:15 \geq	1:15 \geq

Knots and knotholes were the main SRFs of the resource. Drying distortion (i.e., bow, crook, and twist) was insignificant but the percentages of boards with major wane, surface checks, and end splits were substantial. One of the reasons for the existence of wane on the sawn boards was because the sapwood was retained. Surface checks and end splits appeared during the drying stage. Part of these might be related to the checking and end splitting tendencies of plantation eucalypt timbers (Blackburn *et al.* 2010), and part could be related to the performance of the drying regimes used (Vermaas 1995, Innes 1996, Pérez-Peña *et al.* 2016). Mechanical damages and unrecoverable collapse were also substantial in the resource, resulting in a significant loss in the volume of the recovered boards. Mechanical damages were caused during the debarking of the logs and the sawing process (Figure 2).



Figure 2. Machine marks, from debarker (left) and sawing process (centre), and unrecoverable collapse (right) on the finished boards.

The highest loss in the volume of the recovered boards was due to unrecoverable collapse (Figure 3). To both effectively and efficiently use this resource in sawn timber production, there will be a need to optimise the current drying regimes for the resource in the future to reduce the amount of drying defects.

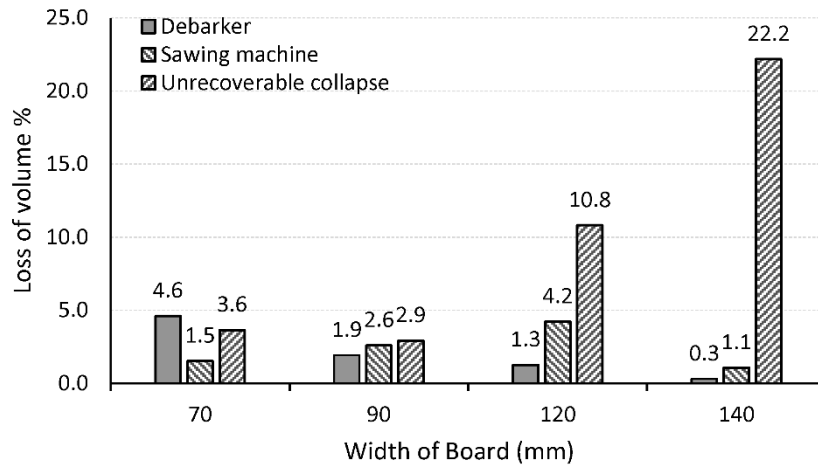


Figure 3. Loss of volume in the recovery of sawn boards during processing of the resource.

MOE, MOR, basic density, and MC of the boards

The average values of adjusted MOE, MOR, basic density, and MC of the boards are given in Table 3. The most frequent failure modes of the boards were knot failure (43.3% of the samples), grain tension failure (36.7% of the samples), catastrophic failure (13.3% of the samples), and compression failure (6.7% of the samples). The ANOVA results showed no significant difference between the flexural properties of the four different widths ($p > 0.05$) (Table 4). The type of knots also did not appear to have a significant effect on the bending strength of the boards tested in this study. This result is different than that reported by Derikvand et al. (2018) for the effects of knot type on the bending strength of fibre-managed plantation *E. nitens* timber. Such differences could be simply due to the variation in the visual characteristics of the boards tested in these two studies.

The tested boards had a wide range of different visual characteristics and SRFs. Slope of grain in the tested boards varied from $1:15 \geq$ to $1:8 \geq x > 1:10$ —measured for each board in accordance with AS 1080.2 (Standards Australia 2006). The ANOVA results showed that both adjusted MOE and MOR of the boards are significantly affected by the changes in slope of grain ($p < 0.001$). The results obtained for the measurements of slope of grain of the boards were divided in different slope classes to enable the statistical analysis, namely boards with

slope of grain of: $1:15 \geq x$, $1:10 \geq x > 1:15$, and $1:8 \geq x > 1:10$. The average adjusted MOE and MOR values decreased by respectively 31.5% and 51.1% with the increase in the slope of grain from $1:15 \geq x$ to $1:8 \geq x > 1:10$.

Table 3. Physical and mechanical properties of the boards.

Width (mm)	Test group	PCW (%)	Adjusted MOE (GPa)	Unadjusted MOE (GPa)	Adjusted MOR (MPa)	Unadjusted MOR (MPa)	Basic density (kg/m ³)	MC (%)
70	Group one	≥ 80	13.0 ± 1.1 ^a	13.2 ± 1.1	62.7 ± 22.6 ^a	65.3 ± 23.5	509.8 ± 42.0 ^a	10.5 ± 0.1 ^a
	Group two	≥ 60 to <80	11.2 ± 0.5	11.4 ± 0.5	39.1 ± 19.0	40.7 ± 19.8	488.7 ± 44.6	10.3 ± 0.3
	Group three	≥ 40 to <60	10.4 ± 1.9	10.6 ± 1.9	46.3 ± 12.4	48.3 ± 12.9	563.5 ± 130.9	10.2 ± 0.2
	Group four	≥ 20 to <40	9.2 ± 1.6	9.3 ± 1.6	38.1 ± 16.5	39.7 ± 17.2	517.5 ± 25.1	10.1 ± 0.1
	Group five	≥ 0 to < 20	8.7 ± 1.7	8.8 ± 1.7	29.6 ± 13.8	30.8 ± 14.4	452.0 ± 62.0	10.5 ± 0.3
Average								
90	Group one	≥ 80	10.5 ± 2.0	10.7 ± 2.0	43.16 ± 18.6	45.0 ± 19.4	506.3 ± 71.1	10.3 ± 0.2
	Group two	≥ 60 to <80	13.8 ± 3.5	14.1 ± 3.6	65.3 ± 29.9	68.1 ± 31.2	475.4 ± 83.5	10.5 ± 0.3
	Group three	≥ 40 to <60	9.9 ± 1.3	10.0 ± 1.4	41.8 ± 8.1	43.5 ± 8.4	458.7 ± 28.3	10.5 ± 0.6
	Group four	≥ 20 to <40	14.6 ± 2.8	14.8 ± 2.8	68.0 ± 22.8	70.8 ± 23.8	557.5 ± 61.5	10.7 ± 0.2
	Group five	≥ 0 to < 20	11.3 ± 1.8	11.5 ± 1.9	37.9 ± 18.1	39.4 ± 18.9	454.2 ± 46.6	10.7 ± 0.6
Average								
120	Group one	≥ 80	12.4 ± 2.6	12.6 ± 2.6	53.5 ± 20.5	54.6 ± 22.2	489.0 ± 59.2	10.5 ± 0.4
	Group two	≥ 60 to <80	11.2 ± 0.6	11.3 ± 0.7	38.3 ± 14.8	33.3 ± 13.3	529.0 ± 31.3	11.7 ± 1.4
	Group three	≥ 40 to <60	10.6 ± 4.8	10.7 ± 4.8	41.8 ± 25.1	43.5 ± 26.1	521.6 ± 88.4	10.7 ± 0.4
	Group four	≥ 20 to <40	9.8 ± 1.1	10.0 ± 1.2	33.6 ± 9.3	35.0 ± 9.7	451.2 ± 31.6	10.9 ± 0.6
	Group five	≥ 0 to < 20	11.3 ± 3.0	11.5 ± 3.0	50.7 ± 10.7	52.8 ± 11.1	473.1 ± 54.0	10.9 ± 0.1
Average								
140	Group one	≥ 80	10.7 ± 2.3	10.9 ± 2.3	39.6 ± 13.8	41.1 ± 14.6	500.9 ± 63.8	11.2 ± 0.5
	Group two	≥ 60 to <80	12.5 ± 1.7	12.5 ± 1.5	51.2 ± 10.5	51.7 ± 8.0	491.9 ± 58.2	11.1 ± 0.7
	Group three	≥ 40 to <60	13.3 ± 0.8	13.4 ± 1.0	59.8 ± 4.9	60.8 ± 6.5	510.7 ± 5.6	11.7 ± 1.0
	Group four	≥ 20 to <40	11.8 ± 0.9	12.0 ± 0.9	45.3 ± 14.3	47.2 ± 14.9	521.6 ± 18.5	11.8 ± 0.9
	Group five	≥ 0 to < 20	9.4 ± 1.5	9.6 ± 1.5	38.4 ± 8.2	40.0 ± 8.5	527.5 ± 64.4	10.9 ± 0.5
Average								
Overall average	Group one	≥ 80	11.7 ± 1.7	11.8 ± 1.6	48.4 ± 10.6	49.5 ± 10.4	505.8 ± 50.1	11.5 ± 0.7
	Group two	≥ 60 to <80	11.3 ± 2.2	11.8 ± 2.3	46.2 ± 16.8	47.8 ± 17.4	498.3 ± 59.1	10.9 ± 0.7

^a: Standard deviation

Table 4. The ANOVA results.

Visual Characteristics and SRFs	MOE	MOR
Annual ring angle	NS	*
Slope of grain	***	***
Slope of grain \times Annual ring angle (SGAR factor)	***	**
Board width	NS	NS
PCW	***	**
Total number of knots in the boards	*	NS
Number of knots in the loading zone of the boards	***	**
Type of knots	NS	NS
Variation in MC	NS	NS
Variation in basic density	*	NS

NS = not significant; * = significant at $P < 0.05$; ** = significant at $P < 0.01$; *** = highly significant at $P < 0.001$.

The impact of annual ring angle was significant on the adjusted MOR ($p < 0.05$) but insignificant on the adjusted MOE of the boards ($p > 0.05$). Transitional boards showed the highest adjusted MOR (52.03 MPa) and MOE values (11.97 GPa). There was no statistically significant difference between the adjusted MOR values of backsawn (46.67 MPa) and transitional boards. Transitional boards were 34.9% stronger than quartersawn boards (38.56 MPa). It must be noted that the visual characteristics and SRFs varied between the tested boards (i.e., the boards were not obtained from clear wood) and this can affect or intensify the impact of annual ring angle on the mechanical properties of the boards. The interaction of slope of grain and annual ring angle (the SGAR factor), PCW, and number of knots in the loading zone also significantly affected both adjusted MOE and MOR values of the boards (Table 4). The results obtained were divided into four groups based on the PCW of the boards tested in order to enable a reasonable statistical analysis, namely, group one $PCW = x \geq 80\%$, group two $PCW = 60\% \leq x < 80\%$, group three $PCW = 40\% \leq x < 60\%$, and group four $PCW = x < 40\%$. The adjusted MOE and MOR of the boards increased respectively by 45% and 48% with an increase in the PCW from $< 40\%$ to $\geq 80\%$. The effect of the number of knots in the loading zone on the adjusted MOE and MOR was negative. The total number of knots in the boards also negatively affected the mechanical properties of the boards but its impact on the adjusted MOR

values was insignificant ($p > 0.05$). The variation of MC between the four board's widths was highly significant ($p < 0.01$). The average MC increased consecutively with the increase in the width of the boards from 70 mm to 140 mm. The variation in MC was taken into account for the calculation of the adjusted MOE and MOR of the boards which is why the impact of the variation in MC on the mechanical properties of the boards was insignificant ($p > 0.05$). The variation in basic density between the four widths was insignificant ($p > 0.05$) but it significantly affected the adjusted MOE of the boards ($p < 0.05$). The impact of the variation in basic density was insignificant on the adjusted MOR values ($p > 0.05$).

Predicted MOE and MOR of the boards

Effectiveness of using log AWV

The correlations between the log MOE and the adjusted MOE and MOR of the boards were positive (Figure 4) however, the R^2 for the correlation between the log MOE and the adjusted MOR of the boards was as low as 0.104. The R^2 obtained for the correlation between the log MOE and board adjusted MOE was 0.534, which means the log MOE can explain more than 53.4% of the variations for the adjusted MOE of the boards.

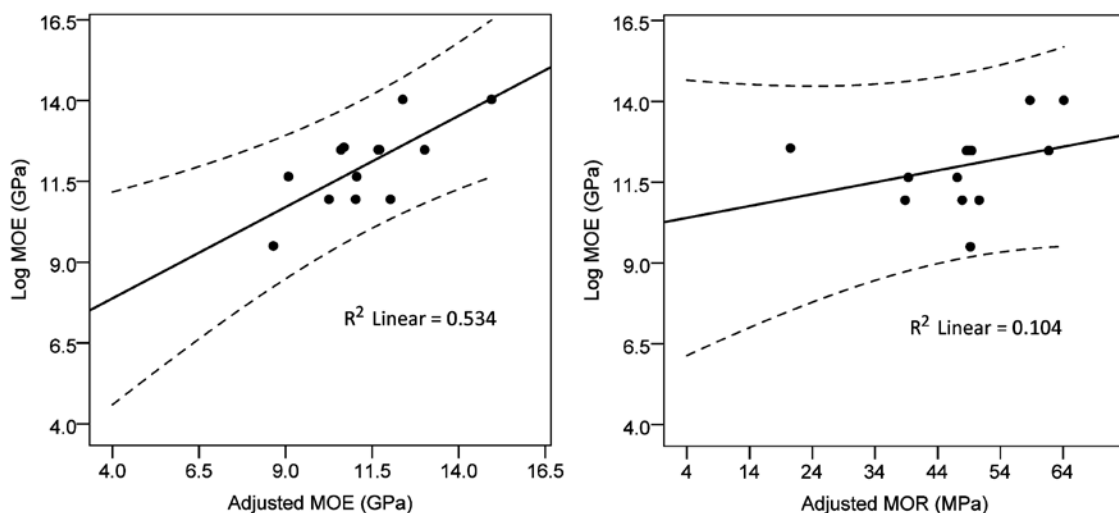


Figure 4. Correlation between the logs MOE and the adjusted MOE (left) and MOR (right) of the boards.

The determination coefficient obtained was close to that reported by Farrell *et al.* (2012) for the correlation between log MOE and static MOE of sawn boards from a plantation *Eucalyptus nitens* resource ($R^2=0.56$).

The results obtained showed that the log MOE measurement using AWV could not be a reasonable tool for the prediction of the adjusted MOR of the boards. This technique however, may be effective for the segregation of the logs based on the target stiffness of the boards (Farrell *et al.* 2012)—with an overall success rate of 53.4%.

ANN modelling results

The ANN models developed in this study explained 78.5% and 79.9% of the variations for the adjusted MOE and MOR of the boards, respectively (Figure 5).

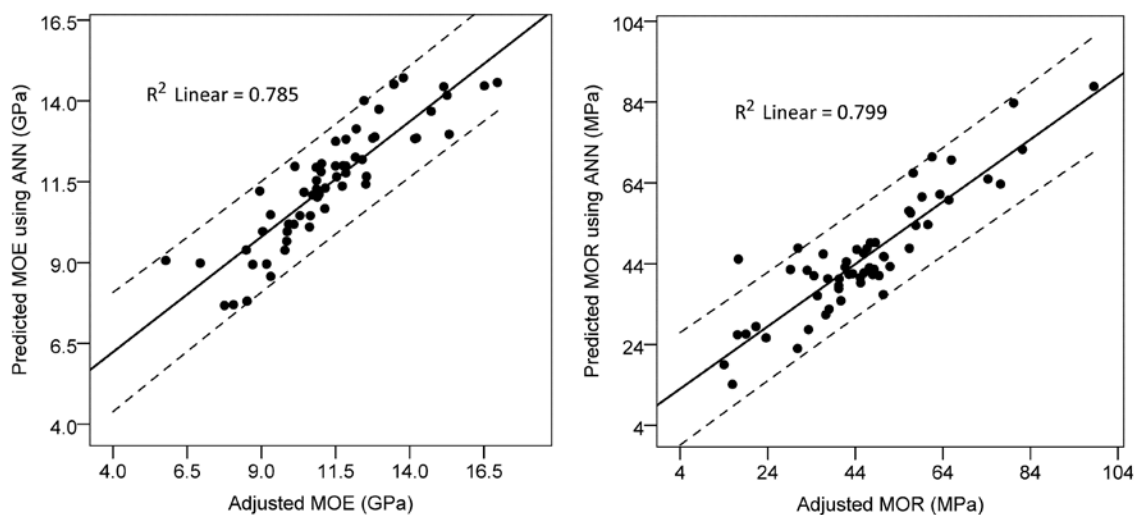


Figure 5. The ANN modelling results for the prediction of the adjusted MOE (left) and MOR (right) of the boards.

Although the tested boards were not obtained from clear wood and had substantial SRFs, the R^2 values obtained by the ANN models in this study for the prediction of MOE and MOR were considerably higher than those obtained by ANN models in previous studies on other wood species (Mansfield *et al.* 2007, Esteban *et al.* 2009). The R^2 value obtained for the prediction of the adjusted MOE ($R^2 = 0.785$) was also comparable to that reported by García-

Iruela *et al.* (2016) for the prediction of the MOE of Radiata pine (*Pinus radiata* D. Don.) timber using ANN modelling and ultrasonic technique ($R^2 = 0.80$).

MLR modelling results

The results showed that the correlation between the board adjusted MOE and MOR values is positive and more than 66.6% of the variance in the adjusted MOR values can be explained by the adjusted MOE (Figure 6).

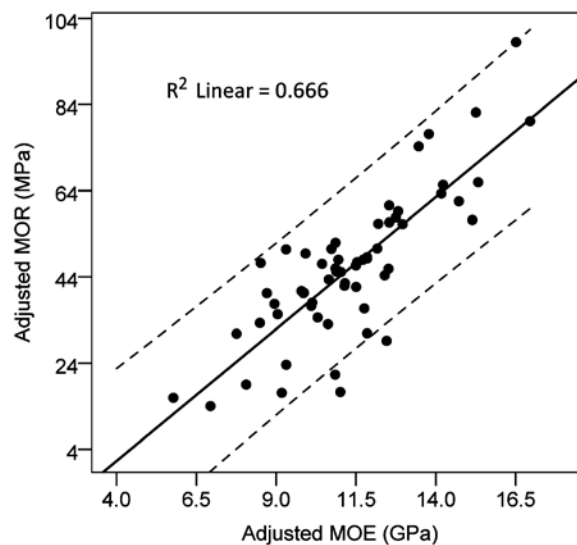


Figure 6. Correlation between adjusted MOR and MOE of the boards.

The correlation between the adjusted MOR and basic density of the boards was positive however, basic density explained only 5.7% of the variance in the adjusted MOR (Figure 7). The correlation between the adjusted MOE and basic density was also positive but only 8.8% of the variance in the adjusted MOE can be explained by basic density (Figure 7). Based on the results of the statistical analysis, an MLR model was developed to predict the adjusted MOE of the boards with several input factors including basic density, slope of grain, annual ring angle, SGAR, PCW, and number of knots in the loading zone of the boards. The same input factors plus the adjusted MOE were used to develop an MLR model for the prediction of the

adjusted MOR of the boards. The results obtained from the two MLR models are shown in Figure 8.

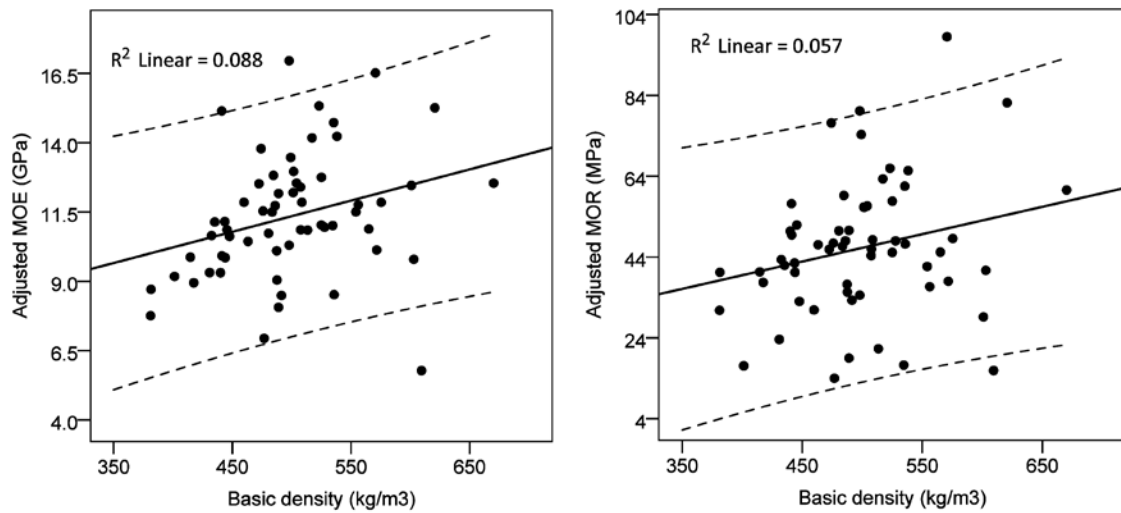


Figure 7. Correlation between adjusted MOE (left) and MOR (right) with basic density of the boards.

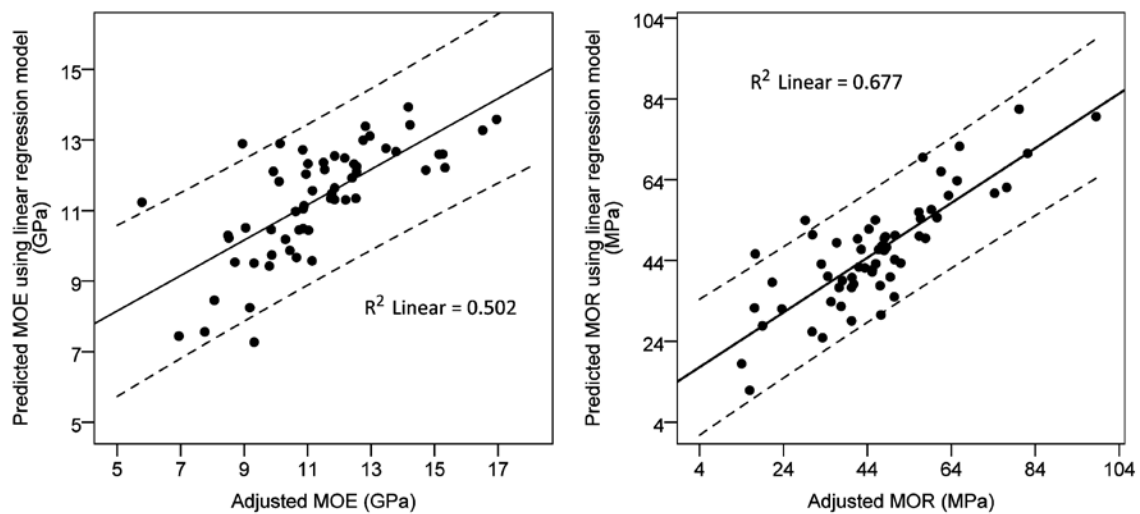


Figure 8. The results of the MLR models developed to predict the adjusted MOE (left) and MOR (right) of the boards.

The MLR modelling showed 50.2% success in predicting the adjusted MOE of the boards using basic density, visual characteristics, and SRFs of the boards as the regressors. Likewise, the MLR modelling exhibited 67.7% success in the prediction of the adjusted MOR

of the boards when the adjusted MOE, basic density, visual characteristics, and SRFs of the boards were used as the regressors. The R^2 value obtained by the MLR modelling for the prediction of the adjusted MOE of the boards ($R^2=0.502$) was comparable to that obtained by the log AWV method ($R^2=0.534$).

Considering the R^2 values, the ability of the MLR modelling in predicting the adjusted MOE values was weaker than that of both the ANN modelling and log AWV measurement techniques. The ability of the MLR modelling in predicting the adjusted MOR values was stronger than that of the log AWV measurement technique, but weaker than that of the ANN modelling approach. In all cases, the ANN models developed in this study were capable to explain a significantly higher percentage of variations in the mechanical properties of the boards in comparison with the MLR models and log AWV measurement technique. Hence, the ANN models developed in this study could be reliable approaches toward predicting the actual MOE and MOR of highly featured timber boards. As the basic density and MC of the boards were also included in the ANN models in this study, this may be possible to generalise and apply these models to other wood species as well. This initial study has proven the effectiveness and necessity of using visual characteristics and SRFs of the boards as effective input factors in the development of ANN models with higher capacities in predicting the bending strength and stiffness of timber than traditional MLR modelling and log AWV measurement. The ANN models in this study however were also associated with some levels of uncertainties which can limit their wider application. Future research with a larger sample size and a wider range of input factors can help to improve the reliability and accuracy of the ANN models developed in this study, which may reduce the need for costly and destructive laboratory testing.

Conclusions

This study was conducted to investigate the recovery rate, visual characteristics, and flexural properties of fibre-managed plantation *E. globulus* sawn timber. The impact of the visual

characteristics on the flexural properties of the boards, the effectiveness of the current timber processing regimes on the resource, the performance of different non-destructive methods in predicting the adjusted MOE and MOR of the timber boards from this resource were studied. The following conclusions were drawn on the basis of the results obtained and their statistical analyses in the study:

- Fibre-managed *E. globulus* can be sawn into structural size boards using conventional timber processing regimes with an overall nominal recovery rate of 31.8%.
- Knots and knotholes were the most frequent natural visual characteristics of the boards recovered from the fibre-managed *E. globulus* resource in this study. The recovered boards also contained significant mechanical damages from debarker and sawing process, wane, unrecoverable collapse, and other drying degradations including surface checks and end splits. Development of novel timber processing and drying approaches for this plantation resource in the future can help to reduce the intensity of these defects.
- The adjusted MOE and MOR were significantly affected by slope of grain, PCW, and number of knots in the loading zone of the boards. The total number of knots in the boards and variation in the basic density significantly affected the adjusted MOE. The adjusted MOR values were also significantly affected by annual ring angle.
- The ANN modelling in this study showed significantly higher accuracy in predicting the adjusted MOE and MOR of the boards in comparison with the MLR modelling and log AWV measurement technique. The ANN models can predict the adjusted MOE and MOR of the boards with respectively 78.5% and 79.9% success when the visual characteristics and SRFs of the boards are used as input factors and MC and basic density of the boards are used as covariates in the development of the models.

Acknowledgments

This study was conducted under the Australian Research Council, Centre for Forest Value, University of Tasmania, TAS, Australia (Grant Reference: IC150100004). The financial support from Forest and Wood Products Australia Limited (FWPA), Melbourne, VIC, Australia is acknowledged (Grant Number: PNB387-1516). The authors are grateful for the support from Forico Pty Ltd. in providing the logs and Britton Timbers. for the milling of the logs and seasoning of the boards.

References

- AS 2082 (2007) Timber - Hardwood - Visually stress graded for structural purposes. *Standards Australia*, Australia.
- AS 4063.1 (2010) Characterisation of structural timber, Part 1: Test Methods. *Standards Australia*, Australia.
- AS 1080.2 (2006) Timber - Methods of test - Slope of grain. *Standards Australia*, Australia.
- AS 2878 (2000) Timber-Classification into Strength Groups. *Standards Australia*, Australia.
- Bardak, S., Tiryaki, S., Bardak, T., and Aydin, A. (2016) Predictive Performance of Artificial Neural Network and Multiple Linear Regression Models in Predicting Adhesive Bonding Strength of Wood. *Strength of Materials*, 48(6), 811-824. <https://doi.org/10.1007/s11223-017-9828-x>.
- Blackburn, D., Hamilton, M., Harwood, C., Innes, T., Potts, B., and Williams, D. (2010) Stiffness and checking of *Eucalyptus nitens* sawn boards: genetic variation and potential for genetic improvement. *Tree genetics & genomes*, 6(5), 757-765. <https://doi.org/10.1007/s11295-010-0289-7>.
- Blackburn, D., Hamilton, M., Williams, D., Harwood, C., and Potts, B. (2014) Acoustic wave velocity as a selection trait in *Eucalyptus nitens*. *Forests*, 5(4), 744-762. <https://doi.org/10.3390/f5040744>.
- Connell, M.J. (2003) *Log Presentation: Log Damage Arising from Mechanical Harvesting or Processing*. Forest and Wood Products Research and Development Corporation, Melbourne, Victoria, Australia, pp.-62
- Denzler, J. K., Weidenhiller, A., & Golser, M. (2015) Property relationships between spruce logs and structural timber. *Scandinavian journal of forest research*, 30(7), 617-623. <https://doi.org/10.1080/02827581.2015.1046479>.
- Derikvand, M., Nolan, G., Jiao, H., and Kotlarewski, N. (2017) What to Do with Structurally Low-Grade Wood from Australia's Plantation Eucalyptus; Building Application?. *BioResources*, 12(1), 4-7. <https://doi.org/10.15376/biores.12.1.4-7>.
- Derikvand, M., Kotlarewski, N., Lee, M., Jiao, H., Chan, A., and Nolan, G. (2018) Visual stress grading of fibre-managed plantation Eucalypt timber for structural building applications. *Construction and Building Materials*, 167, 688-699. <https://doi.org/10.1016/j.conbuildmat.2018.02.090>.
- Edlund, J., Lindström, H., Nilsson, F., & Reale, M. (2006) Modulus of elasticity of Norway spruce saw logs vs. structural lumber grade. *Holz als Roh-und Werkstoff*, 64(4), 273-279. <https://doi.org/10.1007/s00107-005-0091-7>.
- Esteban, L. G., Fernández, F. G., and de Palacios, P. (2009) MOE prediction in *Abies pinsapo* Boiss. timber: Application of an artificial neural network using non-destructive testing. *Computers & Structures*, 87(21), 1360-1365. <https://doi.org/10.1016/j.compstruc.2009.08.010>.
- Farrell, R., Innes, T. C., & Harwood, C. E. (2012) Sorting *Eucalyptus nitens* plantation logs using acoustic wave velocity. *Australian forestry*, 75(1), 22-30. <https://dx.doi.org/10.1080/00049158.2012.10676382>.
- Fernández, F. G., de Palacios, P., Esteban, L. G., García-Iruela, A., Rodrigo, B. G., and Menasalvas, E. (2012) Prediction of MOR and MOE of structural plywood board using an artificial neural network and comparison with a multivariate regression model. *Composites Part B: Engineering*, 43(8), 3528-3533. <https://doi.org/10.1016/j.compositesb.2011.11.054>.

- Fu, Z., Avramidis, S., Zhao, J., and Cai, Y. (2017) Artificial neural network modeling for predicting elastic strain of white birch disks during drying. *European Journal of Wood and Wood Products*, 1-7. <https://doi.org/10.1007/s00107-017-1183-x>.
- García-Iruela, A., Fernández, F. G., Esteban, L. G., de Palacios, P., Simón, C., and Arriaga, F. (2016) Comparison of modelling using regression techniques and an artificial neural network for obtaining the static modulus of elasticity of *Pinus radiata* D. Don. timber by ultrasound. *Composites Part B: Engineering*, 96, 112-118. <https://doi.org/10.1016/j.compositesb.2016.04.036>
- Gavran, M. (2015) *Australian plantation statistics 2015 update*, Australian Bureau of Agricultural and Resource Economics and Sciences, Canberra, Australia.
- Grazide, C., Cointe, A., Coureau, J. L., Morel, S., Dumail, J. F. (2015) Wood heterogeneities and failure load of timber structural elements: a statistical approach. *Wood science and technology*, 49(2), 421-440. <https://doi.org/10.1007/s00226-015-0706-z>
- Innes, T. (1996) Pre-drying of Collapse Prone Wood Free of Surface and Internal Checking. *European Journal of Wood and Wood Products*, 54(3), 195-199. <https://doi.org/10.1007/s001070050165>.
- Jones, T. G., & Emms, G. W. (2010) Influence of acoustic velocity, density, and knots on the stiffness grade outturn of radiata pine logs. *Wood and Fiber Science*, 42(1), 1-9.
- Legg, M., & Bradley, S. (2016) Measurement of stiffness of standing trees and felled logs using acoustics: a review. *The Journal of the Acoustical Society of America*, 139(2), 588-604. <https://doi.org/10.1121/1.4940210>.
- Mackenzie R.K.T. (2009) The non-destructive evaluation of Sitka spruce mechanical properties using acoustic methods. PhD Thesis, Edinburgh Napier University, Edinburgh, UK.
- Mansfield, S. D., Iliadis, L., and Avramidis, S. (2007) Neural network prediction of bending strength and stiffness in western hemlock (*Tsuga heterophylla* Raf.). *Holzforschung*, 61(6), 707-716. <https://doi.org/10.1515/HF.2007.115>.
- Merlo, E., Alvarez, J. G., Santaclara, O., and Riesco, G. (2014) Modelling modulus of elasticity of *Pinus pinaster* Ait. in northwestern Spain with standing tree acoustic measurements, tree, stand and site variables. *Forest Systems*, 23(1), 153-166. <https://dx.doi.org/10.5424/fs/2014231-04706>.
- Nolan, G. B., Greaves, B. L., Washusen, R., Parsons, M., and Jennings, S. (2005) *Eucalypt Plantations for Solid Wood Products in Australia-A Review 'If you don't prune it, we can't use it'*. Forest and Wood Products Research and Development Corporation, Melbourne, Victoria, Australia.
- Pérez-Peña, N., Cloutier, A., Segovia, F., Salinas-Lira, C., Sepúlveda-Villarreal, V., Salvo-Sepúlveda, L., ... and Ananías, R. A. (2016) Hygromechanical strains during the drying of *Eucalyptus nitens* boards. *Maderas. Ciencia y tecnología*, 18(2), 235-244. <https://dx.doi.org/10.4067/S0718-221X2016005000021>.
- Tiryaki, S., & Aydın, A. (2014) An artificial neural network model for predicting compression strength of heat treated woods and comparison with a multiple linear regression model. *Construction and Building Materials*, 62, 102-108. <https://doi.org/10.1016/j.conbuildmat.2014.03.041>.
- Urhan, O. S., Kolpak, S. E., Jayawickrama, K. J., & Howe, G. T. (2014). Early genetic selection for wood stiffness in juvenile Douglas-fir and western hemlock. *Forest ecology and management*, 320, 104-117. <https://doi.org/10.1016/j.foreco.2014.02.020>.
- Vermaas, H.F. (1995) Drying eucalyptus for quality: material characteristics, pre-drying treatments, drying methods, schedules and optimisation of drying quality. *South African Forestry Journal*, 174, 41-49.
- Wang, X., Verrill, S., Lowell, E., Ross, R.J., Herian, V.L. (2013) Acoustic sorting models for improved log segregation. *Wood and Fiber Science*, 45, 343-352.

Appendix D: Paper IV

Publication reference: Derikvand, M., Kotlarewski, N., Lee, M., Jiao, H., & Nolan, G. (2019). Characterisation of Physical and Mechanical Properties of Unthinned and Unpruned Plantation-Grown *Eucalyptus nitens* H. Deane & Maiden Lumber. *Forests*, 10(2), 194.

Characterisation of physical and mechanical properties of unthinned and unpruned plantation-grown *Eucalyptus nitens* lumber

Mohammad Derikvand, Nathan Kotlarewski, Michael Lee, Hui Jiao, Gregory Nolan

Abstract: The use of fast-growing plantation eucalypt (i.e., pulpwood eucalypt) in the construction of high-value structural products has received special attention from the timber industry in Australia and worldwide. There is still however a significant lack of knowledge regarding the physical and mechanical properties of the lumber from such plantation resources as they are mainly being managed to produce woodchips. In this study, the physical and mechanical properties of lumber from a 16-year-old *Eucalyptus nitens* pulpwood resource from the north of Tasmania, Australia was evaluated. The tests were conducted on 318 small wood samples obtained from different logs harvested from the study site. The tested mechanical properties included bending modulus of elasticity (10377.7 MPa) and modulus of rupture (53 MPa), shear strength parallel (5.5 MPa) and perpendicular to the grain (8.5 MPa), compressive strength parallel (42.8 MPa) and perpendicular to the grain (4.1 MPa), tensile strength perpendicular to the grain (3.4 MPa), impact bending (23.6 J/cm²), cleavage (1.6 kN) and Janka hardness (23.2 MPa). Simple Linear regression models were developed using density and moisture content to predict the mechanical properties. The variations in the moisture content after conventional kiln drying within randomly selected samples in each test treatment were not high enough to significantly influence the mechanical properties. A relatively high variation in the density values was observed that showed significant correlations with the changes in the mechanical properties. The presence of knots increased the shear strength both parallel and perpendicular to the grain and significantly decreased the tensile strength of the lumber. The results of this study created a profile of material properties for the pulpwood *E. nitens* lumber that can be used for numerical modelling of any potential structural product from such a plantation resource.

Keywords: static bending; impact bending; tensile strength; compressive strength; shear strength; cleavage; hardness; wood failure modes

1. Introduction

The interest in fast-growing plantation species such as eucalypt is increasing as they may have the potential to ensure a sustainable supply of raw materials for producing mass laminated timber products for different structural building applications [1-6]. The goal of this study was to characterise the

physical and mechanical properties of lumber obtained from a 16-year-old *Eucalyptus nitens* (*E. nitens*) pulpwood resource. This resource is currently under investigation by the Australian timber industry as a potential raw material for the production of structural mass laminated timber.

Eucalypt includes around 900 different species that are almost all endemic to Australia [7]. The plantation hardwood estate in Australia is mainly comprised of *Eucalyptus globulus* and *E. nitens*. The two species of eucalypt are primarily managed in short rotation harvest cycles for pulplong production [8]. Tasmania has the second largest estate of hardwood plantations in Australia. Around 90 per cent of the estate is fibre-grown *E. nitens* plantations that are managed under unthinned and unpruned forestry regimes. In recent years, there has been a growing interest by the timber industry in using this resource for different structural and non-structural products such as sawn lumber [9], plywood [10], laminated veneer lumber [11] and mass laminated timber [12]. The latter case has recently been considered as a potential product option for using pulpwood *E. nitens* in structural building applications at a commercial scale.

Mass laminated timber includes different engineered products that are directly constructed by laminating sawn lumber together using either structural adhesives or mechanical fasteners—such as cross-laminated timber and nail-laminated timber. The production of mass laminated timber from the pulpwood *E. nitens* however requires a robust understanding of the structural performance of the lumber from this resource. Due to the forestry managements procedures used that are based on pulplong production, *E. nitens* lumber contains substantial amount of growth defects such as knots [12,13]. When dealing with plantation resources of this character, understanding the impact of knots on different mechanical properties of lumber is critical and plays a major role at the design stage of structural elements.

The use of a new plantation resource for structural applications also requires establishing its relevant strength groups. This is achievable by testing small clear wood samples from the resource and obtaining the average and lower 5th percentile values for different mechanical properties. These values are already known for commercially available hardwoods and softwoods and can be obtained through relevant standard design codes such as AS 1720.1 [14]. To establish these values for the pulpwood *E. nitens* lumber, an appropriate sampling and testing system needs to be developed. It is therefore necessary to understand how the physical and mechanical properties of the resource are affected by different natural and processing parameters.

In a number of previous studies, the bending properties and basic density of sawn boards from *E. nitens* plantations were examined as functions of parameters related to the characteristics of plantation site, tree age and applied forestry management regimes [9, 15-18]. There is still a significant lack of knowledge around the other physical and mechanical properties of this plantation resource. The available information to date is limited to a few basic mechanical properties of the resource including hardness, bending modulus of elasticity (MOE) and bending modulus of rupture (MOR) under short-term loading conditions [9,17]. Additional experimental works are required to establish relevant design codes and specifications for using this resource in the production of structural products for building applications.

The specific objectives of this study:

- Determined the MOE, MOR, shear strength parallel (SPA) and perpendicular (SPE) to the grain, tensile strength perpendicular to the grain (TPE), compressive strength parallel (CPA) and perpendicular (CPE) to the grain, cleavage, impact bending strength (IBS) and Janka hardness of the pulpwood *E. nitens* lumber.
- Determined the impacts of variations in basic density and minor variations in MC after conventional kiln drying on the mechanical properties.
- Investigated the impact of knot on the SPA, SPE and TPE of the lumber.
- Developed and examined different linear-regression models to predict the mechanical properties of the resource.

- Evaluated the coefficient of variation (COV) in the different physical and mechanical properties of the resource to create a basis for the establishment of an appropriate testing system for obtaining allowable design stress values of the resource in future studies.

2. Materials and Methods

2.1. Lumber

The test samples in this study were extracted from randomly selected lumber obtained from a 16-year-old *E. nitens* pulpwood resource in the north of Tasmania, Australia. The plantation site is located in Woolnorth region with a maximum altitude of 190 m. The required lumber was obtained from six different logs with an average small-end diameter of 359 mm. These logs were randomly selected between 44 logs originally harvested in 2016 for a research project at University of Tasmania that was aimed to develop structural products from this plantation resource for building applications. The harvested logs represent the butt log and come from different trees. After harvesting, the logs were sawn at a local mill using conventional plain sawing method. The sawn lumber was dried in an industrial hardwood kiln and then finished/dressed at a nominal thickness of 35 mm. The finished lumber had a substantial number of knots, surface checks and end splits. The clear wood samples in this study were cut from randomly selected lumber from different logs to ensure a good range of variations in the density and MC values. Variation in MC in this study refers to the differences between MC values of the lumber after the conventional kiln drying. Such differences might be minor. However, there is a lack of information regarding how these minor variations in the MC values can influence the physical and mechanical properties of the lumber. The clear wood samples were taken from different annual growth ring angles (Figure 1) and straight grain wood to reduce the impact of sloping grain on the results obtained.

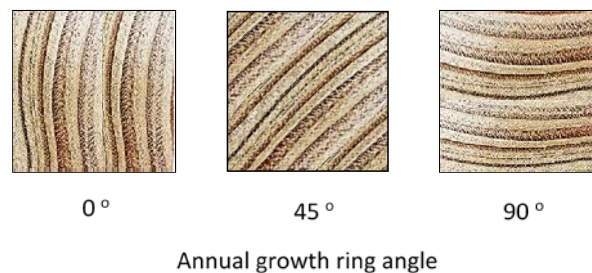


Figure 1. The arrangement of the three general annual growth ring orientations in the cross-section of the samples.

2.2. Sample and test descriptions

2.2.1. Static bending test

The MOE and MOR values of the pulpwood *E. nitens* lumber were determined on clear wood samples with the dimensions of 25 mm × 25 mm × 410 mm using a three-point test set-up and a span length of 360 mm according to ASTM D 143 [19]. The loading rate was set at 1.3 mm/min. The MOE and MOR under three-point bending load were calculated using the following equations:

$$MOE = \frac{L^3(P_2 - P_1)}{4bd^3(\varphi_2 - \varphi_1)} \quad (1)$$

$$MOR = \frac{3P L}{2bd^2} \quad (2)$$

where, b and d are the width (breadth) and depth of the sample (mm), L is the span length (mm), $(P_2 - P_1)$ is the load increment on the load-deflection curve in the linear-elastic range with P_2 and P_1 being

approximately 40% and 10% of the maximum applied load (P) at failure point (N), φ_2 and φ_1 are the maximum mid-span deflections (mm) at P_2 and P_1 loads, respectively.

2.2.2. Janka hardness test

The Janka hardness was assessed on clear wood samples with nominal dimensions of 35 mm × 50 mm × 150 mm. The tests were conducted according to ASTM D143 [19] with the speed of loading of 6 mm/min using a ball bearing fixture with 11.3 mm diameter. The loading of the samples continued until a penetration depth equal to one half of the diameter of the ball bearing was achieved. The test on each sample was repeated six times—twice on the widest surface, twice on the narrowest surface and twice on cross-sections of the samples. In total, sixty tests were conducted for measuring hardness on different surfaces of the samples. The overall Janka hardness was calculated as an average value from all the measurements on different surfaces. The average hardness on the widest and narrowest surfaces (referred to as side hardness) and the two cross-sections (referred to as axial hardness) of the samples were also analysed and reported separately.

2.2.3. IBS Test

The IBS was determined using Charpy Impact Test (CIT) with a 20-kilogram hammer/striker. The dimensions of the test samples were 25 mm × 25 mm × 100 mm. The samples were V-notched in the mid-span to a depth of 3 mm. The samples were hit by the Charpy striker in the mid-span. The energy required to break each sample was determined by measuring the height of the Charpy hammer before and after hitting the sample. The IBS was then calculated using Equation 3.

$$IBS = \frac{\varepsilon}{b \times d} \quad (3)$$

where, IBS is the impact bending strength (J/cm²); ε is the energy absorbed by the sample at failure point (J); b and d are the breadth and the depth of the sample (cm).

The results obtained from the CIT must be converted to the MC of 12% [20]. However, as examining the effect of variation in MC on the IBS was one of the objectives of this study, the results obtained from the CIT were remained at their original values without any conversion.

2.2.4. Cleavage test

The samples for cleavage test had the dimensions of 35 mm × 50 mm × 90 mm. The samples were constructed using a CNC router. The tests were conducted according to the procedures of ASTM D 143 [19] at the loading rate of 2.5 mm/min.

2.2.5. Shear test

Shear strength is a critical property in almost all structural building applications such as bending members, shear walls, trusses and connections. The shear strength of the pulpwood *E. nitens* lumber was measured both parallel and perpendicular to the grain direction. The block shear specimens were constructed in accordance with the procedures described in ASTM D 143 [19]—except for the thickness of the samples that was limited by the thickness of the available boards (i.e., 35 mm). The samples were identically constructed using a CNC router. The impacts of presence of knots and variations in density and MC on the SPA and SPE of the samples were evaluated. For samples that contained a knot (knotted samples), the location of the feature was on the centre line of the applied load in the shear area of the sample (Figure 2). The overall average SPA and SPE were determined on clear wood samples—with no knots or any other defects. The test samples were loaded in shear according to the test procedure of ASTM D 143 [19] at a loading rate of 0.6 mm/min.

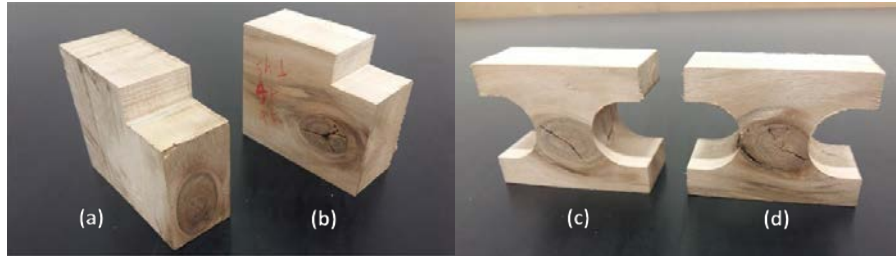


Figure 2. The location of knot in samples prepared for SPA test (a), SPE test (b) and TPE test (c and d).

2.2.6. Tension test

The tensile strength of the lumber was determined perpendicular to the grain (i.e., TPE). The dimension of the test samples was 35 mm × 50 mm × 50 mm. The test samples were fabricated using a CNC router in order to improve the repeatability of the tests and reduce the standard deviation (SD) in the results caused by any variation in the shape and dimensions of the samples. The impacts of presence of knots and variations in density and MC on the TPE of the samples were assessed. For the knotted samples, the location of the knot was on the centre line of the test sample (Figure 2). The TPE samples were tested to ASTM D 143 [19] with a loading rate of 2.5 mm/min.

2.2.7. Compression test

Compressive strength is an important mechanical property in all contact points between structural elements in buildings, especially in compression members such as columns and in contact points where the reaction forces are present (e.g., floor bearers and joists). The compressive strength was evaluated both parallel and perpendicular to the grain direction. The dimensions of the samples were 25 mm × 25 mm × 100 mm for the CPA test and 35 mm × 50 mm × 150 mm for the CPE test. Two samples were extracted from each selected board to test the CPA and CPE of the lumber. The tests were conducted according to the procedures of ASTM D 143 [19]. The speed of loading was 0.3 mm/min for both tests. For the CPE test, the samples were loaded using a square metal bearing plate with the width of 50 mm. The CPE test was continued until a minimum of 2.5 mm deflection was achieved. The CPA test was conducted to the failure point of the samples. The impacts of variations in density and MC on both CPA and CPE were evaluated.

2.2.8. Basic density and MC measurement

The basic density and MC were measured for each sample tested for the different mechanical properties using the oven-dry weight. In total, 159 specimens were collected from the tested samples and assessed. The MC of the samples was calculated using according to AS/NZS 1080.1 [21].

The basic density of the samples was calculated using the following equation:

$$\rho = \frac{m_1}{V} \times \frac{100}{(100 + MC)} \quad (4)$$

where, MC is the moisture content (%), ρ is the basic density (kg/m³), m_0 is the weight of the sample before oven-drying (kg), m_1 is the weight of the sample after oven-drying (kg), V is the volume of the samples before oven-drying (m³).

2.3. Statistical analysis

The experimental design of the study is shown in Table 1.

Table 1. Experimental design of the study.

Test method	Test schematic	Total number of samples
Static bending	a	15
SPA	b	23 (4 knotted samples)
SPE	b	23 (5 knotted samples)
TPE	c	22 (4 knotted samples)
CPA	d	15
CPE	e	15
Cleavage	f	21
IBS	-	15
JH	g	10
Basic density and MC		159
Total number of samples		318

The results obtained were statistically analysed using IBM SPSS Statistics software (version 23). The normal distribution of the data set was examined using the Skewness Test. Analysis of variance (ANOVA) was used to determine the significance of differences between knotted and clear wood samples. Linear-regression models were developed using density and MC as regressors to predict the mechanical properties of the pulpwood *E. nitens* lumber. The coefficient of determination (R^2) was used to evaluate the significance of correlations between density, MC and the mechanical properties of the resource.

3. Results and Discussions

3.1. Basic density and MC

The overall average MC and basic density values obtained from the tested samples are shown in Table 2. The results showed a high variation in the density of the samples with more than 239.6 kg/m³ difference between the minimum and maximum values. However, the COV (i.e., SD divided by mean value) for density was still in the standard range at only 8.5%. Around 67% of the samples showed a density greater than 500 kg/m³. The density of the pulpwood *E. nitens* lumber in this study was 9.2% higher than that of the same plantation resource (480.6 kg/m³) reported by Derikvand et al. [13] and significantly lower than that of *E. nitens* lumber from native forests (670 kg/m³) indicated in AS 2082 [22]. The correlation between MC and density of the plantation *E. nitens* was positive and highly significant ($p < 0.00$). The results indicated that the basic density could explain more than 44% of the variations in the MC values of the samples (Figure 3). The COV for the MC values within all the samples tested in this study was low at less than 4.5%.

Table 2. Average MC and basic density values.

	N	Minimum	Maximum	Mean	SD
Density (kg/m ³)	159	429.4	669.0	523.6	44.6
MC (%)	159	8.2	10.5	9.0	0.4

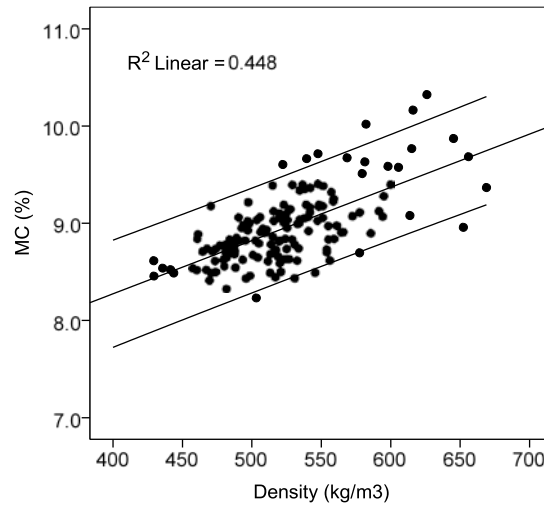


Figure 3. The correlation between MC and basic density.

3.2. Mechanical properties

The mechanical properties along with the density and MC values of the tested samples in each treatment are given in Table 3. The results given in this table represent the properties of small clear wood samples taken from only six logs from the plantation site. The Skewness coefficient values obtained for the mechanical properties were all greater than 0.05, which indicates the normal distribution of the data set for each mechanical property. The ANOVA results for the effect of knots on the SPA, SPE and TPE of the pulpwood *E. nitens* lumber is given in Table 4.

The results indicated that the presence of knot at the centre line of the load axis can increase both SPA and SPE of the lumber (Table 4). The increase in the shear strength was statistically significant for SPA but insignificant for SPE of the samples. The knotted samples also were associated with high COV values in the shear strength (around 41% for both SPA and SPE). These results are in agreement with those reported by Gupta et al. [23] and Cao et al. [24] for the effect of knots on the shear strength of small clear wood samples obtained from other species. The ANOVA results also indicated that the presence of knot in the samples significantly decreased the TPE of the lumber —with the clear wood samples being 92% stronger than the knotted ones.

It must be noted that the effect of knots on the mechanical properties is variable and depends on several different parameters including the grain deviation around knots, knot size parameter and loading conditions. The effect of knots on the mechanical properties of structural size lumber therefore may not necessarily be the same as in the small clear wood samples tested in this study—which could be evaluated in future.

The linear-regression models developed based on the correlations between MC and density with the mechanical characteristics of the pulpwood *E. nitens* lumber are given in Table 5. The regression models in this table are species specific and only valid for density values ranged from 429.4 kg/m³ to 669.0 kg/m³—based on the results obtained in this study. The highest coefficient of determination ($R^2 = 0.79$) was found between hardness and density of the pulpwood *E. nitens* lumber. The density showed a poor correlation with SPA and SPE of the samples. Moderate significant correlations were found between density with TPA, cleavage, CPE and MOE of the samples. The results showed that more than 65% of variations in the MOR, 64% of variations in the IBS and 53% of variations in the CPA of the test samples could be explained by their density values. A coefficient of determination of $R^2 = 0.65$ was obtained between the MOE and MOR values. A high coefficient of determination of $R^2 = 0.68$ was also obtained between axial hardness and side hardness of the samples. In all cases, the variations in MC values of the randomly selected samples in each treatment were not high enough to significantly influence the relevant mechanical characteristic of the pulpwood *E. nitens* in each group.

Table 3. The mechanical properties of the plantation *E. nitens*.

	Minimum	Maximum	Mean	COV (%)
MOR (MPa)	44.5	67.7	53.0	14.7 ^a
MOE (MPa)	6724.1	13218.0	10377.7	16.3 ^b
Density (kg/m ³)	461.2	598.0	526.4	8.0
MC (%)	8.2	9.6	9.0	4.4
Overall average hardness (MPa)	18.5	32.4	23.2	18.5 ^c
Average side hardness (MPa)	15.8	26.1	19.8	16.7
Average axial hardness (MPa)	23.5	45.0	30.2	22.2
Density (kg/m ³)	443.7	669.0	515.2	12.1
MC (%)	8.5	9.4	8.8	3.4
IBS (J/cm ²)	11.7	34.4	23.6	28.8 ^d
Density (kg/m ³)	441.4	599.7	518.4	7.6
MC (%)	8.4	9.4	9.0	3.3
Cleavage (kN)	0.8	2.7	1.6	31.3
Density (kg/m ³)	481.4	645.2	533.1	7.1
MC (%)	8.4	9.9	9.0	4.4
SPA (MPa)	3.0	12.5	5.5	40.0 ^e
Density (kg/m ³)	460.8	605.5	514.1	6.7
MC (%)	8.5	9.7	8.9	3.4
SPE (MPa)	3.9	13.0	8.5	25.9
Density (kg/m ³)	469.9	594.9	528.9	6.2
MC (%)	8.4	10.0	8.9	4.5
TPE (MPa)	0.5	5.5	3.4	41.2
Density (kg/m ³)	464.9	615.1	518.0	7.0
MC (%)	8.6	9.8	9.0	3.3
CPA (MPa)	34.3	54.2	42.8	11.4 ^f
Density (kg/m ³)	429.3	652.3	508.5	13.1
MC (%)	8.5	9.1	8.7	2.3
CPE (MPa)	2.6	5.8	4.1	24.4 ^g
Density (kg/m ³)	480.5	626.1	527.4	8.5
MC (%)	8.3	10.3	9.1	6.6

The suggested COV values by Wood Handbook [25]: a: 16%, b: 22%, c: 20%, d: 25%, e: 14%, f: 18% and g: 28%.

Table 4. Average values of SPA, SPE and TPE of samples with and without knot.

	Sample type	Mean	SD	ANOVA
SPA (MPa)	Clear	5.2	1.1	*
	Knotted	10.4	4.3	
SPE (MPa)	Clear	6.5	1.3	NS
	Knotted	9.8	4.0	
Tensile strength (MPa)	Clear	4.6	0.9	*
	Knotted	2.4	1.30	

NS = Not significant; * = Significant at $P < 0.05$.

Table 5. The correlations between density, MC and mechanical properties.

Dependent Variable	Linear-regression model	Coefficient of determination (R ²)
TPE (MPa)	TPE = -8.77 + 0.02*Density	0.38
	TPE = -11.35 + 1.63*MC	0.16
SPE(MPa)	SPE = -9.79 + 0.03*Density	0.27
	SPE = 1.71 + 0.77*MC	0.02
SPA (MPa)	SPA = -10.17 + 0.03*Density	0.22
	SPA = 0.37 + 0.58*MC	0.01
Cleavage (kN)	Cleavage = -2.97 + 0.0087*Density	0.38
	Cleavage = -3.26 + 0.54*MC	0.13
IBS (J/cm ²)	IBS = -48.46 + 0.14*Density	0.64
	IBS = -0.03 + 2.64*MC	0.01
CPA (MPa)	CPA = -15.4 + 0.05*Density	0.53
	CPA = -24.4 + 7.69*MC	0.12
CPE (MPa)	CPE = -3.5 + 0.01*Density	0.40
	CPE = -3.23 + 0.81*MC	0.22
Average hardness (MPa)	Hardness = -8 + 0.6*Density	0.79
	Hardness = -50.97 + 8.49*MC	0.32
MOE (MPa)	MOE = -3380 + 26.14*Density	0.42
	MOE = 21200 – 1200*MC	0.06
MOR (MPa)	MOR = 14.61 + 3.15*MOE	0.65
	MOR = -23.7 + 0.15*Density	0.61
	MOR = 66.21 – 1.47*MC	0.00

3.3. Failure modes

In general, the failure modes of the clear wood samples were similar to those reported in previous studies for other wood species—e.g., Gupta et al. [23] and Cao et al. [24]. The failure modes of the knotted shear samples loaded parallel to the grain were slightly different than those reported by Cao et al. [24] for the effect of knots on the shear strength of Southern yellow pine. More details about the failure modes of the samples are given in the following sections for each type of test.

3.3.1. Bending samples

As the bending samples were all obtained from straight-grain, defect-free wood, the bending failure modes were relatively consistent. Two general types of failure were observed from these samples, namely, grain tension failure and combined compression and bending tension failure (Figure 4).

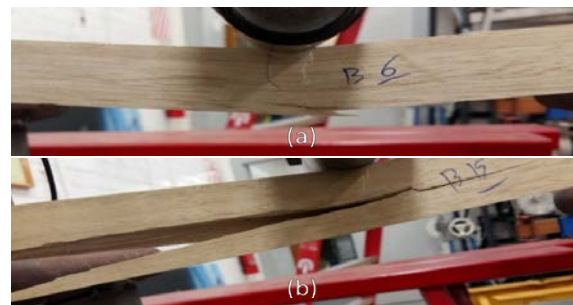


Figure 4. The most frequently observed failure modes of the bending test samples. Combined compression and bending tension failure (a) and grain tension failure (b).

3.3.2. Hardness samples

As the ball bearing fixture penetrated the hardness samples, distinct differences were observed in the fibre deformations between the three different annual growth ring orientations. While the ball

bearing fixture caused a spherical deformation in the samples with 90° annual growth ring orientation, the failure modes in the wood fibre tended to be more irregular as the angle between the loading direction and annual growth rings decreased from 90° to zero degree (Figure 5).

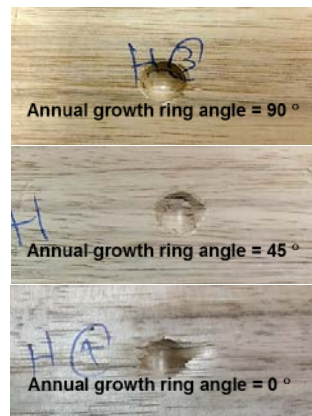


Figure 5. Fibre deformations in hardness samples with different annual growth ring orientations.

3.3.3. IBS samples

The failure mode of the IBS samples was mainly grain tension failure. No brittle failure was observed in these samples.

3.3.4. Cleavage samples

In all cases, the failure of the cleavage samples occurred by the separation of the wood fibres along the longitudinal axis of the samples parallel to the grain direction as shown in Figure 6.



Figure 6. Failure modes of cleavage samples.

3.3.5. Shear samples

The general failure modes of the SPA and SPE samples with and without knot can be seen in Figure 7. The failure mode of the SPA samples without knot was mainly pure shear failure parallel to the grain. The failure in the knotted SPA samples occurred along the fibre direction and was affected by the grain deviations around the knot. No failure in the knot itself was observed in these samples. The failure of the SPE samples was completely different than that of the SPA samples. The failure in these samples started by compression of the wood fibre perpendicular to the grain direction followed by developing cracks and separation of the wood fibres along the grain direction (Figure 7). The failure mode of the SPE samples was not affected by the presence of knot—no failure in the knot was observed.

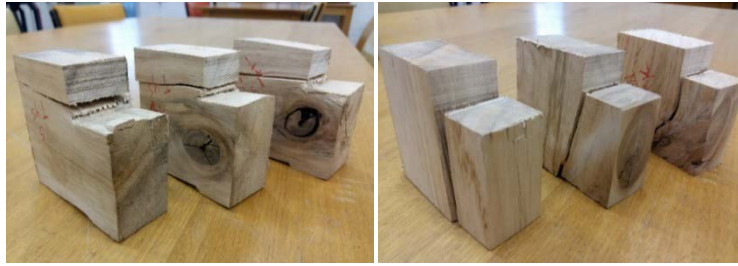


Figure 7. Failure modes of SPE (left) and SPA (right) with and without knot.

3.3.6. Tension samples

The failure mode of the tension samples without knot was purely tension failure along the grain direction (Figure 8). For the knotted samples all the failures occurred in the knot itself.

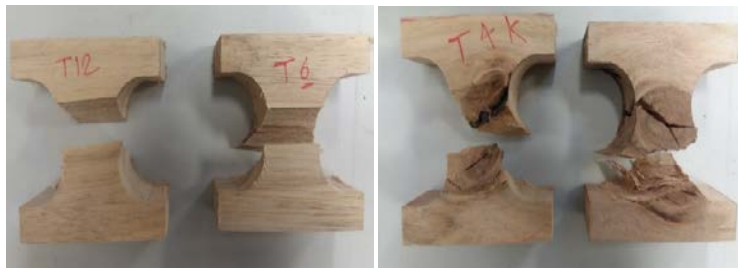


Figure 8. Failure modes of clear (left) and knotted (right) TPE samples.

3.3.7. Compression samples

Three general types of failures were observed in the CPA samples under loading as shown in Figure 9. The failure modes in these samples were classified into different groups in accordance with ASTM D 143 [19], namely, combined compression and shearing parallel to grain, combined end-rolling and shearing and crushing. The failure mode of the CPE samples was typical compression failure with no obvious difference between the three annual growth ring orientations.

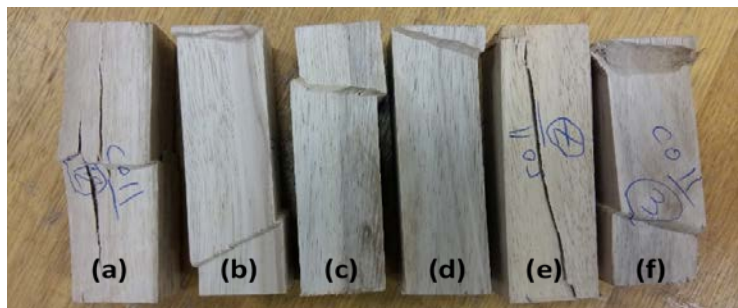


Figure 9. Failure modes of the CPA samples. (a) and (e) compression and shearing parallel to grain, (b) and (f) end-rolling and shearing, (c) and (d) crushing.

3.4. The COV of the mechanical properties

The COV values obtained from the mechanical testing of small clear wood samples in the study were compared to those provided by Wood Handbook [25] for each test as given in Table 3—no COV values are supplied by Wood Handbook [25] for cleavage, SPE and TPE tests.

In this study, except for the IBS and SPA samples, the COV values obtained from the other mechanical tests were lower than those suggested by Wood Handbook [25]. The COV values obtained

from SPA, SPE, cleavage and TPE tests were quite high. Given the fact that the samples tested in this study were taken from only six logs from one plantation site, the COV values in the mechanical properties of the samples may not necessarily be representative of other plantation *E. nitens* resources. The COV of mechanical properties is important in the production, application and quality assurance of different wood products. The COV is also an important indication that determines the repeatability of a given mechanical test, which is of high importance for research purposes. From an engineering perspective, it is usually not a concern if a product is stronger or stiffer than the average. A stronger or stiffer wood product however may also be associated with higher density and hardness—as obtained for most mechanical properties of the lumber tested in this study. A denser and harder product could be difficult to work with and not suitable for an application that requires lightweight materials. Further studies will be required to establish allowable stress values for the studied mechanical properties of the resource. Considering the high COV values obtained for some of the mechanical properties tested in this study, it is highly important in the establishment of allowable design stress values of the pulpwood *E. nitens* lumber to test a reasonably large sample size for each mechanical property from the different growth ring orientations (as in the sampling method in this study) and take into account the influence that the natural variations in density can have on these properties.

4. Conclusions

The aim of this study was to characterise the physical and mechanical properties of fast-growing, pulpwood *E. nitens* lumber as a potential raw material for the production of mass laminated timber for structural building applications.

- A profile of physical and mechanical properties of the pulpwood *E. nitens* lumber was created that can be used in future research for finite element analysis on the structural performance of any potential mass laminated timber product from such a plantation resource.
- There was a high variation in the density values of the pulpwood *E. nitens* lumber that significantly influenced all the studied mechanical properties. The linear-regression models developed in the study using density as the single regressor indicated high coefficient of determinations in predicting the hardness, MOR, IBS and CPA of the lumber. The correlations between the density and TPA, cleavage, CPE and MOE of the lumber were moderate but still statistically significant. The shear strength of the lumber was less sensitive to the natural variations in the density values.
- The variations in the MC of the pulpwood *E. nitens* lumber after conventional kiln drying were low in each test treatment and therefore had no significant influence on the mechanical properties.
- The presence of knot significantly increased the SPA and decreased the TPE of the lumber. The effect of knot on the SPE of the lumber was statistically insignificant—even though an increase in the shear strength was observed in the knotted samples.
- Considering relatively high COV values for some mechanical properties, establishing the allowable stress values of the pulpwood *E. nitens* lumber will require sampling and testing of small clear samples from different growth ring orientations (as used in this study) by taking into account the effect that the density can have on the results.

Author Contributions: Conceptualization, M.D.; methodology, M.D., N.K., M.L., H.J. and G.N.; formal analysis, M.D.; investigation, M.D.; writing—original draft preparation, M.D.; writing—review and editing, M.D., N.K., M.L., H.J. and G.N.; supervision, N.K., H.J. and G.N.

Funding: This research was funded by the Australian Research Council, Centre for Forest Value, University of Tasmania, TAS, Australia, grant number IC150100004. The additional support from Forest and Wood Products Australia Limited (FWPA), Melbourne, VIC, Australia is acknowledged (Grant Number: PNB387-1516). The APC was funded by the Australian Research Council, Centre for Forest Value, University of Tasmania, TAS, Australia.

Acknowledgments: The authors are grateful of the support from Forico Pty Ltd. in providing the logs and Britton Timbers for the milling of the logs, drying and finishing of the boards.

Conflicts of Interest: The authors declare no conflict of interest.

References

1. Gilbert, B.P.; Underhill, I.D.; Bailleres, H.; El Hanandeh, A.; McGavin, R.L. Veneer based composite hollow utility poles manufactured from hardwood plantation thinned trees. *Construction and Building Materials* **2014**, *66*, 458-466. DOI: <https://doi.org/10.1016/j.conbuildmat.2014.05.093>
2. Gilbert, B.P.; Bailleres, H.; Zhang, H.; McGavin, R.L. Strength modelling of Laminated Veneer Lumber (LVL) beams. *Construction and Building Materials* **2017**, *149*, 763-777. DOI: <https://doi.org/10.1016/j.conbuildmat.2017.05.153>
3. Bal, B.C. Some technological properties of laminated veneer lumber produced with fast-growing Poplar and Eucalyptus. *Maderas. Ciencia y tecnología* **2016**, *18*(3), 413-424. DOI: <http://dx.doi.org/10.4067/S0718-221X2016005000037>
4. Crafford, P.L.; Wessels, C.B. The potential of young, green finger-jointed Eucalyptus grandis lumber for roof truss manufacturing. *Southern Forests: a Journal of Forest Science* **2016**, *78*(1), 61-71. DOI: <http://dx.doi.org/10.2989/20702620.2015.1108618>
5. Lara-Bocanegra, A.J.; Majano-Majano, A.; Crespo, J.; Guaita, M. Finger-jointed Eucalyptus globulus with 1C-PUR adhesive for high performance engineered laminated products. *Construction and Building Materials* **2017**, *135*, 529-537. DOI: <https://doi.org/10.1016/j.conbuildmat.2017.01.004>
6. Liao, Y.; Tu, D.; Zhou, J.; Zhou, H.; Yun, H.; Gu, J.; Hu, C. Feasibility of manufacturing cross-laminated timber using fast-grown small diameter eucalyptus lumbers. *Construction and Building Materials* **2017**, *132*, 508-515. DOI: <https://doi.org/10.1016/j.conbuildmat.2016.12.027>
7. ABARES. Australian forest profiles – Eucalypt. Australian Bureau of Agricultural and Resource Economics and Sciences, Canberra, Australia 2016. Retrieved from: http://www.agriculture.gov.au/abares/forestsaustralia/PublishingImages/Forest%20profiles%202016/Eucalypt/AusForProf_2016_Eucalypt_v1.0.0.pdf.
8. Downham, R.; Gavran, M. Australian plantation statistics 2017 update, ABARES, Canberra, Australia 2017. Retrieved from: <http://www.agriculture.gov.au/abares/publications>.
9. Farrell, R.; Innes, T.C.; Harwood, C.E. Sorting Eucalyptus nitens plantation logs using acoustic wave velocity. *Australian Forestry* **2012**, *75*(1), 22-30. DOI: <http://dx.doi.org/10.1080/00049158.2012.10676382>
10. Blackburn, D.; Vega, M.; Yong, R.; Britton, D.; Nolan, G. Factors influencing the production of structural plywood in Tasmania, Australia from Eucalyptus nitens rotary peeled veneer. *Southern Forests: a Journal of Forest Science* **2018**, 1-10. <https://doi.org/10.2989/20702620.2017.1420730>
11. Blackburn, D.; Vega, M. Segregation of Eucalyptus nitens logs from fibre-managed plantations for veneer based engineered wood products. Final report, Centre for Sustainable Architecture with Wood (CSAW) School of Architecture and Design, University of Tasmania, Australia 2017.
12. Derikvand, M.; Nolan, G.; Jiao, H.; Kotlarewski, N. What to Do with Structurally Low-Grade Wood from Australia's Plantation Eucalyptus; Building Application?. *BioResources* **2017**, *12*(1), 4-7. DOI: <https://doi.org/10.15376/biores.12.1.4-7>
13. Derikvand, M.; Kotlarewski, N.; Lee, M.; Jiao, H.; Chan, A.; Nolan, G. Visual stress grading of fibre-managed plantation Eucalypt timber for structural building applications. *Construction and Building Materials* **2018**, *167*, 688-699. <https://doi.org/10.1016/j.conbuildmat.2018.02.090>
14. AS 1720.1. *Timber Structures – Design Methods*, Standards Australia: Sydney, Australia, 2010.
15. Yang, J.L.; Evans, R. Prediction of MOE of eucalypt wood from microfibril angle and density. *Holz als Roh-und Werkstoff* **2003**, *61*(6), 449-452. DOI: <https://doi.org/10.1007/s00107-003-0424-3>
16. Chauhan, S.S.; Walker, J. Relationships between longitudinal growth strain and some wood properties in Eucalyptus nitens. *Australian Forestry* **2004**, *67*(4), 254-260. DOI: <http://dx.doi.org/10.1080/00049158.2004.10674943>
17. Blackburn, D.; Hamilton, M.; Harwood, C.; Innes, T.; Potts, B.; Williams, D. Stiffness and checking of Eucalyptus nitens sawn boards: genetic variation and potential for genetic improvement. *Tree genetics & genomes* **2010**, *6*(5), 757-765. DOI: <https://doi.org/10.1007/s11295-010-0289-7>
18. Medhurst, J.; Downes, G.; Ottenschlaeger, M.; Harwood, C.; Evans, R.; Beadle, C. Intra-specific competition and the radial development of wood density, microfibril angle and modulus of elasticity in plantation-grown Eucalyptus nitens. *Trees* **2012**, *26*(6), 1771-1780. DOI: <https://doi.org/10.1007/s00468-012-0746-z>

19. ASTM D 143. *Standard test methods for small clear specimens of timber*, American Society for Testing and Materials (ASTM) International: United States, 2009.
20. Bal, B.C.; Bektaş, İ. The effects of some factors on the impact bending strength of laminated veneer lumber. *BioResources* **2012**, 7(4), 5855-5863. DOI: <https://doi.org/10.15376/biores.7.4.5855-5863>
21. AS/NZS 1080.1. *Timber – Methods of Test – Moisture Content*, Standards Australia: Sydney, Australia, 2012.
22. AS 2082. *Timber - Hardwood - Visually stress graded for structural purposes*, Standards Australia, Australia, 2007.
23. Gupta, R.; Basta, C.; Kent, S.M. Effect of knots on longitudinal shear strength of Douglas-fir using shear blocks. *Forest Products Journal* **2004**, 54(11), 77-83.
24. Cao, Y.; Street, J.; Mitchell, B.; To, F.; DuBien, J.; Seale, R.D.; Shmulsky, R. Effect of Knots on Horizontal Shear Strength in Southern Yellow Pine. *BioResources* **2018**, 13(2), 4509-4520. <https://doi.org/10.15376/biores.13.2.4509-4520>
25. Wood handbook. *Wood as an engineering material*. General Technical Report FPL-GTR-190. Department of Agriculture, Forest Service, Forest Products Laboratory, Madison, USA, 2010: 508 p.

Appendix E: Paper V

Publication reference: Derikvand, M., Jiao, H., Kotlarewski, N., Lee, M., Chan, A., & Nolan, G. (2019). Bending performance of nail-laminated timber constructed of fast-grown plantation eucalypt. *European Journal of Wood and Wood Products*, 1-17.

Bending performance of nail-laminated timber constructed of fast-grown plantation eucalypt

Mohammad Derikvand, Hui Jiao, Nathan Kotlarewski, Michael Lee, Andrew Chan, Gregory Nolan

Abstract

Australia's hardwood plantation estate is predominantly comprised of *Eucalyptus nitens* and *Eucalyptus globulus*, which are mainly being managed to produce woodchips—a low-value commodity export. There is an increasing interest by the timber industry in developing higher-value structural products from the low-grade timber recovered from these plantation resources. In this experimental study, for the first time, the bending performance of nail-laminated timber (NLT) and NLT-concrete composite (NLTC) floor panels constructed of the low-grade, fibre-managed *Eucalyptus nitens* and *Eucalyptus globulus* timber was evaluated. The test panels were constructed with various span lengths and cross-sectional configurations and subjected to vibration and four-point bending tests. The results indicated that the modulus of elasticity of the *Eucalyptus nitens* NLT panels (11074.6 MPa) was comparable to that of NLT panels made of *Eucalyptus globulus* (11203.2 MPa). The modulus of rupture of the *Eucalyptus globulus* panels was 13.8% higher than that of the *Eucalyptus nitens* ones. The bending properties of the NLT panels constructed of the two plantation species were superior to those of some commercially important mass laminated timber products reported in the literature. Under the limit state design loads, all the NLT and NLTC panels were still in the linear-elastic range. The fundamental natural vibration frequency values of the test panels were above the recommended minimum range of 8-10 Hz for residential and office floors. The two plantation timber species therefore demonstrated sufficient short-term bending performances to be used in the construction of higher-value structural floor products.

Keywords: mass laminated timber; *Eucalyptus nitens*; *Eucalyptus globulus*; bending moment capacity; modulus of elasticity; modulus of rupture; vibration.

Abbreviations

BMC = Bending moment capacity
CLT = Cross-laminated timber
GLT = Glue-laminated timber
LCC = Load-carrying capacity
LSD = Limit state design
ULS = Ultimate limit state
SLS = Serviceability limit state

MOE = Modulus of elasticity
MOR = Modulus of rupture
NLT = Nail-laminated timber
NLTC = Nail-laminated timber-concrete
NLTC#1 = Nail-laminated timber-concrete type one
NLTC#2 = Nail-laminated timber-concrete type two
NLTC#3 = Nail-laminated timber-concrete type three

Geometrical and mechanical parameters

a = One-third of span length
b = Breadth
d = Depth
D = Weight of panels
 $EI_{eff,0}$ = Effective stiffness of panels with no composite action
 $EI_{eff,1}$ = Effective stiffness of panels with full composite action
 $EI_{eff,em}$ = Empirical effective flexural stiffness
 $EI_{eff,ser}$ = Empirical effective flexural stiffness at SLS load
 G_1 = Permanent load from the self-weight
 G_2 = Superimposed permanent load
 G_T = Total permanent load
I = The second moment of area
L = Span length
 L_p = Panel length
M = Actual bending moment
 M_{ULS} = Design bending moment

\emptyset = Diameter
 ϵ = Composite efficiency of connections
P = Maximum applied load
 P_1 = 10% of maximum applied load
 P_2 = 40% of maximum applied load
 P_G = Analytical uniformly distributed load at SLS
 P_S = Experimental imposed load
 P_{Su} = Experimental uniformly distributed load at SLS
 Q_o = Design imposed load for office buildings
 Q_R = Design imposed load for residential buildings
SLC = Specific load-carrying capacity
 W_{ULS} = Combination of permeant and imposed loads
 δ_{SLS} = Serviceability deflection limit
 ϕ_1 = Deflection at P1
 ϕ_2 = Deflection at P2
 ϕ_s = Maximum deflection at P_S

1. Introduction

As demand for using timber in building constructions continuous to grow, sustainable supply of timber for structural purposes is of high importance. In this context, fast-growing species such as eucalypt have attracted the timber industry in Australia and worldwide (Blackburn et al. 2011; Derikvand et al. 2017, 2018 a, b, 2019; Gilbert et al. 2017; Lara-Bocanegra et al. 2017; Liao et el. 2017; Lu et al. 2018). Eucalypt is the most widely planted hardwood species in the world. In Australia, eucalypt plantations are mostly managed to produce woodchips—a low-value product—for pulp and paper industry. Forestry management regimes applied to these plantation resources are generally aimed to increase wood volume production—rather than wood quality. As a result, sawn timber recovered from such plantation resources is structurally low-grade (Derikvand et al. 2017, 2018a, b). This creates challenges against using this timber directly as individual boards in most structural applications, especially when the structural element is exposed to high service loads. Nevertheless, there may be still a good potential for this timber resource to be used in producing innovative structural mass laminated timber products for building applications.

The use of mass laminated timber products in the construction of residential and non-residential buildings has increased in popularity in the last few years (Raftery and Rodd 2015; Lu et al. 2018; Mai et al. 2018; Wang et al. 2018). A mass laminated timber product is made of several layers of solid timber boards laminated together with either structural glue or mechanical fasteners such as nails and screws. When exposed to external loads, the timber boards in each layer are able to transfer a portion of the

loads to the boards in their adjacent layers. In such a system, stiffer boards will attract more load than weaker boards and once a single failure occurs, the stiffer boards will carry increased loads—which results in a load redistribution in the system (Brandner and Schickhofer 2006). This creates a reliable load sharing factor which helps to decrease the impacts of strength-reducing features such as knots on the overall performance of the product (Kandler et al. 2018).

To date, limited studies have been conducted to investigate the potential of fast-grown plantation eucalypt species in the production of mass laminated timber (Lara-Bocanegra et al. 2017; Dugmore 2018; Pröller et al. 2018). Liao et al. (2017) investigated the feasibility of using a hybrid plantation eucalypt timber resource (*Eucalyptus urophylla* × *Eucalyptus grandis*) in producing cross-laminated timber (CLT). These researchers demonstrated that producing CLT from the hybrid plantation eucalypt timber can be a promising alternate application for this resource as demands of woodchips for pulp and paper industry decreases. An important challenge in using the fast-grown plantation eucalypt timber in producing CLT however was reported to be the poor bond performance of such a timber resource due to its relatively high density, poor adhesive penetration, and high internal stress and percentage of juvenile wood (Lu et al. 2017).

Nail-laminated timber (NLT) is another example of an engineered, mass laminated timber product that has effectively been adapted to use in different structural applications such as floor systems, timber decks, and timber bridges (Weckendorf et al. 2016; Hong 2017; Zhou et al. 2017). NLT is composed of a series of timber boards placed on their edges and nailed together on their sides (i.e., the widest face). The use of NLT in building construction has many advantages that can make it an appropriate product option for the low-grade timber of fibre-managed plantation eucalypt. Some of these advantages are highlighted as follow:

- Unlike CLT and glue-laminated timber (GLT), NLT is a mechanically laminated product. Hence, its strength and stiffness are independent than the adhesion properties of the timber used in its construction. This enables the use of highly featured (low-grade) timber without any extensive pre-thicknessing processes, which are normally required for producing CLT and GLT from hardwood (Lu et al. 2018).
- NLT is less variable in strength and stiffness compared to solid timber and its characteristic strength is higher than that of solid timber of the same dimensions (Hong 2017). This results in a higher allowable design stress.
- NLT production requires no high-tech equipment or necessarily unique manufacturing facilities and can be even produced locally in a variety of sizes to suit different structural applications.
- Structural NLT components can be prefabricated off-site and assembled on-site, which leads to reduced building construction time and cost.
- Due to its high load sharing factor, NLT enables the possibility of using structurally medium-grade to low-grade boards in building construction and also in combination with higher grade

ones. This allows for custom structural requirements in building components and could maximise the use of timber boards from low grade levels in structural applications.

Although opportunities exist in developing higher-value mass laminated timber products from the Australian fibre-managed eucalypt plantations, no information is available in the literature regarding the performance of these timber resources in the construction of such products. The available information to date is related to the potential of the fibre-managed plantation eucalypt in producing sawn timber (Farrell et al. 2012; Derikvand et al. 2018a, b), plywood (McGavin et al. 2015; Blackburn et al. 2018), and laminated veneer lumber (Blackburn and Vega 2017).

The overall aim of this experimental study was to evaluate the performance of low-grade timber recovered from fast-growing, fibre-managed plantation *Eucalyptus nitens* (*E. nitens*) and *Eucalyptus globulus* (*E. globulus*) in the construction of high-mass NLT and NLT-concrete (NLTC) composite elements with a target application in the structural floor systems. In the recent years, there has been a growing interest by the Australian plantation forest and timber industries in developing higher-value structural mass laminated timber products from the low-grade timber recovered from these plantation resources (Derikvand et al. 2017, 2018a, b). The objectives of this study were to:

- Determine the bending modulus of elasticity (MOE) and modulus of rupture (MOR) of NLT floor panels constructed of *E. nitens* and *E. globulus* under four-point bending load.
- Determine the specific load-carrying capacity (SLC) and empirical effective flexural stiffness ($EI_{eff,em}$) of NLT and NLTC panels constructed of the two timber species.
- Evaluate the composite efficiency of the NLTC panels constructed using conventional screw-type shear connectors.
- Compare the structural bending capacity of the NLT panels made of the two plantation species with other types of commercially important mass laminated timber products reported in the literature.
- Examine and verify the performance of the NLT and NLTC panels constructed of the two plantation species against the limit state design (LSD) requirements for bending moment capacity (BMC) and serviceability of structural floor systems, with respect to both vibration and deflection, in residential self-contained dwellings and office buildings.

2. Materials and Methods

2.1. Floor panel production

The timber boards were obtained from a 16 years old fibre-managed plantation *E. nitens* resource and a 26 years old fibre-managed plantation *E. globulus* resource harvested from the north of Tasmania, Australia. The stands were unthinned and unpruned and the recovered boards had substantial strength-reducing features such as knots and surface checking. The boards were processed (sawn, dried, and machine dressed) under normal commercial procedures. The thickness of the finished boards was 35

mm. The widths of the boards used were 70 mm, 90 mm, and 140 mm. The length of the boards varied depending on the required length of the test panels. The boards were used with continuous length without any end jointing. A total of 112 timber boards were used in the production of the test panels in this study. The average oven-dry densities of the *E. nitens* and *E. globulus* boards used were $493.2 \pm 61.3 \text{ kg.m}^{-3}$ and $505.2 \pm 54.0 \text{ kg.m}^{-3}$, respectively. The average MOE and MOR values of the plantation *E. nitens* timber used in this study were reported to be respectively 10.8 GPa and 43.6 MPa (Derikvand et al. 2018a). The plantation *E. globulus* timber also has shown an average MOE of 11.3 GPa and an average MOR of 46.2 MPa in a previous study by Derikvand et al. (2018b).

Two types of floor panels, with concrete (NLTC) and without concrete (NLT), were constructed and tested from both timber species. The NLT component in each panel was constructed by nailing eight boards together vertically on their sides using a pneumatic nail gun. The dimensions of the nails used are depicted in Fig. 1. The nailing pattern used allowed a nominal spacing of 300 mm between the nails in each row (Fig. 2). The edge distance of the nails was 20 mm in all test treatments (Robertson et al. 2018).

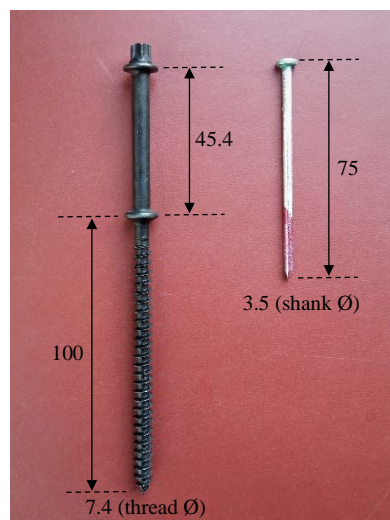


Fig. 1. SFS Shear connector (left) and nail (right) used (measurements in mm).

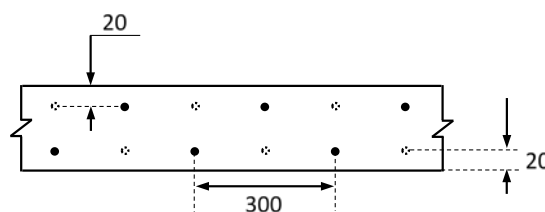
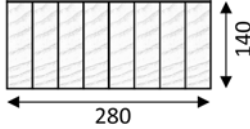
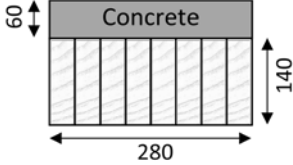
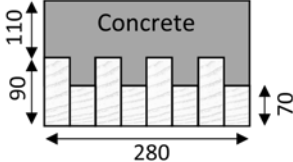


Fig. 2. The nailing pattern used (measurements in mm).

The NLTC panels were produced with two different cross-sectional patterns as depicted in Table 1. In the construction of the NLTC panels, one row of SFS shear connectors was installed into the centre line

of the top surface of the panels with the use of pre-drilled holes that were 3.5 mm smaller in diameter than the SFS shear connectors.

Table 1. Experimental design of the study.

Sample type	Cross-sectional configuration (mm)	Sample code	Species	Span length (mm)	Replicates
NLT (without concrete)		NLT	<i>E. nitens</i>	3300	2
			<i>E. globulus</i>	3300	2
NLTC (with concrete)		NLTC#1	<i>E. nitens</i>	3300	2
			<i>E. globulus</i>	3300	2
		NLTC#2	<i>E. nitens</i>	4600	1
			<i>E. globulus</i>	4600	1
		NLTC#3	<i>E. nitens</i>	3300	2
			<i>E. globulus</i>	3300	2

The dimensions of the SFS connectors are shown in Fig. 1. Each row consisted of two rows of the SFS connectors inclined at 45° angle to the horizontal plane in opposite directions with an embedment depth of 100 mm (Fig. 3). The SFS connectors were amongst the first generations of shear connectors specifically designed for timber-concrete structures and are widely used in the construction and repair of structural floor systems (Popovski and Gavric 2015; Rijal et al. 2015; Mai et al. 2018; Oudjene et al. 2013, 2018). This type of connectors was selected as they are cheap and simple to use, although their structural efficiency on plantation eucalypt timber is unknown.



Fig. 3. Shear connectors on NLTC#3 samples before casting the concrete.

After installing the shear connectors, reinforcement concrete wire mesh was installed on the shear connectors and plywood formwork was fixed around each NLTC panel to cast the concrete onto the specimen. The top surface of the NLTC panels was covered by a layer of BondCrete to prevent the timber from absorbing moisture from the wet concrete. The specific gravity of the BondCrete was 1.08. After the BondCrete was fully dried, the concrete was poured into the formwork and left in the laboratory environment to cure for 28 days prior to testing. Normal concrete was used for this purpose. The compressive strength of the concrete used was 32 MPa—provided by the supplier of the concrete based on cylinder tests. The concrete was kept moist by daily spraying water for two weeks. The formwork was removed after the concrete had fully cured.

2.2. Experimental tests description

2.2.1. Vibration test

All the test panels in the study were subjected to vibration assessment prior to four-point bending tests. For the vibration tests, the panels were simply supported with the span lengths given in Table 1. Each panel was excited three times at the centreline of the panels on the top surface and allowed to vibrate freely. Sufficient time was considered between each excitation so that the previous vibration can fully damp out without influencing the next one. A 450 g basketball dropped from 100 cm height was used as the excitation impulse. This method was adapted from a similar testing system by Hamilton (2014), Taoum (2016), and Kan et al. (2017). The vertical acceleration resulting from each excitation was recorded using an accelerometer (Bosch Sensortech BMC150 Acceleration Sensor) with a resolution of 0.0383 m.sec⁻² placed at the mid-span of the panels. The fundamental natural vibration frequency of the panels was identified using a Fast Fourier Transform taken from the acceleration time-history data obtained from the vibration tests.

2.2.2. Static bending test

The NLT and NLTC panels were then tested using a four-point bending test set-up in accordance with AS/NZS 4063.1 (Standards Australia 2010). The speed of loading was 7.5 mm.min⁻¹. The deflection resulting from the loads was measured from the bottom surface at mid-span of the panels. The loading of each sample continued until either a full failure occurred in the panels or an unrecoverable drop was observed in the load graph. The maximum slip between the NLT component and the concrete slab in the NLTC panels, resulting from the bending load, was measured using two dial gauges fixed at both ends of the panels. The BMC of the test panels was calculated using Equation 1:

Equation 1

$$M = \frac{P L}{6}$$

where, M is the actual BMC of the panels (kN.m), P is the maximum applied load (kN), L is the span length (m).

The MOE and MOR of the NLT panels were calculated using Equation 2 and Equation 3, respectively:

Equation 2

$$MOE = \frac{23L^3(P_2 - P_1)}{108bd^3(\varphi_2 - \varphi_1)}$$

Equation 3

$$MOR = \frac{P L}{bd^2}$$

where, b and d are the width (breadth) and depth of the panels (mm), L is the span length (mm), P_2 and P_1 are respectively 40% and 10% of the maximum applied load (P) at failure point (N), φ_2 and φ_1 are the maximum deflections (mm) at P_2 and P_1 loads, respectively.

The empirical effective flexural stiffness of the NLT and NLTC panels was calculated at P_2 (or 40% of the maximum applied load) (Mai et al. 2018) using Equation 4.

Equation 4

$$EI_{eff,em} = \frac{3aP_2L^2 - 4P_2a^3}{48\varphi_2}$$

where, $EI_{eff,em}$ is the empirical effective flexural stiffness (N.mm²) at P_2 , a is one-third of the span length (mm), φ_2 is the maximum deflection at P_2 (mm), and L is the span length (mm).

The SLC of the test panels was calculated using Equation 9:

Equation 5

$$SLC = \frac{P}{D}$$

where, SLC is the specific load-carrying capacity or the amount of load a unit weight of each panel can carry (N/N), P is the maximum applied load at failure point (N), and D is the weight of the panel (N).

2.3. Evaluation of the interlayer connections

The composite efficiency of the timber-concrete connections (ϵ) in the NLTC panels was estimated as a percentage value by using the following equation (Piazza and Ballerini 2000; Ballerini et al. 2002; Mai et al. 2018):

Equation 6

$$\epsilon = \frac{EI_{eff,em} - EI_{eff,0}}{EI_{eff,1} - EI_{eff,0}} \times 100$$

where, $EI_{eff,em}$ is the empirical effective flexural stiffness of the NLTC panels (N.mm²), $EI_{eff,1}$ is the effective flexural stiffness of the NLTC panels with a theoretical full composite action with no slip at the interface of the concrete and NLT component (N.mm²), $EI_{eff,0}$ is the effective flexural stiffness of the NLTC panels with a theoretical no composite action and no force couple resisted by the composite cross-section (N.mm²).

The $EI_{eff,1}$ for the NLTC panels was modelled using the gamma-method and a shear bond coefficient of one (Yeoh et al. 2010; Mai et al. 2018). The $EI_{eff,0}$ values were calculated in the same way but by making use of a shear bond coefficient of zero.

2.4. Ultimate limit state (ULS) verification

A series of analytical calculations were conducted to see if the NLT and NLTC floor panels made from the two plantation eucalypt species can meet the ULS requirements for bending capacity under short-term loading conditions. For this purpose, the ULS design loads were calculated for each panel as a combination of uniformly distributed permanent load (i.e., the weight of the panel itself or dead load) plus uniformly distributed imposed load (i.e., live load) in accordance with AS/NZS 1170.1 (Standards Australia 2002). In AS/NZS 1170.1 (Standards Australia 2002), the imposed load relevant to the structural floor systems in office buildings is different than that of residential buildings (self-contained dwellings). For the design of structural floors in offices with general use, AS/NZS 1170.1 (Standards Australia 2002) suggests a uniformly distributed imposed load (Q) of 3 kPa, whereas for general floor areas in residential buildings the suggested uniformly distributed imposed load is equal to 1.5 kPa. The uniformly distributed imposed load per one metre length of the panels for office buildings (Q_O) and residential buildings (Q_R) is calculated as:

Equation 7

$$Q_{O \text{ or } R} = bQ$$

where, b is the width of the panels (m).

The amount of permanent load (G_1) resulting from the self-weight per one metre length of each panel (kN/m) was calculated using Equation 8.

Equation 8

$$G_1 = \frac{D}{L_p}$$

where, D is the weight of the panels (kN), L_p is the panel length (m).

A superimposed permanent load (G_2) of 1 kPa (or 0.28 kN/m per one metre length of the panels) was also considered in the ULS calculations to account for the dead loads resulting from the weight of non-structural elements and semi-permanent members in the building (Yeoh et al. 2011). The total permanent load (G_T) was calculated as:

Equation 9

$$G_T = G_1 + G_2$$

The combination of the two types of loads (w_{ULS}) for ULS verification was calculated using Equation 10—in accordance with AS/NZS 1170.0 (Standards Australia 2002):

Equation 10

$$w_{ULS} = 1.2G_T + 1.5Q_{(O \text{ or } R)}$$

The load combinations used for the LSD verifications in the study are summarised in Table 2.

Table 2. Permanent and imposed loads and different load combinations used for LSD verifications.

Species	Sample code	Replicate	Mass (kg)	G _T (kN/m)	Office buildings (kN/m)		Residential buildings (kN/m)	
					Q _o	1.2 G _T + 1.5Q _o	Q _R	1.2 G _T + 1.5Q _R
<i>E. nitens</i>	NLT	1	85	0.51	0.84	1.87	0.42	1.24
		2	75	0.48	0.84	1.84	0.42	1.21
	NLTC#1	1	240	0.93	0.84	2.38	0.42	1.75
		2	235	0.92	0.84	2.36	0.42	1.73
	NLTC#2	1	295	0.88	0.84	2.32	0.42	1.69
	NLTC#3	1	325	1.17	0.84	2.66	0.42	2.03
		2	340	1.21	0.84	2.71	0.42	2.08
	<i>E. globulus</i>	NLT	1	90	0.53	0.84	1.89	0.42
2			75	0.48	0.84	1.84	0.42	1.21
NLTC#1		1	235	0.92	0.84	2.36	0.42	1.73
		2	240	0.93	0.84	2.38	0.42	1.75
NLTC#2		1	320	0.93	0.84	2.38	0.42	1.75
NLTC#3		1	355	1.25	0.84	2.76	0.42	2.13
		2	335	1.19	0.84	2.69	0.42	2.06

Based on the calculated load combinations, the ULS bending moment (design bending moment in kN/m) was estimated using the following equation:

Equation 11

$$M_{ULS} = \frac{w_{ULS}L^2}{8}$$

where, L is the span length of the panels (m).

The estimated M_{ULS} values were compared with the actual BMC values of the tested panels without applying any material reduction/capacity factor.

2.5. Short-term serviceability limit state (SLS) verification

The test panels made from the two plantation species were checked against the SLS requirements for deflection of structural floor elements under bending loads according to AS/NZS 1170.0 (Standards Australia 2002). For structural floors in offices with general uses and general floor areas in residential buildings the suggested deflection limit (δ_{SLS}) is calculated as:

Equation 12

$$\delta_{SLS} = \frac{\text{Span}}{300}$$

For structural floor elements in both office and residential buildings, the maximum deflection under the uniformly distributed imposed load of 3 kPa for offices and 1.5 kPa for residential buildings shall not be greater than the δ_{SLS} . To check this requirement, the experimental imposed loads (P_s) at SLS in kN were obtained from the load-deflection curve as the load corresponding to a deflection of span/300. The equivalent experimental uniformly distributed load (P_{Su}) in kN/m were then calculated using the equivalence of the deflection as follow:

Equation 13

$$\frac{5P_{Su}L^4}{384(EI)_{eff,Ser}} = \frac{3aP_sL^2 - 4P_s a^3}{48(EI)_{eff,Ser}}$$

hence,

Equation 14

$$P_{Su} = \frac{8(3aP_sL^2 - 4P_s a^3)}{5L^4}$$

where, $EI_{eff,Ser}$ is the empirical effective flexural stiffness (N.mm²) at serviceability load, a is one-third of the span length (mm), P_s is the experimental imposed load (N), and L is the span length (mm).

3. Results and Discussions

3.1. Failure modes of the test panels

The failure modes of the NLT panels from both timber species under four-point bending load were mostly simple tension and cross-tension failures (see Fig. 4 a, b, c, d, e, g). The tension failures were mostly due to high slope of grain in the boards (Fig. 4e) or local grain deviation around knots (Fig. 4 a, b, g). In several cases, the high slope of grain in some boards caused sudden tension failure along the fibre direction. Surface checking of the boards also accelerated the failure propagation in the tension zone of a few NLT samples (Fig. 4d). Compression failure on the top edge of a few boards was observed in some of the NLT panels constructed from both *E. nitens* and *E. globulus* timber (Fig. 4f). This may

suggest that the ratio of compression to bending strength of the two plantation timber species is low compared to other species, which needs to be evaluated in the future research. The failure in the NLTC panels started by the fracture of weak boards in the NLT component followed by developing cracks and slip in the concrete.



Fig. 4. Failure modes of the test panels.

The failure mode of the NLTC#1 and NLTC#2 panels from both species was generally combined tension and compression failure. This type of failure occurred due to the fact that the centroid of the interface of the NLT component and concrete slab was not reasonably close to the centroid of the composite section. The failure in the NLTC#3 panels started with tension failure at the bottom of the concrete slab (Fig. 4 i and j). This type of failure in the NLTC#3 panels occurred because the centroid of the interface of the NLT and concrete slab was in the tension zone of the panels—as the concrete slab was thicker than the NLT component. In a few cases, apart from the horizontal slip, gap opening was also observed between the NLT component and concrete slab at both ends of the NLTC panels (Fig. 4h).

3.2. SLC and EI of the panels

The general slope of load-deflection curves of the test panels in the elastic region can be seen in Fig. 5. The gross values and the average values of load-carrying capacity (LCC) of the test panels can be seen in Fig. 6 and Table 3, respectively. The NLT panels had a significantly lower average LCC than the comparable NLTC panels with the same span length (i.e., NLTC#1 and NLTC#3).

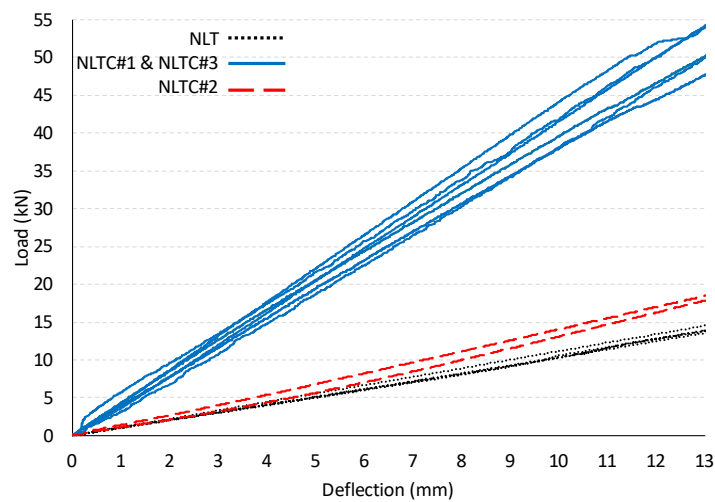


Fig. 5. Load-deflection curves up to 13 mm deflection (elastic range) at mid-span.

Table 3. The average LCC values of the test panels in each test treatment.

Species	Average LCC (kN)				
	Overall	NLT	NLTC#1	NLTC#2 ²	NLTC#3
<i>E. nitens</i>	74.7 ± 13.0 ¹	60.3 ± 2.8	89.7 ± 3.0	60.5	81.3 ± 0.9
<i>E. globulus</i>	71.7 ± 13.0	68.6 ± 11.5	82.0 ± 8.5	50.9	75.1 ± 6.9

¹ Standard deviation (SD).

² This treatment had only one replicate, therefore, no SD is provided.

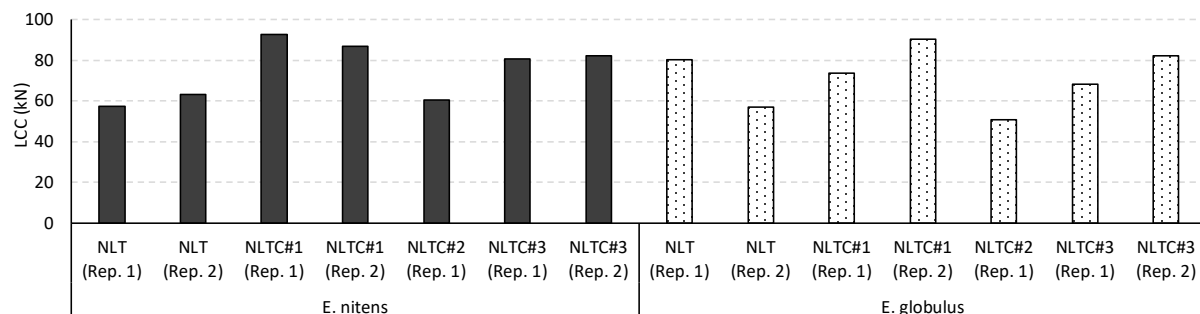


Fig. 6. The LCC of the test panels.

The overall average LCC of the test panels made of *E. nitens* was 4.2% higher than that of the test panels made of *E. globulus*. However, the NLT panels from *E. globulus* showed almost 14% higher average LCC than the identical NLT panels from *E. nitens*.

The SLC values obtained from the test panels in the study are shown in Fig. 7. The overall average SLC of the test panels made from both timber species were almost the same (Table 4)—with an average difference of less than 1%. The average SLC of NLT panels from *E. globulus* was 8.8% higher than that of the identical NLT panels made of *E. nitens*. However, in all other test treatments, NLTC panels from *E. nitens* indicated higher average SLC values than the NLTC panels constructed of *E. globulus* (Table 4).

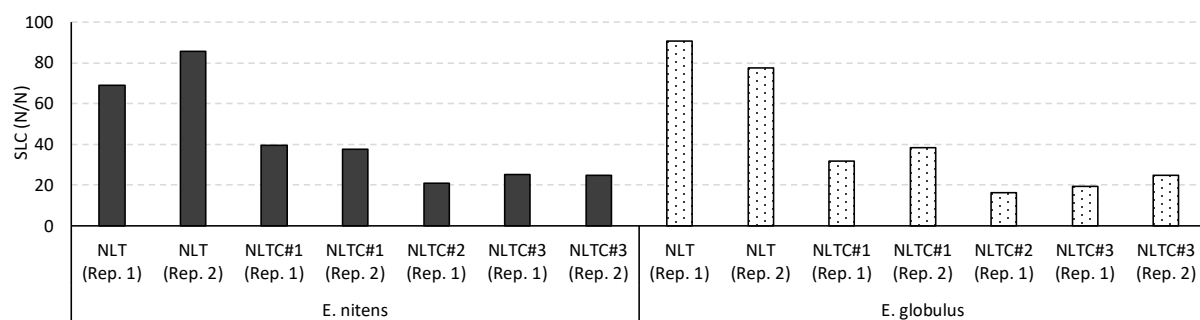


Fig. 7. The SLC of the test panels.

Table 4. The average SLC values of the test panels in each test treatment.

Species	Average SLC (N/N)				
	Overall	NLT	NLTC#1	NLTC#2 ¹	NLTC#3
<i>E. nitens</i>	43.2 ± 22.9	77.3 ± 8.4	38.5 ± 0.9	20.9	24.9 ± 0.3
<i>E. globulus</i>	42.8 ± 27.3	84.1 ± 6.5	35.2 ± 3.3	16.2	22.3 ± 2.7

¹ This treatment had only one replicate, therefore, no SD is provided.

As can be derived from Fig. 6 and Fig. 7, while the overall LCC was higher in NLTC panels than comparable NLT panels, the NLTC panels had significantly lower SLC than the NLT ones—with an average difference of 62% in *E. nitens* and an average difference of 69% in *E. globulus*. While LCC is an important design criterion, a more rational decision can be made on the selection of structural materials for different building applications when their SLC values are also taken into account. A low SLC of a building material can be a result of either its low LCC or its high weight. The latter case, which was observed in the NLTC panels, can be problematic in the construction of timber-rich multi-story buildings. A low SLC resulting from the high weight of the structural elements can cause extreme reaction forces in timber columns and support beams that are supposed to carry a combination of different loads including the permanent loads created from the self-weight of the structural elements above them.

The values of $EI_{eff,em}$ obtained from the experiments, MOR, and MOE of the NLT panels are given in Table 5. The difference between the average MOE values of the two timber species was as low as 1.1%, whereas the NLT panels made of *E. globulus* exhibited an average MOR value that was 13.8% higher than that of the identical panels made of *E. nitens*. A high variation was observed in the bending properties of the NLT panels, which partly could be due to the limitations of this study related to the small sample size tested for each species. A more accurate comparison between the properties of the two species could be made by testing a larger sample size in future studies. The average $EI_{eff,em}$ values of NLTC panels from both species were significantly higher than that of NLT panels (Table 6). The average $EI_{eff,em}$ values of NLTC panels from both *E. nitens* and *E. globulus* were almost 3.6 times greater than that of NLT panels.

Table 5. The MOE, MOR, and $EI_{eff,em}$ of the NLT panels.

Species	Sample code	Replicate	MOE (MPa)	$EI_{eff,em}$ (N.mm ² × 10 ¹¹)	MOR (MPa)
<i>E. nitens</i>	NLT	1	10942.3	6.88	34.5
		2	11206.9	6.85	37.9
	Average		11074.6 ± 132.3	6.87 ± 0.02	36.2 ± 1.7
<i>E. globulus</i>	NLT	1	11929.8	7.50	48.1
		2	10473.5	6.68	34.3
	Average		11203.2 ± 728.2	7.09 ± 0.41	41.2 ± 6.9

Table 6. The $EI_{eff,em}$ of the NLTC panels.

Species	Sample code	Replicate	$EI_{eff,em}$ (N.mm ² × 10 ¹²)
<i>E. nitens</i>	NLTC#1	1	2.65
		2	2.46
	NLTC#2	1	2.49
		2	2.33
	NLTC#3	1	2.40
		2	2.40
Average			2.47 ± 0.11
<i>E. globulus</i>	NLTC#1	1	2.67
		2	2.56
	NLTC#2	1	2.42
		2	2.45
	NLTC#3	1	2.45
		2	2.55
Average			2.53 ± 0.09

The bending performance (MOE and MOR) of the NLT panels in this study was compared to some other types of commercially important mass laminated timber products and the results are shown in Fig. 8.

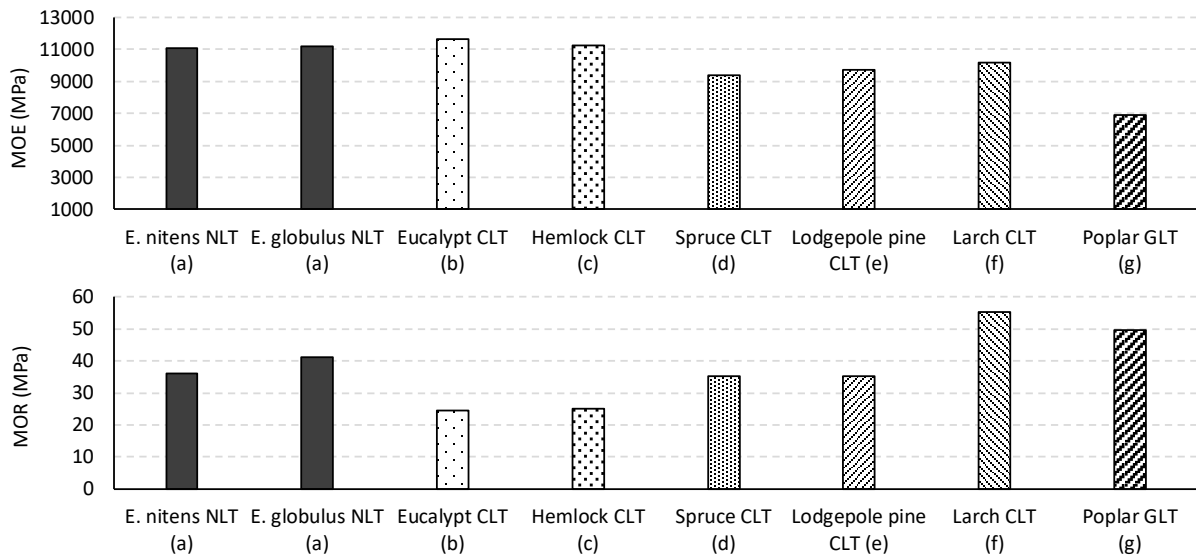


Fig. 8. The bending properties (MOE and MOR) of NLT panels in this study (a) vs those of CLT and GLT reported in the literature. (b): Liao et al. (2017); (c): He et al. (2018); (d): Buck et al. (2016); (e): Wang et al. (2015); (f): Song and Hong (2018); (g): Bayatkashkoli et al. (2012).

The average MOE values of the NLT panels from both timber species in this study were comparable to that of the CLT panels constructed of a hybrid plantation eucalypt timber resource (11466 MPa) reported by Liao et al. (2017) and Canadian hemlock CLT panels (11671 MPa) reported by He et al. (2018). The average MOR values of the NLT panels made of the plantation *E. nitens* and *E. globulus* however, were respectively 47.8% and 68.2% higher than that of the hybrid eucalypt CLT panels (24.5 MPa) and 43.8% and 63.6% higher than that of the Canadian hemlock CLT panels (25.18 MPa). The MOE values of the NLT panels were also noticeably higher than that of Spruce CLT, Lodgepole pine CLT, Larch CLT, and Poplar GLT reported in the literature (Fig. 8).

3.3. Efficiency of the interlayer connections

The total values of maximum slip between the NLT component and concrete slab in the NLTC panels were ranged from a minimum of 3.8 mm up to 11.0 mm in *E. nitens* and from 3.4 mm up to 11.9 mm in *E. globulus* samples (Fig. 9 and Fig. 10). In some cases in *E. nitens* panels, while the slip at one end was close to zero (shown in Fig. 9 as lowest slip end), moderate to large slips were observed at the other end of the panels (shown in Fig. 9 as highest slip end). The same behaviour was observed in *E. globulus* samples, although the slip level at the two ends of these samples was more uniform than the *E. nitens* ones.

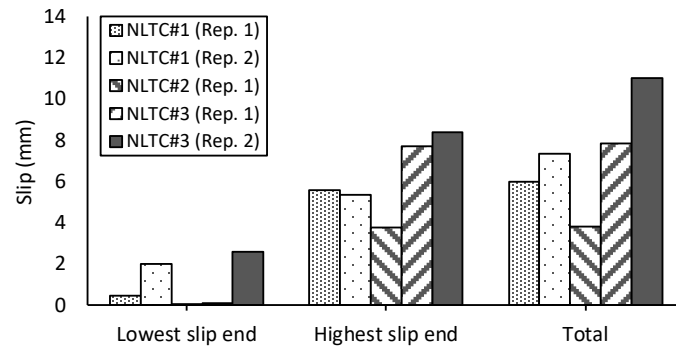


Fig. 9. The slip range in the *E. nitens* NLTC panels.

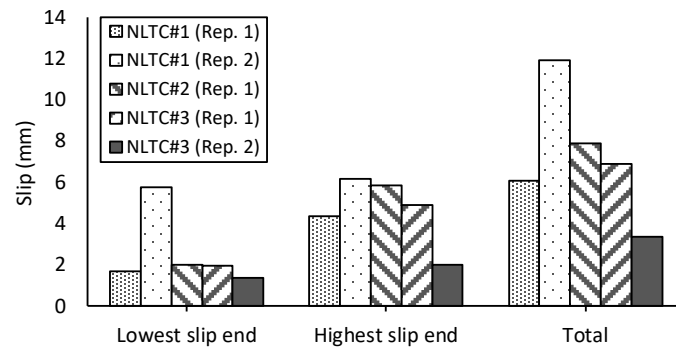


Fig. 10. The slip range in the *E. globulus* NLTC panels.

The average values of ϵ of the conventional screw-type shear connectors used in the study were 68.9% and 71.3% for *E. nitens* and *E. globulus* panels, respectively—with an overall average value of 70.1% (Table 7). The $EI_{eff,1}$ values for a theoretically full composite section were from 1.19 times to 1.33 times greater than the $EI_{eff,em}$ values obtained from the NLTC panels made of both species.

Although the dimensions of the test specimens and the number of connectors were different, the composite action obtained for the NLTC floors in this study was significantly lower than that reported by Mai et al. (2018) for CLT-concrete floors constructed using the same type of connectors. The CLT-concrete floors designed by Mai et al. (2018) had 900 mm width and 6000 mm length and were comprised of four rows of inclined SFS screws with a nominal spacing of 150 mm. The depth ratio of CLT to concrete slab in their study was 1.5. These researchers concluded that a full degree of composite action (100%) can be achieved for the CLT-concrete floors using the SFS screws inclined at 45° angle and the proposed floor system.

Additional studies are required to improve the composite efficiency of the NLTC panels constructed of the two timber species by making use of novel, more appropriate timber-concrete shear connectors (Yeoh et al. 2010; Dias et al. 2015, 2018; Djoubissie et al. 2018).

Table 7. The composite efficiency obtained using the screw-type shear connectors.

Species	Sample code	Replicate	$EI_{eff, l} (N.mm^2 \times 10^{12})$	$EI_{eff, o} (N.mm^2 \times 10^{12})$	ϵ (%)
<i>E. nitens</i>	NLTC#1	1	3.17	0.86	77.49
		2	3.17	0.86	69.26
	NLTC#2	1	3.17	0.86	70.56
		1	3.09	1.10	61.81
	NLTC#3	2	3.09	1.10	65.33
		1	3.19	0.87	77.59
<i>E. globulus</i>	NLTC#1	2	3.19	0.87	72.84
		1	3.19	0.87	66.81
	NLTC#2	1	3.11	1.11	67.00
		2	3.11	1.11	72.00
	NLTC#3	1	3.11	1.11	67.00
		2	3.11	1.11	72.00

3.4. ULS verification

The actual BMC of the test panels and the design bending moment (M_{ULS}) at ULS loads are given in Table 8. On average, the BMC of the test panels constructed of *E. nitens* was 4.7% higher than that of panels made of *E. globulus*. Except for replicate one in the NLT panels made of *E. globulus*, the BMC values of NLTC panels from both species were higher than that of NLT panels—with an overall average difference of 26%. The actual BMC of replicate one in the NLT panels made of *E. globulus* was unexpectedly 4% higher than the average BMC of the NLTC panels from the same species.

Table 8. The M_{ULS} and the actual BMC of the panels.

Species	Sample code	Replicate	Office buildings (kN.m)			Residential buildings		
			M_{ULS} (kN.m)	BMC (kN.m)	Ratio (BMC/ M_{ULS})	M_{ULS} (kN.m)	BMC (kN.m)	Ratio (BMC/ M_{ULS})
<i>E. nitens</i>	NLT	1	2.55	31.58	12.38	1.69	31.58	18.69
		2	2.51	34.70	13.82	1.65	34.70	21.03
	NLTC#1	1	3.24	50.97	15.73	2.38	50.97	21.42
		2	3.22	47.68	14.81	2.36	47.68	20.20
	NLTC#2	1	6.14	46.42	7.56	4.47	46.42	10.38
		1	3.62	44.23	12.22	2.76	44.23	16.03
	NLTC#3	2	3.69	45.22	12.25	2.83	45.22	15.98
	Average		3.57 ± 1.13	42.97 ± 6.57	12.68 ± 2.45	2.59 ± 0.88	42.97 ± 6.57	17.68 ± 3.62
	NLT	1	2.57	44.02	17.13	1.72	44.02	25.59
		2	2.51	31.40	12.51	1.65	31.40	19.03
<i>E. globulus</i>	NLTC#1	1	3.22	40.45	12.56	2.36	40.45	17.14
		2	3.24	49.74	15.35	2.38	49.74	20.90
	NLTC#2	1	6.30	39.00	6.19	4.63	39.00	8.42
		1	3.75	37.52	10.01	2.90	37.52	12.94
	NLTC#3	2	3.66	45.07	12.31	2.81	45.07	16.04
	Average		3.61 ± 1.19	41.03 ± 5.49	12.29 ± 3.28	2.64 ± 0.93	41.03 ± 5.49	17.15 ± 5.13

The actual BMC values of both NLT and NLTC panels made of the two timber species were considerably higher than the M_{ULS} values calculated at the ULS loads. The overall average values of the BMC were 11.7 times and 16.1 times higher than that of the M_{ULS} values for office and residential buildings, respectively. This indicates that the bending capacity of the panels from both species is sufficient to meet the ULS requirements under short-term loading conditions. It must be noted that there were some limitations for the ULS verifications in this study. Most of these limitations were related to the lack of test data, useable for structural design purposes, on the mechanical properties of the two timber species used in the study. A full ULS verification of the bending strength of the panels can be

done in the future by taking into account different loading conditions (i.e., point loads and uniformly distributed loads) and applying different material capacity factors for both long-term and short-term service conditions. For this purpose, material capacity factors (known as K factors) as well as the characteristic bending strength and creep rate of the timber are required—which do not currently exist for the fibre-managed plantation *E. nitens* and *E. globulus* timber. The K factors however are outlined in AS 1720.1 (Standards Australia 2010) and their values are independent than timber species.

3.5. SLS verification

The experimental imposed loads corresponding to a deflection limit of span/300 mm are given in Table 9. The experimental imposed load capacities of the NLT panels made from both species were on average 5.8 times and 11.6 times larger than the design imposed loads for floor systems in office (Q_o) and residential buildings (Q_R) at SLS. The experimental imposed loads obtained from the NLTC panels were also on average 17.6 times and 35.2 times larger than the design imposed loads for office and residential buildings.

Table 9. Experimental and analytical imposed load capacities of the panels corresponding to the serviceability deflection limit.

Species	Sample code	Replicate	δ_{SLS} (mm)	Q_o (kN/m)	Q_R (kN/m)	P_{Su} (kN/m)
<i>E. nitens</i>	NLT	1	11	0.84	0.42	4.82
		2	11	0.84	0.42	4.83
	NLTC#1	1	11	0.84	0.42	18.65
		2	11	0.84	0.42	17.12
	NLTC#2	1	15.3	0.84	0.42	6.48
		2	11	0.84	0.42	16.09
	NLTC#3	1	11	0.84	0.42	16.48
		2	11	0.84	0.42	16.48
<i>E. globulus</i>	NLT	1	11	0.84	0.42	5.07
		2	11	0.84	0.42	4.72
	NLTC#1	1	11	0.84	0.42	19.60
		2	11	0.84	0.42	18.93
	NLTC#2	1	15.3	0.84	0.42	6.34
		2	11	0.84	0.42	17.13
	NLTC#3	1	11	0.84	0.42	17.13
		2	11	0.84	0.42	17.84

The results indicated that the test panels constructed of fibre-managed *E. nitens* and *E. globulus* are able to satisfy the SLS requirements for deflection. The capacity of the test panels was well beyond the standard requirements for deflection outlined in AS/NZS 1170.0 (Standards Australia 2002). The serviceability of the NLT and NLTC panels with respect to long-term structural performance under sustained loads needs to be investigated and verified in the future studies.

3.6. Vibration serviceability

The typical acceleration time-history plots obtained from the test panels are shown in Fig. 11 and Fig. 12. The resulting fundamental natural vibration frequency values of the panels are given in Table 10.

The fundamental natural frequency values obtained from all the test panels were higher than the recommended minimum range of 8-10 Hz—below which floor vibration induces the most discomfort (Bernard 2008; Rijal et al. 2015; Santos et al. 2015). There was no clear trend in fundamental natural vibration frequency differences between the two plantation timber species.

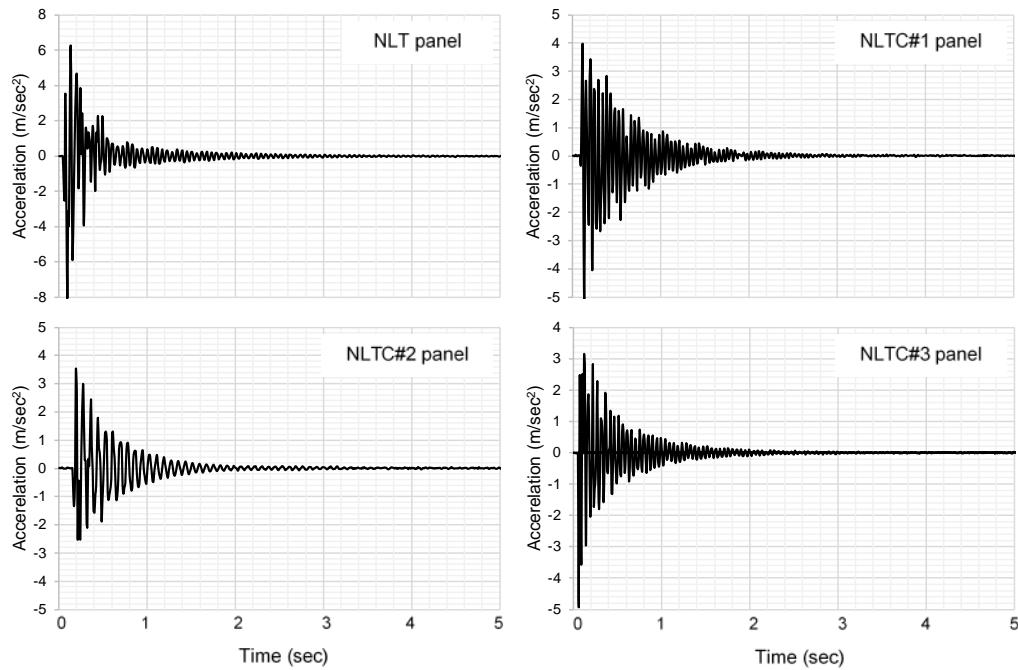


Fig. 11. Typical acceleration time-history plots recorded for *E. nitens* panels.

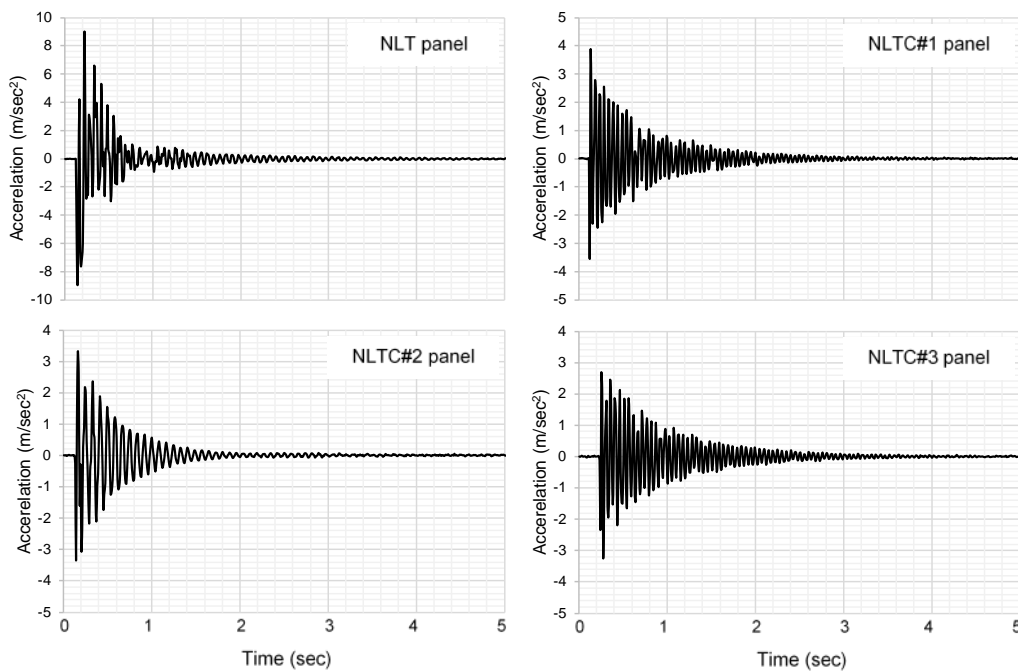


Fig. 12. Typical acceleration time-history plots recorded for *E. globulus* panels.

Table 10. The results of vibration tests.

Sample code	Replicate	Number of tests	Fundamental natural vibration frequency (Hz)		
			<i>E. nitens</i>	<i>E. globulus</i>	Ratio (<i>E. nitens</i> / <i>E. globulus</i>)
NLT	1	3	16.1 ± 0.35	16.4 ± 0.42	0.98
	2	3	17.3 ± 0.50	16.8 ± 0.51	1.03
NLTC#1	1	3	19.2 ± 0.45	19.3 ± 0.62	0.99
	2	3	18.7 ± 0.20	19.0 ± 0.37	0.98
NLTC#2	1	3	11.0 ± 0.39	10.3 ± 0.34	1.07
NLTC#3	1	3	15.3 ± 0.46	15.0 ± 0.27	1.02
	2	3	15.1 ± 0.40	15.9 ± 0.65	0.95

On average, the NLT panels showed 8.6% higher natural frequency than the NLTC#3 panels—whose concrete slab was thicker than the NLTC#1 and NLTC#2 panels. The average fundamental natural frequency of the NLT panels was 14.4% lower than the NLTC#1 panels. The NLTC#2 panels also showed the lowest natural frequency values amongst the other panel configurations—even though these values were still above the range of 8-10 Hz. As the NLTC#1 and NLTC#2 had the same cross-sectional configurations, the lower fundamental natural frequency in the NLTC#2 panels was mainly due to their longer span length compared to that of the NLTC#1 panels. This result, together with the results of ULS verification, proved that with increased span length the structural design of a timber-concrete floor system will be limited more by serviceability than by strength requirements (Rijal et al. 2015). As supported by the results of this study, the natural vibration frequency is mainly a function of stiffness, mass, and span length of the panels (Taoum 2016; Hong 2017). The vibrational behaviour can also be affected by the width of the panels through its influence on the transverse stiffness (Lukaszewska 2009; Robertson et al. 2018). This effect can be evaluated using experimental and numerical methods developed in previous studies (Monteiro et al. 2015; Santos et al. 2015).

The results of vibration serviceability assessment together with those of SLS and ULS verifications suggest that the NLTC#1 and NLTC#2 could be better solutions than the other panel configurations tested in this study. The fundamental natural vibration frequency values of NLTC#2 panels however were only marginally above the minimum range of 8-10 Hz that is recommended for structural floor systems in residential and office buildings. This suggests that future research will need to focus on improving the serviceability of such panels which could be possible by developing more appropriate timber-concrete connection systems that can lead to increased stiffness and span length.

4. Conclusions

This study was conducted to investigate the potential of producing higher-value structural NLT and NLTC floor panels from fast-growing, fibre-managed plantation *E. nitens* and *E. globulus*. The test panels were constructed with different cross-sectional configurations and span lengths and examined under four-point bending load. The following conclusions were drawn based on the results obtained:

- The NLT panels made of *E. globulus* showed higher average LCC and SLC values than the *E. nitens* NLT panels, while the average LCC and SLC values of NLTC panels made of *E. nitens* were meaningfully higher than those of the identical panels made of *E. globulus*.
- No meaningful difference was observed in the NLT panels made from both species with respect to average MOE values. However, the NLT panels made of *E. globulus* exhibited 13.8% higher MOR than the *E. nitens* ones. The MOE and MOR of the NLT panels in this study were superior to some commercially important mass laminated timber products made of other timber species reported in the literature.
- The NLTC panels made of *Eucalyptus globulus* had 2.4% higher $EI_{eff,em}$ than the *Eucalyptus nitens* panels. The conventional screw-type shear connectors resulted in a partial composite action in the NLTC panels. Considering the $EI_{eff,em}$ values obtained, the composite efficiency of the conventional screw-type shear connectors used ranged from 61.8% to 77.6%—which allowed a moderate slip between the NLT component and concrete slab. An appropriate timber-concrete connection system needs to be developed in the future studies for NLTC panels made of the two plantation timber species to improve their composite actions.
- The use of concrete in the NLTC panels resulted in an enhanced BMC by an average of 26% compared with the NLT panels from both species. The actual BMC values obtained from all the test panels were significantly higher than those created from the uniformly distributed design loads based on ULS requirements of structural floors in both office and residential buildings. The failure did not occur in the panels until the ULS requirements for short-term BMC were well passed—under ULS loads, all the NLT and NLTC panels were still in the linear-elastic range. The experimental imposed loads obtained were also significantly larger than the actual design imposed loads (SLS loads) corresponding to a deflection limit of span/300.
- The fundamental natural vibration frequency values obtained from all the test panels with various cross-sectional configurations and span lengths were above the recommended range of 8-10 Hz. However, when the span length increased from 3300 mm to 4600, the fundamental natural vibration frequency of the NLTC panels decreased significantly. The fundamental natural vibration frequency of the NLTC panels with 4600 mm span length was only marginally above the recommended range of 8-10 Hz.
- Overall, the structural performance of the two timber species, as potential raw materials for the construction of floor systems, was sufficient to meet the short-term, serviceability loading conditions in both office and residential buildings. More studies need to be conducted in future to determine the long-term structural performances of the two timber species under both ULS and SLS conditions.

Funding: This study was undertaken under the Australian Research Council, Centre for Forest Value, University of Tasmania, TAS, Australia (Grant Reference: IC150100004). The financial support from

Forest and Wood Products Australia Limited (FWPA), Melbourne, VIC, Australia is acknowledged (Grant Number: PNB387-1516). The authors are also grateful of the support from Forico Pty Ltd. in providing the logs and Britton Timbers for the milling of the logs and drying and finishing of the boards.

Conflict of Interest: The authors declare that they have no conflict of interest.

References

1. AS 1720.1 (2010) Timber Structures – Design Methods. Standards Australia, Australia.
2. AS/NZS 1170.0 (2002) Structural design actions. Part 0: General principles. Standards Australia/Standards New Zealand, Australia.
3. AS/NZS 1170.1 (2002) Structural design actions. Part 1: Permanent, imposed and other actions. Standards Australia/Standards New Zealand, Australia.
4. AS/NZS 4063.1 (2010) Characterisation of structural timber. Part 1: Test Methods. Standards Australia/Standards New Zealand, Australia.
5. Ballerini M, Crocetti R, Piazza M (2002) An experimental investigation of notched connections for timber-concrete composite structures. In proceedings of the 7th World Conference on Timber Engineering WCTE 2002, Shah Alam, Malaysia, pp. 171-178.
6. Bayatkashkoli A, Shamsian M, Mansourfard M (2012) The effect of number of joints on bending properties of laminated lumber made from poplar (*Populus nigra*). Forestry Studies in China 14(3): 246-250. <https://doi.org/10.1007/s11632-012-0313-0>
7. Bernard E (2008) Dynamic serviceability in lightweight engineered timber floors. Journal of Structural Engineering 134: 258–268. [https://doi.org/10.1061/\(ASCE\)0733-9445\(2008\)134:2\(258\)](https://doi.org/10.1061/(ASCE)0733-9445(2008)134:2(258))
8. Blackburn D, Vega M (2017) Segregation of Eucalyptus nitens logs from fibre-managed plantations for veneer based engineered wood products. Final report, Centre for Sustainable Architecture with Wood (CSAW) School of Architecture and Design, University of Tasmania, Australia.
9. Blackburn D, Vega M, Yong R, Britton D, Nolan G (2018) Factors influencing the production of structural plywood in Tasmania, Australia from Eucalyptus nitens rotary peeled veneer. Southern Forests: a Journal of Forest Science 1-10. <https://doi.org/10.2989/20702620.2017.1420730>
10. Blackburn DP, Hamilton MG, Harwood CE, Innes TC, Potts BM, Williams D (2011) Genetic variation in traits affecting sawn timber recovery in plantation-grown *Eucalyptus nitens*. Annals of Forest Science 68(7). <https://doi.org/10.1007/s13595-011-0130-y>
11. Brandner R, Schickhofer G (2006) System effects of structural elements-determined for bending and tension. In proceedings of the 9th World Conference on Timber Engineering (WCTE 2006), Portland.
12. Buck D, Wang XA, Hagman O, Gustafsson A (2016) Bending properties of cross laminated timber (CLT) with a 45 alternating layer configuration. BioResources 11(2): 4633-4644. <https://doi.org/10.15376/biores.11.2.4633-4644>
13. Derikvand M, Kotlarewski N, Lee M, Jiao H, Chan A, Nolan G (2018a) Visual stress grading of fibre-managed plantation Eucalypt timber for structural building applications. Construction and Building Materials 167: 688-699. <https://doi.org/10.1016/j.conbuildmat.2018.02.090>
14. Derikvand M, Kotlarewski N, Lee M, Jiao H, Nolan G (2018b) Flexural and visual characteristics of fibre-managed plantation Eucalyptus globulus timber. Wood Material Science & Engineering 1-10. <https://doi.org/10.1080/17480272.2018.1542618>
15. Derikvand M, Kotlarewski N, Lee M, Jiao H, Nolan G (2019) Characterisation of physical and mechanical properties of unthinned and unpruned plantation-grown Eucalyptus nitens H.Deane & Maiden lumber. Forests 10(2): 194. <https://doi.org/10.3390/f10020194>
16. Derikvand M, Nolan G, Jiao H, Kotlarewski N (2017) What to do with structurally low-grade wood from Australia's plantation eucalyptus; building application?. BioResources 12(1): 4-7. <https://doi.org/10.15376/biores.12.1.4-7>
17. Dias AM, Kuhlmann U, Kudla K, Mönch S, Dias AMA (2018) Performance of dowel-type fasteners and notches for hybrid timber structures. Engineering Structures 171: 40-46. <https://doi.org/10.1016/j.engstruct.2018.05.057>

18. Dias AMPG, Martins ARD, Simões LMC, Providência PM, Andrade AAM (2015) Statistical analysis of timber–concrete connections–Mechanical properties. *Computers & Structures* 155: 67-84. <https://doi.org/10.1016/j.compstruc.2015.02.036>
19. Djoubissie DD, Messan A, Fournely E, Bouchaïr A (2018) Experimental study of the mechanical behavior of timber-concrete shear connections with threaded reinforcing bars. *Engineering Structures* 172: 997-1010. <https://doi.org/10.1016/j.engstruct.2018.06.084>
20. Dugmore MK (2018) Evaluation of the bonding quality of *E. grandis* cross-laminated timber made with a one-component polyurethane adhesive. Doctoral dissertation, Stellenbosch: Stellenbosch University.
21. Farrell R, Innes TC, Harwood CE (2012) Sorting *Eucalyptus nitens* plantation logs using acoustic wave velocity. *Australian Forestry* 75(1): 22-30. DOI: <http://dx.doi.org/10.1080/00049158.2012.10676382>
22. Gilbert BP, Bailleres H, Zhang H, McGavin RL (2017) Strength modelling of laminated veneer lumber (LVL) beams. *Construction and Building Materials* 149: 763-777. <https://doi.org/10.1016/j.conbuildmat.2017.05.153>
23. Hamilton J (2014) Use of low grade timber in residential flooring systems. Bachelor's Thesis, University of Tasmania.
24. He M, Sun X, Li Z (2018) Bending and compressive properties of cross-laminated timber (CLT) panels made from Canadian hemlock. *Construction and Building Materials* 185: 175-183. <https://doi.org/10.1016/j.conbuildmat.2018.07.072>
25. Hong KEM (2017) Structural performance of nail-laminated timber-concrete composite floors. Master's dissertation, University of British Columbia.
26. Kan J, Ross RJ, Wang X, Li W (2017) Energy harvesting from wood floor vibration using a piezoelectric generator. Research Note, FPL–RN–0347. Madison, WI: US Department of Agriculture, Forest Service, Forest Products Laboratory, 9 p.
27. Kandler G, Lukacevic M, Füssl J (2018) Experimental study on glued laminated timber beams with well-known knot morphology. *European Journal of Wood and Wood Products* 76(5): 1435-1452. <https://doi.org/10.1007/s00107-018-1328-6>
28. Lara-Bocanegra AJ, Majano-Majano A, Crespo J, Guaita M (2017) Finger-jointed *Eucalyptus globulus* with 1C-PUR adhesive for high performance engineered laminated products. *Construction and Building Materials* 135: 529-537. <https://doi.org/10.1016/j.conbuildmat.2017.01.004>
29. Liao Y, Tu D, Zhou J, Zhou H, Yun H, Gu J, Hu C (2017) Feasibility of manufacturing cross-laminated timber using fast-grown small diameter eucalyptus lumbers. *Construction and Building Materials* 132: 508-515. <https://doi.org/10.1016/j.conbuildmat.2016.12.027>
30. Lu Z, Zhou H, Liao Y, Hu C (2018) Effects of surface treatment and adhesives on bond performance and mechanical properties of cross-laminated timber (CLT) made from small diameter eucalyptus timber. *Construction and Building Materials* 161: 9-15. <https://doi.org/10.1016/j.conbuildmat.2017.11.027>
31. Lukaszewska E (2009) Development of prefabricated timber-concrete composite floors. Doctoral dissertation, Luleå University of Technology.
32. Mai KQ, Park A, Nguyen KT, Lee K (2018) Full-scale static and dynamic experiments of hybrid CLT–concrete composite floor. *Construction and Building Materials* 170: 55-65. <https://doi.org/10.1016/j.conbuildmat.2018.03.042>
33. McGavin RL, Bailleres H, Hamilton MG, Blackburn DP, Vega M, Ozarska B (2015) Variation in rotary veneer recovery from Australian plantation *Eucalyptus globulus* and *Eucalyptus nitens*. *BioResources* 10(1): 313-329. <https://doi.org/10.15376/biores.10.1.313-329>
34. Monteiro SR, Dias AM, Lopes SM (2015) Bi-dimensional numerical modeling of timber–concrete slab-type structures. *Materials and Structures* 48(10): 3391-3406. <https://doi.org/10.1617/s11527-014-0407-3>
35. Oudjene M, Meghlat EM, Ait-Aider H, Batoz JL (2013) Non-linear finite element modelling of the structural behaviour of screwed timber-to-concrete composite connections. *Composite Structures* 102: 20-28.

36. Oudjene M, Meghlat EM, Ait-Aider H, Lardeur P, Khelifa M, Batoz JL (2018) Finite element modelling of the nonlinear load-slip behaviour of full-scale timber-to-concrete composite T-shaped beams. *Composite Structures* 196: 117-126. <https://doi.org/10.1016/j.compstruct.2018.04.079>
37. Piazza M, Ballerini M (2000) Experimental and numerical results on timber-concrete composite floors with different connection systems. In proceedings of the World Conference on Timber Engineering WCTE 2002. Whistler Resort, British Columbia, Canada.
38. Popovski M, Gavric I (2015) Performance of a 2-story CLT house subjected to lateral loads. *Journal of Structural Engineering* 142(4): E4015006. [https://doi.org/10.1061/\(ASCE\)ST.1943-541X.0001315](https://doi.org/10.1061/(ASCE)ST.1943-541X.0001315)
39. Pröller M, Nocetti M, Brunetti M, Barbu MC, Blumentritt M, Wessels CB (2018) Influence of processing parameters and wood properties on the edge gluing of green *Eucalyptus grandis* with a one-component PUR adhesive. *European Journal of Wood and Wood Products* 76(4): 1195-1204. <https://doi.org/10.1007/s00107-018-1313-0>
40. Raftery GM, Rodd PD (2015) FRP reinforcement of low-grade glulam timber bonded with wood adhesive. *Construction and building materials* 91: 116-125. <https://doi.org/10.1016/j.conbuildmat.2015.05.026>
41. Rijal R, Samali B, Shrestha R, Crews K (2015) Experimental and analytical study on dynamic performance of timber-concrete composite beams. *Construction and Building Materials* 75: 46-53. <https://doi.org/10.1016/j.conbuildmat.2014.10.020>
42. Robertson M, Holloway D, Taoum A (2018) Vibration of suspended solid-timber slabs without intermediate support: assessment for human comfort. *Australian Journal of Structural Engineering* 19(4): 266-278. <https://doi.org/10.1080/13287982.2018.1513783>
43. Santos PGD, Martins CEDJ, Skinner J, Harris R, Dias AMPG, Godinho LMC (2015) Modal frequencies of a reinforced timber-concrete composite floor: Testing and modeling. *Journal of Structural Engineering* 141(11): 04015029. [https://doi.org/10.1061/\(ASCE\)ST.1943-541X.0001275](https://doi.org/10.1061/(ASCE)ST.1943-541X.0001275)
44. Song YJ, Hong SI (2018) Performance evaluation of the bending strength of larch cross-laminated timber. *Wood Research*, 63(1), 105-115.
45. Taoum A (2016) Application of local post-tensioning to new and existing structures. Doctoral dissertation, University of Tasmania.
46. Wang JB, Wei P, Gao Z, Dai C (2018) The evaluation of panel bond quality and durability of hem-fir cross-laminated timber (CLT). *European Journal of Wood and Wood Products* 76(3): 833-841. <https://doi.org/10.1007/s00107-017-1283-7>
47. Wang Z, Gong M, Chui YH (2015) Mechanical properties of laminated strand lumber and hybrid cross-laminated timber. *Construction and Building Materials* 101: 622-627. <https://doi.org/10.1016/j.conbuildmat.2015.10.035>
48. Weckendorf J, Toratti T, Smith I, Tannert T (2016) Vibration serviceability performance of timber floors. *European Journal of Wood and Wood Products* 74(3): 353-367. <https://doi.org/10.1007/s00107-015-0976-z>
49. Yeoh D, Fragiocomo M, De Franceschi M, Heng Boon K (2010) State of the art on timber-concrete composite structures: Literature review. *Journal of structural engineering* 137(10): 1085-1095. [https://doi.org/10.1061/\(ASCE\)ST.1943-541X.0000353](https://doi.org/10.1061/(ASCE)ST.1943-541X.0000353)
50. Yeoh D, Fragiocomo M, Deam B (2011) Experimental behaviour of LVL-concrete composite floor beams at strength limit state. *Engineering Structures* 33(9): 2697-2707. <https://doi.org/10.1016/j.engstruct.2011.05.021>
51. Zhou J, Chui YH, Gong M, Hu L (2017) Elastic properties of full-size mass timber panels: Characterization using modal testing and comparison with model predictions. *Composites Part B: Engineering* 112: 203-212. <https://doi.org/10.1016/j.compositesb.2016.12.027>

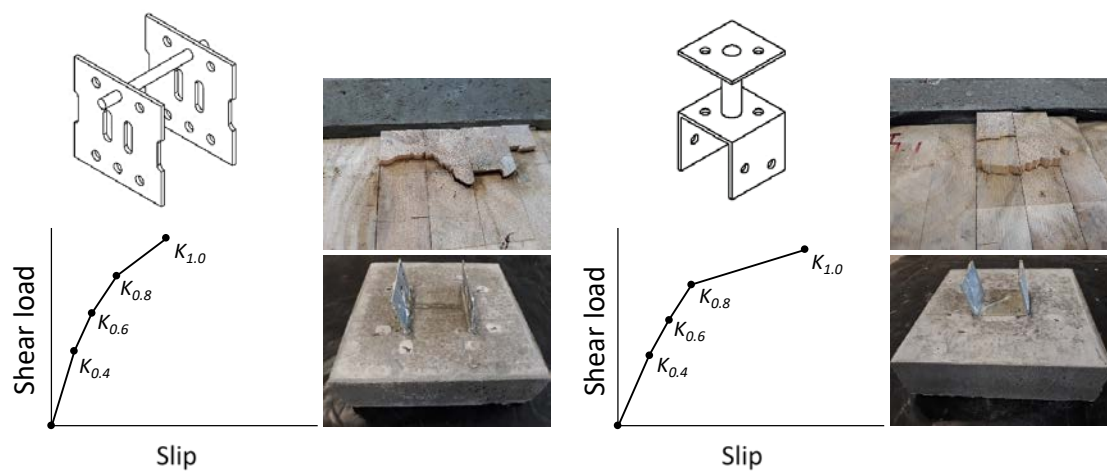
Appendix F: Paper VI

This paper is under review by an international journal.

Timber-concrete composite connections for hybrid nail-laminated timber floor systems

Mohammad Derikvand, Nathan Kotlarewski, Michael Lee, Hui Jiao, Andrew Chan, Gregory Nolan

Graphical abstract



Abstract

Meeting the required composite action necessary for timber-concrete floor structures is achievable through design and utilisation of shear connections with high structural capacity. The aim of this experimental study was to develop and test timber-concrete shear connections for hybrid nail-laminated timber (NLT) floor systems constructed of low-grade plantation eucalypt. Two new types of glued-in shear connections were developed using a full stirrup timber post anchor and two hot galvanised steel plates welded together with a reinforcing bar and installed perpendicular to the longitudinal direction of the NLT component. Notched connections (round dovetail notch and oblong dovetail notch) and inclined screw connections (coach screws and SFS screws) were also manufactured and tested to create a basis for comparison with the new glued-in connections. The tests were performed under uniaxial pushout load. Based on the results, the glued-in steel plates with reinforcing bar showed the highest shear strength (56.9 kN) and slip modulus at serviceability limit state (26.3 kN/mm) and ultimate limit state (22.6 kN/mm). The failure in these connections occurred mostly in the NLT component through shear parallel to the grain. Considering the post-peak response under loading, the glued-in steel plates

with reinforcing bar represented a pure ductile behaviour which makes it an effective shear connector for the construction of hybrid NLT floors from low-grade plantation eucalypt.

Keywords: eucalypt; nail-laminated timber; shear connector; shear strength; slip modulus; timber-concrete.

1. Introduction

Eucalyptus nitens (*E. nitens*) is the main hardwood plantation specie in Tasmania, Australia. The timber obtained from *E. nitens* plantations is structurally low-grade as this resource is predominately managed to produce pulplog and woodchips (Derikvand et al. 2018a, b). Nevertheless, the forest industry in Australia is keen to add value to *E. nitens* plantations by developing structural and non-structural products from the timber obtained from these resources (Blackburn et al. 2018; Derikvand et al. 2017, 2018a, b).

In a previous study at University of Tasmania, it was demonstrated that plantation *E. nitens* timber has satisfactory structural performance to be used in the construction of nail-laminated timber (NLT) and hybrid NLT-concrete floor panels (Derikvand et al. 2019). However, the conventional dowel-type fasteners used as shear connectors in the construction of the NLT-concrete panels from this resource resulted in a poor composite action. To address this issue, various shear connection systems were developed and tested in this study for NLT-concrete floors constructed of plantation *E. nitens* timber.

The structural efficiency of a timber-concrete composite (TCC) floor is a function of its level of composite action (Dias 2005; Deam et al. 2008; Yeoh et al. 2010; Khorsandnia et al. 2018). TCC shear connections that result in high composite action are those with high shear strength and slip modulus (Yeoh et al. 2010, 2011; Dias et al. 2018; Suárez-Riestra 2019). The effectiveness of a TCC shear connection is generally dependent on its structural capacity (Dias 2005; Auclair et al. 2016), possibility of prefabrication (Lukaszewska et al. 2008; Jacquier and Girhammar 2012; Crocetti et al. 2015), and ease and cost of manufacture (Oudjene et al. 2018).

Although dowel-type fasteners are cheap and simple to use (Dias et al. 2018), the full composite action of a TCC floor may not always be achievable as these fasteners are not rigid under shear loads (Yeoh 2010; Rijal et al. 2015; Hong 2017). Connection systems with higher rigidity and slip modulus, such as adhesive-bonded TCC connections (Eisenhut et al. 2016), glued-in continuous steel meshes with reinforcing bars (Otero-Chans et al. 2018; Suárez-Riestra et al. 2019), and long notched connections with dowel (Dias et al. 2018), are usually more expensive to use and/or difficult to manufacture than the dowel-type fasteners alone.

Otero-Chans et al. (2018) tested several different configurations of glued-in steel plates with and without reinforcing bars in TCC connections made with solid timber. These researchers concluded that, using glued-in steel plates, it is possible to design TCC structures with a composite action close to 100% when the direction of the shear loads is parallel to the longitudinal direction of the steel plates and the

timber component. Such steel plate connectors can be used in NLT-concrete structures during the production process of NLT component by inserting the steel plates between the timber boards (layers) before nail-laminating them together (Hong 2017). Using glued-in steel plates however is not quite practical on prefabricated NLT products. The use of glued-in steel plates with longitudinal arrangement in the construction of TCC structures requires cutting long slots parallel to the length of the timber component. In the construction of a prefabricated NLT panel however there is normally a row of steel nails in every 150 to 200 mm of the length of the panel (Hong 2017; Robertson et al. 2018; Derikvand et al. 2019). Therefore, the glued-in steel plates, with limited dimensions, can be installed on prefabricated NLT panels only within this 150 to 200 mm space between the nail rows (as shown in Figure 1).

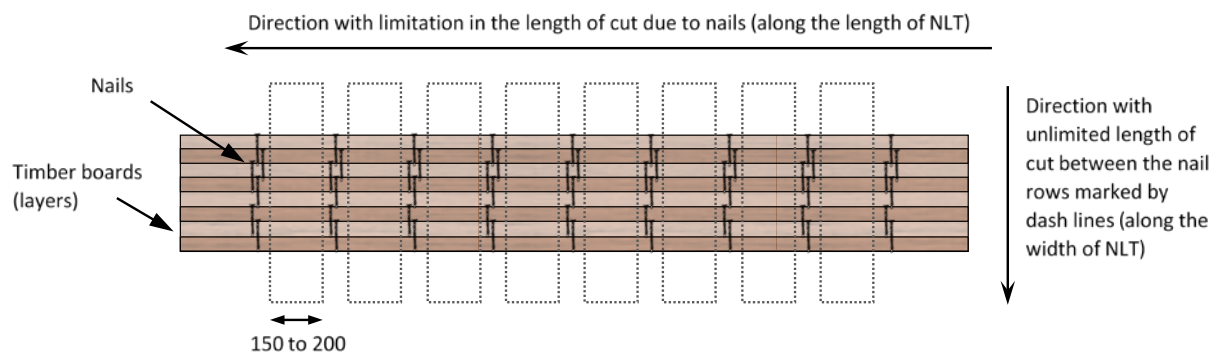


Figure 1. The plan view of a part of an NLT panel with multiple nail rows (measurements are in mm).

The structural capacity of some of the TCC shear connections with high slip modulus may also rely on the properties of the timber used in their construction—such as shear strength parallel to the grain (Suárez-Riestra et al. 2019). Therefore, the behaviour of conventional TCC connections on plantation *E. nitens* timber could be completely different—as the material properties of timber from such plantation resources is highly variable (Derikvand et al. 2018b). The need for developing appropriate TCC connection systems for a potential high-value NLT-concrete floor product from *E. nitens* plantations is therefore warranted.

The objective of this experimental study was to develop and examine shear connections for hybrid NLT-concrete floor panels constructed from plantation *E. nitens* timber. Two new connections were developed using glued-in timber post anchor and glued-in steel plates welded together with a reinforcing bar. The timber post anchor used is an off-the-shelf product that has been repurposed in this study with its original design to be tested as a shear connector in TCC floors. The shear strength, stiffness, and failure modes of the connections were studied under uniaxial pushout loads. To create a basis for comparison with the glued-in connections, two notched connections, namely round dovetail notch and oblong dovetail notch, were also tested to represent rigid connections with a possible brittle behaviour. Two types of conventional dowel-type shear connectors (i.e., SFS screws and coach screws) were also

tested to represent less rigid connections with more ductile behaviour. The structural capacities of the studied connections are compared and discussed.

2. Materials and Methods

2.1. Timber

The timber boards used in this study were obtained from a 16 years old fibre-managed plantation *E. nitens* resource harvested from the north of Tasmania, Australia. The boards were of low structural grade and had substantial defects such as knots, end splits, and surface checking. The nominal thickness and width of the boards used were 34 mm and 140 mm, respectively. The average oven-dry density of the boards was $513 \pm 67 \text{ kg.m}^{-3}$. The modulus of elasticity and modulus of rupture of timber from the same plantation resource were reported to be respectively 10.80 GPa and 43.55 MPa in a previous study by Derikvand et al. (2018b).

2.2. Description of the test connections

The general configuration and dimensions of the NLT component and the concrete slab in the test connections are shown in Figure 2. The NLT component in each sample was produced by nail-laminating eight boards together on their sides using a pneumatic nail gun. The length and diameter of the nails used were 75 mm and 3.5 mm, respectively. A zigzag nailing pattern comprised of two rows of nails with a nominal longitudinal spacing of 150 mm was utilised. The edge distance and the end distance of the nails were respectively 20 mm and 55 mm in all test treatments. The top surface of the NLT component in the samples was covered by a layer of Polythene film to prevent the timber from absorbing moisture from the wet concrete.

Two new glued-in connections, two types of notched connections, and two types of inclined screw connections were developed and tested in this study as given in Table 1.

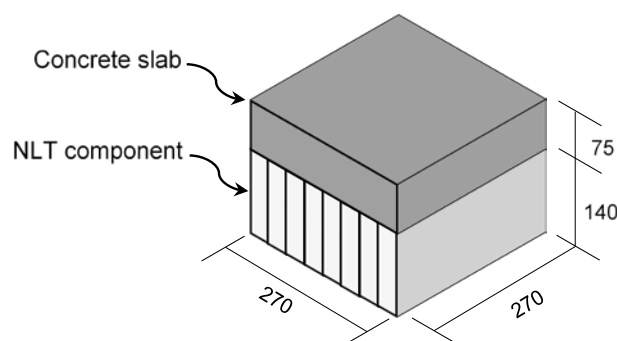


Figure 2. Configuration and dimensions of the shear samples.

Table 1. Experimental design.

Category	Connector type	Symbol	Number of replicates
Glued-in connections	Timber post anchor	GA1	3
	Steel plates with reinforcing bar	GA2	3
Notched connections	Round dovetail notch	NA1	3
	Oblong dovetail notch	NA2	3
Inclined screw connections	SFS screws	SA1	3
	Galvanised coach screws	SA2	3

2.2.1. Glued-in connections

For the glued-in connections, the examined connectors were a) a full stirrup timber post anchor and b) two steel plates welded together using a reinforcing bar. The configurations and dimensions of these connectors along with the direction of the shear loads resisted by these connectors during the tests are depicted in Figure 3.

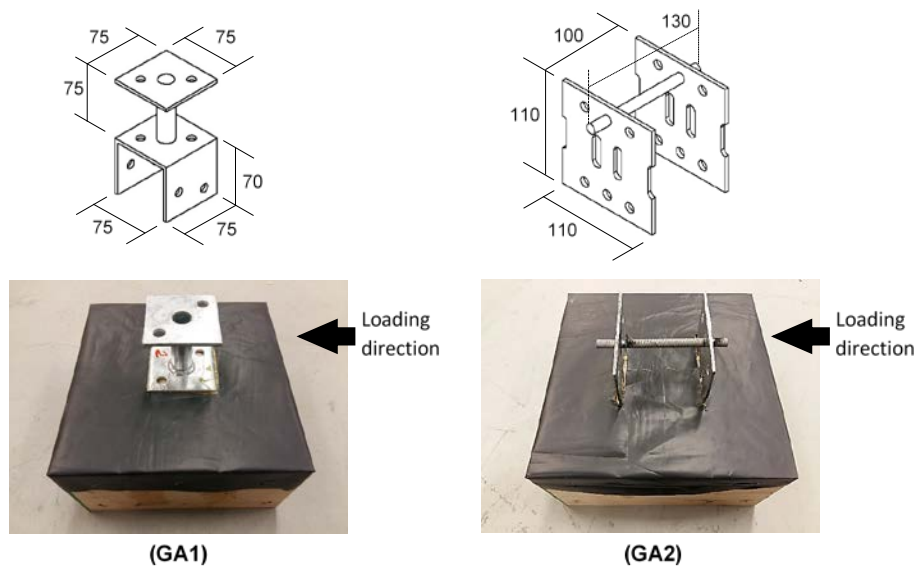


Figure 3. Configurations of the glued-in connections (measurements in mm); timber post anchor (GA1); steel plates with reinforcing bar (GA2).

To install the glued-in connectors, two slots of 3.2 mm wide and 70 mm deep were cut from the top surface of the NLT component perpendicular to the lamination direction of the timber boards. The slots were filled with a one-component polyurethane glue (Gendron et al. 2016) and the connectors were then inserted. The samples were left to cure for 24 hours.

2.2.2. Notched connections

The configuration and dimensions of the round and oblong dovetail notched connections are depicted in Figure 4. The notched connections were produced using a Computer Numerical Control (CNC) router and a dovetail router bit with a 25 mm depth of cut. These connections were designed with dovetailed

sections so that they can hold the concrete slab and the NLT component together—accounting for any upward buckling in a full-scale floor under bending loads. No screw or bolt was used in the construction of these connections so that the level of shear strength and stiffness of the notch itself can be properly determined and a brittle behaviour can occur in the connection—to create a basis for comparison with ductile connections.

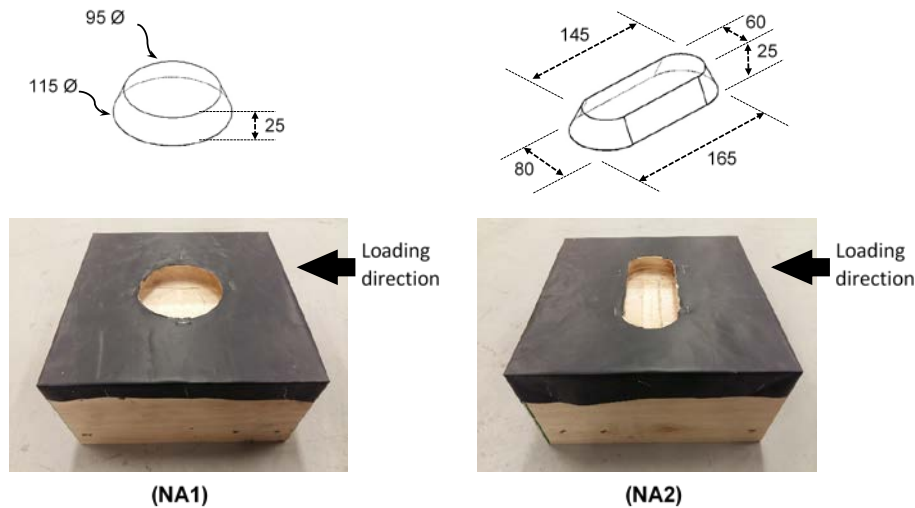


Figure 4. Configurations of the notched connections (measurements in mm); round dovetail notch (NA1); oblong dovetail notch (NA2).

2.2.3. Inclined screw connections

The inclined screw connections were constructed using conventional SFS connectors and galvanised coach screws (Figure 5). Both types of screw connections were constructed by installing two connectors inclined at 45° angle in opposite directions. The embedment depths were 100 mm and 90 mm respectively for the SFS screws and the coach screws. The SFS connectors had the same dimensions as in Deam et al. (2008) and Mai et al. (2018b).

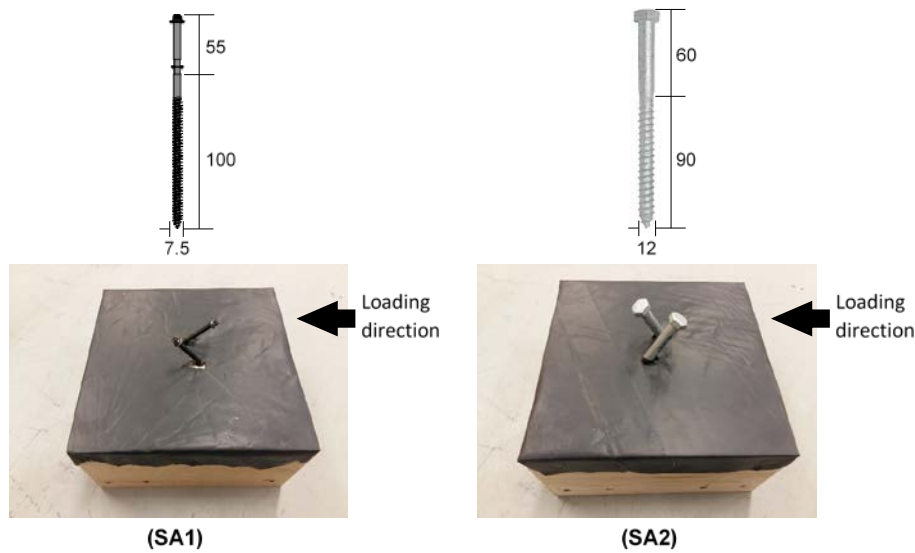


Figure 5. Configurations of the inclined screw connections (measurements in mm); SFS screws (SA1); coach screws (SA2).

2.2.4. Concrete casting

A high-strength premixed concrete with nominal 28-day grade of 55 MPa was used in producing the slabs. To cast the concrete, a steel reinforcement wire mesh was installed and a plywood formwork was fixed around each sample. After the concrete was poured into the formwork, the samples were left to cure in the laboratory environment for a month prior to testing. The formwork was removed after the concrete had fully cured.

2.3. Pushout test description

The pushout loading set-up used in this study is shown in Figure 6. The loading procedure was based on the European Standard, CEN 26891 (1991). Two layers of 5 mm thick Teflon were used between the test jig and the concrete surface to create a low-friction contact—as in Otero-Chans et al. (2018) and Suárez-Riestra et al. (2019). The samples were initially loaded up to almost 40% of their estimated maximum load-carrying capacity (F_{est}). The load was maintained at this level for 30 seconds and then reduced to almost 10% of the F_{est} . The load was maintained at this level again for 30 seconds and then increased with the same loading rate up to failure point (F_{max}) of the samples. The F_{est} can be obtained from experience, calculations, or from the results of actual testing (as per CEN 26891 1991). The F_{est} was estimated in this study based on the results of testing reported in the literature relevant to each type of connectors—a method used by Khorsandnia et al. (2018) for investigating the structural performance of TCC connections. After testing the first sample in each treatment, the F_{est} was adjusted for the rest of the samples only if the F_{max} obtained deviated from the F_{est} by more than 20% (Dias 2005; Suárez-Riestra et al. 2019). The slip between the concrete slab and NLT component was measured using a Linear Variable Differential Transformer (LVDT) from the bottom of the concrete slab (Figure 6).

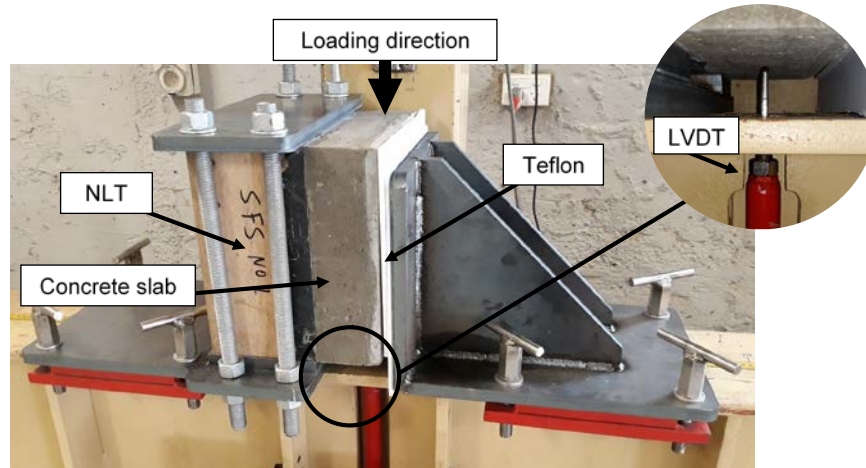


Figure 6. Test set-up.

The shear strength was quantified as the peak applied load (or F_{\max}) resisted by each test connection. The stiffness of the connections was quantified by calculating the slip modulus at 40% (or service load, $K_{0.4}$), 60% ($K_{0.6}$), 80% ($K_{0.8}$), and 100% ($K_{1.0}$) of F_{\max} .

Piece-wise linear curves were created from the non-linear load-slip behaviour of the connections in each category using the averaged F_{\max} and averaged slip modulus values at 40%, 60%, 80%, and 100% of F_{\max} .

2.4. Statistical data analysis

The results obtained were statistically analysed using IBM SPSS Statistics software (version 23). The importance of differences in the average values of slip modulus and F_{\max} between the test connections was determined using the Duncan's multiple range test at 95% level of confidence. As only three samples were tested for each connection type, it must be acknowledged that the statistical analysis in this study only shows the general trend in differences between various groups.

3. Results and Discussions

3.1. Failure modes and load-slip curves

The failure modes of the tested connections are shown in Figure 7 and further summarised in Table 2.

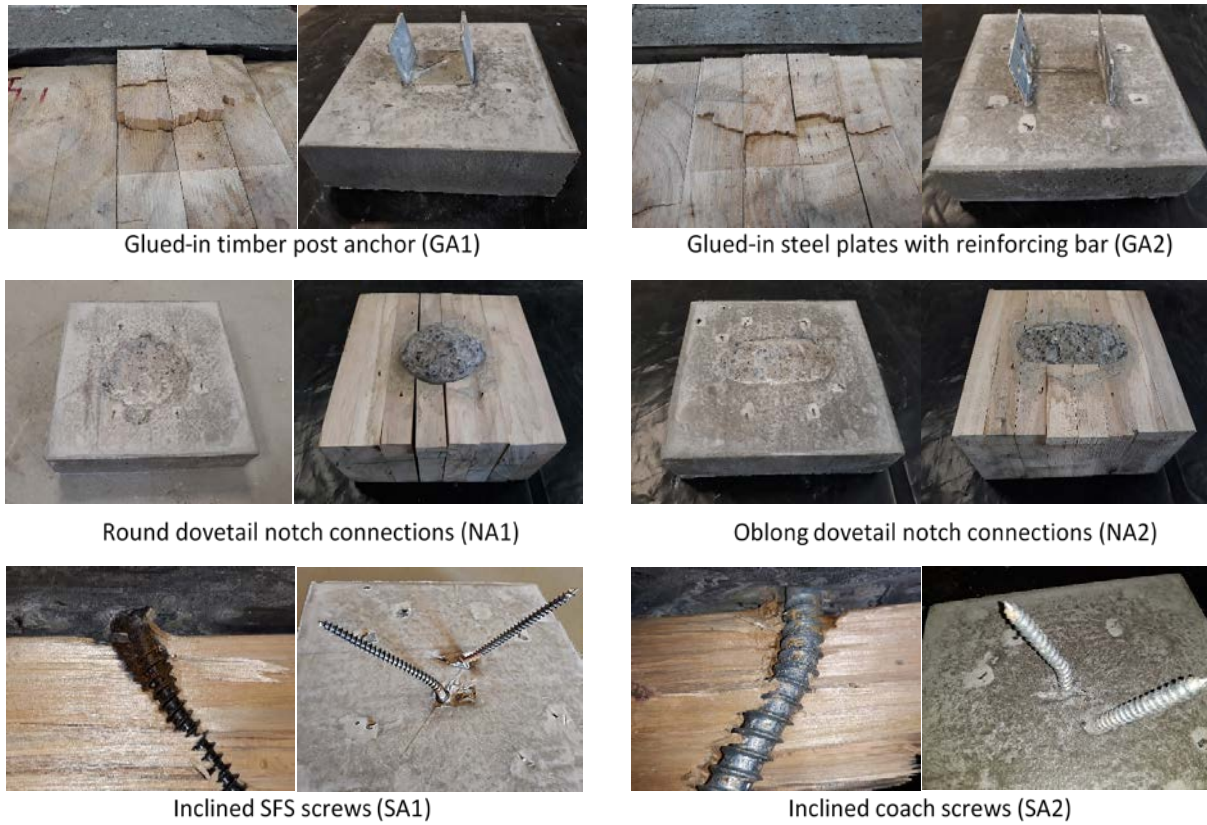


Figure 7. Failure modes of the TCC connections tested in this study.

Table 2. Failure modes of the test connections.

Connection type	Post-peak behaviour		NLT component		Concrete slab		Connector	
	Ductile	Brittle	Crushing	Shear	Fracture	Cracking	Fracture	Bending deformation
GA1	Yes	No	No	Yes	No	No	No	Yes
GA2	Yes	No	No	Yes	No	No	No	Yes
NA1	No	Yes	No	Yes	Yes	No	Yes	No
NA2	No	Yes	No	Yes	Yes	No	Yes	No
SA1	Yes	No	Yes	No	No	No	No	Yes
SA2	Yes	No	Yes	No	No	No	No	Yes

The failures in the glued-in connections (GA1 and GA2) generally happened in the NLT component through shear parallel to the grain (Figure 7). Bending deformation in the connectors was also observed in these specimens. No failure was observed in the concrete slabs or the connectors.

The failure mechanism in the inclined screw connections (SA1 and SA2) was mainly compression/crushing of wood fibres around the screws followed by bending deformation in the screws. No failure in the concrete slab was detected in these specimens.

In the notched connections (NA1 and NA2), the failure started in some of the boards in the NLT component by shear parallel to the grain followed by shear fracture in the concrete slab.

The load-slip curves of the test connections under uniaxial pushout test are depicted in Figure 8. The post-peak behaviour of the connections was quantified by calculating the ratio of $F_{\max}/F_{10\text{mm}}$ where $F_{10\text{mm}}$ is the maximum load at 10 mm slip of the connection. It is suggested that when this ratio is above 50% the connection is ductile and a ratio less than 50% represents a brittle connection (Yeoh et al. 2011; Mai et al. 2018b). Accordingly, a ductile connection in this paper refers to a connection that can reach 10 mm slip with less than 50% reduction in its shear strength. The post-peak behaviour of each connection type is given in Table 2.

The post-peak behaviour of the glued-in connections was purely ductile even after the NLT component was failed in shear parallel to the grain. The nails used in the construction of the NLT component together with the connector itself deformed gradually under loading which helped to distribute the shear loads between different layers (boards) and prevented the NLT component from sudden brittle failure. Except for one of the connections with SFS screws, the failure in the inclined screw connections (i.e., coach screws and SFS screws) was totally ductile. This result on the post-peak behaviour of the SFS screws is different than that reported for the same type of connectors by Mai et al. (2018b) on hybrid cross-laminated timber-concrete CLT-concrete floors. The species of timber and the type of timber component was different in this study than the above-mentioned ones, which might have led to such differences.

Pure brittle failures were observed in the notched connections. The maximum shear strength in these connections was achieved at a slip less than 10 mm after which the load-carrying capacity dropped to zero due to complete fracture in the concrete notch (Figure 8). Brittle failure in such connections could be avoided to some degree by inserting dowel-type fasteners in the centre of the notch (Deam et al. 2008; Dias et al. 2018).

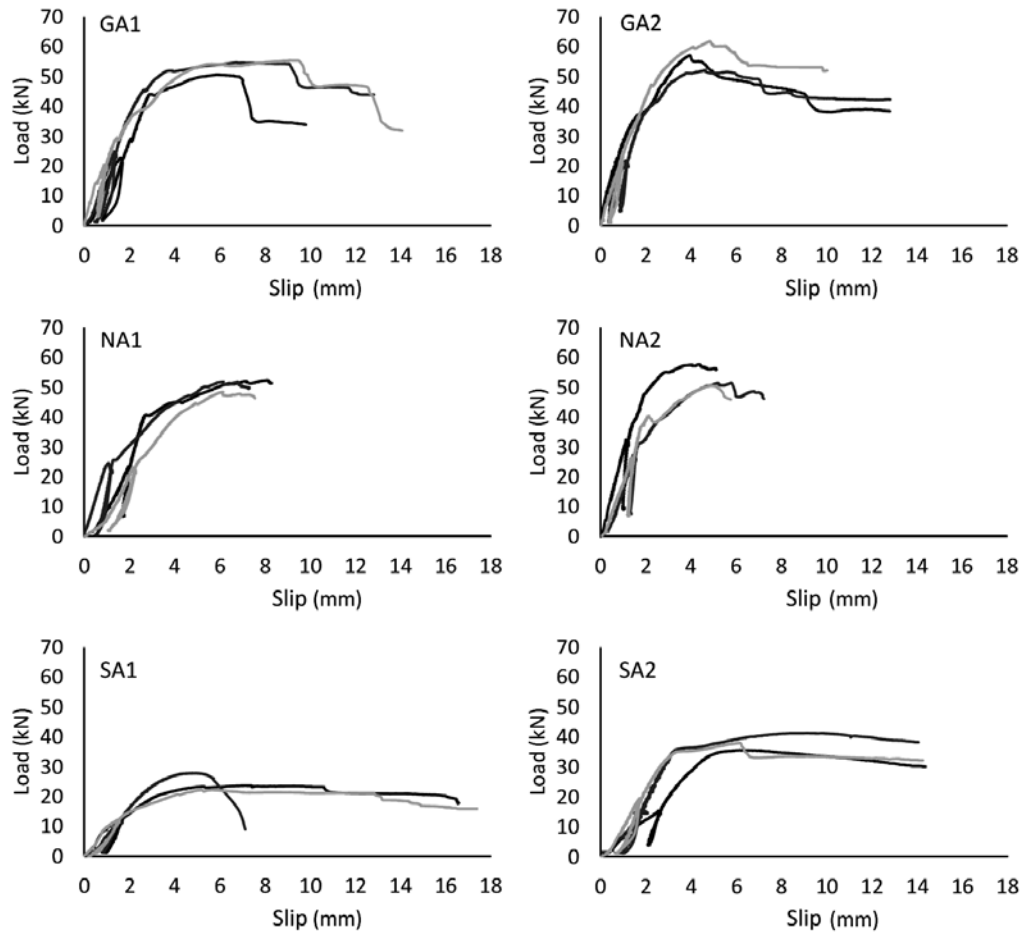


Figure 8. Load-slip curves from the tested connections.

The piece-wise linear load-slip curves for the tested connections are shown in Figure 9. It can be seen from this figure that the connections made with glued-in steel plates with reinforcing bar (GA2) had a better load-slip response under uniaxial pushout loads compared to other connections. The SFS screws also resulted in connections with a much less favourable load-slip response. There was a similar trend in the load-slip curve of the glued-in timber post anchor (GA1), glued-in steel plates with reinforcing bar (GA2), and the oblong dovetail notch connections (NA2) up to 80% of failure load.

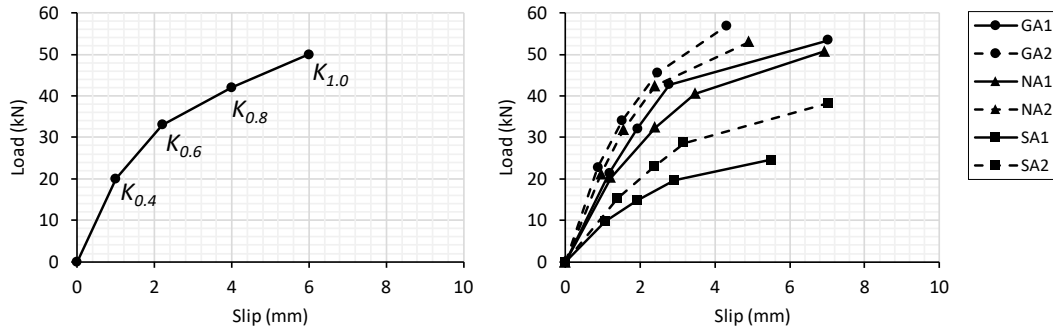


Figure 9. An example of a piece-wise load-slip curve with depicted slip modulus symbols (a) and the actual piece-wise linear load-slip curves obtained for the connections in this study (b).

3.2. Shear strength and slip modulus of the connections

The average shear strength and slip modulus values of the connections along with the Duncan's multiple range test results are given in Table 3.

The highest average shear strength (F_{max}) was obtained by the connections made with glued-in steel plates with reinforcing bar (GA2) followed respectively by the connections made with glued-in timber post anchor (GA1), oblong dovetail notch (NA2), round dovetail notch (NA1), and inclined coach screws (SA2). The connections made with inclined SFS screws (SA1) also exhibited the lowest shear strength values.

Based on the Duncan's multiple range test results, the differences in the shear strength values between the glued-in connections and the notched connections was insignificant ($p > 0.05$). There was a significant difference ($p < 0.05$) in the shear strength between the connections with inclined SFS screws and coach screws—with coach screws being 55.7% stronger. The shear strength of the SFS screws in this study was comparable to that reported by Mai et al. (2018b) on hybrid CLT-concrete floors (23.4 kN).

Table 3. Maximum shear strength (F_{max} in kN) and slip modulus values ($K_{0.4}$, $K_{0.6}$, $K_{0.8}$, $K_{1.0}$ in kN/mm) of the connections at different load levels.

Connection type	Replicate	F_{max}	Duncan's group ^a	$K_{0.4}$	Duncan's group ^a	$K_{0.6}$	Duncan's group ^a	$K_{0.8}$	Duncan's group ^a	$K_{1.0}$	Duncan's group ^a
GA1	1	54.6		18.9		18.2		17.7		8.1	
	2	50.5		15.0		13.9		15.3		8.6	
	3	55.3		20.6		17.9		13.4		6.1	
	Mean	53.5	A	18.2	ABC	16.7	BC	15.4	AB	7.6	B
GA2	1	57.0		30.2		24.0		17.7		14.4	
	2	52.0		23.0		20.0		16.5		11.3	
	3	61.7		25.8		23.6		21.3		13.9	
	Mean	56.9	A	26.3	A	22.6	A	18.5	A	13.2	A
NA1	1	52.3		14.0		13.1		12.9		6.4	
	2	51.7		25.4		14.9		12.3		7.6	
	3	48.3		11.1		10.0		10.0		7.9	
	Mean	50.7	A	16.8	BCD	12.7	CD	11.7	BC	7.3	B

NA2	1	57.5		27.8		26.4		25.0		13.2	
	2	51.3		18.6		18.1		13.7		8.9	
	3	50.5		20.1		16.9		14.5		10.3	
	Mean	53.1	A	22.2	AB	20.5	AB	17.7	A	10.8	A
SA1	1	23.7		9.1		7.3		6.5		3.3	
	2	27.9		8.1		8.0		7.9		5.8	
	3	22.2		10.5		8.0		5.9		4.3	
	Mean	24.6	C	9.2	D	7.8	D	6.7	C	4.5	C
SA2	1	35.6		6.5		7.1		6.9		5.6	
	2	41.2		14.3		10.6		10.8		4.5	
	3	38.0		12.3		11.3		11.2		6.2	
	Mean	38.3	B	11.0	CD	9.7	D	9.7	BC	5.4	BC

^a : Different letters indicate significant differences between the connection types at 95% level of confidence

In the TCC structures, the slip modulus at 40% of maximum load (i.e., $K_{0.4}$) is used for serviceability design and the slip modulus at 60% of maximum applied load (i.e., $K_{0.6}$) is used for ultimate limit state. As given in Table 3, the highest $K_{0.4}$ and $K_{0.6}$ values were obtained by the connections made with glued-in steel plates with a reinforcing bar (GA2). There was no significant difference ($p > 0.05$) in the $K_{0.4}$ and $K_{0.6}$ values between the GA2 connections and oblong dovetail notch connections (NA2). The NA2 connections however had respectively 15.6% and 9.3% lower $K_{0.4}$ and $K_{0.6}$ values than the GA2 connections. There was also no significant difference ($p > 0.05$) between the average $K_{0.4}$ and $K_{0.6}$ values of the connections made with glued-in timber post anchor (GA1) and those of the NA2 connections. The average $K_{0.4}$ and $K_{0.6}$ values of the GA1 connections however were lower than those of the NA2 connections. The difference in the average $K_{0.6}$ values between the GA1 and GA2 connections was statistically significant ($p < 0.05$)—with the GA2 connections having 35.3% higher slip modulus at 60% of failure load.

There was no significant difference ($p > 0.05$) in the average slip modulus values between the round dovetail notch connections (NA1) and the inclined screw connections (SA1 and SA2) up to 80% of the F_{max} —although the NA1 connections showed higher slip modulus values at all the various load levels. Coach screws exhibited respectively 19.6% and 24.4% higher average $K_{0.4}$ and $K_{0.6}$ values than the SFS screws. These differences however were not statistically significant within the sample size tested in this study ($p > 0.05$).

Table 4 represents the stiffness degradation in the tested connections. The stiffness degradation values in this table were calculated as a ratio of slip modulus at various load levels on that at 40% of failure load (i.e., $K_{0.4}$ used for serviceability limit state). The glued-in timber post anchor (GA1), oblong dovetail notch (NA2), and coach screws (SA2) exhibited the lowest stiffness degradation when the applied load increased from 40% to 80% of failure load. The round dovetail notched connections (NA1) showed the highest stiffness degradation. With an increase in the load from 40% to 80% of failure load, the second highest stiffness degradation of approximately 30% was observed in the glued-in steel plates

with reinforcing bar (GA2). This must be noted that even with this level of stiffness degradation the glued-in steel plates with reinforcing bar still had a $K_{0.8}$ value (18.5 kN/mm) that was considerably greater than that of all the other connections tested (Table 3). The glued-in steel plates with reinforcing bar had the lowest stiffness degradation when the ultimate load-carrying capacity of the connections was reached ($K_{1.0}/K_{0.4}$).

Table 4. Stiffness degradation in the tested connections.

Connection type	$K_{0.4}/K_{0.4}$	$K_{0.6}/K_{0.4}$	$K_{0.8}/K_{0.4}$	$K_{1.0}/K_{0.4}$
GA1	1	0.919	0.851	0.419
GA2	1	0.857	0.703	0.501
NA1	1	0.753	0.696	0.434
NA2	1	0.925	0.799	0.488
SA1	1	0.841	0.731	0.485
SA2	1	0.876	0.874	0.492

3.3. Overview of the performance of the glued-in connections

In general, considering the shear strength, stiffness, failure modes, and post-peak behaviour, the two glued-in connections in this study exhibited a better performance on NLT-concrete elements than the other types of connections tested. The glued-in connections represented a ductile behaviour under pushout loads while still exhibiting the highest shear strength values.

Although a direct comparison might be irrelevant given the fact that different timber products, species, and connector dimensions were used, it could be pointed out that the glued-in connections loaded perpendicular to the steel plates have produced lower slip modulus values than connections loaded parallel to the steel plates in some previous studies on other types of timber products (e.g., Lukaszewska et al. 2008; Otero-Chans et al. 2018; Hong 2017). In addition, based on the failure modes observed, the shear strength and stiffness of the two glued-in connections relies predominantly on the shear strength of the NLT component. Compared to the other connections tested, the use of glued-in connections in the construction of NLT-concrete floors can be relatively more expensive. Therefore, the use of such connections can be justified only when a higher composite action in NLT-concrete elements is of interest—e.g., long-span floors. For NLT-concrete floors with short span, the use of dowel-type connectors could be much more economically viable in which case inclined coach screws are recommended. The significance of differences between the bending performance of full-scale NLT-concrete floors constructed with the TCC connectors examined in this research can be studied and verified in future using both experimental and analytical approaches—such as the gamma-method described in the Annex B of Eurocode 5 (CEN 2004).

4. Conclusions

This experimental study was performed to develop and investigate the structural performance of TCC shear connections that could be used in the construction of hybrid NLT-concrete floors from low-grade plantation *E. nitens* timber. The test connections were comprised of a glued-in connection made with timber post anchor, a glued-in connection made with two steel plates with reinforcing bar, two types of notched connections (round dovetail notch and oblong dovetail notch), and two types of connections with inclined screws (SFS screws and coach screws). The following conclusions were drawn based on the results obtained:

- The connections made with inclined SFS screws and coach screws exhibited the lowest shear strength and slip modulus. These connections represented a ductile behaviour on the NLT component.
- Between the six different connections tested, the oblong dovetail notch connections had the third highest shear strength (53.1 kN) and the second highest slip modulus at service load (22.2 kN/mm). The notched connections however had a brittle behaviour under pushout loads.
- The glued-in connections made with timber post anchor exhibited the second highest shear strength (53.5 kN) and the third highest slip modulus at service load (18.2 kN/mm). Considering the post-peak behavior, the glued-in timber post anchor was classified as a ductile connector. Shear parallel to the grain failure in the NLT component was the most common failure mode in the glued-in connections.
- The glued-in connection comprised of two steel plates welded together by a reinforcing bar showed the highest shear strength (56.9 kN) and slip modulus (26.3 kN/mm) at service load. This type of connections exhibited a remarkable post-peak behaviour resulting in a better ductile behavior compared to the other connection tested.

Acknowledgment: The authors are grateful of the support from Forico Pty Ltd. in providing the logs and Britton Timbers for the milling of the logs and drying and finishing of the boards. The feedback from Dr. Chris Beadle on this paper and technical support from Mr. Robin Green from University of Tasmania in preparing the test specimens are acknowledged.

Funding: This study was undertaken under the Australian Research Council, Centre for Forest Value, University of Tasmania, TAS, Australia (Grant Reference: IC150100004). Additional support was provided by Forest and Wood Products Australia Limited (FWPA), Melbourne, VIC, Australia (Grant Number: PNB387-1516).

Conflict of Interest: The authors declare that they have no conflict of interest.

References

- [1] Auclair SC, Sorelli L, Salenikovich A (2016) A new composite connector for timber-concrete composite structures. *Construction and Building Materials* 112: 84-92. <https://doi.org/10.1016/j.conbuildmat.2016.02.025>
- [2] Blackburn D, Vega M, Yong R, Britton D, Nolan G (2018) Factors influencing the production of structural plywood in Tasmania, Australia from *Eucalyptus nitens* rotary peeled veneer. *Southern Forests: a Journal of Forest Science* 1-10. <https://doi.org/10.2989/20702620.2017.1420730>
- [3] Crocetti R, Sartori T, Tomasi R (2015) Innovative timber-concrete composite structures with prefabricated FRC slabs. *Journal of Structural Engineering* 141(9): 04014224. [https://doi.org/10.1061/\(ASCE\)ST.1943-541X.0001203](https://doi.org/10.1061/(ASCE)ST.1943-541X.0001203)
- [4] Deam BL, Fragiaco M, Buchanan AH (2008) Connections for composite concrete slab and LVL flooring systems. *Materials and Structures* 41(3): 495-507. <https://doi.org/10.1617/s11527-007-9261-x>
- [5] Derikvand M, Jiao H, Kotlarewski N, Lee M, Chan A, Nolan G (2019) Bending performance of nail-laminated timber constructed of fast-grown plantation eucalypt. *European Journal of Wood and Wood Products* 77(3) 421–437. <https://doi.org/10.1007/s00107-019-01408-9>
- [6] Derikvand M, Kotlarewski N, Lee M, Jiao H, Chan A, Nolan G (2018b) Visual stress grading of fibre-managed plantation Eucalypt timber for structural building applications. *Construction and Building Materials* 167: 688-699. <https://doi.org/10.1016/j.conbuildmat.2018.02.090>
- [7] Derikvand M, Kotlarewski N, Lee M, Jiao H, Nolan G (2018a) Flexural and visual characteristics of fibre-managed plantation *Eucalyptus globulus* timber. *Wood Material Science & Engineering*. <https://doi.org/10.1080/17480272.2018.1542618>
- [8] Derikvand M, Nolan G, Jiao H, Kotlarewski N (2017) What to Do with Structurally Low-Grade Wood from Australia's Plantation Eucalyptus; Building Application?. *BioResources* 12(1): 4-7. <https://doi.org/10.15376/biores.12.1.4-7>
- [9] Dias AMPG (2005) Mechanical behaviour of timber-concrete joints. Doctoral Dissertation, Delft University of Technology, Germany.
- [10] Dias AMPG, Kuhlmann U, Kudla K, Mönch S, Dias AMA (2018) Performance of dowel-type fasteners and notches for hybrid timber structures. *Engineering Structures* 171: 40-46. <https://doi.org/10.1016/j.engstruct.2018.05.057>
- [11] EN 1995-1-1 Eurocode 5 - Design of timber structures - Part 1-1: General - Common rules and rules for buildings. Brussels: CEN 2004.

- [12] Eisenhut L, Seim W, Kühnborn S (2016) Adhesive-bonded timber-concrete composites—Experimental and numerical investigation of hygrothermal effects. *Engineering Structures* 125: 167-178. <https://doi.org/10.1016/j.engstruct.2016.05.056>
- [13] European Committee for Standardization (1991) Timber structures—Joints made with mechanical fasteners—General principles for the determination of strength and deformation characteristic. EN 26891, Brussels, Belgium.
- [14] Fragiaco M (2012) Experimental behaviour of a full-scale timber-concrete composite floor with mechanical connectors. *Materials and structures* 45(11): 1717-1735. <https://doi.org/10.1617/s11527-012-9869-3>
- [15] Gendron B, Salenikovich A, Sorelli L (2016) Timber concrete composite beams with ductile failure modes. In *Proceedings of World Conference on Timber Engineering*, Vienna, Austria.
- [16] Hong KEM (2017) Structural performance of nail-laminated timber-concrete composite floors. Master's dissertation, University of British Columbia.
- [17] Jacquier N, Girhammar UA (2012) Tests on shear connections in prefabricated composite cross-laminated-timber and concrete elements. In *World Conference on Timber Engineering*: 15/07/2012-19/07/2012 (pp. 441-450). New Zealand Timber Design Society.
- [18] Khorsandnia N, Valipour H, Bradford M (2018) Deconstructable timber-concrete composite beams with panelised slabs: Finite element analysis. *Construction and Building Materials* 163: 798-811. <https://doi.org/10.1016/j.conbuildmat.2017.12.169>
- [19] Lukaszewska E, Johnsson H, Fragiaco M (2008) Performance of connections for prefabricated timber-concrete composite floors. *Materials and structures* 41(9): 1533-1550. <https://doi.org/10.1617/s11527-007-9346-6>
- [20] Mai KQ, Park A, Lee K (2018b) Experimental and numerical performance of shear connections in CLT-concrete composite floor. *Materials and Structures* 51(4): 84. <https://doi.org/10.1617/s11527-018-1202-3>
- [21] Mai KQ, Park A, Nguyen KT, Lee K (2018a) Full-scale static and dynamic experiments of hybrid CLT-concrete composite floor. *Construction and Building Materials* 170: 55-65. <https://doi.org/10.1016/j.conbuildmat.2018.03.042>

- [22] Otero-Chans D, Estévez-Cimadevila J, Suárez-Riestra F, Martín-Gutiérrez E (2018) Experimental analysis of glued-in steel plates used as shear connectors in Timber-Concrete-Composites. *Engineering Structures* 170: 1-10. <https://doi.org/10.1016/j.engstruct.2018.05.062>
- [23] Oudjene M, Meghlat EM, Ait-Aider H, Lardeur P, Khelifa M, Batoz JL (2018) Finite element modelling of the nonlinear load-slip behaviour of full-scale timber-to-concrete composite T-shaped beams. *Composite Structures* 196: 117-126. <https://doi.org/10.1016/j.compstruct.2018.04.079>
- [24] Rijal R, Samali B, Shrestha R, Crews K (2015) Experimental and analytical study on dynamic performance of timber-concrete composite beams. *Construction and Building Materials* 75: 46-53. <https://doi.org/10.1016/j.conbuildmat.2014.10.020>
- [25] Robertson M, Holloway D, Taoum A (2018) Vibration of suspended solid-timber slabs without intermediate support: assessment for human comfort. *Australian Journal of Structural Engineering* 19(4): 266-278. <https://doi.org/10.1080/13287982.2018.1513783>
- [26] Suárez-Riestra F, Estévez-Cimadevila J, Martín-Gutiérrez E, Otero-Chans D (2019) Perforated shear+ reinforcement bar connectors in a timber-concrete composite solution. Analytical and numerical approach. *Composites Part B: Engineering* 156: 138-147. <https://doi.org/10.1016/j.compositesb.2018.08.074>
- [27] Yeoh D, Fragiaco M, De Franceschi M, Heng Boon K (2010) State of the art on timber-concrete composite structures: Literature review. *Journal of Structural Engineering* 137(10): 1085-1095. [https://doi.org/10.1061/\(ASCE\)ST.1943-541X.0000353](https://doi.org/10.1061/(ASCE)ST.1943-541X.0000353)
- [28] Yeoh D, Fragiaco M, Deam B (2011) Experimental behaviour of LVL–concrete composite floor beams at strength limit state. *Engineering Structures* 33(9): 2697-2707.

Appendix G: Paper VII

Publication reference: Derikvand, M., Kotlarewski, N., Lee, M., Jiao, H., Chan, A., & Nolan, G. (2019). Short-term and long-term bending properties of nail-laminated timber constructed of fast-grown plantation eucalypt. *Construction and Building Materials*, 211, 952-964.

Short-term and long-term bending properties of nail-laminated timber constructed of fast-grown plantation eucalypt

Mohammad Derikvand, Nathan Kotlarewski, Michael Lee, Hui Jiao, Andrew Chan, Gregory Nolan

Abstract

Developing higher-value structural products from fast-growing eucalypt plantations—that are currently managed for woodchip production—can create new markets for these plantation resources and ensure a sustainable supply of timber for building construction. In this study, structural nail-laminated timber (NLT) panels with different span lengths were manufactured from a 16-year-old fast-grown *Eucalyptus nitens* plantation using a lamination system that can maximise the use of lower-grade boards in NLT production. The short-term bending performance in the elastic region and the effects of environmental conditions and structural grade of timber on long-term bending creep deflection of the panels were evaluated. The data analysis revealed that the current visual stress-grading method is incapable of estimating the actual modulus of elasticity (MOE) of the plantation *Eucalyptus nitens* timber. A linear regression model was proposed using the actual MOE of the boards that can predict the MOE of NLT panels with an average accuracy of 98%. The NLT panels made with higher-grade boards showed 22.4% greater MOE values than the NLT panels made with lower-grade boards. The lamination system used resulted in NLT panels with predictable and customised MOE with a remarkable average coefficient of variance of less than 2.6%. The long-term bending creep deflection of the test panels was significantly affected by daily variations in the relative humidity of the environment and structural grade of the timber used. The results of this study can be used in the development of an appropriate NLT production system from fast-grown plantation eucalypt.

Keywords: mass laminated timber; eucalyptus; bending test; creep test; lamination system; visual stress-grading.

1. Introduction

Timber as a natural and recyclable material represents a green solution to building construction (Evison et al. 2018; Smith et al. 2018). When used as individual boards, timber also has some limitations that can influence its wider applications for structural building purposes. Solid timber has a higher variability in the mechanical properties compared to some other construction materials such as steel that can be manufactured under controlled production conditions (Ramage et al. 2017). Solid timber also has limitations in terms of length and cross-sectional dimensions. Laminated assemblies such as nail-laminated timber (NLT) offer practical solutions to these limitations of solid timber (Hong 2017). The main goal of this study was to evaluate the short-term elastic bending performance and long-term

bending creep deflection of NLT floor panels constructed of a fast-growing, fibre-managed plantation *Eucalyptus nitens* (*E. nitens*) resource that is currently managed to produce woodchips—a low-value product. Developing higher-value structural products from plantation eucalypt timber can create new markets for such plantation resources.

NLT is a mass laminated timber product that is constructed by nailing together timber boards on their sides to achieve a section with more consistent structural properties than a solid timber of the same dimensions (Hong 2017; Robertson et al. 2018). NLT can be produced in any desired length and width. NLT components can be found in a wide range of different structural applications in bridges, timber decks, and both modern and historical buildings (Janssens 2015; Weckendorf et al. 2016; Zhou et al. 2017). In building construction, NLT is most commonly used in structural flooring systems as either a continuous member (i.e., as a floor panel) or a beam-type bearer (Hong 2017; Robertson et al. 2018). One important aspect of mass laminated timber products, such as NLT, cross-laminated timber (CLT), and glue-laminated timber (GLT), is that most of their important mechanical properties can be properly estimated through analytical and numerical models and then used for structural design purposes (Okabe et al. 2014; Fossetti et al. 2015; Fink et al. 2015; Oh et al. 2015, Hong 2017; Ussher et al. 2017). This however requires a precise estimation of the structural properties of the timber boards used in their construction (Kandler et al. 2015).

The structural properties of commercially available hardwood species, such as eucalypt from native forests, are conventionally estimated through a process called visual stress-grading (VSG). The VSG method estimates the structural grade of timber boards according to some specific visual criteria (e.g., knot size, slope of grain, wane, etc.) that are regulated for each structural grade in the relevant standard methods. These criteria are based on the relationships between the strength-reducing features (SRF), that are visually assessable, and mechanical properties of timber (Derikvand et al. 2018b). These relationships are obtained through extensive experimental studies and statistical approaches. Each structural grade obtained from the VSG method corresponds to an F-grade (or stress-grade) using which different mechanical properties of timber including its flexural modulus of elasticity (MOE) can be estimated. Although it is associated with human factor, the VSG method is still an acceptable procedure in structural grading of mature hardwood timber from native forests with known properties. Previous studies, however, have shown that the VSG method might not give accurate results when dealing with young, fast-growing timber species such as fibre-managed plantation eucalypt (Derikvand et al. 2018b). In Australia, eucalypt plantations are mostly managed for pulplog production. The timber boards recovered from such plantation resources contain significant amount of SRF and juvenile wood (Derikvand et al. 2018 a, b). Due to this, the physical and mechanical properties of the timber from fast-growing eucalypt plantation could be completely different in the relationship between visual SRFs and structural properties from those of mature native forest timber of the same species (Derikvand et al. 2017, 2018a, b). As the interest in using fast-growing plantation eucalypt in building construction is

rapidly growing around the world (Liao et al. 2017; Lu et al. 2018), establishing an acceptable structural grading system for this timber resource is of high importance.

The structural grade of timber is an important criterion that both timber manufacturers and structural engineers can use to estimate the bending properties and other mechanical characteristics of different mass laminated timber products (Fink et al. 2015, Kandler et al. 2015). Producing mass laminated timber based on the outcome of an inappropriate grading system can lead to a high variation in the mechanical properties of the final product.

Numerous analytical and numerical methods have been developed and proposed in previous studies to estimate the structural capacity of different mass laminated timber products (Shim et al. 2009; Okabe et al. 2014; Fink et al. 2015; Fossetti et al. 2015; Oh et al. 2015; Christovasilis et al. 2016; Ussher et al. 2017). Zhou et al. (2017) examined a modal testing method that could predict the MOE of industrial size CLT panels made of Norway spruce (*Picea abies*) with at least 90% accuracy. In another study, a numerical finite element model was developed by Kandler et al. (2015) that was able to predict the effective stiffness of Norway spruce GLT beams with a high level of accuracy. This model predicts the stiffness of the GLT beams using the longitudinal stiffness profile of each lamella (boards). These researchers calculated the longitudinal stiffness profile of the lamellas using the local fibre orientation on the surfaces of the lamellas which was obtained by an optical scanning device. Lee et al. (2005) established a model using the transformed section method and optimised knot and MOE distributions of lamellas as the main input variables that could successfully predict the bending properties of GLT beams constructed of Japanese Larch (*Larix kaempferi*).

Apart from their acceptable accuracy, most of the prediction models in the previous studies either are heavily calculations-based or come with a high level of complexity which could make it difficult to apply them in a practical commercial production scale of mass laminated timber. Depending on the type of mass laminated timber, appropriate prediction models are also usually species specific due to the fact that timber's most physical and mechanical properties could be different between species and even within species (Shim et al. 2009; Frihart and Beecher 2016).

Such species-based information and simplified prediction models currently does not exist for a potential mass laminated timber product from fibre-managed plantation eucalypt timber. In order to verify the mechanical properties of timber from such plantation resources for any structural applications, questions need to be addressed on how the fibre-managed plantation eucalypt timber performs under both short-term and long-term service conditions. Furthermore, as the recovery rate of higher-grade boards from fibre-managed eucalypt plantations is relatively low (Derikvand et al. 2018b), research is needed to establish practical solutions to maximise the use of lower-grade boards in the production of a potential mass laminated timber from such plantation resources.

A preliminary research at University of Tasmania, Australia, demonstrated that the structural design of NLT from plantation eucalypt timber is more limited by serviceability—which is a function of stiffness—than by strength requirements (Derikvand et al. 2019). It was also observed that when the

timber boards are randomly nail-laminated together, the resulting NLT panels will have a high variability in their stiffness values. One of the aims of this study was therefore to optimise the construction of such NLT panels by developing a lamination system that can reduce such variabilities while still maximising the use of lower-grade boards in the NLT construction. The specific objectives of the study were to:

- Determine the performance of VSG method in estimating the flexural MOE of individual boards of fibre-managed plantation *E. nitens* timber.
- Compare the accuracy of simple regression models in predicting the flexural MOE of the NLT panels based on the VSG results and the actual MOE of the boards obtained from four-point bending test.
- Develop a lamination system to effectively use both lower-grade and higher-grade boards from plantation *E. nitens* in the production of NLT panels and to reduce the variations in the flexural MOE of the panels.
- Examine and verify the performance of the NLT panels, produced using the proposed lamination system, against the serviceability requirements according to the relevant building design code.
- Determine the impacts of structural grade of the boards and environmental conditions, including relative humidity (RH) and temperature, on the long-term creep deflection of the NLT panels under serviceability bending loads.

2. Materials and Methods

2.1. Timber boards

The timber boards used in this study were obtained from a 16-year-old fibre-managed plantation *E. nitens* resource in the north of Tasmania, Australia. As this plantation resource was originally managed to produce pulplog, the stands were unthinned and unpruned. The recovered boards therefore contained substantial SRF. The thickness and width of the boards were 35 mm and 140 mm, respectively. The lengths of the boards were 2600 mm and 3600 mm, which correspond to the lengths of the test NLT panels. The average oven-dry density of the 16-year-old fibre-managed plantation *E. nitens* timber used in this study was reported by Derikvand et al. (2018b) to be $480.58 \pm 49.46 \text{ kg/m}^3$. In total, 72 boards were used in the construction of the NLT panels in this study. The timber boards were visually graded in accordance with AS 2082 (Timber - Hardwood - Visually stress graded for structural purposes, Standards Australia 2007). The grade of the boards was mostly limited by the knot size parameter. After obtaining the structural grade of the boards using visual grading, the relevant F-grade (stress-grade) was allocated to each board. Based on the F-grades, the expected MOE values of the boards were extracted from AS 1720.1 (Standards Australia 2010). The F-grades can be different from one species to another.

For *E. nitens*, four F-grades are outlined in AS 2082 (Standards Australia 2007). The expected minimum MOE values for each of these F-grades are given in Table 1.

After visual grading, the boards were subjected to an edgewise four-point bending test to obtain their actual MOE values according to AS/NZS 4063.1 (Standards Australia/Standards New Zealand 2010). The four-point bending test was conducted in the linear-elastic range and non-destructively without breaking the samples. This method has been used in previous studies to determine the flexural stiffness of timber and mass timber products such as CLT and glulam (O’Ceallaigh et al. 2014; Viguier et al. 2015; Thilén 2017).

Table 1. The F-grades assigned to E. nitens and their expected MOE values.

Species	Structural grade from VSG ^a	Relevant F-grade ^a	Expected MOE of the boards (GPa) ^b
<i>E. nitens</i>	Structural grade No. 1	F22	16
	Structural grade No. 2	F17	14
	Structural grade No. 3	F14	12
	Structural grade No. 4	F11	10.5

^a According to AS 2082 (Standards Australia 2007)

^b According to AS 1720.1 (Standards Australia 2010)

The level of applied load varied based on the length of the boards. For the boards with the lengths of 2600 mm and 3600 mm, the applied loads were 1.96 kN and 0.98 kN, respectively. The loading velocity was 5 mm.min⁻¹. The following equation was used to calculate the actual MOE of the boards (Derikvand et al. 2018a, b).

Equation 1

$$MOE = \frac{23L^3(F_2 - F_1)}{108bd^3(w_2 - w_1)}$$

where, *b* and *d* are the thickness and the width of boards (mm), *L* is the span length (mm), *F*₂ and *F*₁ are respectively maximum applied load and 10% of the maximum load (N), *w*₂ and *w*₁ are maximum displacement (mm) at *F*₂ and *F*₁ loads, respectively.

The actual MOE of the boards were compared to the expected MOE values of the boards obtained from visual grading.

2.2. NLT lamination pattern

The NLT panels in this study were constructed with two different lengths of 2600 mm and 3600 mm. The depth and width of the panels were 140 mm and 280 mm, respectively. After obtaining the actual MOE of the boards through four-point bending test, the boards with the length of 2600 mm were divided into two groups of lower-grade and higher-grade boards. The lower-grade boards had MOE values equivalent to an F-grade lower than F11 (< F11). The MOE values of higher-grade boards were

equivalent to an F-grade of F11 or higher. The lower-grade and higher-grade boards were used to produce lower-grade and higher-grade NLT panels. The NLT dimensions in each test treatment are given in Table 2.

Table 2. Specification and dimensions of the NLT panels.

Code	Panel grade	Specimen No.	Depth (mm)	Breadth (mm)	Length (mm)	Number of laminated boards	Nail spacing (mm)
L-NLT	Higher-grade	Specimen 1	140	280	3600	8	150
	//	Specimen 2	//	//	//	//	//
	//	Specimen 3	//	//	//	//	//
LS-NLT	Lower-grade	Specimen 1	140	280	2600	8	150
	//	Specimen 2	//	//	//	//	//
	//	Specimen 3	//	//	//	//	//
HS-NLT	Higher-grade	Specimen 1	140	280	2600	8	150
	//	Specimen 2	//	//	//	//	//
	//	Specimen 3	//	//	//	//	//

The NLT panels were produced by nail-laminating eight boards together on their sides using a pneumatic nail gun. The nails used in producing the test panels had 3.5 mm diameter and 75 mm length. The nailing system utilised in this study had a zigzag pattern with two rows as depicted in Figure 1. Some of the timber boards had substantial bow and crook which created difficulties in the lamination process of the panels. The bow and crook in the boards were fixed using F-style clamps during the nailing process.

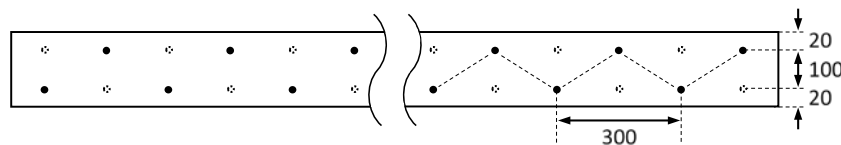


Figure 1. The nailing pattern used in producing the test panels (measurements in mm).

The lamination arrangement/pattern used in producing the NLT panels is shown in Figure 2. Using the presented lamination pattern, the boards used in the construction of the NLT panels were selected in such a way that in each test treatment the average MOE values of the boards in the test panels were almost equal. This method of boards selection was utilised to see whether the MOE of NLT panels can be customised using such a lamination system and then properly predicted by simple regression models. For this purpose, a specific MOE value was targeted for the panels in each test treatment. The target MOE values for L.NLT, LS.NLT, and HS.NLT panels were nominal 11.70 GPa, 9.27 GPa, and 11.81 GPa, respectively. To maximise the use of lower-grade boards in the construction of each panel, the boards were selected in a way that at least half of them (or more) had an MOE less than the target MOE of the panel itself. During the lamination process, the stiffer boards in each panel were distributed in different layers near the edges and in the centre of the panels to avoid any localised variation in the

stiffness of the panels along the width. Using this method, the weaker boards were directly laminated to stiffer boards in their adjacent layers in an alternate arrangement (Figure 2).

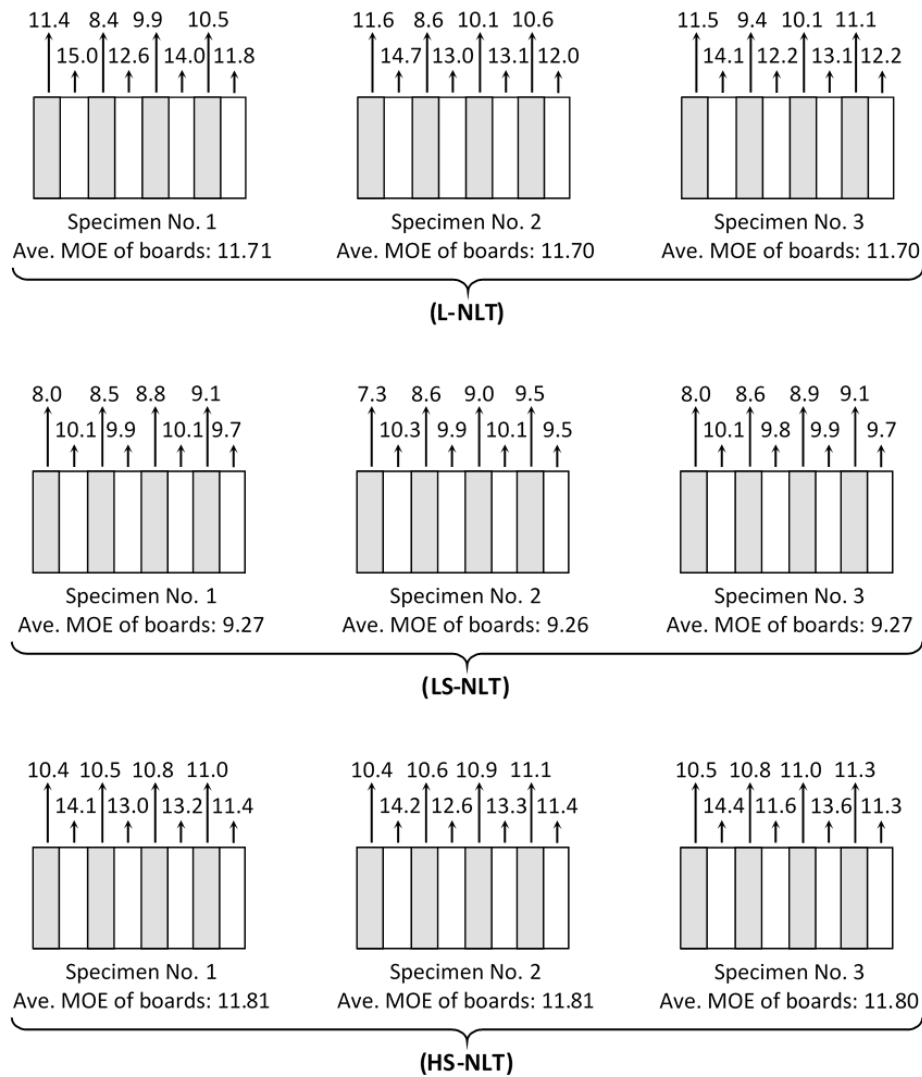


Figure 2. Cross-sectional view of the lamination pattern used and average actual MOE (GPa) of the boards in each test panel. The numbers above each board represents its MOE value in GPa.

In the lamination system used in this study, the SRF zones in weaker boards (such as large knots) were covered by the clear sections of stiffer boards in their adjacent layers (Figure 3). In such a system, while the panel will deflect as a whole under loading, the stiffer boards are likely to carry a higher level of load than the weaker ones. It was assumed that this effect can improve the performance of the NLT panels from low-grade timber by reducing the regional influence of SRF on the overall load-carrying capacity of the panels.



Figure 3. Examples of SRF zones in lower-grade boards supported by the clear sections of stiffer boards in the adjacent layers.

2.3. Short-term bending test

The NLT panels were tested on their widest face by applying loads in the linear-elastic range using the four-point bending test apparatus shown in Figure 4. The load levels for testing the panels with the length of 2600 mm and 3600 mm were 11.77 kN and 6.87 kN, respectively. These levels of loads ensured that the serviceability loads are well passed and the deflections in the test panels are big enough to calculate their MOE values properly. The MOE of the panels was calculated using Equation 1.



Figure 4. The four-point bending test apparatus.

In conjunction with AS/NZS 1170.1 and AS/NZS 1170.0 (Standards Australia/Standards New Zealand 2002), for structural floor elements in general areas in office buildings, the maximum deflection under a uniformly distributed imposed load (Q) of 3 kPa (or 0.84 kN/m for the panel width of 280 mm) shall not exceed span/300. To evaluate the serviceability of floor elements in some of the previous studies, a uniformly distributed superimposed dead load (G) of 1 kPa (or 0.28 kN/m for the panel width of 280 mm) was also added to the standard imposed load to take into account the dead loads resulting from the self-weight of non-structural and semi-permanent members in the building (Yeoh et al. 2011). The midspan deflection of the test panels in this study at the serviceability bending load were compared to the deflection limit provided by AS/NZS 1170.0 (Standards Australia/Standards New Zealand 2002)

under a combination (SSD) of serviceability short-term imposed load and superimposed dead load as follows:

Equation 2

$$SSD = G + 0.7Q = 0.87 \text{ kN/m}$$

The above load combination is uniformly distributed. The equivalent experimental four-point SSD loads were calculated using the equivalence of the bending moment as follow:

Equation 3

$$\frac{PL}{6} = \frac{qL^2}{8}$$

hence,

Equation 4

$$P = \frac{3qL}{4}$$

where, q is the load combinations (SSD) (kN/m), P is the experimental four-point bending load equivalent to q (kN), and L is the span length of the panels (m).

To verify the serviceability of the NLT panels, the deflections of the test panels obtained from the experimental load-deflection curves at the experimental equivalence of SSD load were compared to the deflection limit of span/300.

2.4. Long-term bending creep test

To study the long-term creep deflection in the midspan of the test panels, after obtaining the actual MOE under short-term bending loads, the panels were loaded by the uniformly distributed serviceability bending load specified for structural floors in office buildings in AS 1170.1 (Standards Australia/Standards New Zealand 2002). This included the load combination given in Equation 5 which is comprised of long-term, uniformly distributed imposed load of 3 kPa (Q) and superimposed dead load of 1 kPa (G) equivalent to approximately 63 kgf.m⁻¹ based on the width of the panels in this study.

Equation 5

$$\text{Sustained load} = G + 0.4Q$$

Typical concrete blocks were used for loading the test panels as shown in Figure 5 (Musselman et al. 2018). The test was performed in an indoor laboratory environment with variable temperature and RH. As studying the influence of environmental conditions on the creep deflection of the panels was an

objective of this study, it is worth mentioning that the creep test was conducted at the Discipline of Architecture and Design, University of Tasmania, Launceston, Tasmania, Australia. The daily variations in the temperature and RH therefore represent the environmental conditions during the test in Launceston region.



Figure 5. The bending creep test set-up.

The long-term bending deflections in the midspan of the panels were measured daily for 90 days—from October 2018 to January 2019. The temperature and RH in the laboratory environment were recorded for every deflection measurement using a sensor connected to a Pasco Xplorer GLX datalogger (Model: PS-2002). Relative creep values in the panels were calculated using the following equation:

Equation 6

$$w(t) = \frac{\omega(t)}{\omega(i)} - 1$$

where, $w(t)$ is relative creep at time (t); $\omega(t)$ is the midspan deflection at time (t); $\omega(i)$ is the initial deflection of the panels after loading.

2.5. Statistical data analysis

The statistical analyses throughout this study were performed using IBM SPSS Statistics software (version 23). One-way analysis of variance (ANOVA) test was used to determine the significance of differences in the MOE values between HS.NLT and LS.NLT panels. The significance of correlations between different test variables was determined using the Pearson correlation coefficient. The coefficient of determination (R^2) was used to investigate the prediction accuracy of different linear and nonlinear regression models developed in this study.

3. Results and Discussions

3.1. The effectiveness of VSG on the plantation *E. nitens* boards

The F-grades allocated to the individual boards based on both VSG and the actual MOE of the boards are given in Table 3. The VSG method on the plantation *E. nitens* boards had a poor accuracy of less than 34%. The VSG method overestimated the stress-grade of more than 44% of the boards. More than 22% of the boards were also downgraded by the VSG method.

From an engineering perspective, down-grading the boards may not be an issue as this can result in a higher safety in the design of the building. Over-grading the boards, however, could be unsafe as these boards might be used under a service load with a level of intensity higher than their expected load-carrying capacities.

Historically, the VSG method was first developed for grading and sorting mature native forest timber in the mill and done by certified timber graders (ALS 1970). In this method, the MOE is one of the main grade-determining mechanical properties (Piazza and Riggio 2008). Another important grade-determining characteristic is density (Olsson and Oscarsson 2017). The timber grader can estimate the grade of the boards based on their visual characteristics, but the density of the boards is not visually measurable. In this procedure, the age and the source (e.g., plantation or native forests) of the timber is also not considered—which could be a concern when it comes to a fibre-managed plantation resource that can have a high variation in the density and mechanical properties.

As the percentage of overestimated F-grades in this study were considerably high, the current VSG method will not be a reliable grading system for the fibre-managed plantation *E. nitens* timber. This result is in agreement with those reported by Derikvand et al. (2018b) on structural grading of *E. nitens*.

Table 3. The VSG results versus actual F-grades of individual boards.

F-grade based on VSG	Percentage of boards in each grade based on VSG (%)	Actual F-grade of the boards in each group ^a (%)					Total error of VSG (%)
		F22	F17	F14	F11	< F11	
F22	11.1	-	2.8	2.8	1.4	4.2	11.1
F17	2.8	-	-	-	2.8	-	2.8
F14	29.2	-	-	2.8	8.3	18.1	26.4
F11	25	-	4.2	6.9	11.1	4.2	13.9
< F11	31.9	-	1.4	5.6	4.2	19.4	12.5
Total	100	-	8.3	18.1	27.8	45.8	66.7

^a Allocated based on the actual MOE of the boards

3.2. The MOE of NLT panels

The ANOVA results, given in Table 4, revealed that the average MOE of the panels made with lower-grade boards (LS-NLT panels) was significantly different than that of the panels made with higher-grade ones (HS-NLT panels). The results showed that more than 94% of variations in the empirical MOE of the NLT panels in all test treatments can be explained by the actual average MOE of the boards (Table 5). The empirical MOE of NLT panels throughout this paper refers to the experimental MOE of

the panels calculated using Equation 1. The average MOE of the boards in each panel obtained by the VSG method however had a nonsignificant, negative correlation with the MOE of the NLT panels. The load-deflection curves of the test panels in the linear-elastic region are shown in Figure 6.

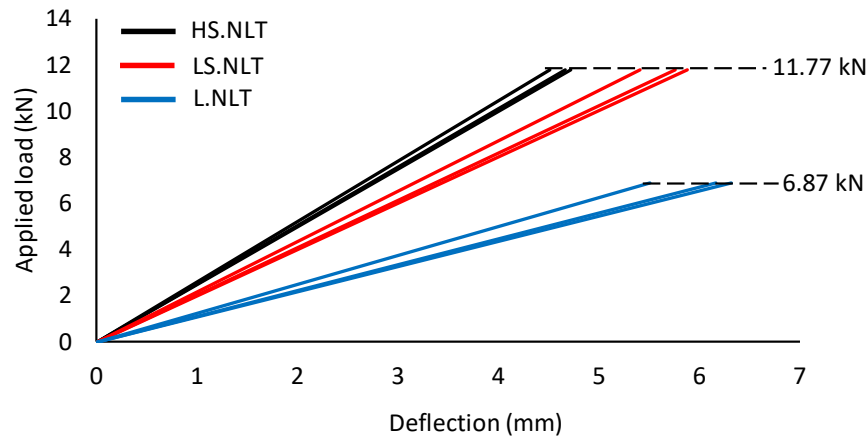


Figure 6. Load-deflection curves of the panels in the linear-elastic region. The length of the panels was 2600 mm for HS.NLT and LS.NLT and 3600 mm for L.NLT.

The average MOE of the boards in each test panel obtained by both VSG and four-point bending test as well as the empirical MOE of the test panels are given in Table 6. In all cases, HS-NLT panels showed a higher MOE value than the LS-NLT panels. The HS-NLT panels were on average 22.4% stiffer than the LS-NLT ones. The empirical MOE of the test panels was more than 97% (on average) close to the average actual MOE of the boards that was targeted in each panel during the lamination process. This indicates an appropriate load-sharing capacity between the boards in the test panels.

Table 4. The ANOVA results.

Source	Type III Sum of Squares	df	Mean Square	F	Sig.
Panel type (LS-NLT vs HS-NLT)	6.58	1	6.58	61.07	0.001
Error	0.43	4	0.11		
Total	656.98	6			

^a $R^2 = 0.94$ (Adjusted R^2 Squared = 0.92)

Table 5. The correlations between empirical MOE of the panels and average MOE of the boards in each panel.

		Empirical MOE of panels	Actual average MOE of boards	Average MOE of boards based on VSG
Empirical MOE of panels	Pearson Correlation	1	0.97**	-0.11
	Sig. (2-tailed)		0.00	0.79
	N	9	9	9
Actual average MOE of boards	Pearson Correlation		1	0.01
	Sig. (2-tailed)			0.98
	N		9	9

** Correlation is significant at 99% level of confidence.

Table 6. Empirical and predicted MOE values of the NLT panels.

Panel code	Specimen No.	Ave. MOE of boards (GPa)		Empirical MOE of panels (GPa)	Predicted MOE of panels (GPa)			
		Actual values	Based on VSG		Equation 8	Diff. (%)	Equation 7	Diff. (%)
L-NLT	1	11.71	13.28	11.28	11.27	-0.03	10.55	-6.48
	2	11.70	10.00	11.41	11.27	-1.19	10.81	-5.23
	3	11.70	10.16	11.08	11.27	1.70	10.80	-2.58
Average		11.70 (0.02) ^a	11.15 (16.6) ^a	11.26 (1.4) ^a	11.27 (0.02) ^a	0.01	10.72 (1.4) ^a	-4.8
HS-NLT	1	11.81	9.98	11.75	11.36	-3.33	10.81	-7.99
	2	11.81	10.53	11.45	11.36	-0.80	10.77	-5.94
	3	11.80	13.31	11.17	11.35	1.67	10.55	-5.57
Average		11.81 (0.03)	11.27 (15.8)	11.46 (2.5)	11.36 (0.03)	-0.9	10.71 (1.3)	-6.5
LS-NLT	1	9.27	10.54	9.77	9.33	-4.54	10.77	10.21
	2	9.26	11.59	9.23	9.32	1.03	10.68	15.71
	3	9.27	11.41	9.09	9.33	2.65	10.70	17.72
Average		9.27 (0.04)	11.18 (5.0)	9.36 (3.9)	9.33 (0.04)	-0.3	10.72 (0.4)	14.5

^a Coefficient of variance in parenthesis

The lamination arrangement used resulted in NLT panels with consistent and less variable flexural stiffness in each test treatment. The average coefficient of variance in the MOE values obtained from all the tested NLT panels (i.e., nine specimens) as low as 2.6% (Table 6). Reducing the coefficient of variance in the mechanical properties can help to improve the lower fifth percentile value of strength of the final product. This effect can be studied using the presented lamination arrangement in future by testing a large sample size to failure point.

In Figure 7, the empirical MOE values of the test panels are compared to the MOE of individual boards in each panel. In each one of the HS-NLT panels, the MOE values of most of the boards were lower than that of the panel itself. This shows a high contribution of the stiffer boards in the overall stiffness of the panels. This effect was slightly different in the L-NLT panels in which the MOE values of the individual boards were less uniform—even though the average empirical MOE of these panels was close to that of the HS-NLT ones. Based on these results, it could be pointed out that laminating higher-grade and lower-grade boards, with known MOE, in an alternate arrangement has the potential to increase the use of lower-grade boards in NLT production while still exhibiting an appropriate bending performance.

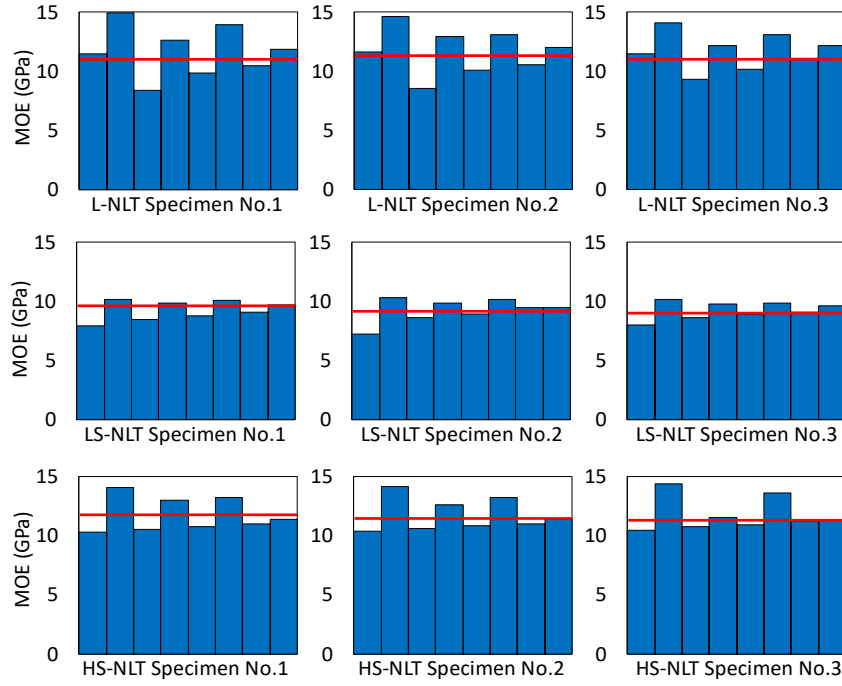


Figure 7. The empirical MOE of the test panels (red line) versus the MOE of individual boards in each panel according to the actual lamination arrangement (blue bars).

Based on the statistical analysis results, two simplified regression equations were developed to predict the empirical MOE of the NLT panels. Both equations were developed using the MOE of the boards as the single regressor. The first equation was created using the average MOE of the boards in each panel estimated by the VSG method as follow:

Equation 7

$$MOE_{Panel} = 11.61 - (0.08 \times MOE_{VSG})$$

The second equation was created using the average actual MOE of the boards in each panel obtained by four-point bending test as follow:

Equation 8

$$MOE_{Panel} = 1.91 + (0.8 \times MOE_{Actual})$$

where, MOE_{Panel} is the predicted MOE of the NLT panels (GPa), MOE_{VSG} is the average MOE of the boards in each panel estimated by the VSG method (GPa), and MOE_{Actual} is the average MOE of the boards in each panel obtained by four-point bending test (GPa).

The results demonstrated that a regression model based on the average MOE of the boards obtained by the VSG method (Equation 7) has a considerably low R^2 of less than 0.012. The differences between the empirical MOE values of the panels and those obtained by Equation 7 ranged from -7.99% to 17.72%. This equation showed conservative predictions for the MOE of L-NLT and HS-NLT panels. It also significantly overestimated the MOE of LS-NLT panels. The differences between the actual MOE of

the LS-NLT panels and the predicted values using Equation 7 ranged from 10.21% to 17.72%. This result proved that predicting the flexural MOE of the *E. nitens* NLT panels based on the VSG results might not be a safe and reliable procedure.

The differences between the empirical MOE values of the NLT panels and those obtained by Equation 8 were from -4.54% to 2.65%—with an average difference of less than 1.9%. The R^2 obtained by this equation was 0.941. This suggests that prediction of the MOE of NLT panels based on the actual MOE of the boards used in their constructions can be a much more reliable method. As the only regressor in Equation 8 was the actual MOE of the boards, such equation can even be used as a simple prediction model at a larger scale with a potential application in the commercial production of NLT panels. This however requires a good estimate of the MOE of the timber—which is not achievable through the VSG method. Developing an appropriate grading system for the timber recovered from the fibre-managed plantation eucalypt resources is therefore warranted. In practice, it has been demonstrated that a very good estimate of the actual MOE of individual boards can be obtained through machine stress grading and commercially available timber scanning devices (Kandler et al. 2015; Pošta et al. 2016).

3.3. Short-term serviceability verification

The deflection values of the test panels at the short-term serviceability load combination were extracted from the load-deflection curves of the panels and the results are depicted in Figure 8.

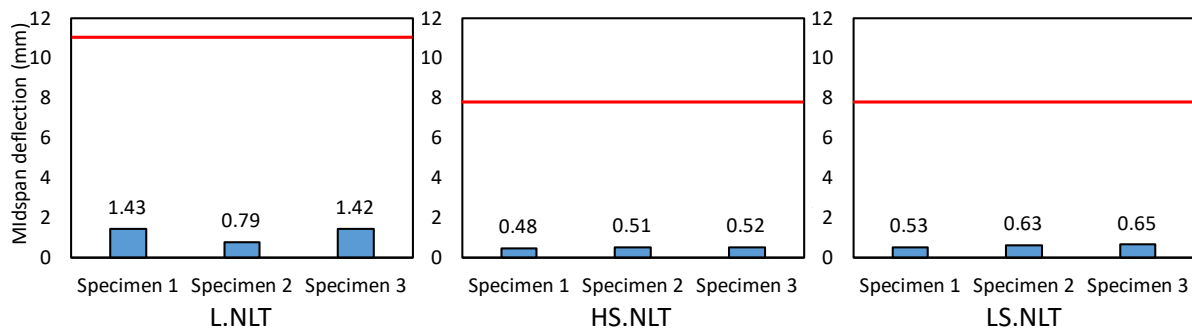


Figure 8. Midspan deflection of the NLT panels at serviceability load. Red line indicates the deflection limit of $span/300$ for each panel type.

The midspan deflection in the LS-NLT panels was higher than that in the HS.NLT ones. For the L-NLT panels, the serviceability deflection limit ($span/300$) was 10 times greater than the experimental midspan deflection of the panels. The serviceability deflection limit was respectively 16 times and 13.3 times greater than the experimental midspan deflection of HS.NLT and LS.NLT panels as well. The plantation *E. nitens* NLT panels therefore showed appropriate short-term serviceability performances to be used as structural flooring elements in office buildings.

3.4. Long-term bending behaviour

The long-term (creep) deflections in the midspan of the test panels under serviceability bending load and the daily variations in the RH and temperature of the laboratory environment are depicted in Figure 9. A similar, nonlinear trend was observed in the long-term deflection behaviour of the test panels from different span lengths and structural grades.

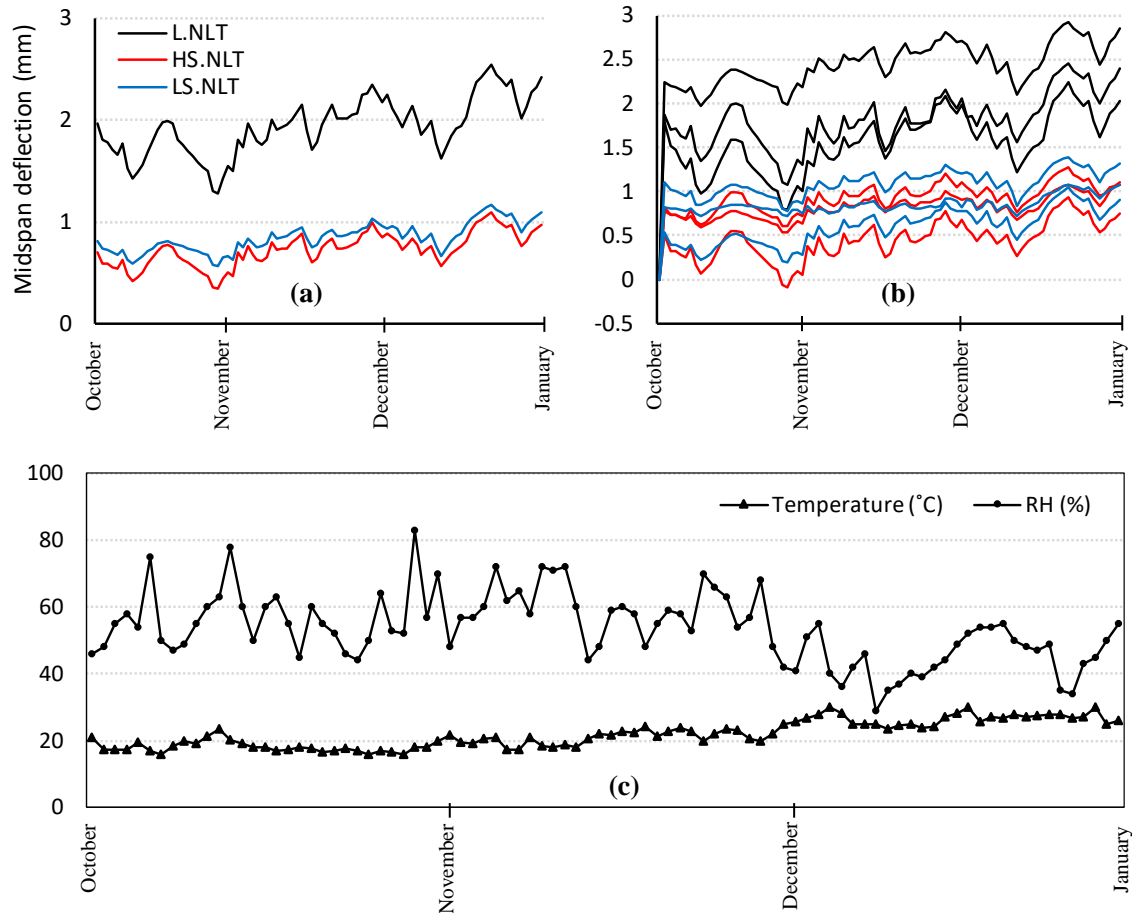


Figure 9. The average long-term midspan deflection of each panel type (a) and that of individual panels (b) as well as daily variations in RH and temperature of the laboratory environment (c).

Within the first 30 days of initial loading, a considerably large reduction in the midspan deflection of the panels was detected. The average midspan deflections then started to increase gradually for the following 60 days, although the nonlinearity in the time-deflection curves continued with periods of sudden increase and decrease in the deflection of the panels.

The initial midspan deflections and the peak relative creep values of the test panels within the first 30 days, 60 days, and 90 days are given in Table 7. In general, the panels made of higher-grade boards (HS.NLT panels) exhibited a lower initial deflection and relative creep values than the panels made of lower-grade boards (LS.NLT panels). The peak relative creep after 90 days in the LS.NLT panels was 15.7% higher than that in the HS.NLT panels. The L.NLT panels also showed the lowest peak relative

creep values after 90 days even though the span length in these panels was 1000 mm longer than that in the HS.NLT and LS.NLT panels.

Overall, the relative creep in the LS.NLT panels was 1.2 times and 2.0 times greater than that in the HS.NLT and L.NLT ones, respectively. These results demonstrated that the structural grade of the boards has a meaningful effect on the long-term bending performance of the NLT panels made of fibre-managed planation *E. nitens* timber.

On average, after 90 days the relative creep in all the test panels was 5.6 times higher than that within the first 30 days of testing. The relative creep in the test panels after 60 days was also 3.9 times higher than that within the first 30 days of testing—which indicates the significant influence of loading duration on the relative creep of the NLT panels.

The RH of the laboratory environment varied considerably from a minimum of 29% to a maximum of 83%. The variations in the temperature also ranged from 15 °C to 30 °C, averaging 21 °C for the duration of the test.

Table 7. Peak values of relative creep in the panels over periods of 30, 60, and 90 days.

Panel code	Specimen No.	Initial midspan deflection (mm)	Peak values of relative creep		
			$w(t_{30})$	$w(t_{60})$	$w(t_{90})$
L.NLT	Specimen No. 1	2.24	0.07	0.25	0.31
	Specimen No. 2	1.79	None	0.17	0.37
	Specimen No. 3	1.87	0.07	0.16	0.20
	Average	1.97	0.07	0.19	0.29
HS.NLT	Specimen No. 1	0.51	None	0.17	0.25
	Specimen No. 2	0.82	None	0.65	0.96
	Specimen No. 3	0.77	0.04	0.14	0.32
	Average	0.7	0.04	0.32	0.51
LS.NLT	Specimen No. 1	1.11	0.09	0.52	0.82
	Specimen No. 2	0.53	0.21	0.46	0.55
	Specimen No. 3	0.82	0.01	0.31	0.40
	Average	0.82	0.10	0.43	0.59

To study the effect of the environmental conditions on the long-term midspan deflection of the panels, the correlations between daily variations in RH and daily variations in the midspan deflections of the panels were determined. The results of this analysis are illustrated in Figure 10 using scatter charts. The significance of the correlations is determined by the coefficient of determination (R^2) values depicted in this figure. The same method was used to determine the correlations between daily variations in the temperature and daily variations in the midspan deflection of the test panels. The results of this analysis are also shown using scatter charts in Figure 11.

The results indicated that RH has a significant influence on the long-term midspan deflection of the panels under serviceability bending loads. Generally, the midspan deflection of the panels increased with the increase in the RH of the environment. This result is in agreement with those reported by Musselman et al. (2018) for the effect of RH on the long-term bending deflection of laminated-veneer lumber beams made of Douglas Fir-Larch.

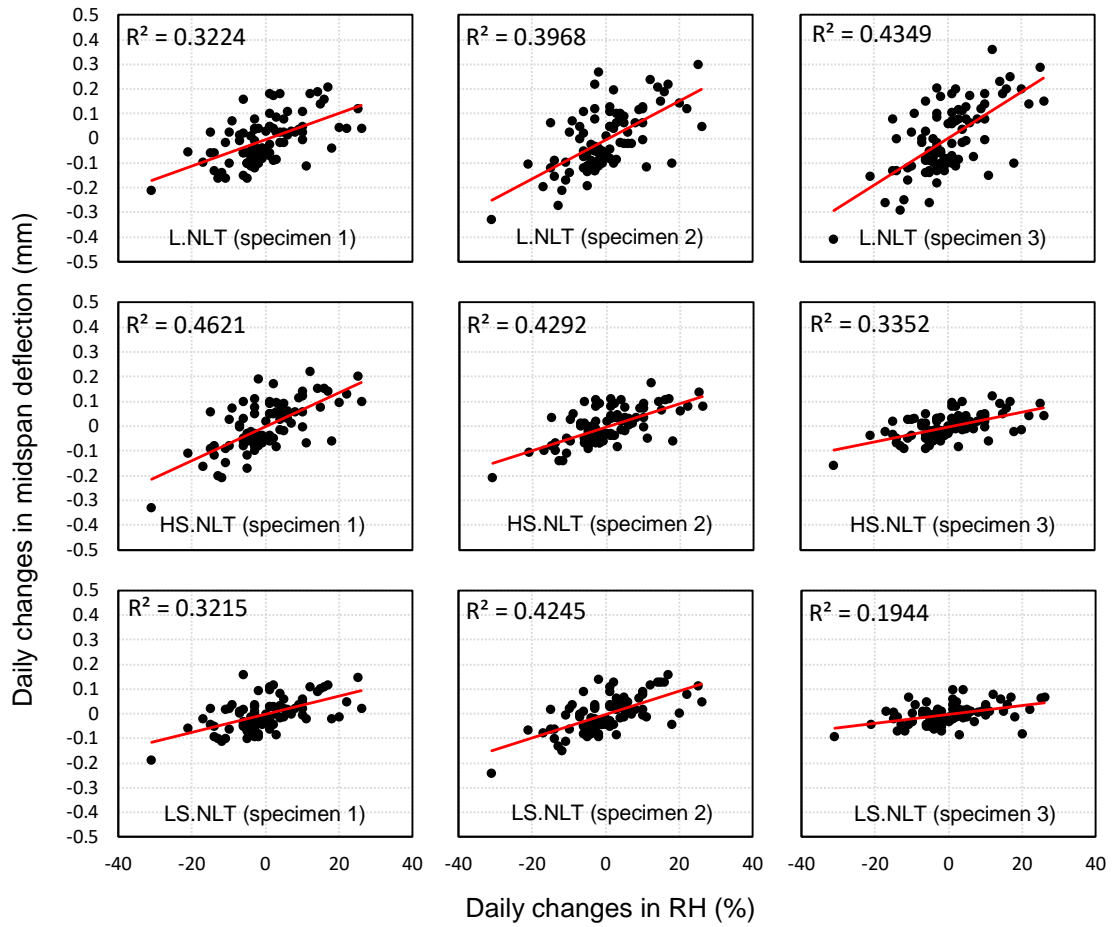


Figure 10. Correlations between daily changes in midspan deflection and RH.

Timber buildings are always exposed to variable temperature and RH. In general, the moisture content of timber increases with the RH of the environment until an equilibrium point is reached (Simpson 2007). With the increase in the moisture content, the deflection of the timber element under sustained loads increases as well. This phenomenon is known as mechano-sorptive creep (Takeda and Arima 2006). The mechano-sorptive creep is independent of time and can occur in any environment with varying RH. The long-term deflections (creep) in the timber elements therefore can be divided into time-dependent and time-independent components. The time-dependent component of creep is a deflection that gradually increases as a result of a sustained load towards a maximum point in a given period. Part of this deflection is recoverable and disappears after the timber element is unloaded, and part is unrecoverable which is known as permanent creep in the element. The time-independent component of creep, resulting from an increase in the RH of the environment, is also usually mostly recovered as the RH decreases—although cyclic changes in the RH can accelerate or even increase the creep rate in the timber elements (Huang 2016). The results obtained in this study clearly supports this logic (Figure 9).

Considering the coefficient of determination (R^2) values obtained, the daily variations in the temperature of the laboratory environment showed no important correlations with the daily variations

in the long-term midspan deflection of the panels (Figure 11). This result indicates that within a range of 15 °C to 30 °C, where the temperature is mostly around an average of 21 °C, the influence of the daily variations in the temperature on the long-term deflection of the NLT panels is not tangible. It must be noted however that this result does not suggest that a higher range of variations in the temperature will not influence the long-term deflection of the timber elements.

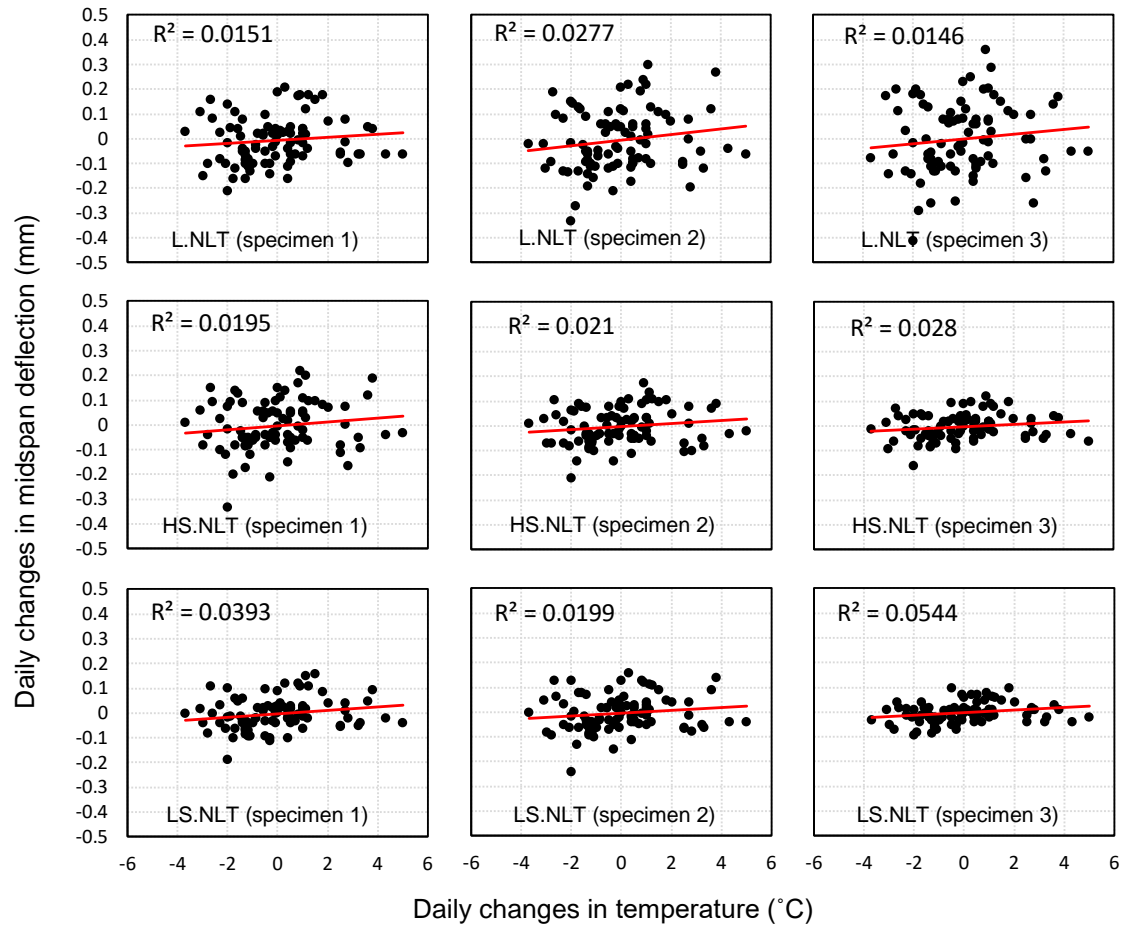


Figure 11. Correlations between daily changes in midspan deflection and temperature.

Based on the statistical analysis results, the nonlinear regression model presented in Equation 9 was fitted to the experimental data of the long-term bending creep deflection of the test panels. This is a purely statistical model that was achieved through an extensive trial-and-error process which involved several other types of linear and nonlinear regression expressions including exponential, logarithmic, and power models.

Three variables that can influence the long-term behaviour of the panels were used in developing this model, namely, time (in days), temperature (in °C), and RH (in %). The model is comprised of four constant parameters, namely, α_1 , α_2 , α_3 , and α_4 . The estimated constant parameters for each panel type are given in Table 8. The experimental and model time-deflection curves for each panel type under long-term serviceability bending loads are shown in Figure 12.

Equation 9

$$w = \alpha_1 \times (time)^{\alpha_2} \times (Temp.)^{\alpha_3} \times (RH)^{\alpha_4}$$

where, w is the long-term (creep) deflection in the midspan of the panels.

Table 8. Estimated constant parameters for Equation 9.

Panel code	Estimated parameters				R ²
	α_1	α_2	α_3	α_4	
L.NLT	0.050	0.032	0.648	0.391	0.71
HS.NLT	0.019	0.062	0.666	0.391	0.74
LS.NLT	0.003	0.085	0.901	0.619	0.75

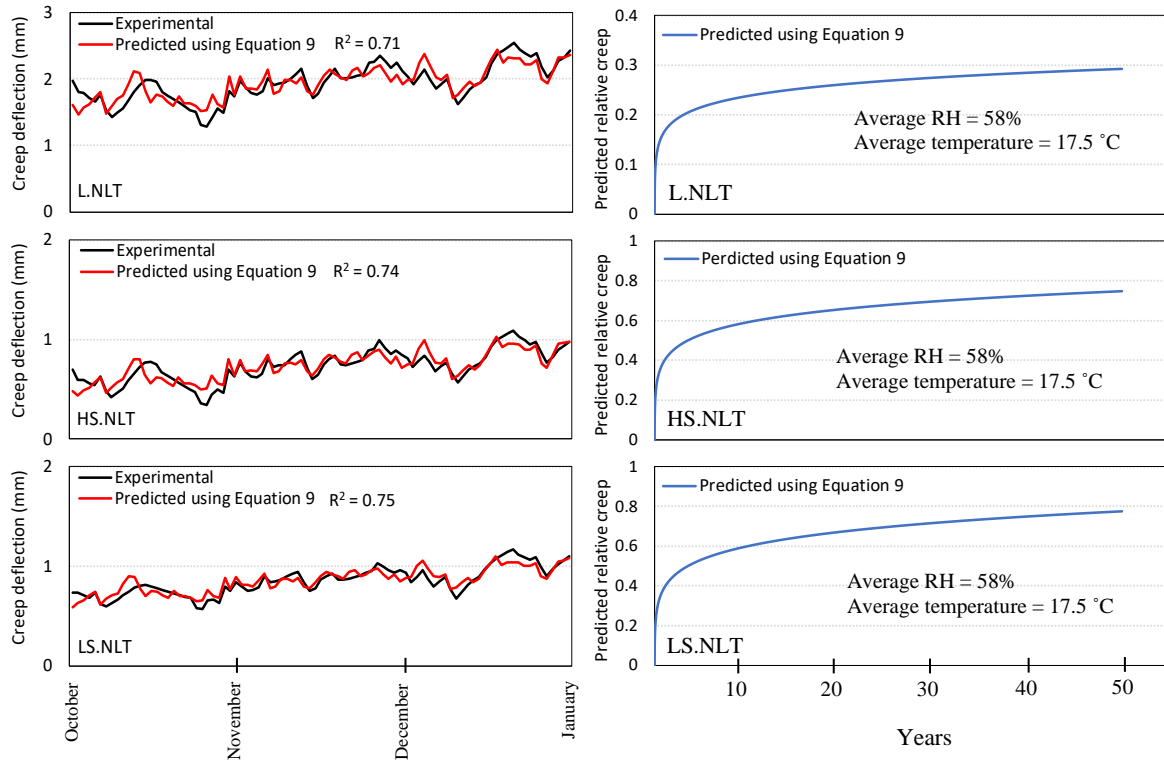


Figure 12. Experimental and model (by Equation 9) time-deflection curves (left) and predicted relative creep in the panels under long-term serviceability bending load for 50 years (right).

The coefficient of determination (R^2) values between the experimental and model curves were 0.71 for the L.NLT panels, 0.74 for the HS.NLT panels, and 0.75 for the LS.NLT panels. While the long-term midspan deflection of the panels was highly nonlinear, the regression model in Equation 9 represented the best fitting with the experimental data compared to the other linear and nonlinear models evaluated during the creation of this model. This model takes into account the effect of daily variations in the temperature and RH of the environment on the long-term midspan deflection of the panels in addition to the number of days during which the panels are affected by the load. It must be noted that, as Equation

9 has been created using the experimental data of creep deflection based on the daily variations in RH and temperature in Tasmania, its accuracy and the effectiveness of its application in predicting the bending creep deflection of NLT panels in other areas with different environmental conditions could vary—which can be studied in future research.

The relative creep under long-term serviceability bending loads for each panel type were predicted for 50 years using Equation 9 and the results are illustrated in Figure 12. For predicting the relative creep values in the panels, the average temperature and RH were used in the model and it was assumed that the temperature and RH of the environment will not change dramatically from one year to another. It must be noted that the results presented in Figure 12 for 50 years are the total relative creep values in the panels for each year which are different than the peak values of relative creep that were calculated for different periods.

The peak relative creep values presented in Table 7 were affected by both time-dependent creep and mechano-sorptive creep, whereas the total creep values predicted by Equation 9 are only for the time-dependent creep itself—as the average RH and temperature were used for this purpose. The predicted total relative creep values after 50 years for the L.NLT, HS.NLT, and LS.NLT panels were respectively 0.30, 0.75, and 0.78—which corresponds to 30%, 75%, and 78% increase in the initial deflection of the panels.

Considering the short-term deflection of the panels under serviceability loads discussed in section 0, the total relative creep values obtained from each panel type after 50 years will not significantly influence the deflection serviceability of the panels for the given span lengths. This result suggests that, for the span lengths tested in this study, the fibre-managed plantation *E. nitens* timber will have satisfactory long-term performance to meet the serviceability requirements for deflection.

The area of long-term creep in timber however is quite complex, especially under variable temperature and RH. The creep deflection in any timber product relies on several parameters such as density, MOE, load level, and moisture content (Lu and Leicester 1997). There are also many factors that can influence the long-term behaviour of a timber product in general. Other than the creep deflection that was evaluated in this study, possible reductions in the stiffness and strength after a given period (usually 50 years in most design codes) can also influence the suitability of a timber resource for structural building applications. Especially, when it comes to fibre-grown plantation eucalypt that is not originally managed for structural applications, such factors are of high importance and need to be evaluated experimentally to guarantee a safe use of the final product in any target structural application.

4. Conclusions

In this study, structural NLT panels were constructed from a 16-year-old fibre-managed *E. nitens* plantation that is being managed for producing woodchips. The performance of the VSG method in estimating the MOE of individual boards from the fibre-managed plantation *E. nitens* was evaluated.

The reliability of simple regression models in predicting the MOE of the NLT panels was determined using the average MOE of the boards obtained from both VSG method and four-point bending test as the single regressors. The influence of environmental conditions (temperature and RH) on the long-term behaviour of the panels was also evaluated under serviceability bending loads. The following conclusions were drawn on the basis of the results obtained:

- The current VSG standard method showed a poor accuracy of less than 34% in predicting the actual MOE of the individual boards from the fibre-managed plantation *E. nitens*. The MOE of the NLT panels therefore could not be properly estimated using the VSG results.
- A linear regression model was developed in this study based on the actual MOE of the boards as the single regressor that could predict the MOE of the NLT panels with more than 98% average accuracy.
- All the test panels constructed of the fibre-managed plantation *E. nitens* successfully passed the short-term serviceability requirements for the deflection limit of span/300.
- A lamination pattern was developed that resulted in a remarkable average coefficient of variance of about 2.6% in the flexural MOE of the NLT panels—this coefficient of variance was achieved from a total of nine panels in this study that were precisely and carefully constructed. This lamination pattern can be used to customise the MOE of NLT panels and maximise the use of lower-grade boards in their constructions.
- The long-term creep deflection of the panels was significantly affected by the variation in RH and structural grade of the timber boards used. The correlation between the daily variations in the temperature and the long-term creep deflection of the panels was insignificant within the range of 15 °C to 30 °C—where the average temperature is usually around 21 °C. The peak relative creep after 90 days in NLT panels made with lower-grade boards was 15.7% higher than that in NLT panels made with higher-grade boards. A nonlinear regression model was developed based on the experimental results of long-term bending creep test. The relative creep values predicted by this model for 50 years indicated that the fibre-managed plantation *E. nitens* timber has satisfactory long-term bending performance to meet the serviceability requirements of deflection in structural floor systems.

Acknowledgment

This study was undertaken under the Australian Research Council, Centre for Forest Value, University of Tasmania, TAS, Australia (Grant Reference: IC150100004). The support from Forest and Wood Products Australia Limited (FWPA), Melbourne, VIC, Australia is acknowledged (Grant Number: PNB387-1516). The authors are also grateful of the support from Forico Pty Ltd. in providing the logs and Britton Timbers for the milling of the logs and drying and finishing of the boards.

References

- [1] ALS. (1970). American lumber standard board of review. American Softwood Lumber Standard PS 20–70 (ALS). American Lumber Standards Committee. Washington, DC: U.S. Department of Commerce.
- [2] AS 1720.1. (2010). Timber Structures – Design Methods. Standards Australia, Australia.
- [3] AS 2082. (2007). Timber - Hardwood - Visually stress graded for structural purposes. Standards Australia, Australia.
- [4] AS/NZS 1170.0. (2002). Structural design actions. Part 0: General principles. Standards Australia/Standards New Zealand, Australia.
- [5] AS/NZS 1170.1. (2002). Structural design actions. Part 1: Permanent, imposed and other actions. Standards Australia/Standards New Zealand, Australia.
- [6] AS/NZS 4063.1. (2010). Characterisation of structural timber. Part 1: Test Methods. Standards Australia/Standards New Zealand, Australia.
- [7] Christovasilis, I. P., Brunetti, M., Follesa, M., Nocetti, M., & Vassallo, D. (2016). Evaluation of the mechanical properties of cross laminated timber with elementary beam theories. *Construction and Building Materials*, 122, 202-213. <https://doi.org/10.1016/j.conbuildmat.2016.06.082>
- [8] Derikvand, M., Kotlarewski, N., Lee, M., Jiao, H., & Nolan, G. (2018a). Flexural and visual characteristics of fibre-managed plantation Eucalyptus globulus timber. *Wood Material Science & Engineering*, 1-10. <https://doi.org/10.1080/17480272.2018.1542618>
- [9] Derikvand, M., Kotlarewski, N., Lee, M., Jiao, H., Chan, A., & Nolan, G. (2018b). Visual stress grading of fibre-managed plantation Eucalypt timber for structural building applications. *Construction and Building Materials*, 167, 688-699. <https://doi.org/10.1016/j.conbuildmat.2018.02.090>
- [10] Derikvand, M., Kotlarewski, N., Lee, M., Jiao, H., Chan, A., & Nolan, G. (2019). Bending performance of nail-laminated timber constructed of fast-grown plantation eucalypt. *European Journal of Wood and Wood Products*, in press.
- [11] Derikvand, M., Nolan, G., Jiao, H., & Kotlarewski, N. (2017). What to do with structurally low-grade wood from Australia's plantation eucalyptus; building application?. *BioResources*, 12(1), 4-7. <https://doi.org/10.15376/biores.12.1.4-7>
- [12] Evison, D. C., Kremer, P. D., & Guiver, J. (2018). Mass timber construction in Australia and New Zealand—status, and economic and environmental influences on adoption. *Wood and Fiber Science*, 128-138.
- [13] Fink, G., Frangi, A., & Kohler, J. (2015). Probabilistic approach for modelling the load-bearing capacity of glued laminated timber. *Engineering Structures*, 100, 751-762. <https://doi.org/10.1016/j.engstruct.2015.06.015>
- [14] Fossetti, M., Minafò, G., & Papia, M. (2015). Flexural behaviour of glulam timber beams reinforced with FRP cords. *Construction and Building Materials*, 95, 54-64. <https://doi.org/10.1016/j.conbuildmat.2015.07.116>
- [15] Frihart, C. R., & Beecher, J. F. (2016). Factors that lead to failure with wood adhesive bonds. In *World Conference on Timber Engineering, WCTE 2016, August 22-25, 2016, Vienna, Austria*.
- [16] Hong, K. E. M. (2017). *Structural performance of nail-laminated timber-concrete composite floors* (Master's dissertation, University of British Columbia).
- [17] Huang, Y. (2016). Creep behavior of wood under cyclic moisture changes: interaction between load effect and moisture effect. *Journal of wood science*, 62(5), 392-399. <https://doi.org/10.1007/s10086-016-1565-4>
- [18] Janssens, M. L. (2015). Full-scale tests in a furnished living room to evaluate the fire performance of protected cross-laminated and nail laminated timber construction. Final Report, Southwest Research Institute, TX, USA.
- [19] Kandler, G., Füssl, J., Serrano, E., & Eberhardsteiner, J. (2015). Effective stiffness prediction of GLT beams based on stiffness distributions of individual lamellas. *Wood Science and Technology*, 49(6), 1101-1121. <https://doi.org/10.1007/s00226-015-0745-5>
- [20] Lee, J. J., Park, J. S., Kim, K. M., & Oh, J. K. (2005). Prediction of bending properties for structural glulam using optimized distributions of knot characteristics and laminar MOE. *Journal of wood science*, 51(6), 640-647. <https://doi.org/10.1007/s10086-005-0704-0>

- [21] Liao, Y., Tu, D., Zhou, J., Zhou, H., Yun, H., Gu, J., & Hu, C. (2017). Feasibility of manufacturing cross-laminated timber using fast-grown small diameter eucalyptus lumbers. *Construction and Building Materials*, 132, 508-515. <https://doi.org/10.1016/j.conbuildmat.2016.12.027>
- [22] Lu, J. P., & Leicester, R. H. (1997). Mechano-sorptive effects on timber creep. *Wood science and technology*, 31(5), 331-335. <https://doi.org/10.1007/BF01159152>
- [23] Lu, Z., Zhou, H., Liao, Y., & Hu, C. (2018). Effects of surface treatment and adhesives on bond performance and mechanical properties of cross-laminated timber (CLT) made from small diameter Eucalyptus timber. *Construction and Building Materials*, 161, 9-15. <https://doi.org/10.1016/j.conbuildmat.2017.11.027>
- [24] Musselman, E. S., Dinehart, D. W., Walker, S. M., & Mancini, M. L. (2018). The effect of holes on the creep behavior and flexural capacity of laminated veneer lumber (LVL) beams. *Construction and Building Materials*, 180, 167-176. <https://doi.org/10.1016/j.conbuildmat.2018.05.186>
- [25] O'Ceallaigh, C., Harte, A., Sikora, K., & McPolin, D. (2014). Enhancing Low Grade Sitka Spruce Glulam Beams with Bonded-in BFRP Rods. In *Proc. of COST Action FP1004 Conference, Experimental Research with Timber*, Prague, Czech Republic.
- [26] Oh, J. K., Lee, J. J., & Hong, J. P. (2015). Prediction of compressive strength of cross-laminated timber panel. *Journal of wood science*, 61(1), 28-34. <https://doi.org/10.1007/s10086-014-1435-x>
- [27] Okabe, M., Yasumura, M., Kobayashi, K., & Fujita, K. (2014). Prediction of bending stiffness and moment carrying capacity of sugi cross-laminated timber. *Journal of wood science*, 60(1), 49-58. <https://doi.org/10.1007/s10086-013-1377-8>
- [28] Olsson, A., & Oscarsson, J. (2017). Strength grading on the basis of high resolution laser scanning and dynamic excitation: a full scale investigation of performance. *European Journal of Wood and Wood Products*, 75(1), 17-31. <https://doi.org/10.1007/s00107-016-1102-6>
- [29] Piazza, M., & Riggio, M. (2008). Visual strength-grading and NDT of timber in traditional structures. *Journal of Building Appraisal*, 3(4), 267-296. <https://doi.org/10.1057/jba.2008.4>
- [30] Pošta, J., Ptáček, P., Jára, R., Terebesyová, M., Kuklík, P., & Dolejš, J. (2016). Correlations and differences between methods for non-destructive evaluation of timber elements. *Wood Research*, 61(1), 129-140.
- [31] Ramage, M. H., Burridge, H., Busse-Wicher, M., Fereday, G., Reynolds, T., Shah, D. U., ... & Allwood, J. (2017). The wood from the trees: The use of timber in construction. *Renewable and Sustainable Energy Reviews*, 68, 333-359. <https://doi.org/10.1016/j.rser.2016.09.107>
- [32] Robertson, M., Holloway, D., & Taoum, A. (2018). Vibration of suspended solid-timber slabs without intermediate support: assessment for human comfort. *Australian Journal of Structural Engineering*, 19(4), 266-278. <https://doi.org/10.1080/13287982.2018.1513783>
- [33] Shim, K. B., Kim, K. M., & Park, J. S. (2009). Improvement of prediction accuracy of glulam modulus of elasticity by considering neutral axis shift in bending. *Wood and Fiber Science*, 41(1), 90-96.
- [34] Simpson, W. T. (2007). Predicting equilibrium moisture content of wood by mathematical models. *Wood and fiber science*, 5(1), 41-49.
- [35] Smith, R. E., Griffin, G., Rice, T., & Hagehofer-Daniell, B. (2018). Mass timber: evaluating construction performance. *Architectural Engineering and Design Management*, 14(1-2), 127-138. <https://doi.org/10.1080/17452007.2016.1273089>
- [36] Takeda, T., & Arima, T. (2006). Creep of the beam in Japanese conventional structures composed of green and kiln-dried timber II: predictive model for relative deflections. *Journal of wood science*, 52(5), 383-388. <https://doi.org/10.1007/s10086-002-0797-7>
- [37] Thilén, J. (2017). Testing of CLT-Concrete Composite decks. Report number: TVBK-5259, Lunds University, Sweden.
- [38] Ussher, E., Arjomandi, K., Weckendorf, J., & Smith, I. (2017). Prediction of motion responses of cross-laminated-timber slabs. *Structures* 11, 49-61. <https://doi.org/10.1016/j.istruc.2017.04.007>
- [39] Viguier, J., Jehl, A., Collet, R., Bleron, L., & Meriaudeau, F. (2015). Improving strength grading of timber by grain angle measurement and mechanical modeling. *Wood Material Science & Engineering*, 10(1), 145-156.

- [40] Weckendorf, J., Toratti, T., Smith, I., & Tannert, T. (2016). Vibration serviceability performance of timber floors. *European Journal of Wood and Wood Products*, 74(3), 353-367. <https://doi.org/10.1007/s00107-015-0976-z>
- [41] Yeoh, D., Fragiaco, M., & Deam, B. (2011). Experimental behaviour of LVL–concrete composite floor beams at strength limit state. *Engineering Structures*, 33(9), 2697-2707. <https://doi.org/10.1016/j.engstruct.2011.05.021>
- [42] Zhou, J., Chui, Y. H., Gong, M., & Hu, L. (2017a). Elastic properties of full-size mass timber panels: Characterization using modal testing and comparison with model predictions. *Composites Part B: Engineering*, 112, 203-212. <https://doi.org/10.1016/j.compositesb.2016.12.027>